INTERNATIONAL HYDROLOGICAL PROGRAMME

Modelling erosion, sediment transport and sediment yield

Edited by Wolfgang Summer and Desmond E. Walling

A contribution to IHP-V Projects 2.1 and 6.2

IHP-VI | Technical Documents in Hydrology | No. 60
UNESCO, Paris, 2002

SC-2002/WS/48

CONTENTS

INTRODUCTION

In July 1998, the International Commission on Continental Erosion of the International Association of Hydrological Sciences organised a symposium in Vienna, Austria, with the theme *Modelling Soil Erosion, Sediment Transport and Closely Related Hydrological Processes*. The symposium was co-sponsored by UNESCO, as a contribution to IHP-V and more particularly to IHP-V Project 2.1 dealing with *Vegetation, Land-Water Use and Erosion Processes* and Project 6.2 concerned with *Land Use, Deforestation, Erosion and Sedimentation in the Humid Tropics*. The symposium was held at the headquarters of the IAEA, and was widely agreed to have been a very successful meeting. The proceedings were published by IAHS Press (*Modelling Soil Erosion, Sediment Transport and Closely Related Hydrological Processes*, Proceedings of the Vienna Symposium, July 13-17, 1998, eds. W. Summer, E. Klaghofer and W. Zhang, IAHS Publication no. 249, 1998) and the 50 papers were contributed by authors from many different regions of the world.

The formal and informal discussion sessions at the meeting emphasised the diversity of the approach to modelling erosion and sediment yield and the need for closer integration of field monitoring and modelling activities, but nevertheless provided clear evidence of many significant advances and achievements within the general area. The discussions also highlighted the central role that modelling must play in dealing with the many environmental problems associated with erosion and sediment transport and in the development of effective catchment management and sediment control strategies.

To build on the success of the symposium and to contribute further to IHP-V Projects 2.1 and 6.2, it was agreed to assemble a collection of papers dealing with recent work on the field of modelling erosion, sediment transport and sediment yield, that could be published in the UNESCO Technical Documents in Hydrology Series, in order to demonstrate the state-of-the-art in this important area. Many of the papers built on contributions to the symposium, but others were solicited to extend the scope of the collection.

The process of collating the papers into the final electronic form proved a lengthy task and the editors are grateful to the authors for their forbearance in accepting the resulting delays and in responding to requests for additional material. Particular thanks are extended to Dr Adrian Collins from the Department of Geography at the University of Exeter, UK, for his help with the final stages of the collation process.

Wolfgang Summer
Hagenbrunn, Austria

Desmond Walling
Department of Geography, University of Exeter, UK.

What approach to the modelling of catchment scale erosion and sediment transport should be adopted?

R. J. Wasson
Centre for Resource and Environmental Studies,
Australian National University,
Canberra, Australia

Abstract

At the catchment scale, spatial and temporal organisation emerges from a large number of physical and biological processes operating at lower levels. The long-standing method of understanding and modelling these lower level processes, from which it is claimed higher level organisation can be simulated, has thus far not produced the anticipated results. Many landscape modellers remain stuck at lower levels, and the catchment scale models required for management and scientific understanding are either not available or are too complex for meaningful use. Emphasis should now be given to either directly modelling the high level, or emergent, properties of catchments, or producing models that can reproduce these high level properties. Sediment budgets are used to explore these ideas.

Introduction

A commonplace assumption in the modern world of hydrological and sediment transport modelling is that processes understood at point scale can be scaled to basin areas of tens to hundreds of thousands of square kilometres. Large and expensive modelling efforts in many countries are based on this assumption, following a tradition that comes largely from classical physics. Once constructed, such models are seen as useful tools for understanding particular catchments and for predicting the impact of land use and climate change on erosion and sediment transport.

There are two reasons for questioning the assumption that bottom-up process-based modelling is the best and only way to produce useful models:

1. A practical objection – models of the natural variability of rainfall infiltration, run off, erodibility, cover, channel characteristics, and sediment storage demand enormous data inputs. Such data are rarely if ever available for areas much larger than a few tens of square kilometres, and the cost of data collection is prohibitive in most countries. Highly parameterised models of the kind needed to exploit such data are essentially untestable, and while the accurate simulation of measured runoff and/or sediment yield may be obtained, it is not possible to know if it is because of correct model configuration or because of the tuning that is almost always needed to successfully simulate outputs.

2. A philosophical objection – catchments are complex systems in which the dynamics are likely to be best understood by examining across - system organisation rather than concentrating on the parts from which a whole system view is constructed. The interaction of components produces results that generally cannot be simulated from the components; that is, the whole is emergent from a wide range of processes and interactions that are neither predictable from, deducible from, nor reducible to the parts alone (Anderson, 1992).

In what follows, the top-down approach is adopted, whereby emergent properties of catchment are identified as a starting point for modelling, rather than the traditional approach of continuum mechanics in which processes are modelled and combined, usually in a spatial setting, using GIS, to reproduce an emergent property such as runoff or sediment yield.

Support for the top-down approach

The top-down approach has been traditionally used by geomorphologists and ecologists, although not necessarily explicitly described in this way.

The muddle of physical and biological processes that occur at small spatial scales and on short time scales across the landscape are partly responsible for the spatial and temporal organisation that is investigated by geomorphologists. For example, river drainage networks are well ordered, drainage density and hillslope length and gradient are mutually adjusted, and the hydraulic geometry of river channels changes as flows of sediment and water change.

There is growing evidence that these, and other examples of systems-level organisation, are self-organised (Phillips, 1995). That is, orderly or repetitive spatial patterns emerge from processes that are internal to the system, and do not require external stimuli to develop. Energy is imported into an open system, such as a catchment, and dissipated to produce order. Such systems may be self-organised to a critical, far from equilibrium, state such that the internal dynamics of the system produce widely varying responses to the same forcing (Bak et al., 1987).

Many aspects of ecosystems are also self-organised and are described as complex adaptive systems (Kauffman, 1993). A large number of agents operating on the basis of local information interact to produce emergent properties. Adaptive behavior appears as individual agents learn from exposure to new information. This adaptive capacity produces emergent properties that are highly organised and, at an appropriate hierarchic level, change in predictable ways.

Harris (1998) identifies some important emergent properties in ecosystems, particularly features of nutrient and energy cycling, size spectra of organisms, trophic structures, and stoichiometric ratios of elements in the biota. In geomorphic systems, as

already noted, hydraulic geometry, drainage networks, and mutual adjustments between channels and hillslopes are examples of emergent properties. There are many others, some of which will be discussed below.

Paraphrasing Harris (1998), systems ecology, biogeochemistry and geomorphology can be viewed as a science of meta-rules, where the emergent properties are the objects of interest, and the muddle of processes operating at lower levels are important in so far as they help to construct the meta-rules. But whatever modelling approach is adopted, it is the emergent properties that must be the target.

After decades of waiting largely in vain for the bottom-up approach to produce plausible models of whole systems, such as catchments, it is time to put a lot more effort into top-down approaches. Many geomorphologists during the 1970's and 1980's adopted the bottom-up approach, and became lost in the muddle of processes operating at levels much lower than the emergent properties. Those who have stuck to the task of understanding landscape level organisation and processes are now positioned, along with some physicists and ecologists, to develop a science of meta-rules. This should be our aim.

The idea of emergence saw formal definition by G.H. Lewis in 1875 (see Goldstein, 1999) where a distinction was drawn between resultant and emergent chemical compounds. A resultant is either a sum or a difference of co-operating forces and can be readily traced to its components. An emergent, by contrast, cannot be reduced either to the sum or difference of co-operating forces. Since this first formal usage of the idea of emergence, there have been other uses of the idea, most notably in animal behaviour, philosophy and entomology (see Goldstein, 1997 for a history).

Is emergence a concept that can be disposed of as understanding of micro-level processes improves? Wilson (1998) argues that micro level process understanding is improving and will eventually allow construction of the whole, like the assumption that point scale process can be scaled to whole catchments. In this case, emergence is a provisional concept based on the inadequacy of current theory for reproducing macro-level features from the micro-level.

Goldstein (1999) points to the fundamental deterministic unpredictability of emergents caused by the non-linearity of complex systems and resulting mathematical intractability. This suggests that hard-core reductionism, which only recognises one level of understanding, will be defeated by the mathematics of the processes that is the basis of the approach. But there are two other reasons for arguing that the study of emergents is not just a provisional approach. The first has already been stated, that when choosing a macro level on which to focus, it is being recognised that the phenomena at this level ' hang together' (Goldstein, 1999) more strongly than phenomena at other levels. Secondly while recognizing that micro-level processes play a role in producing macro-level phenomena, macro-level phenomena affect micro-level processes. There is, therefore, both upward and downward causality.

Emergent properties of catchment scale erosion and sediment transport

Material budgets in ecology and geomorphology

Vollenweider (1976) was able to construct predictive models of the relationship between total phosphorus load and phytoplankton biomass in oligotrophic lakes. He was successful because he restricted his analysis to the key nutrient and to temporally averaged biomass, a fundamental emergent property of lake ecosystems.

Ecologists have long argued that the currency of exchange which is common to all ecosystems is energy and/or material (Odum, 1971). Harris (1997) returns to this theme, and argues that models able to predict algal biomass must be based on flows and stocks of materials both in catchments and waterbodies. This is an extension of Vollenweider's idea, and enables the coupling of the various subsystems identifiable in a catchment-lake system, while capturing key emergent properties. Models of fluxes of particulate and dissolved nutrients, including detritus, are called for. Such models of material budgets are fundamental to quantification of systems states, analysis of the cascade response to perturbations, and form a natural link to economic analysis; particularly ecologic-economic analysis. A fine example is Stigebrandt and Wulff (1987).

Budgets in catchments – global patterns

Material budgets are also important in physical geomorphic systems, but their role as an emergent property of value in comparative studies of catchment types and system states is not widely appreciated (O'Sullivan, 1979; Phillips-Howard, 1985). Their role in decision making in catchment management is hardly recognised. Application of systems modelling to global, regional and local material budgets, along with clear demonstration of utility, should increase awareness. Preoccupation with bottom-up modelling hampers the fundamentally important use of material budgets for both scientific and management purposes. Some examples follow of material budgets as emergent properties, beginning at the global scale. Emphasis is on material budgets because of the link thereby made possible with ecological studies, and because material budgets provide a way of quickly seeing the whole catchment. They also provide a focus for identifying key controlling factors, and so of setting priorities for process research. Therefore, in what follows, controls on budgets are also considered.

Material yield at any point in a catchment is the net result of all processes of production and loss/storage upstream of that point. Yield is therefore a high order property, which is also one term in a material budget equation. It is also a property that has thus far not been simulated from micro-level processes.

Mean annual sediment yield (SY; t x 10^6/yr) from catchments across the globe is related to catchment area by power functions (Milliman and Syvitski, 1992):

$$SY = cA^b \quad (1)$$

where A is catchment area, c is the yield at 1 x $10^6 km^2$, and b averages 0.57. The intercepts (C) are an exponential function of catchment elevation (E), a variable along with A used to distinguish sediment yield regions of the globe, and expressed as:

$$\text{Log } c = \log 2.34 + 1.66 \times 10^{-3} E \quad (2)$$

where c is t/yr (x 10^6)and E is the mean of the elevation classes (m above sea level) used by Milliman and Syvitski; $r^2 = 0.91$.

Across the globe, Milliman and Syvitski distinguished seven coherent sets of sediment yields from catchments ranging in size from 10 to $10^6 km^2$. In all but one case, where yield is high in small catchments it is also high downstream. Similarly, where yield is low in small catchments it is also low downstream. The exponential function (2) allows interpolation between the sets, allowing generalisation of most of the global data.

From this correlation analysis it can be inferred that because high elevation catchments worldwide are steep (Chorley et al., 1984), they yield large amounts of sediment and water. But a deeper understanding is needed, and there are at least two plausible interpretations of the observations. First, the headwater regions yield almost all of the

sediment transported downstream, and channels and slopes in downstream areas contribute very little sediment. Second, while large amounts of sediment are contributed to rivers from steep headwaters, high runoff rates and sediment yields produced in headwaters lead to channel instability and substantial channel erosion downstream, which contributes to river sediments loads. Whatever the explanation and it is like to differ between catchments, high sediment yields in headwaters are accompanied by high yields downstream.

The power functions for the seven global sets of sediment yield data account for between 70 and 82% of the variance of yield. Catchment area is a surrogate for river discharge, although Milliman and Syvitski show that discharge does not correlate strongly with sediment yield implying that yield is controlled more by sediment supply than transport capacity. The residual variance not accounted for by the power functions is therefore likely to relate to supply, and the most plausible parameters, following Phillips' (1990) global analysis, are slope, runoff and rainfall erosivity. Phillips used a stream power model to assess the contribution to soil loss of the factors identified in the Universal Soil Loss Equation and similar soil erosion models. Soil shear strength (erodibility), surface roughness (a result of land management and landscape properties), and slope length account for less than 0.5% of the variance of soil loss. Land use, as a surrogate for land management, may not therefore be a significant variable globally when only a single time period is analysed and sheet and rill erosion alone are considered.

The conclusion about land use is not supported, however, when yields from both disturbed and undisturbed catchments are analysed together. Mozzherin (1994) separated disturbed and undisturbed (or little disturbed) temperate zone catchments and showed that the difference in mean annual yield of the former is about 21 times the latter for catchments $<1000km^2$ in area, and falls to a factor of 5 for catchments $>25,000km^2$ because of sediment storage, particularly on floodplains in large catchments.

Coherent patterns of yields from headwaters to catchment outlets occur globally, identifying an emergent property that warrants deeper understanding. Phillips (1990) has shown the utility of a simple stream power model in disentangling controls on soil loss, analogous in approach to the Vollenweider model. The empirical analysis by Milliman and Syvitski has successfully discriminated regions of coherent variation of SY and A in catchments varying in size by seven orders of magnitude, relying only upon surrogates for discharge (catchment area) and gradient (elevation class).

This is consistent with the formulation used by Sinclair and Bell (1996) to simulate drainage network evolution, where local erosion and sediment transport in a section of river can be described by using only A and S. This local erosion law has been used, in conjunction with suitable topographic rules, to simulate Horton's power law distributions of stream branching.

Sediment budgets – regional patterns

Wasson (1994) showed that coherent relationships between SY and A can be defined for different regions of Australia, analogous to those defined globally by Milliman and Syvitski. Eight power functions were defined, for large parts of the country, accounting for between 79 and 97% of sediment yield variance. The intercepts of the equations (Equation 1) are not straightforwardly a function of elevation as they are globally (Equation 2). They are also not a function of any single variable, such as soil erodibility or rainfall erosivity.

By combining rainfall erosivity (the R factor of the USLE, taken from Rosewell, 1997) erodibility class (Rosewell, 1997), and relief class of Milliman and Syvitski (MS), the intercepts (c) in (Equation 1) can be accounted for as follows:

$$\text{Logc} = \log 4.69 + 2.15 \times 10^{-4} 1 \quad (3)$$

$$\text{where } 1 = \text{R.K.MS} \quad (4)$$

This analysis includes the majority of the yield regions defined by Wasson (1994), excludes regions 6 and 11 because they are not well defined statistically, and also excludes region 10 (arid Australia) and region 4 (Murray-Darling Lowlands) because they appear to conform to a relationship different from that in (3). Equation (3) therefore accounts for most Australian data ($r^2 = 0.87$) in the lowland, highlands and mountain categories of Milliman and Syvitski.

The terms of (Equation 3) and (Equation 4) are set out in Table 1, from which it is evident that the intercept (c) does not vary systematically with any individual independent variable. The highest value of c (Darling Downs) is not paired with the highest value of R, occurs in the highland category (not mountains category), but is correlated with the highest soil erodibility. The Darling Downs is an area of highly erodible black earth soils, is intensively cultivated, and experiences moderately high erosivity. By contrast, the lowest value of c (Adelaide Hills) is an area of lowlands (despite its name) with higher than average erodibility but the lowest erosivity.

This example of regional patterns in SY, a key term in any sediment budget, shows that soil and rainfall properties are more important than they appear to be where data are aggregated globally. Phillips (1990) came to the same conclusion in his analysis of factors controlling soil loss on hillslopes. Unlike the global patterns, discharge (in the form of A) and gradient are not sufficient to account for the patterns seen in the Australian data (cf. Wasson, 1994). Nonetheless, Equations (3) and (4), while largely empirical, have considerable explanatory power and a minimum number of parameters.

Another approach to analysing regional (and local) patterns of sediment budgets has been developed by De Ploey (1990). Using the ratio of volume of eroded sediment/input of energy or geomorphic work, De Ploey defines erosional susceptibility as follows:

$$E_s = \frac{V_e}{A.P.g(horRS/2)} \quad (5)$$

Where *Es* is an erodibility coefficient (s^2/m^2), *Ve* is the volume (or mass) in m^3 of soil eroded over a surface area A (m^2), P is total volume of precipitation per m^2 during a period t, g is gravitational acceleration, h is the elevation head loss (m) corresponding to mean depth over which Ve was removed, R is the hydraulic radius (depth in m) of overland flow, and S is representative gradient. The term g.R. S/2 is equivalent to U_o^2, where U_o^2 is proportional to flow shear stress. The general expression (Equation 5) is modified for different processes, such as sheet and rill erosion, gullying, landsliding, and creep (De Ploey et al., 1995).

This formulation focuses on yield, as in other examples discussed earlier, and depends on a few easily determined parameters. P, rather than a more usual erosivity measure such as R in the USLE, is used by De Ploey et al. (1995) because all rainfall affects the soil vegetation system by generating resistance to erosion in the form of vegetation and soil organic matter, and by driving erosion. This is particularly important for long term values of Es. Es is, therefore, a measure of an emergent property produced by the interaction of rainfall, soil and geomorphic processes. Es has characteristic values for different soil-vegetation regions and land use, so it is not dependent solely on natural (ie non-human) phenomena.

Table 1 Relationships between sediment yield and catchment area for different regions of Australia

Region	Average rainfall erosivity	Erodibility class K	MS	I	C
2. Darling Downs	2500	4	2	20,000	480
5. Sub-humid Central and Northern Queensland	2400	3.5	2	16,800	248
9. Ord River	2500	3	2	15,000	96
1. Southern Uplands	1240	3	3	11,160	33
8. Monsoonal Northern Territory	3750	2.5	1	9,375	17
12. Adelaide Hills	625	3	1	1,875	13

R – in SI units [MJ.mm/(ha.h.y)]
K – soil erodibility class (1 low, 4 high)
MS – elevation class: 1, lowlands: 2, highlands; 3, mountains
I – R.K.MS
C – intercept in equation (1) at A = 1 x 10^6km^2

Values of Es compiled by De Ploey et al. (1995) range between 5 x 10^{-1} and 1 x 10^{-7} s^2/m^2. Landslides/debris flows have Es values between 5 x 10^{-3} and 5 x 10^{-1} s^2/m^2, rill and interill erosion has Es values between 1 x 10^{-4} and 1 x 10^{-2} s^2/m^2, gullies have values between 1 x 10^{-6} and 1x 10^{-4} s^2/m^2, and creep has values between 1 x 10^{-7} and 1 x 10^{-6}s^2/m^2.

Globally, therefore, landslides and debris flows most efficiently convert energy into sediment production, followed by rill and interrill erosion, gullying and creep. This conclusion is strongly moderated by particular settings, so that, in any particular catchment, soil characteristics, land use/management, and gradient affect the range of values of Es.

Sediment budgets – local patterns

By local is meant individual catchments, but there is considerable overlap with regional patterns. Also aggregation from local to global scale is possible as demonstrated with values of Es and the relative geomorphic efficiency of eroding processes. The role of individual sediment producing processes is of greater significance at the catchment scale than at regional or global scale.

Sediment producing processes can be thought of as occurring at or between three end members: landsliding/debris flows, sheet and rill erosion, and channel erosion. This classification excludes glacial systems. Examples of catchments dominated by each of the end-members are given by: Oguchi (1996), for landslide/debris flow systems in Japan, and other circum-Pacific temperate regions of high relief and frequent rainstorms; Trimble (1983) for sheet and rill erosion systems in the MidWest of the USA; and Wasson et al. (1998) for channel erosion systems in southeastern Australia. Usually only small catchments are dominated by landsliding and debris flows.

Following Phillips (1991), catchment sediment yield (SY) for any size catchment (A), over a time period t, is given by:

$$SY = P_t A\, D_{r,t} D_{l,t}\, D_{c,t} \qquad (6)$$

where P_t is average sediment production (or erosion) rate, D_r is the ratio of sediment reaching stream channels to total hillslope sheet and rill erosion, D_l similarly for landslides/debris flows, and D_c similarly for channel erosion. The product D_{rt}. D_{lt}. D_{ct} is the catchment sediment delivery ratio (SDR), or the ratio of yield to total erosion. Equation (6) is a useful way of examining SY and SDR, two high level properties of a catchment. Most values of the

SDR are <1.0, showing that sediment is stored between sediment producing areas and the point of yield. But there is little local information content in the SDR, particularly about where the sediment is stored.

Sediment production (Pt) is distributed between yield, colluvial storage (Sc), and alluvial storage (Sa):

$$S_{c,t} = (1 - D_{s,t})\ (1\text{-}D_{l,t})\ P_t A \quad (7)$$

$$S_{a,t} = (1 - D_{c,t})\ P_t\ A\ D_s\ D_{lt} \quad (8)$$

Equations (6-8) have been applied by various authors (e.g., Phillips, 1991; Reid and Dunne, 1996) to estimate the system state of various catchments where observations of sediment production, storage and yield have been made. The partial summaries of existing sediment budgets in Phillips (1991) and Reid and Dunne (1996) show that most fall between the end-members defined earlier, although where landslides/debris flows are common they dominate the sediment budget; perhaps because this process of sediment production is, according to De Ploey's Es, the most efficient.

The allocation of sediment between the various components of Equations (7 and 8) changes through time. Change is: in response to catchment management (eg soil conservation, logging – Trimble, 1983; Roberts and Church, 1986); is the inexorable result of processes triggered by initial human disturbance (Wasson et al., 1998); and the result of climate change. While poorly documented in existing sediment budgets, it is likely that the contribution by various sediment producing processes also changes through time. As Phillips (1991) observes, the '….basic sediment budget should be understood to represent a "snapshot" valid for a particular period of time and representing a spatial average of its contributing hillslopes and tributary basins' (p. 233).

While sediment budgets and the SDR are high level properties of catchments, and so are of great interest in the context of this paper, they are poorly understood. Attempts to model the SDR rely upon correlations with morphometric measures. For example, ASCE (1975) suggests a power function relationship:

$$\text{LogSDR} = b\ \text{log}A + \text{log}k \quad (9)$$

where b generally lies between –0.01 and –0.25. This relationship, derived for the USA, is unlikely to be globally applicable. For example Dedkov and Mozzherin (1984) document cases where b is positive. Other investigations of the SDR include a study by Roehl (1962) in which the SDR was found to depend on A, stream length, relief-length ratio, and the bifurcation ratio. Roehl worked in an area of the USA where sheet and rill erosion dominate the sediment budget, while Mou and Meng (1980), working in part of China where gully erosion is an important source, showed that the SDR is directly controlled by gully density.

Walling (1983) stresses the limitations of the SDR, a spatially and temporally lumped parameter, which fails to reproduce the distributed and time-varying nature of erosion and sediment transport. To Richards (1993), this suggests that process models such as TOPMODEL are required. But Richards also argues for greater use of network density and hillslope – channel connectivity to understand SDRs. The linkage between SDRs and the spatial structure of catchments therefore appears to be a useful path for catchment scale modellers. It is thereby hoped to understand, more completely, observations like those by Ichim (1997), who demonstrated differing relationships between SDR and stream order depending on the relative erodibility and runoff rates of catchments.

The dominance of landslides/debris flows in some sediment budgets is understood to relate to hillslope gradient and soil thickness. Oguchi (1996) showed that in the Japanese mountains, annual sediment yield from a catchment is directly proportional to the volume of slope failure triggered by a single storm. Also, both the volume of slope failure and sediment yield per unit area are power functions of hillslope gradient. Without sufficient soil, the

relationship between yield and volume of slope failure would change through time, and there is no evidence of this in Oguchi's data, although his time series may not be long enough to show such an effect.

The boundary between catchments (or parts of catchments) dominated by landslides/debris flows and other sediment producing processes is not rigorously known. Equally, the reasons for some catchments being dominated by sheet and rill erosion while others are dominated by channel erosion are not clear. The relative erosion rate of hillslopes and valley floors is a likely key factor, and so the erodibility of surface hillslope soils and both surface and subsurface valley bottom soils, requires attention. Here again is a field ripe for systematic observations and modelling.

Conclusions

The current widespread re-evaluation of approaches to the analysis and modelling of natural systems is one that must be taken seriously by those modelling erosion and sediment transport at catchment scales. A focus on emergent properties of catchments immediately lifts the modeller's gaze above the detail of low level process, and demands attention to high level properties of the kind that need to be understood if catchment management is to be effective. Ecologists have, to some degree, shown the way, and physicists and others are beginning to develop a science of meta-rules.

Geomorphologists concerned with the spatial arrangements of catchments, and with their operation through time, have traditionally dealt with emergent properties. A fascination for detailed process studies did, for a time, divert attention away from high level properties to the muddle of processes from which order emerges. But now, with increasing interest in top-down analysis, the geomorphology of catchments should be a major interest of modellers.

The examples given in this paper of the value of high level properties are drawn from sediment budgets, although they involve aspects of spatial ordering and temporal change. There are many other high level properties of catchments that could have been discussed and which warrant attention by modellers. Among them are: the statistical properties of drainage networks as they move from a pre to a post disturbance state; the stoichiometry and partitioning of nutrient and carbon between organic and inorganic components of catchments; the distribution of roughness elements in catchments; and types of temporal responses to perturbations. There is much to be conceptualised and modelled.

Bibliography

ANDERSON, P.W (1972) 'More is different'. Science, 177, p. 393-396.

ASCE (1998) Sedimentation engineering, Amer. Soc. Civil Engineers, Manuals and Reports on Engineering Practice, No. 54, Am. Soc. Civ. Eng., New York.

BAK, P.; C. TANG and K. WIESENFELD (1987) 'Self-organised criticality: an explanation of 1/*f* noise'. Phys. Rev. Letters, 59, p. 381-384.

BAK, P (1997) *How nature works*. Oxford University Press, 212 p.

CHORLEY, RJ.; S.A. SCHUMM and D.E. SUGDEN (1984) *Gomorphology*. Methuen, London, 589 p.

DEDKOV, A.P. and V.I. MOZZHERIN (1984) *Erosion and sediment yield on the Earth.* Kazan University Press (in Russian).

DE PLOEY, J. (1990). 'Modelling the erosional susceptibility of catchments in terms of energy'. Catena, 17, p. 175-183.

DE PLOEY, J.; J. MOEYERSONS and D. GOOSSENS (1995) 'The De Ploey erosional susceptibility model of catchments'. Es. Catena, 25, p. 269-314

GOLDSTEIN, J. (1999) 'Emergence as a construct: history and issues'. Emergence, 1 (1), p. 49-72.

HADLEY, R.F. and S.A. SCHUMM (1961) 'Sediment sources and drainage basin characteristics in Upper Cheyenne River basin'. US Geol Survey Water Supply Paper, 1531, p. 135-198.

HARRIS, G. P. (1997) 'Algal biomass and biogeochemistry in catchments and aquatic ecosystems: scaling of processes, models and empirical- tests'. In A. Howard (ed.), *Algal modelling: processes and management*. Hydrobiologia, 349, p. 19-26.

HARRIS, G. P. (1998) 'Predictive models in spatially and temporally variable freshwater systems'. Aust J Ecol., 23, p. 80-94.

ICHIM, I. (1990). 'The relationship between sediment delivery ratio and stream order: a Romanian case study'. In: *Erosion, transport and deposition processes* (Proc. Jerusalem Workshop, 1987). IAHS Publ. No 189, p. 79-86.

KAUFFMAN, SA, (1993) *The origins of order: self-organisation and selection in evolution*. Oxford Univ. Press, New York.

MILLIMAN, J.D. and J.P.M. SYVITSKI (1992) 'Geomorphic/tectonic control of sediment discharge to the ocean: the importance of small mountains and rivers'. J. Geol., 100, p. 525-544.

MOU, J and Q. MENG (1980). Sediment delivery ratio as used in the computation of the watershed sediment yield. Chinese Soc. Hydraulic Eng., Beijing.

MOZZHERIN, V.I. (1994) *Geomorphological analysis of river solids discharge: plains of temperate regions*. DSc Dissertation, Kazan University. (in Russian).

ODUM, E.P., (1971) *Fundamentals of ecology (Third Edition)*. Saunders, Philadelphia.

OGUCHI, T (1996). 'Hillslope failure and sediment yield in Japanese regions with different storm intensity'. Bull. Dept Geog., Univ Tokyo, 28, p. 45-54.

O'SULLIVAN, P.E. (1979) 'The ecosystem-watershed concept in the environmental sciences - a review'. Intern. J. Envir. Studs., 13, p. 273-281.

PHILLIPS, J.D (1990) 'Relative importance of factors influencing fluvial soil loss at the global scale'. Amer. J. Sci., 290, p. 547-568.
PHILLIPS, J.D. (1991) 'Fluvial sediment budgets in the North Carolina Piedmont'. Geomorphology, 4, p. 231-241.
PHILLIPS, J. D. (1995) 'Self-organisation and landscape evolution'. Progress in Physical Geography,19, p. 309-321.
PHILLIPS-HOWARD, K.D. (1985) 'The anthropic catchment-ecosystem concept: an Irish example. Human Ecology, 13, p. 209-240.
REID, L. M. and T. DUNNE (1996) *Rapid evaluation of sediment budgets*. Geoecology Paperback, Catena Verlag, Reiskirchen, Germany, 164 p.
RICHARDS, K.S. (1993) Sediment delivery and the drainage network. In: K. Bevan and M.J. Kirkby (eds.), *Channel network hydrology*, p. 221-254, Wiley, Chichester.
ROBERTS, R.G and M. CHURCH (1986) 'The sediment budget in severely disturbed watersheds Queen Charlotte Ranges, British Columbia'. Can. J. For. Res., 16, p. 1092-1106.
ROEHL, E.J. (1962) 'Sediment source areas, delivery ratios and influencing morphological factors'. IAHS Publ. No. 59, p. 202-213.
ROSEWELL, C.J. (1997) 'Potential sources of sediments and nutrients: sheet and rill erosion and phosphorus sources'. Australia, State of the Environment. Tech. Paper Series (Land and Waters), DEST, Canberra.
SINCLAIR, K and R.C. BALL (1996) 'Mechanism for global- optimisation of river networks from local erosion rules'. Phys. Rev. Letters, 76 (18), p. 3360-3363.
STIGEBRANDT, A and F. WULFF (1987) 'A model for the dynamics of nutrients and oxygen in the Baltic proper'. J. Mar Res., 45, p. 729-759.
TRIMBLE, SW. (1983) 'A sediment budget for Coon Creek, the Driftless Area,Wisconsin, 1853-1977'. Amer. J. Sci., 283, p. 454-474.
WALLING, D.E. (1983) 'The sediment delivery problem'. J. Hydrol., 65, p. 209-237.
WASSON, R.J. (1994) 'Annual and decadal variation of sediment yield in Australia, and some global comparisons'. In: *Variability in stream erosion and sediment transport* (Proc. Canberra Symposium) IAHS Publ. No. 224, p. 269-279.
WASSON, R.J.; R.K. MAZARI; B. STARR and G. CLIFTON (1998) 'The recent history of erosion and sedimentation on the Southern Tablelands of Southeastern Australia: sediment flux dominated by channel incision'. Geomorphology .

Soil erosion by water prediction technology developments in the United States

D. C. Flanagan, M. A. Nearing, and L. D. Norton
USDA-ARS National Soil Erosion Research Laboratory,
West Lafayette, IN 47907-1196, USA

Introduction

Soil erosion by water continues to be a serious problem throughout the world. Development of improved soil erosion prediction technology is required to provide conservationists, farmers and other land users with the tools they need to examine the impact of various management strategies on soil loss and sediment yield and plan for the optimal use of the land. Additionally, soil erosion prediction technology allows policymakers to assess the current status of the land resource and the potential need for enhanced or new policies to protect soil and water resources. Erosion prediction is most needed by conservationists at the field level who work directly with farmers and other land users, which has large implications for development and adoption of this technology.

Within the United States, work began in the mid-1980s on two erosion prediction technology efforts. The first was development of a physical process-based erosion simulation model that would provide both temporal and spatial estimates of soil loss within small watersheds and for hillslope profiles within small watersheds. This effort later became known as the Water Erosion Prediction Project (WEPP). The second effort was aimed at rapidly developing an updated replacement for the empirically-based Universal Soil Loss Equation (USLE) that could be used as an intermediate product for erosion estimates on hillslope profiles during the longer period required for the development, parameterization, and validation of the process-based simulation model. Eventually the update to the USLE became known as the Revised Universal Soil Loss Equation (RUSLE), and ultimately was developed as a program for use on personal computers as well.

This paper will discuss RUSLE and WEPP model development, components and current status. We will also provide information on current activities to develop common interfaces and databases for the RUSLE, WEPP, WEPS (Wind Erosion Prediction System), and RWEQ (Revised Wind Erosion Equation) models.

The water erosion prediction project

Model development history

Work on the process-based WEPP model began in 1985 and the project was led by Dr. George R. Foster, USDA-ARS (United States Department of Agriculture - Agricultural Research Service), National Soil Erosion Research Laboratory (NSERL), West Lafayette, Indiana. The major cooperating agencies at that time were the USDA-ARS, USDA-Natural Resources Conservation Service (NRCS), USDA-Forest Service (FS), and United States Department of the Interior (USDI) - Bureau of Land Management (BLM). Initial project efforts created a Core Team of scientists and user agency representatives to be responsible for development, testing, experimental parameterization studies, and validation of the various process model components and the model as a whole. The scientists and users worked together to develop a set of User Requirements (Foster and Lane, 1987) that documented the ways in which the model was to be applied, model functionality, and science to be included. The User Requirements provided the direction for the model development and experimental parameterization studies. During 1985-1987, Dr. Foster developed the initial Fortran model framework and erosion component for the WEPP computer program that would be used as a foundation for all subsequent work on model code development. Dr. Leonard J. Lane assumed the duties of WEPP Project Leader in 1987 following Dr. Foster's departure from ARS, and model programming efforts transferred to the USDA-Southwest Watershed Research Center in Tucson, Arizona.

From 1987-1989 all of the necessary components (hydrology, plant growth, water balance, etc.) required to conduct a continuous hillslope profile erosion simulation were incorporated into the WEPP code, with the ARS-Tucson group leading the model code development and the individual scientists on the WEPP Core Team providing components to that group.

During 1987-88 a set of rainfall simulation experiments were conducted on 33 important cropland soils to obtain baseline soil erodibility parameters for WEPP (Elliot et al., 1989). Dr. John M. Laflen led this effort in which interrill erodibility, rill erodibility, and critical hydraulic shear stress were determined for soils in a freshly-tilled condition having minimal plant residues. In addition to runoff, sediment, and flow topography measurements, a complete set of tests on each site's soil physical and chemical properties were conducted to allow examination of relationships between the erodibility parameters and soil properties.

A similar set of rainfall simulation experiments were conducted in 1988-89 on a group of rangeland soils (Simanton et al., 1991). Since rangeland conditions do not include tillage disturbance, these experiments measured the impacts of plant cover by taking measurements on clipped and unclipped plot conditions. Interrill erodibility, rill erodibility, and critical hydraulic shear stress were computed using optimization techniques developed by Nearing et al. (1989).

Dr. John Laflen was named WEPP leader in August 1989. Also at that time a prototype of the WEPP model (Lane and Nearing, 1989) that could be applied to hillslope profiles was delivered to ARS, NRCS, FS, and BLM at a special meeting in Lafayette, Indiana. This version of WEPP (v89) was able to perform a continuous simulation of simple cropping situations. However, it did not include all required components, including non-uniform hydrology, winter processes or irrigation. Additionally, v89 did not include the components necessary to conduct small watershed simulations with runoff and sediment routing from hillslope profiles to channels and impoundments. This version was run from the DOS command line using ASCII input files, and a climate generator was available to create the daily weather input file. There were also

some very early file builder programs provided to assist in creating the slope, soil, and management input files for the model, but no overall interface program was available.

Work continued from 1990 through 1994 on development of the WEPP hillslope model. Non-uniform hydrology down a slope profile was incorporated into the model in 1990, and this also required significant enhancement to the erosion component. The ability to simulate fixed sprinkler and furrow irrigation was added to the model during this time (Kottwitz, 1995). Winter processes of frost and thaw development, snow accumulation and melting were incorporated into WEPP during 1990-91 with computations initially on a daily basis, and then later on an hourly basis during 1993-94 (Savabi et al., 1995). Major changes to both the cropland plant growth components and the residue decomposition components were also made in 1990-91. EPIC (Williams, 1995) plant growth functions were incorporated for cropland, and decomposition day theory was used for residue decomposition predictions for cropland (Stott et al., 1995). Representatives of the 5 agencies then involved in WEPP developed a coding convention. Also, a systematic model recoding effort converted the majority of the Fortran model code to an accepted standard during 1991-1994, with the goal of improving model maintainability, performance, and stability.

A complete interface program was developed during 1991-95 to assist users in creating the input files for the model, as well as organizing simulation runs. The main purpose of this program was initially to assist scientists developing and testing model components, as well as conducting validation studies (Flanagan et al., 1994). A hillslope interface became publicly available in 1994, followed by a watershed interface in 1995. The interface programs were DOS-based, and contained mainly text input screens, with some graphical data input and model output viewing capabilities. Users could set up groups of model simulation scenarios to reuse at later times, and could edit any WEPP model inputs.

Expansion of the WEPP program to allow simulation of small watersheds began in 1991. Many of the channel routing routines in the CREAMS (Knisel, 1980) model were directly used within WEPP, and modified and improved as necessary (Ascough et al., 1995; Ascough et al., 1997; Baffaut et al., 1997). A new component to predict sediment deposition in impoundments was also developed (Lindley et al., 1995).

Model infiltration parameterization studies were conducted during 1993-94, using the USLE natural runoff plot database information available at the NSERL. This work resulted in equations and procedures to accurately estimate baseline effective hydraulic conductivity from soil properties (Risse et al., 1994) and adjustments to these baseline values for cropped conditions (Zhang et al., 1995a, 1995b). WEPP could now be used with the baseline equations and soil property information to make good uncalibrated predictions of runoff volumes.

Validation studies on WEPP hillslope model performance were conducted from 1993-95, largely using information from the USLE natural runoff plot database stored at the USDA-ARS National Soil Erosion Research Laboratory (Zhang et al., 1996). Additional results on WEPP watershed model performance with data from small experimental watersheds were reported in 1997 (Liu et al., 1997). The overall results of these and other studies have shown the model predictions to adequately represent observed runoff and sediment yield data for a majority of locations both within and outside the U.S. Some problem areas that were identified were winter processes and erosion prediction in the Palouse (McCool et al., 1998), as well as furrow irrigation predictions in southern Idaho (Bjorneberg et al., 1997).

The complete WEPP model for hillslope and channel applications, model documentation (Flanagan and Nearing, 1995; Flanagan and Livingston, 1995), interfaces, training materials, and hillslope validation data sets and results were delivered to ARS, NRCS, FS, and BLM in a special WEPP/WEPS Symposium held in Des Moines, Iowa in July 1995.

Since 1995, the project has been in a maintenance and implementation phase, with major work in development of improved user interfaces and databases, and minimal work on development of expanded scientific components. A major impediment to acceptance of the model by field NRCS users was lack of sufficiently easy-to-use interfaces. To address this need, work began in 1996 on development of a computer interface for field conservation users, which would be developed initially for Windows™ 95/98/NT platforms. A prototype Beta version (Flanagan et al., 1998) was released in April 1998 for testing by NRCS and others. This version allowed full hillslope simulations, but did not include watershed functionality or contain all management editing functions. A Beta-2 version of the interface was released in January 1999 for further in-house testing, and a Beta-3 version was released for public testing and feedback in May 1999. The Beta-3 version was fully functional for WEPP hillslope profile simulations and management editing, and also contained simple watershed functionality (single channel and up to three hillslopes). Additional work is continuing on creating a fully functional watershed Windows™ interface, with an evaluation version planned for early 2000.

Three areas of current work on WEPP model science testing and enhancement are winter hydrology, furrow irrigation, and impoundment simulations. These efforts are being conducted through cooperative efforts with ARS scientists in Pullman, Washington and Kimberly, Idaho,

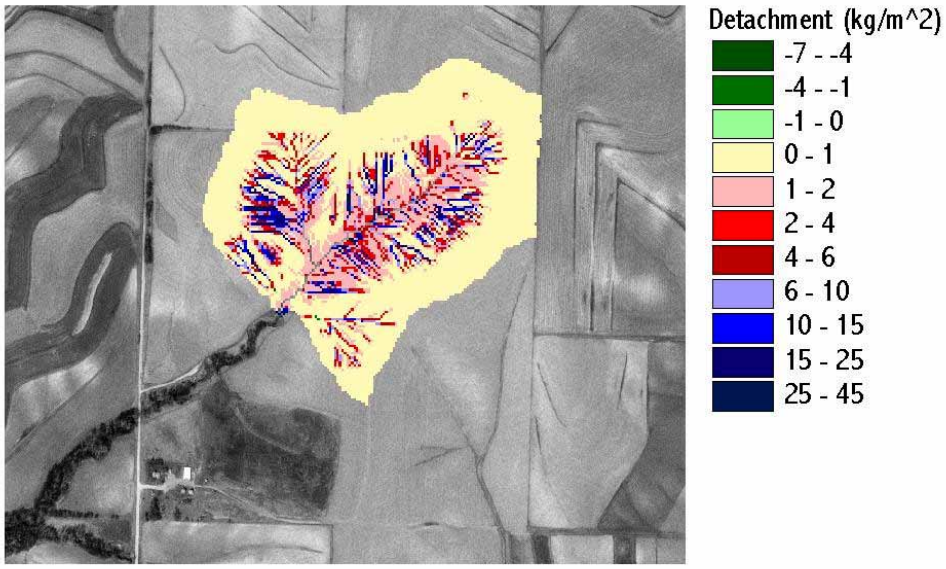

Fig. 1 The WEPP model was applied to thousands of flowpaths within this watershed in Treynor, Iowa using digital elevation data and a GIS (Cochrane and Flanagan, 1999). Average annual rates of soil detachment and deposition are depicted spatially, using results from the WEPP model simulations

and FS scientists in Moscow, Idaho, respectively. An initial stage of the impoundment component enhancement has been completed, and suggested changes are currently being evaluated and incorporated into the official WEPP model code. Improvements to the WEPP winter component should be complete by early 2001. Additional testing of the WEPP furrow irrigation routines across a range of typical locations and soils in the U.S. are planned in 2000 to determine if changes may be required in the model sediment transport relationships for these low slope and low flow conditions.

Other efforts at the NSERL have focused on linkage of the WEPP watershed model with Geographic Information Systems (GIS). Recent work has developed procedures and interfaces to automatically delineate watershed boundaries, channels, hillslope regions, and representative slope profiles from Digital Elevation Model (DEM) data. This work has shown that automatic techniques can be successfully used to rapidly set up accurate WEPP model simulation topographic inputs, potentially reducing the work required of users conducting watershed simulations (Cochrane and Flanagan, 1999). Future efforts will attempt to transfer the research findings and software to the Windows™ interface programs.

The WEPP team is also working with the Wind Erosion Prediction System (WEPS) modeling group in a joint effort to ultimately develop a single process-based model that can be used for either water or wind erosion simulations. This common model would assure that all computations related to hydrology, water balance, crop growth, residue decomposition, effects of tillage, etc. would be identical for the wind or water simulations when applied with the same slope, soil, management, and climate. This consistency between predictions is very important for action agencies (for example, NRCS) that plan to apply both models in conservation planning activities. Plans are to develop a common wind and water model by the end of 2001.

WEPP model components

WEPP is a continuous simulation model, and can use either observed or generated climatic inputs to drive the runoff and erosion processes. The CLIGEN (Nicks et al., 1995) weather generator was developed specifically to create daily climate inputs for WEPP, based upon long-term weather station statistics. CLIGEN has a database of over 1300 weather stations in the United States.

Critical components of WEPP are the infiltration and runoff computations. A Green-Ampt Mein-Larson model (Mein and Larson, 1973) as modified for unsteady rainfall (Chu, 1978) is used to predict the cumulative infiltration depth. Depressional storage is estimated as a function of random roughness and slope steepness (Onstad, 1984). When rainfall rate exceeds the infiltration rate, rainfall excess begins to be computed. Runoff is the total rainfall excess minus any reduction due to the surface depressional storage (Stone et al., 1995).

Peak runoff rate is a very important parameter in WEPP, as it is used in calculations to estimate flow depth and ultimately flow shear stress. WEPP uses either a semi-analytical solution of the kinematic wave model (Stone et al., 1992) or an approximation of the kinematic wave model to determine the peak runoff rate (Stone et al., 1995). Runoff rate, rill roughness and rill channel characteristics are used with the Darcy-Weisbach equation to estimate flow depth and hydraulic radius. Flow shear stress is computed as the product of the weight density of water times the hydraulic radius times the sine of the average slope profile angle (Foster et al., 1995). Shear stress is partitioned between that acting on the soil and that acting on various roughness elements through use of the Darcy-Weisbach friction factor values (Gilley and Weltz, 1995). Sediment transport capacity is computed using a simplified function of shear stress raised to the 3/2 power, times a coefficient that is determined through application of the Yalin (1963) equation at the end of the slope profile (Finkner et al., 1989).

The WEPP model uses a steady-state sediment continuity equation to predict sediment load down a hillslope profile:

$$\frac{dG}{dx} = D_f + D_i \tag{1}$$

where G is sediment load ($kg \cdot s^{-1} \cdot m^{-1}$), x is distance downslope (m), D_f is rill erosion rate ($kg \cdot s^{-1} \cdot m^{-2}$), and D_i is interrill sediment delivery rate ($kg \cdot s^{-1} \cdot m^{-2}$) (Foster et al., 1995).

Interrill sediment delivery to rills is predicted in WEPP using the following equation:

$$D_i = K_{iadj} I_e \sigma_{ir} SDR_{RR} F_{nozzle} \frac{R_s}{w} \tag{2}$$

where K_{iadj} is the adjusted interrill erodibility factor ($kg \cdot s \cdot m^{-4}$), I_e is effective rainfall intensity ($m \cdot s^{-1}$), σ_{ir} is the interrill runoff rate ($m \cdot s^{-1}$), SDR_{RR} is a sediment delivery ratio that is a function of random roughness, row side-slope and the interrill particle size distribution, F_{nozzle} is an adjustment factor to account for sprinkler irrigation nozzle impact energy variation, R_s is the rill spacing (m), and w is the rill width (m).

Rill erosion rate may be either positive in the case of detachment or negative in the case of deposition. Rill detachment in WEPP is predicted when the flow sediment load is below transport capacity, and flow shear stress acting on the soil exceeds critical shear stress. In that case, D_f is predicted with:

$$D_f = K_{radj}(\tau - \tau_{cadj})(1 - \frac{G}{T_c}) \tag{3}$$

where K_{radj} is the adjusted rill erodibility factor ($s \cdot m^{-1}$), τ is flow shear stress (Pa), τ_{cadj} is adjusted critical shear stress of the soil (Pa), G is sediment load in the flow ($kg \cdot s^{-1} \cdot m^{-1}$), and T_c is flow sediment transport capacity ($kg \cdot s^{-1} \cdot m^{-1}$).

Deposition in rills is predicted when flow sediment load exceeds transport capacity. In this case the model predicts the rill erosion rate using:

$$D_f = \frac{\beta v_{eff}}{q}(T_c - G) \tag{4}$$

where β is a raindrop-induced turbulence factor, v_{eff} is an effective fall velocity for the sediment ($m \cdot s^{-1}$), q is flow discharge per unit width ($m^2 \cdot s^{-1}$), and T_c and G are as previously defined. β is currently assigned a value of 0.5 for rain impacted flows, and a value of 1.0 for other cases such as snow melt or furrow irrigation erosion.

Other model components include a soil component to adjust roughness, infiltration, and erodibility parameters as affected by tillage and consolidation (Alberts et al., 1995), a plant growth component to provide daily values of crop canopy, biomass, and plant water use (Arnold et al., 1995), and a daily water balance to determine the impacts of soil evaporation, plant transpiration, infiltration, and percolation on soil water status (Savabi and Williams, 1995). Crop residue levels are also updated daily, with adjustments for decomposition as well as the impacts of tillage or other management operations (Stott et al., 1995). WEPP contains components to estimate frost, thaw and snow depths, as well as snow melt runoff in regions that experience freezing temperatures (Savabi et al., 1995). Additionally, the model can be used to determine the impact of furrow and sprinkler irrigation on soil erosion (Kottwitz, 1995).

In watershed applications, WEPP allows simulations of groups of hillslopes, channels, and impoundments. Daily water balance, plant growth, and soil and residue status for channels are predicted identically to that on hillslopes. Channel peak runoff rates are predicted using either a modified Rational Equation similar to that in the EPIC (Williams et al., 1995) model, or the CREAMS (Smith and Williams, 1980) peak runoff equation. Channel erosion is estimated using a steady-state sediment continuity equation:

$$\frac{dq_{sed}}{dx} = D_L + D_F \tag{5}$$

where q_{sed} is the sediment load in the channel ($kg \cdot s^{-1} \cdot m^{-1}$), x is distance down the channel (m), D_L is lateral inflow of sediment along the channel ($kg \cdot s^{-1} \cdot m^{-2}$), and D_F is detachment or deposition by flow in the channel ($kg \cdot s^{-1} \cdot m^{-2}$) (Ascough et al., 1995). For a channel in an active detachment mode that has not reached a nonerodible layer, a rectangular channel is assumed and the erosion rate is:

$$E_{ch} = w_c K_{ch} (\tau_{ave} - \tau_{cr}) \tag{6}$$

where E_{ch} is the soil loss per unit channel length ($kg \cdot s^{-1} \cdot m^{-1}$), w_c is channel width (m), κ_{ch} is a channel erodibility factor ($s \cdot m^{-1}$), τ_{ave} is average channel flow shear stress acting on the soil (Pa), and τ_{cr} is critical shear stress of the channel soil (Pa). See Foster et al. (1980) for equations describing detachment and channel widening after a nonerodible layer is reached.

If sediment load of all particle types is larger than flow sediment transport capacity, then sediment deposition in the channel is predicted using:

$$D_F = \frac{v_f}{q_w} (T_c - q_{sed}) \tag{7}$$

where v_f is particle fall velocity ($m \cdot s^{-1}$), q is flow discharge per unit width ($m^2 \cdot s^{-1}$) and T_c is channel flow sediment transport capacity ($kg \cdot s^{-1} \cdot m^{-1}$). For cases in which sediment load is near transport capacity, shifting of transport capacity from particle classes with excess to those with a deficit is predicted, as described in detail by Ascough et al. (1995) and Foster et al. (1980).

Current status and activities

The WEPP project leader is Dr. Dennis Flanagan, who assumed lead scientific and administrative duties in April 1999. Current WEPP model staff at the USDA-ARS National Soil Erosion Research Laboratory consists of two agricultural engineers (Dennis Flanagan and John Laflen), and two computer specialists (Charles Meyer and Jim Frankenberger). Additional programming support is provided through cooperative agreements with Purdue University.

WEPP activities are currently in five major areas. The highest priority task is development of improved interfaces for application of the watershed and hillslope models. This task involves work on both stand-alone interfaces unique to WEPP, as well as development work on a common interface to run WEPP, WEPS, RUSLE, or RWEQ (see section on MOSES below). A WEPP watershed Windows™ interface is almost complete, and plans are to explore other interface options, including a Web browser-based interface. The project computer specialists are also significantly involved in the development of the MOSES common interface. The second major area is partnering with other scientists to improve certain components of the model scientific code, as discussed in the last section with the winter, irrigation, and impoundment components. The third area of WEPP work is model code maintenance and support - which consists of assisting users in applying the model and fixing "bugs" as necessary in either the scientific model or the interface programs. Model testing for observed and simulated scenarios is the fourth work area, and is important to assure that model response is as

expected and appropriate. The last major work area is development of a common water and wind erosion process model, in a cooperative effort with the USDA-ARS Wind Erosion Research Unit at Manhattan, Kansas.

An updated version of the scientific model and interface programs is provided on approximately an annual basis. All WEPP materials are provided free of charge and distributed from the NSERL internet site. The most current version of WEPP is version 99.5, which was released in May 1999 in conjunction with the Beta-3 Windows interface version. Both the DOS and Windows interfaces can be downloaded from the NSERL Web site with the v99.5 scientific model.

Inquiries concerning the WEPP project and model may be directed to the email address wepp@ecn.purdue.edu. The WEPP model software, documentation, and other information are available from the USDA-ARS National Soil Erosion Research Laboratory web site at:

http://topsoil.nserl.purdue.edu/weppmain/wepp.html

The revised universal soil loss equation (RUSLE)

Model development history

Plans for RUSLE were developed in 1984-85, however there was no progress on the project until 1987, when Dr. Ken Renard, USDA-ARS, Tucson, Arizona, was named project leader. Staff at the NSERL (ARS and Purdue University) wrote the initial RUSLE computer program in the C programming language, and the model equations were incorporated within a user interface designed to run under the DOS operating system. NRCS users evaluated the first RUSLE prototype in 1990, and this led to significant modifications and enhancements of the program.

The RUSLE program was first released for public use in late 1992. Updated versions have been released periodically since then to correct errors and enhance the program's functionality. Upon Dr. Renard's retirement from ARS in 1994, Dr. George Foster became the official RUSLE project leader. Agricultural Handbook 703 (Renard et al., 1997a) was published in 1997, describing the RUSLE model science as well as providing instructions on using the computer software. At that time the documentation described RUSLE version 1.05.

The USDA-Natural Resources Conservation Service (NRCS) has implemented RUSLE technology throughout its system of field offices, though in most cases the computer program has not been used. In most states, NRCS released RUSLE in paper form (hardcopy tables and figures) placed in the Field Office Technical Guides.

The most current version of RUSLE available is version 1.06. New features include estimates of deposition on concave slopes, in terrace channels, and in sediment basins as a function of sediment characteristics. Version 1.06 also predicts deposition in terrace channels as a function of an estimated incoming sediment load and the transport capacity in the terrace channel. The slope length factor is estimated from the ratio of rill to interrill erosion, slope steepness, and land use.

RUSLE model components

The basic equation within RUSLE is the same as the Universal Soil Loss Equation:

$$A = R \cdot K \cdot L \cdot S \cdot C \cdot P \tag{8}$$

where A is average annual soil loss (tons·acre^{-1}·yr^{-1}), R is a rainfall-runoff erosivity factor (ft-tonf·in[acre·h·yr]$^{-1}$), K is a soil erodibility factor (ton·acre·h[hundreds of acre·ft-tonf·in]$^{-1}$), L is a slope length factor, S is a slope steepness factor, C is a cropping management factor, and P is a conservation practices factor (Renard et al., 1997a).

The R factor in RUSLE has been significantly improved over that in the USLE, particularly for the western United States. Precipitation data from more than 1200 locations were used to create a greatly improved isoerodent map (Renard et al., 1991). RUSLE recommends a reduction in R values for flat slopes in regions of the country having long duration and intense storm events, to account for decreases in soil loss due to pondage of water. A special equivalent R factor for the northwestern U.S. wheat and range area was also developed to better account for the unique rill erosion that occurs there due to soil surface thawing and snowmelt/rainfall runoff events (Renard et al., 1997b).

New sets of regression equations have been developed to estimate the soil erodibility factor, K. In RUSLE, erodibility has been made seasonally variable, with weighting of an instantaneous value of K in proportion to the fraction of the annual R value (Renard et al., 1991). This allows the model to simulate relatively higher erodibility after winter freeze-thaw periods as compared to lower values for compacted or frozen soils.

The slope length factor (L) in RUSLE is computed using:

$$L = (\lambda / 72.6)^m \tag{9}$$

where is λ slope length (ft), and m is a slope length exponent computed using:

$$m = \mathrm{B}/(1 + \mathrm{B}) \tag{10}$$

where B is the ratio of rill to interrill erosion. B can be estimated in RUSLE using the following equation:

$$\mathrm{B} = (\sin\theta / 0.0896)/[3.0(\sin\theta)^{0.8} + 0.56] \tag{11}$$

where θ is the slope angle (McCool et al., 1997).

For slopes longer than 15 ft and having steepness less than 9%, the slope steepness factor (S) is computed using:

$$S = 10.8 \sin\theta + 0.03 \tag{12}$$

while for slopes greater than or equal to 9%,

$$S = 16.8 \sin\theta - 0.50 \tag{13}$$

RUSLE also uses additional equations for computing S factors for short slopes or for recently tilled and thawing soil in a weakened state (Romkens et al., 1997).

The cropping management factor C is computed as a weighted average of soil loss ratios (SLRs) representing soil loss for a given condition to that for the unit plot (bare tilled fallow conditions). C is computed with the distribution of EI (fraction of R) through a year, using the equation:

$$C = PLU \cdot CC \cdot SC \cdot SR \cdot SM \quad (14)$$

where PLU is a prior land use subfactor, CC is a canopy cover subfactor, SC is a surface cover subfactor, SR is a surface roughness subfactor and SM is a soil moisture subfactor. Details on computation of each of these subfactors is provided in Chapter 5 of Agricultural Handbook 703 (Yoder et al., 1997). RUSLE also contains a residue decomposition model that predicts the decrease in surface and subsurface residue mass as a function of residue characteristics and climate.

Significant improvements have been made in how RUSLE computes support practice P factors, compared to USLE. Additional experimental data for practices such as contouring, strip-cropping, and terracing were analyzed, and supplemented by results of simulations with the CREAMS (Knisel, 1980) model. RUSLE also includes new P factor estimation procedures for conservation practices on rangeland. The reader is referred to Chapter 6 of the Agricultural Handbook 703 (Foster et al., 1997) for complete details on P factor computations.

All RUSLE-1 versions function very similarly to an application of USLE, in that each of the factors (R, K, L, S, C, and P) are computed independently, then the average values are multiplied together to obtain the average annual soil loss. Most of the factors in RUSLE-1 are computed at 15 day (or less) breakpoints through a year, but these breakpoint values of the individual factors are not multiplied together, then summed. The product of the average factor values can predict soil loss rates that differ by up to 20-25% from those computed using a breakpoint product procedure (Yoder and Lown, 1995). The RUSLE-2 program currently being developed departs from the independent USLE factor approach and instead uses a breakpoint integration procedure.

Current status and activities

Dr. Matt Romkens, USDA-ARS National Sedimentation Laboratory (NSL), Oxford, Mississippi is the current RUSLE project leader. Continuing model development efforts are being conducted through a cooperative agreement between the NSL and the University of Tennessee (Dr. Daniel Yoder, PI). Dr. George Foster retired from ARS in 1998, but is continuing work on RUSLE in a consultant position through the University of Tennessee.

RUSLE Version 1.06 is the current public version freely available from the USDA-Agricultural Research Service (ARS) for general use, and can be downloaded from the following web site:

http://www.sedlab.olemiss.edu/rusle

Current activities in the RUSLE project are development of a graphical user interface for application of RUSLE-2 technology on Windows™ 95/98/NT operating systems, as well as incorporation of the RUSLE technology within the MOSES common interface system.

Evaluation studies of the soil erosion models

It is important that soil erosion models be evaluated for their intended use. For the Water Erosion Prediction Project (WEPP) model, seven individual points were defined relative to "Validation Criteria" (Foster and Lane, 1987). These included subjective statements such as: "(a) The model is valid if it serves its intended purpose as defined by these specific User Requirements."; "(b) The model is based on scientific principles…"; (d) "The model gives results that are more useful for agency program objectives than those given by the USLE and applies to situations not appropriate for the USLE." These types of criteria are important and necessary. Another type of evaluation criteria for models, and perhaps the most commonly considered one, is the comparison of model predictions to measured erosion data. The WEPP criteria (Foster and Lane, 1987) also addressed this type of evaluation: "(f) Judgements on the "goodness of fit" of the estimates from the procedure to observed data are to be based on the data sets as a whole and not on a few specific isolated data sets. Quantitative measures of the "goodness of fits" will be calculated and presented, but a specific quantitative level of accuracy figure is not being required because of the great variation in the experimental data that will be used in the validation."

Recently, a series of studies have been conducted to compare erosion model predictions of soil loss to measured data. These include studies on WEPP, the USLE, and RUSLE. Risse et al. (1993) applied the Universal Soil Loss Equation (USLE) to 1700 plot·years of data from 208 natural runoff plots. Average observed soil loss on an annual basis was 3.51 $kg \cdot m^{-2}$. Using the USLE, annual values of predicted soil loss averaged 3.22 $kg \cdot m^{-2}$ with an average magnitude (absolute value) of error of 2.13 $kg \cdot m^{-2}$, or approximately 60% of the mean. Rapp (1994) applied the RUSLE model to the same set of data as Risse et al., and annual values of predicted soil loss averaged 3.16 $kg \cdot m^{-2}$. The average magnitude (absolute value) of error was not reported, but it is apparent that the two models performed similarly overall in terms of soil loss prediction. Zhang et al. (1996) applied the WEPP computer simulation model to 290 annual values and obtained an average of 2.18 $kg \cdot m^{-2}$ for the measured soil loss, with an average magnitude of error of 1.34 $kg \cdot m^{-2}$, or approximately 61% of the mean. In both cases the relative errors tended to be greater for the lower soil loss values. All three studies were conducted without model calibration. Model input parameters were not adjusted from initial default values for the specific data used in the comparisons.

What is reported above is obviously a very "broad brush" picture of the performance of the three erosion models, but in essence, the results indicate that for the prediction of *soil loss,* the three models appear to perform approximately on the same level of accuracy. However, there are a couple of important points to be considered. In the first place, all three models do predict soil loss, but only the WEPP model is specifically designed to predict sediment yield. Thus if prediction of average soil loss on the eroding portion of a hillslope is the goal, one might conclude from the studies that any of the three models work equally well. However, if one needs to know the deposition rates in the toe-slope of the hill, how much sediment might be transported off-site, sediment load from a channeled area, or the distribution of erosion along the hillslope, only WEPP will provide that information. Also, with regard to RUSLE vs. the USLE, one should note that though no calibration was done to the data, the data used in this study was the same or quite similar to the data used to develop the USLE[1]. RUSLE, however, was largely a

[1] Risse et al. (1993) and Rapp (1994) actually discuss this point in their papers, and delineate the consequence of the issue. It turns out that USLE and RUSLE perform about equally on the portion of the data used to develop the models as on that not used.

response to a need to improve predictions of soil loss in regions or situations not well represented in the data used in the Risse et al. and Rapp studies, such as semi-arid rangelands, no-till crops, and for the erosivity factor, the entire western U.S. In those situations, certainly, one might expect that RUSLE will perform better than the USLE.

The modular soil erosion system (MOSES)

Introduction

MOSES is a cooperative project among several agencies, universities, and locations to develop a multiplatform common interface program with common databases to allow users to access and use the RUSLE, WEPP, WEPS and RWEQ programs. Participants include the USDA - Agricultural Research Service, USDA - Natural Resources Conservation Service, USDA - Forest Service, Purdue University, University of Tennessee, and Kansas State University. A major reason behind this effort is the need for a single product that field users can learn to operate only once but will allow use of multiple erosion simulation models. Another benefit is a potential reduction in duplication of effort in software coding, maintenance and database development.

MOSES development history

Discussions on the possibility of creating a common interface to run the RUSLE and WEPP programs was first discussed during a meeting between the two projects in Knoxville, Tennessee in October 1996. An additional meeting was held in Lubbock, Texas in January 1997 that also included staff from the Revised Wind Erosion Equation (RWEQ) and the Wind Erosion Prediction System (WEPS) projects. The four groups decided at that time to begin design and development of a common interface with common databases to run any of the models. Mr. Charles Meyer, USDA-ARS, West Lafayette, Indiana was chosen as MOSES project leader. MOSES was initiated as the first virtual project within ARS, and operated initially with time and resources contributed from the individual projects. In 1998 and 1999, some additional funding was provided by NRCS to ARS to assist with MOSES programming tasks.

During 1997 and 1998 a large amount of work was devoted to the design of the main interface screens. There were four main design committees - 1.) Slope View, 2.) Plan View, 3.) Management View, and 4.) Location View. Additionally a committee was formed to determine the optimal outputs (text and graphics) for NRCS as well as other potential users. In addition to developing plans for the screen views and functions in the MOSES product, many of the features discussed in the committees were incorporated within the individual project stand-alone interface programs.

In October 1998, urgent needs of NRCS resulted in decisions to only initially incorporate RUSLE and WEPS in a MOSES-1 product. In August 1999, the MOSES group and programmers determined that the best approach to meet a short-term deadline of October 2000 for an initial MOSES prototype was to use a modified RUSLE-2 stand-alone interface and merge the WEPS-1 model beneath it. In the long-term, the RUSLE-2 framework may not be sufficient as additional models (WEPP watershed model, complete WEPS for multiple regions, RWEQ) need to be incorporated. Alternative approaches for MOSES past October 2000 are being considered.

Current status and activities

At present, work is progressing on the first prototype of the MOSES interface that will initially include the RUSLE and WEPS models. Plans are to release a beta version of MOSES to NRCS for initial testing by October 1, 2000. Following this initial release, work will continue to incorporate WEPP and RWEQ within a complete MOSES framework. An operational version of MOSES for NRCS field office testing should be available by sometime in 2002. Information on the MOSES project can be found at the following Web site:

http://horizon.nserl.purdue.edu/MOSES

Bibliography

ALBERTS, G.A.; M.A. NEARING; M.A. WELTZ; L.M. RISSE; F.B. PIERSON; X.C. ZHANG; J.M. LAFLEN and J.R. SIMANTON (1995) 'Chapter 7. Soil component'. In: D.C. Flanagan and M.A. Nearing (eds.), *USDA-Water Erosion Prediction Project hillslope profile and watershed model documentation*. NSERL Report No. 10, USDA-ARS National Soil Erosion Research Laboratory, West Lafayette, Indiana.

ARNOLD, J.C.; M.A. WELTZ; E.E. ALBERTS and D.C. FLANAGAN (1995) 'Chapter 8. Plant growth component'. In: D.C. Flanagan and M.A. Nearing (eds.), *USDA-Water Erosion Prediction Project hillslope profile and watershed model documentation*. NSERL Report No. 10, USDA-ARS National Soil Erosion Research Laboratory, West Lafayette, Indiana.

ASCOUGH, J.C. II; C. BAFFAUT; M.A. NEARING and D.C. FLANAGAN (1995) 'Chapter 13. Watershed model channel hydrology and erosion processes'. In: D.C. Flanagan and M.A. Nearing (eds.), *USDA-Water Erosion Prediction Project hillslope profile and watershed model documentation*. NSERL Report No. 10, USDA-ARS National Soil Erosion Research Laboratory, West Lafayette, Indiana.

ASCOUGH, J.C. II; C. BAFFAUT; M.A. NEARING and B.Y. LIU (1997) 'The WEPP watershed model: I. Hydrology and erosion'. Trans. Am. Soc. of Agric. Eng., 40(4), p. 921-933.

BAFFAUT, C.; M.A. NEARING; J.C. ASCOUGH II and B.Y. LIU (1997) 'The WEPP watershed model: II. Sensitivity analysis and discretization on small watersheds'. Trans. Am. Soc. of Agric. Eng., 40(4), p. 935-943.

BJORNEBERG, D.L.; J.K. AASE and T.J. TROUT. (1997) 'WEPP model evaluation under furrow irrigation'. ASAE Paper 97-2115. American Society of Agricultural Engineers, St. Joseph, Michigan, 18 p.

COCHRANE, T.A. and D.C. FLANAGAN (1999). 'Assessing water erosion in small watersheds using WEPP with GIS and digital elevation models'. J. Soil and Water Cons. (in press).

CHU, S.T. (1978) 'Infiltration during an unsteady rain'. Water Resour. Res., 14(3), p. 461-466.

ELLIOT, W.J.; A.M. LIEBENOW; J.M. LAFLEN AND K.D. KOHL (1989) *A compendium of soil erodibility data from WEPP cropland soil field erodibility experiments 1987 & 1988.* NSERL Report No. 3. USDA-Agricultural Research Service National Soil Erosion Research Laboratory, West Lafayette, Indiana.

FINKNER, S.C.; M.A. NEARING; G.R. FOSTER and J.E. GILLEY (1989) 'A simplified equation for modeling sediment transport capacity'. Trans. Am. Soc. of Agric. Eng., 32(5), p. 1545-1550.

FLANAGAN, D.C.; D.A. WHITTEMORE; S.J. LIVINGSTON; J.C. ASCOUGH II and M.R. SAVABI (1994) 'Interface for the Water Erosion Prediction Project model'. ASAE Paper No. 94-2105. American Society of Agricultural Engineers, St. Joseph, Michigan, 16 p.

FLANAGAN, D.C. and M.A. NEARING (eds.) (1995) *USDA-Water Erosion Prediction Project hillslope profile and watershed model documentation.* NSERL Report No. 10, USDA-ARS National Soil Erosion Research Laboratory, West Lafayette, Indiana.

FLANAGAN, D.C. and S.J. LIVINGSTON (eds.) (1995) *USDA-Water Erosion Prediction Project (WEPP) version 95.7 user summary.* NSERL Report No. 11, USDA-ARS National Soil Erosion Research Laboratory, West Lafayette, Indiana.

FLANAGAN, D.C.; H. FU; J.R. FRANKENBERGER; S.J. LIVINGSTON and C.R. MEYER (1998) 'A Windows® interface for the WEPP erosion model'. ASAE Paper No. 98-2135. American Society of Agricultural Engineers, St. Joseph, Michigan, 14 p.

FOSTER, G.R.; L.J. LANE; J.D. NOWLIN; J.M. LAFLEN and R.A. YOUNG (1980) 'Chapter 2. A model to estimate sediment yield from field-sized areas: development of model'. In: W.G. Knisel (ed.), *CREAMS: a field-scale model for chemicals, runoff, and erosion from agricultural management systems*. USDA Conservation Research Report No. 26, p. 35-64.

FOSTER, G.R. and L.J. LANE (compilers) (1987) *User requirements: USDA-Water Erosion Prediction Project (WEPP)*. NSERL Report No. 1, USDA-ARS National Soil Erosion Research Laboratory, West Lafayette, IN, 43 p.

FOSTER, G.R.; D.C. FLANAGAN; M.A. NEARING; L.J. LANE; L.M. RISSE and S.C. FINKNER (1995) 'Chapter 11. Hillslope erosion component'. In: D.C. Flanagan and M.A. Nearing (eds.), *USDA-Water Erosion Prediction Project hillslope profile and watershed model documentation*. NSERL Report No. 10, USDA-ARS National Soil Erosion Research Laboratory, West Lafayette, Indiana.

FOSTER, G.R.; G.A. WEESIES; K.G. RENARD; D.C. YODER; D.K. MCCOOL and J.P. PORTER (1997) 'Chapter 6. Support practice factor (P)'. In: K.G. Renard, G.R. Foster, G.A. Weesies, D.K. McCool and D.C. Yoder (compilers), *Predicting soil erosion by water: a guide to conservation planning with the Revised Universal Soil Loss Equation (RUSLE)*. USDA Agricultural Handbook No. 703, p. 183-251.

GILLEY, J.E. and M.A. WELTZ (1995) 'Chapter 10. Hydraulics of overland flow'. In: D.C. Flanagan and M.A. Nearing (eds.), *USDA-Water Erosion Prediction Project hillslope profile and watershed model documentation*. NSERL Report No. 10, USDA-ARS National Soil Erosion Research Laboratory, West Lafayette, Indiana.

KNISEL, W.G. (ed.) (1980) *CREAMS: A field-scale model for chemicals, runoff, and erosion from agricultural management systems*. USDA Conservation Research Report No. 26, 640 pp.

KOTTWITZ, E. R. (1995) 'Chapter 12. Irrigation component'. In: D.C. Flanagan and M.A. Nearing (eds.), *USDA-Water Erosion Prediction Project hillslope profile and watershed model documentation*. NSERL Report No. 10, USDA-ARS National Soil Erosion Research Laboratory, West Lafayette, Indiana.

LANE, L.J. and M.A. NEARING (eds.) (1989) *USDA-Water Erosion Prediction Project: hillslope profile model documentation*. NSERL Report No. 2, USDA-ARS National Soil Erosion Research Laboratory, West Lafayette, Indiana.

LINDLEY, M.R.; B.J. BARFIELD and B.N. WILSON (1995) 'Chapter 14. Surface impoundment element model description'. In: D.C. Flanagan and M.A. Nearing (eds.), *USDA-Water Erosion Prediction Project hillslope profile and watershed model documentation*. NSERL Report No. 10, USDA-ARS National Soil Erosion Research Laboratory, West Lafayette, Indiana.

LIU, B.Y.; M.A. NEARING; C. BAFFAUT and J.C. ASCOUGH II (1997) 'The WEPP watershed model: III. Comparisons to measured data from small watersheds'. Trans. Am. Soc. of Agric. Eng., 40(4), p. 945-952.

MCCOOL, D.K.; G.R. FOSTER and G.A. WEESIES (1997) 'Chapter 4. Slope length and steepness factors (LS)'. In: K.G. Renard, G.R. Foster, G.A. Weesies, D.K. McCool and D.C. Yoder (compilers), *Predicting soil erosion by water: a guide to conservation planning with the Revised Universal Soil Loss Equation (RUSLE)*. USDA Agricultural Handbook No. 703, p. 101-141.

MCCOOL, D.K.; C.D. PANNKUK; C.H. LIN and J.M. LAFLEN (1998) 'Evaluation of WEPP for temporally frozen soil'. ASAE Paper 98-2048, American Society of Agricultural Engineers, St. Joseph, Michigan, 9 p.

MEIN, R.G. and C.L. LARSON (1973) 'Modeling infiltration during a steady rain'. Water Resour. Res., 9(2), p. 384-394.

NEARING, M.A.; D.I. PAGE; J.R. SIMANTON and L.J. LANE (1989) 'Determining erodibility parameters from rangeland field data for a process-based erosion model'. Trans. Am. Soc. Agric. Eng., 32(3), p. 919-924.

NICKS, A.D.; L.J. LANE and G.A. GANDER (1995) 'Chapter 2. Weather generator'. In: D.C. Flanagan and M.A. Nearing (eds.), *USDA-Water Erosion Prediction Project hillslope profile and watershed model documentation*. NSERL Report No. 10, USDA-ARS National Soil Erosion Research Laboratory, West Lafayette, Indiana.

ONSTAD, C.A. (1984) 'Depression storage on tilled soil surfaces'. Trans. Am. Soc. Agric. Eng., 27(3), p. 729-732.

RAPP, J.F. (1994) *Error assessment of the Revised Universal Soil Loss Equation using natural runoff plot data*. M.S. Thesis, School of Renewable Natural Resources, Univ. of Arizona, Tucson, AZ.

RENARD, K.G.; G.R. FOSTER; G.A. WEESIES and J.P. PORTER (1991) 'RUSLE: Revised Universal Soil Loss Equation'. J. Soil and Water Cons., 46(1), p. 30-33.

RENARD, K.G.; G.R. FOSTER; G.A. WEESIES; D.K. MCCOOL and D.C. YODER (compilers) (1997a) *Predicting soil erosion by water: a guide to conservation planning with the Revised Universal Soil Loss Equation (RUSLE)*. USDA Agricultural Handbook No. 703, 404 p.

RENARD, K.G.; D. K. MCCOOL; K.R. COOLEY; G.R. FOSTER; J.D. ISTOK and C.K. MUTCHLER (1997b) 'Chapter 2. Rainfall-runoff erosivity factor (R)'. In: K.G. Renard, G.R. Foster, G.A. Weesies, D.K. McCool and D.C. Yoder (compilers), *Predicting soil erosion by water: a guide to conservation planning with the Revised Universal Soil Loss Equation (RUSLE)*. USDA Agricultural Handbook No. 703, p. 19-64.

RISSE, L.M.; M.A. NEARING; A.D. NICKS and J.M. LAFLEN (1993) 'Assessment of error in the Universal Soil Loss Equation'. Soil Science Soc. of Am. J., 57, p. 825-833.

RISSE, L.M.; M.A. NEARING and M.R. SAVABI (1994) 'Determining the Green-Ampt effective hydraulic conductivity from rainfall-runoff data for the WEPP model'. Trans. Am. Soc. of Agric. Eng., 37(2), p. 411-418.

ROMKENS, M.J.M.; R.A. YOUNG; J.W.A. POESEN; D.K. MCCOOL; S.A. EL-SWAIFY and J.M. BRADFORD (1997) 'Chapter 3. Soil erodibility factor (K)'. In: K.G. Renard, G.R. Foster, G.A. Weesies, D.K. McCool and D.C. Yoder (compilers), *Predicting soil erosion by water: a guide to conservation planning with the Revised Universal Soil Loss Equation (RUSLE)*. USDA Agricultural Handbook No. 703, p. 65-99.

SAVABI, M.R. and J.R. WILLIAMS (1995) 'Chapter 5. Water balance and percolation'. In: D.C. Flanagan and M.A. Nearing (eds.), *USDA-Water Erosion Prediction Project hillslope profile and watershed model documentation*. NSERL Report No. 10, USDA-ARS National Soil Erosion Research Laboratory, West Lafayette, Indiana.

SAVABI, M.R.; R.A. YOUNG; G.R. BENOIT; J.M. WITTE and D.C. FLANAGAN (1995) 'Chapter 3. Winter hydrology'. In: D.C. Flanagan and M.A. Nearing (eds.), *USDA-Water Erosion Prediction Project hillslope profile and watershed model documentation*. NSERL Report No. 10, USDA-ARS National Soil Erosion Research Laboratory, West Lafayette, Indiana.

SIMANTON, J.R.; M.A. WELTZ and H.D. LARSEN (1991) 'Rangeland experiments to parameterize the water erosion prediction project model: vegetation canopy cover effects'. J. of Range Mgmt., 44(3), p. 276-282.

SMITH, R.E. and J.R. WILLIAMS (1980) 'Chapter 1. Simulation of the surface water hydrology'. In: W.G. Knisel (ed.), *CREAMS: A field-scale model for chemicals, runoff, and erosion from agricultural management systems*. p. 13-35.

STONE, J.J.; L.J. LANE and E.D. SHIRLEY (1992) 'Infiltration and runoff simulation on a plane'. Trans. Am. Soc. Agric. Eng., 35(1), p. 161-170.

STONE, J.J.; L.J. LANE; E.D. SHIRLEY and M. HERNANDEZ (1995) 'Chapter 4. Hillslope surface hydrology'. In: D.C. Flanagan and M.A. Nearing (eds.), *USDA-Water Erosion Pediction Project hillslope profile and watershed model documentation*. NSERL Report No. 10, USDA-ARS National Soil Erosion Research Laboratory, West Lafayette, Indiana.

STOTT, D.E.; E.E. ALBERTS and M.A. WELTZ (1995) 'Chapter 9. Residue decomposition and management'. In: D.C. Flanagan and M.A. Nearing (eds.), *USDA-Water Erosion Prediction Project hillslope profile and watershed model documentation*. NSERL Report No. 10, USDA-ARS National Soil Erosion Research Laboratory, West Lafayette, Indiana.

WILLIAMS, J.R. (1995) 'Chapter 25. The EPIC model'. In: V.P. Singh (ed.), *Computer models of watershed hydrology*. Water Resources Publications, Littleton, Colorado, p. 909-1100.

YALIN, M.S. (1963) 'An expression for bed-load transportation'. J. Hydraulics Division ASCE, 98(HY3), p. 221-250.

YODER, D.C. AND J.B. LOWN (1995) 'The future of RUSLE: inside the new revised universal soil loss equation'. J. Soil and Water Cons., 50(5), p. 484-489.

YODER, D.C.; J.P. PORTER; J.M. LAFLEN; J.R. SIMANTON; K.G. RENARD; D.K. MCCOOL and G.R. FOSTER (1997) 'Chapter 5. Cover-management factor (C)'. In: K.G. Renard, G.R. Foster, G.A. Weesies, D.K. McCool and D.C. Yoder (compilers), *Predicting soil erosion by water: a guide to conservation planning with the Revised Universal Soil Loss Equation (RUSLE)*. USDA Agricultural Handbook No. 703, p. 143-181.

ZHANG, X.C.; M.A. NEARING and L.M. RISSE (1995a) 'Estimation of Green-Ampt conductivity parameters: part I. row crops'. Trans. Am. Soc. of Agric. Eng., 38(4), p. 1069-1077.

ZHANG, X.C.; M.A. NEARING and L.M. RISSE (1995b) 'Estimation of Green-Ampt conductivity parameters: part II. perennial crops'. Trans. Am. Soc. of Agric. Eng., 38(4), p. 1079-1087.

ZHANG, X.C.; M.A. NEARING; L.M. RISSE and K.C. MCGREGOR (1996) 'Evaluation of runoff and soil loss predictions using natural runoff plot data'. Trans. Am. Soc. of Agric. Eng., 39(3), p. 855-863.

Erosion and sediment yield modelling in the former USSR

N.N. Bobrovitskaya
State Hydrological Institute,
23 Second Line, 199053 St. Petersburg, Russia

Introduction

At the present time, the soil erosion and sediment yield models available in Russia and neighbouring countries are used for a number of purposes, including:
- estimating the rate of overland soil scour and ravine erosion;
- substantiating the success of anti-erosion measures in irrigated/non-irrigated crop fields;
-assessing the impacts of soil improvement, road construction, etc.;
- computing sediment inflow to rivers, ponds and reservoirs to assess rates of siltation;
- predicting sediment transport in rivers and canals;
- documenting sediment inflow to seas and the World Ocean;
- quantifying the role of sediment runoff in temporary streams and rivers as a factor of contaminant transport and deposition.

A dense network of hydrometeorological stations has been installed to observe soil erosion on slopes, water discharges, sediment yields and the principal factors which determine these processes (i.e. precipitation, soil moisture content, soil freeze-up, etc). This hydrological monitoring programme incorporates the following range of drainage scales:
- from 0.000 - 2.0 km^2 - temporary streams on slopes and in micro-hollows;
- 2 – 10 km^2 - big streams in hollows;
- 10 – 2000 km^2 - small rivers;
- 2000 - 50000 km^2 - medium-size rivers;
- > 50000 km^2 - large rivers.

Thousands of references are available on studies of soil erosion and suspended sediment yield. This brief contribution focuses upon models and methods for the assessment of overland scour.

Model types

Water erosion is a powerful factor in landscape evolution. As a result of enhanced erosion, soil fertility is decreasing considerably and rivers, canals and reservoirs are experiencing accelerated siltation. In addition, the products of erosion, i.e. sediments, act as a vector and potential store of contaminants.

The urgent need to understand and control soil erosion arose at the boundary of the 19-20th Centuries and remains important today. Throughout this period, a number of fundamental studies have been conducted on soil erosion. In Russia, research in recent decades has greatly assisted the improvement of scientific knowledge of erosion phenomena (Zaslavsky, 1979). The most important results of this research include:

- determination of soil properties and the development of soil classification (Dokuchaev, Reports for 1888-1900, publications for 1888 - 1951; Kachinsky, 1963; Kovda, 1985; etc.);
- the mapping of soil distribution and an improved understanding of the factors of soil formation for different natural zones in Russia and the former USSR (Kachinsky, 1963; Kovda, 1985; etc.);
- the undertaking of studies on hydrological and morphological features of the formation of hydrographical networks, including slope relief and the spatial distribution of soil types with respect to slope relief elements (Kozmenko, 1937, 1957);
- the identification of the major processes of soil erosion and determination of erosion rates for different natural zones and for different kinds of land use (Dokuchaev, 1888-1951; Kozmenko, 1937-1957; Sobolev, 1970);
- the development and use of qualitative and quantitative methods to assess the rate of soil erosion by water and wind and the establishment of soil protection measures based on accounting procedures for soil properties, husbandry management and hydromorphological factors (Kostyakov, 1948; Kozmenko, 1937,1957; Zaslavsky, 1979, 1983; etc.);
- the development of pioneering research on soil erosion taking into account hydrometeorological factors and soil-geomorphologic conditions using a combination of ground and remote methods (Bogolyubova, 1975; Anon, 1979; Bobrovitskaya, 1979, 1986, 1990; etc.);
- the development of methods and models for estimating water erosion based on taking into account the features of soil erosion and soil properties (Mirtskhoulava, 1970; Schwebs, 1981, 1991; Bogolyubova and Karaushev, 1979; Bobrovitskaya, 1979, 1991; Kuznetsov, 1981; Barabanov and Garshinev, 1991; Surmach, 1976; Kosov and Zorina, 1989; Borzilov, 1991; Larionov, 1993; etc.);
- the development of methods for large-scale cartographic and mathematical modelling of water and wind erosion (Sachok, 1984,1994; Kondratjyev, 1989; Grigorjyev and Sidorchuk, 1995; Dolgilevitch et al., 1995; Nazarov, 1996; etc.).

Four principal types of erosion models can be identified which have been used in Russia: empirical, logical, mathematical, and hydromechanical. There is some overlap in this classification scheme because mathematical relationships are used for information processing within empirical models, and all mathematical models are based on important empirical relationships between erosion characteristics and a range of forcing factors. Let us consider briefly the models most frequently applied in practice to assess soil washout from slopes.

Empirical models

Early examples of empirical models include those developed by:
a) Kornev and Kostyakov (1937):

$$W = a\, I^{0.75}\, L^{0.5}\, h^{1.5} \quad (1)$$

where W = washout (specific sediment yield); I = slope of ploughed lands;
L = slope length; h = water return rate; a = correction factor.

b) Glushkov and Polliakov (1946):

$$a = S/\ 10\quad \sqrt[4]{I} \quad (2)$$

where a = erosion coefficient; S = mean annual sediment concentration (g/m^3); I = channel slope.

c) Svetitsky (1962):

$$a_c = P_s /N^{1.22} \quad (3)$$

where a_c = erosion coefficients; P_s= mean annual sediment yield; N = energy characteristic.

In 1977, Bogoliubova and Karaushev (1979) developed a method for the computation of soil scour, based on the use of equations for transportation capacity and information on stream network density:

$$W = 1/2\ K_w \sum_{i=1}^{n} (x^2_i - x^2_{i-1})\ N_i \quad (4)$$

$$N_i = K^{n-1}_N \quad (5)$$

where W = total scour on the slope produced by all kinds of brooklets, from i up to n long; x_i = total length of the brooklet of the *i*-th order from the head to the outlet; x_1 = length of the brooklet of the 1st order; x_2 = length of the last order; K_N = bifurcation coefficient assumed to be equal to 2; N_i = the member of flows of different orders, after Horton.

Another example is the 'graphoanalytical model' proposed by Bobrovitskaya (1979, 1986). This model is based upon the use of the natural micro-watersheds of hollows as a basis for studying water flow and sediment transport. These hollows can exhibit a number of hydrological and morphological characteristics, including either, natural or anthropogenic micro-watersheds and a variety of positions in the hydrographic system. In addition, they are observed over all types of soils and subsoils; they have longitudinal profiles and cross-sections, which are variable over slopes as well as pathway networks of 1-111 types which are connected with the lower links of the hydrographic network; and they possess a capacity for self-organisation. A procedure has been developed for the empirical study of water outflow and sediment yield, which combines the use of field and remote-sensing methods.

According to this model, the mean annual soil washout for the period of crop rotation ($M_{sop\%}$) can be calculated from:

$$M_{sop\%} = \sum (M_{sp\%} + M'_{sp\%})/N \quad (6)$$

$$M_{smp\%} = h^n_{\ mp\%}\ a\ b\ k_i \quad (7)$$

$$M'_{smp\%} = h_{mp\%\,a}\, a_1\, h\, k_1 \quad (8)$$

where M_{smp} and $M'_{smp\%}$ = specific sediment yields from slopes for the period of snow-melting and floods of the specified probability of exceedance for a brooklet of m order (t/ha); h_p = runoff depth of the same probability of exceedence for the period of the snowmelt flood or rainfall floods (mm); a_m and N = parameters dependent on the type of the brooklet network on the slopes, on the agrotechnical practice and on the soil types; b = a coefficient, which takes into account the effects of the agrotechnical practice during the previous year and the soil scour; K_i = a coefficient which takes into account the slope steepness. The fact that the model does not take into direct account the slope length is compensated for by consideration of the type of brooklet network depending on slope length.

Another example is the model by Surmach (1979) which can be expressed as follows:

$$W = K/10\ a^{1/2} F^n L^n \gamma Y^i U P_\tau P_g P_w P_e A_a \quad (9)$$

where K = a coefficient reducing the value of initial sediment content in water to the standard conditions; a = 75 m; F = the inclination on the corresponding site of the slope; L = the slope length (m); y = the sediment content in slope runoff (g/m^3) near the water divide at the slope site of 75 m long and inclination of 0.004; Y = the melt or heavy rain flow layer with the prescribed probability or during the period of a single rain (mm); I = the power within the flow layer (changing from 1.06 to 1.14 for rain flow, and from 0.94 to 0.89 for melt water flow); U = the coefficient of snow accumulation character; Pr, Pe = the coefficients taking into account the washout effects of mechanical composition, washout and the extent of soil erosion; A = the coefficient of agricultural engineering.

It is advantageous that this model uses the characteristics of mechanical composition and the extent of soil erosion. Unfortunately, however, it is frequently necessary to determine soil washout using a method developed for measuring creek channels and considerable errors inevitably result from this procedure.

Logical and mathematical models

Progress in studying and understanding the physical features of erosion allowed the development of logical and mathematical models of soil erosion. One of the first models was proposed by Schwebs (1974, 1981, 1991). The dependence of mean annual specific sediment yield on heavy rain is expressed as follows:

$$\overline{W}_{ë} = \delta_{ë} \sum_{n=1}^{m} \left[\frac{x_{cì}^{2,7}}{\Delta t_{CÒ}^{1,7}} \left(1 + 17{,}5 \frac{\grave{A} X_{\Delta t_{\tilde{N}Ò}}}{\Delta t_{CÒ}} \right) \right] = \delta_{ë} \hat{E}_{\tilde{A}\grave{l}} \quad (10)$$

$$\overline{W_{ë}} = 1{,}2 \cdot 10^{-4}\, j_R e^{-\lambda_P (0{,}85 - 100m)} \sum_{i=1}^{m} K_{\tilde{A}\grave{l}} I^n L^{0{,}5} \quad (11)$$

where jk = the relative soil washout; the washout for the ordinary argillaceous chernozem is taken as unity; lp = the factor taking into account the effects of vegetation cover on soil washout; m = the underlying surface roughness; I = the slope inclination; L = the slope length;

n = the power with the inclination depending on soil type, anti-erosion sustainability and the character of underlying surface; $K_{\Gamma m}$ = the hydrometeorological coefficient.

A major advantage of this model is that, in principle, the value of $K_{\Gamma m}$ can be determined for any soils and any surface condition. However, due to the shortage of prototype materials, Schwebs considers it to be sufficient to use in the washout model $K_{\Gamma m}$ for a bare surface of standard soil with the relative washout being unity. In this case the value of $K_{\Gamma m}$ can be mapped, which is an advantage of the model in practice. However, this assumption means that in all cases differing from the standard, $K_{\Gamma m}$ is represented by fictitious values determined only by the intensity and sediment layer. In addition, the model has been based upon the data from field studies of 1 m long runoff sites, which makes it impossible to take into account the non-linearity of relations between water and sediment runoff both with transfer from grounds to slopes and with water discharges of different probability. The Schwebs model has several modifications, for instance, to take into account washout for the period of snow melt or the effects of tree location in regulating erosion, etc. (Schwebs, 1991).

Hydromechanical models

The laws of hydromechanics underpin the available hydrometeorological models. These are best represented by the studies of Mirtskhoulava (1970, 1991) and Kuznetsov (1992), etc. In these hydromechanical models, the flow bed is schematically represented by complicated homogeneous spherical assemblies, which are interconnected by cohesion.

A great number of input parameters are required by these models and this frequently represents a severe problem for applying them on unstudied slopes. Therefore, to assess the risk of erosion and the impact of anti-erosion precautions, existing empirical models are most generally employed.

Without going into detail, (cf. Mirtskhoulava, 1966, 1970, 1989), the equations for permissible non-eroding mean velocities $V_{n\ per}$ and near-bed velocities $V_{\Delta\ per}$ can be expressed as:

$$V_{n.per.} = \left(\lg\frac{8.8H}{d}\right)\sqrt{\frac{2m}{2.6p_o n}\left[(p_s - p_o)gd + 1.25\left(C_f^s k + \sigma_{ob}\right)\right]} \qquad (12)$$

$$V_{\Delta n.per.} = 1.25\sqrt{\frac{2m}{2.6p_o n}\left[(p_s - p_o)gd + 1.25\left(C_f^s k + \sigma_{ob}\right)\right]} \qquad (13)$$

where H = flow depth; d = the mean diameter of entrained aggregates, assumed equal to 0.004 m; m = the coefficient of working conditions including the effect of various factors of channel conditions; n = overload coefficient accounting for the eroding capacity of flow due to velocity fluctuations; p_o = density of water; p_s = density of soil grains; g = free fall acceleration; k = coefficient to characterise probability of deflection of cohesion from mean value.

The quantity of soil washed off from a plot (having unit width and length) in a watershed to the end of the erodible part of slope can be determined by formulae. For the

determination of the total wash-off, the obtained result is multiplied by the slope area (χ_2 b), where b is the slope width (Mirtskhoulava, 1970):

$$q_{\chi_2 T} = 11 \cdot 10^{-4} g p_s \omega d \left[\frac{308(\sigma n_o)^{0.6} i^{0.7} m_1^{1.4} I^{0.6} \chi_2^{1.6}}{V_{\Delta per}^2} + \frac{13 \cdot 10^{-6} V_{\Delta per}^{3.32}}{(\sigma n_o) i^{1.16} m_1^{2.32}} - \chi_2 \right] \frac{T}{\chi_2} \tag{14}$$

where ϖ = the average frequency of pulsation velocities; m = a coefficient accounting for the deviation of the sheet flow motion from the accepted smooth water surface motion.

Mathematical models

The hydrodynamic model by Kondratjyev (1989) gives a description of non-steady surface runoff as a continuous layer and sediment transport based on the system of differential equations in partial derivatives. These are the continuity equation for running water and the equation expressing the law of conservation of the mass of transported sediment particles:

$$\frac{\partial h}{\partial t} + \frac{\partial q}{\partial x} = r - f \tag{15}$$

$$\frac{\partial}{\partial t}(Sh) + \frac{\partial}{\partial x}(Sq) + \rho \frac{\partial \eta}{\partial t} = 0 \tag{16}$$

where q = $q = \sqrt{i} h^{5/3} / n$; h = the depth of surface flow; q = the unit water discharge; r = the rate of precipitation; f = the rate of infiltration; S = the sediment concentration in the stream; η = the mark of the surface; i = slope of ploughed lands; n = the Manning's roughness coefficient; ρ = the deposit density; x, t = the spatial and temporal co-ordinates. For an individual creek the initial system of equations is as follows:

$$\frac{\partial \omega}{\partial t} + \frac{\partial Q}{\partial x} = (r - f) b \tag{17}$$

$$\frac{\partial}{\partial t}(S\omega) + \frac{\partial}{\partial x}(SQ) + \rho P \frac{\partial \eta}{\partial t} = 0 \tag{18}$$

where $Q = \frac{\sqrt{i} \omega^{5/3}}{n P^{2/3}}$ w = is the cross-section area; Q = the water discharge; P = the wetted perimeter; b = the brooklet width.

The runoff from slopes resulting from the brooklets system and the washout caused by it can be simulated using the following system of equations:

$$\frac{\partial \omega^*}{\partial t} + \frac{\partial Q^*}{\partial x} = (r - f) B \tag{19}$$

$$\frac{\partial}{\partial t}\left(S\omega^{*}\right)+\frac{\partial}{\partial x}\left(SQ^{*}\right)+\rho P^{*}\frac{\partial \eta}{\partial t}=0 \qquad (20)$$

where $Q^{*}=\sqrt{i}\omega^{*5/3}/nP^{*2/3}N^{2/3}\varpi^{*}$ =*N*. ϖ = the total cross-section area of all the creeks; P* = the total wetted perimeter; N = the number of creeks in the section X; B = the slope width.

The model is supplemented with a block allowing calculation of water percolation into soil by the Phillip's formula. The sediment concentration in the flow S is assumed to correspond with transportation capacity:

$$S \cong S_{\grave{O}} = KQ^{2} \qquad (21)$$

where *K* = the parameter whose value depends on the layer of soil washed out. The model requires calibration for a number of conditions.

Mapping the characteristics of soil erosion

The cartographic version of the model by Bobrovitskaya (1986, 1991) is convenient for helping to evaluate soil erosion in large territories (Figure 1). Erosion is deciphered using aerial photos (1:25000 scale). Such maps of erosion-threatened lands (of potential soil erosion) can be used to target anti-erosion precautions. This mapping technique has been developed at the Moscow State University (Larionov, 1993). Soil washout is calculated by modified equations: for the summer period by the equations of Wischmeier and Smith, and for the snow melt period by the model of Bobrovitskaya (1979). A fragment of such a map is shown in Figure 2.

Computer erosion modelling is successfully used in studies by Garshinev and Barabanov (1991) to calculate soil washout and the necessary distances between tree belts to control over erosion. In Belarus, a set of programmes has been developed for computer modelling of sediment runoff (Sachok, 1994). It allows mapping of both 'actual' characteristics of water erosion corresponding to the current relief and the prediction of soil erosion taking into account potential changes in environmental conditions. These maps can be applied in a wide range of territory sizes: individual fields, farms, administrative regions. The graphoanalytical model by Bobrovitskaya (1979, 1986) has been combined with cartographic modelling. The fragments of a computer map derived from this procedure are shown in Figures 3-9.

Problems of calibrating and validating soil erosion models

The absence of extensive empirical information represents a major problem for verifying the estimates of soil loss provided by available soil erosion models. Application of these models requires much information e.g. hydrometeorological, hydraulic and topographical data as well as numerous measures of soil and vegetation characteristics. Moreover, these characteristics should be measured not only in the laboratory or on runoff plots, but along the slopes, too. When models are tested on the basis of measurements from runoff plots or in the laboratory,

the errors in sediment yield calculation may be quite significant. Field data are required for reliable testing.

The key research needs for improving soil erosion models

In future it is very important to make an intercomparison of different models, both mathematical and empirical ones. Such work should be based upon the use of standard field sites representative of different natural zones of the world with contrasting anthropogenic pressures. In Russia and the countries of the former USSR, these sites are readily available around water-balance stations. Examples include, the Valdai Branch of the State Hydrological Institute (Valdai Upland), Nijnedevitskaya water-balance station (in the forest steppe zone of the Central Russian Upland), and a site representing Kamennaya Steppe (a steppe zone of the European part of Russia), where for the past 80 years a unique experiment has been conducted on controlling erosion by using tree belts, different types of ploughing, etc. Observations of water and sediment yield have been undertaken at these stations over 40-50

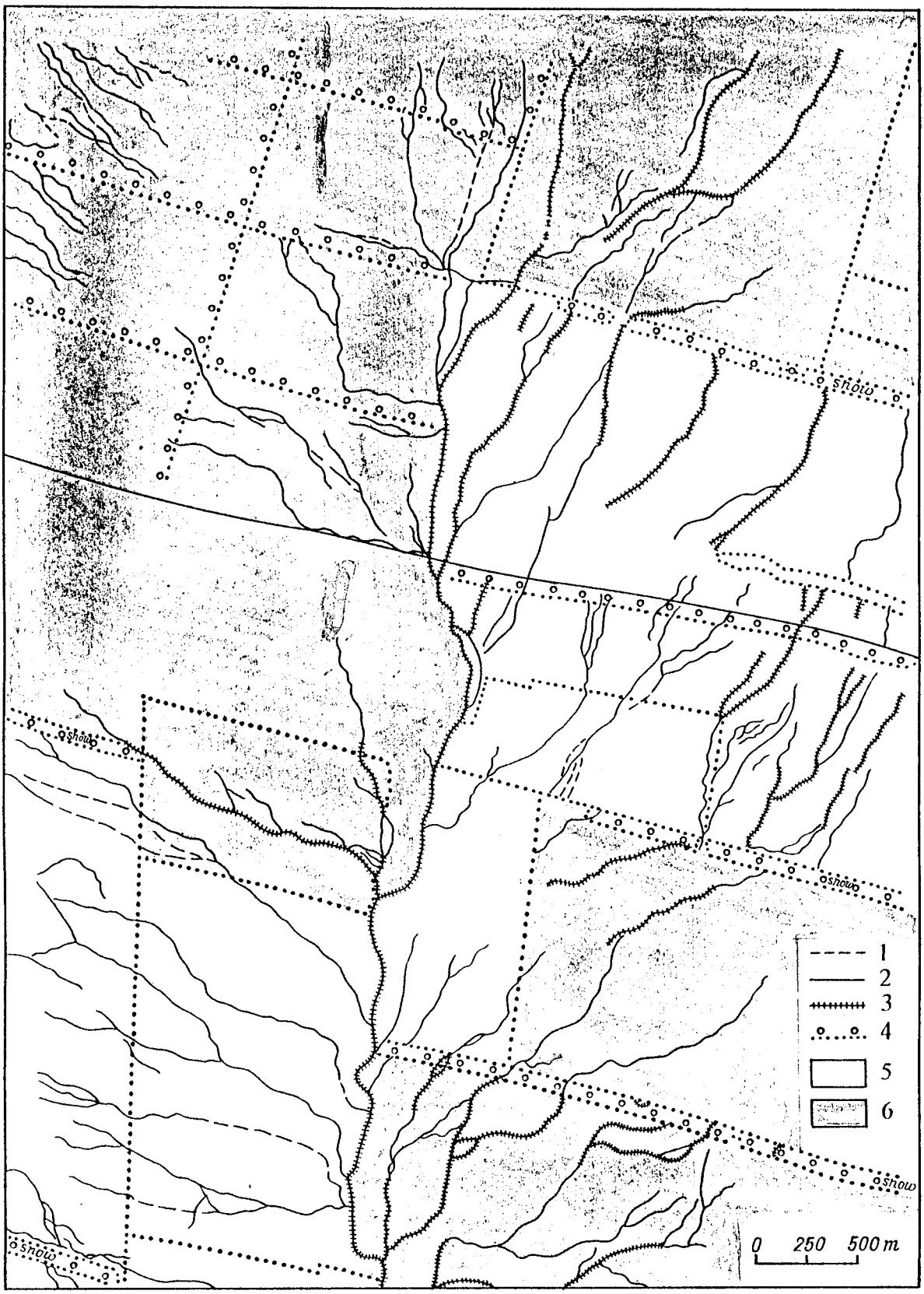

Fig. 1 Erosion formations on the right slope of the Aley River at Geelyevo in the Altai Region (Bobrovitskaya and Zubkova, 1991). Symbols: 1 – channels of brooklet type II; 2, 3 – channels of brooklets of type III: cutting and not cutting through the humus layer; 4 – tree belts; 5 – the slope sites with boardless ploughing on which only large brooklets of type III are deciphered; 6 – the fields ploughed in the autumn ready for sowing in the spring

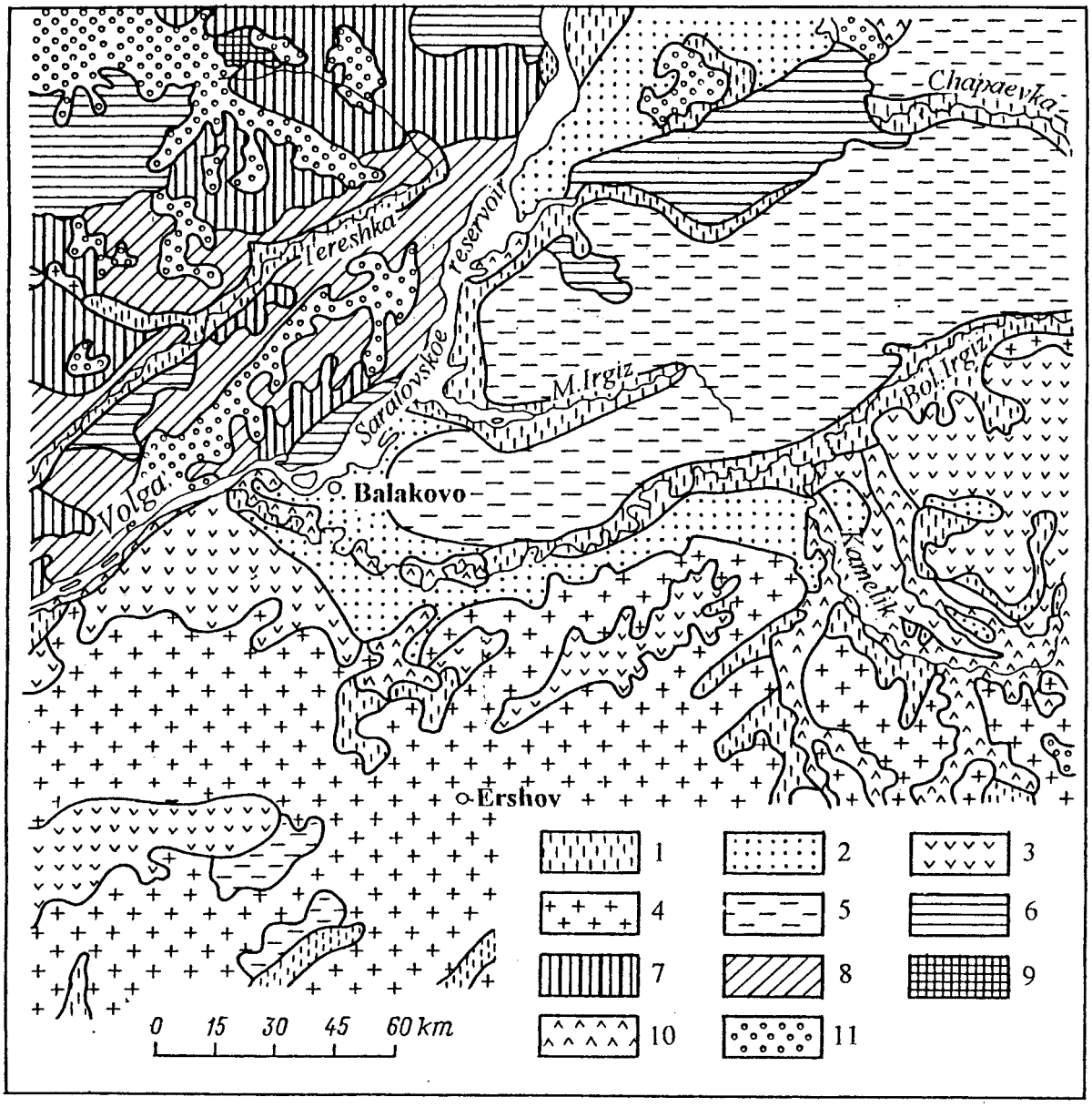

Fig. 2 A fragment of the map of erosion lands in the European territory of the USSR and the Caucasus. The mean rate of wash away (t ha^{-1} yr^{-1}) on the ploughed land: 1 - <0.5; 2 – 0.5-1; 3 – 1-2; 4 – 2-3; 5 – 3-4; 6 – 4-7; 7 – 5-7; 8 – 7-10; 9 – 10-11. On the natural fodder fields: 10 <0.5; 11 – in the forest (Larinov, 1993)

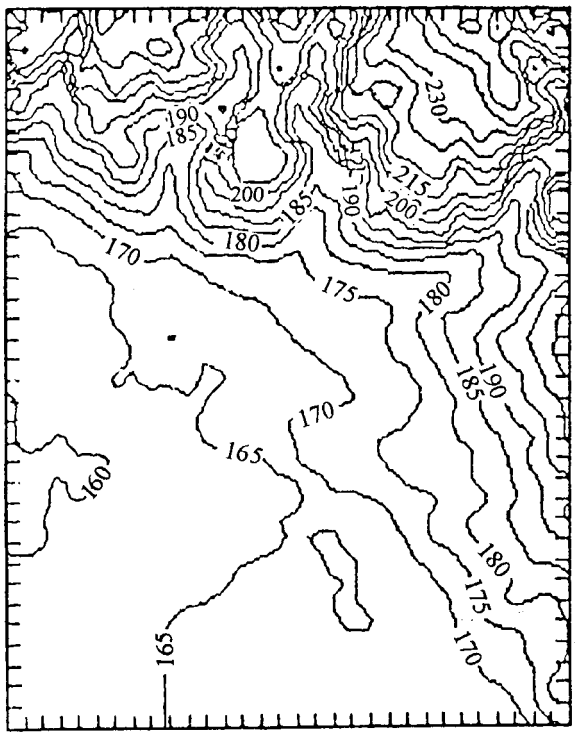

Fig. 3 Absolute altitudes of relief (Sachok, 1994)

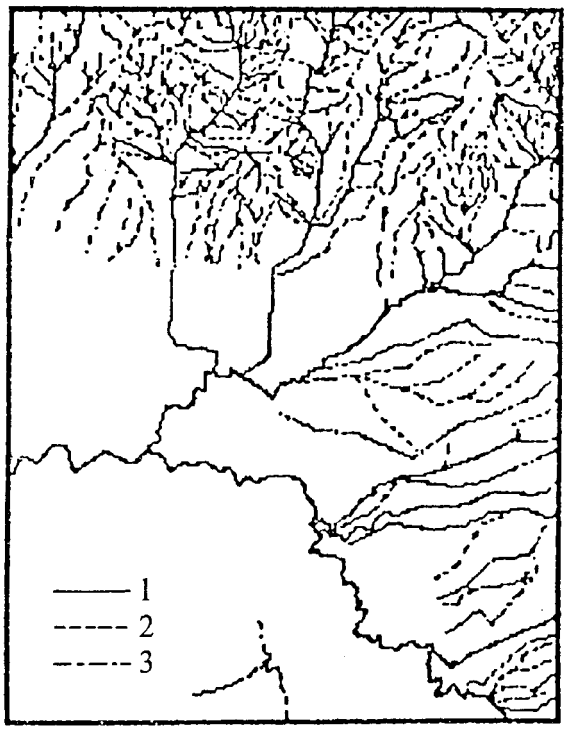

Fig. 4 Hydrological network (Sachok, 1994)
1 – river channels;
2 – hollows;
3 – watershed divides

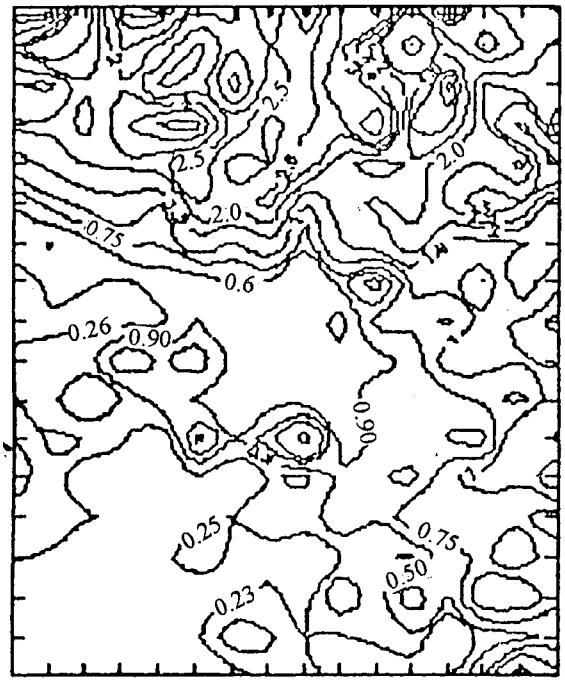

Fig. 5 Gradient of slope in degrees (Sachok, 1994)

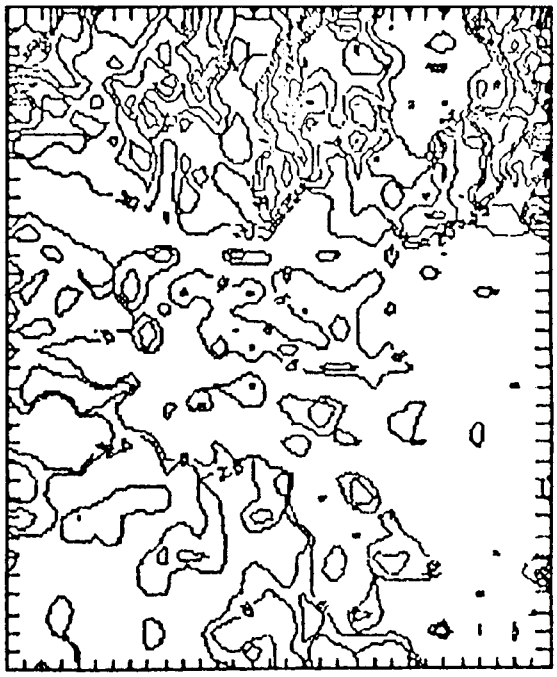

Fig. 6 Sediment yield for the spring snowmelt flood (t/ga) (Sachok, 1994)

Fig. 7 Sediment yield for the period of summer floods (t/ga) (Sachok, 1994)

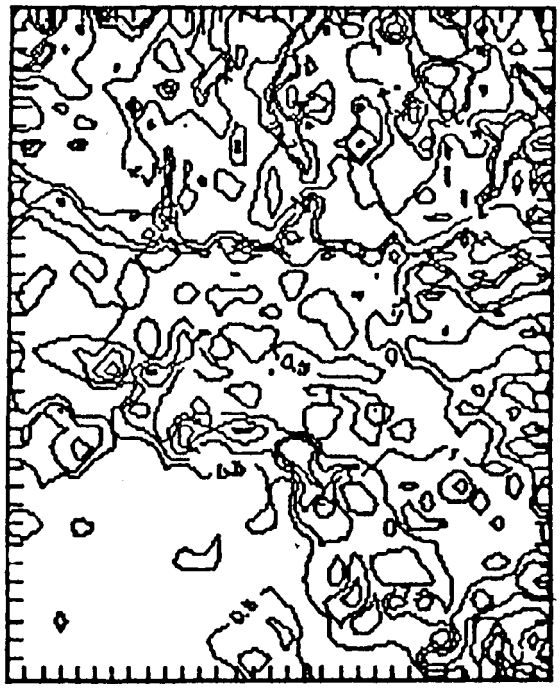

Fig. 8 Annual sediment yield (mm) (Sachok, 1994)

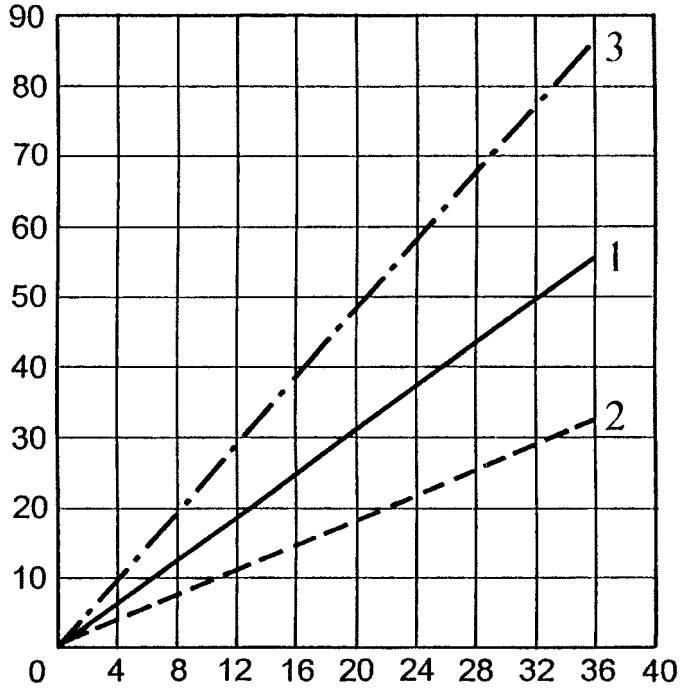

Fig. 9 Dependence sediment yield (t/ga) from gradient of slope (Sachok, 1994)
1 – sediment yield for the spring snowmelt flood (t/ga)
2 – sediment yield for the period of floods (t/ga)
3 – annual sediment yield (t/ga)

years, thereby making them suitable for testing a range of soil erosion and sediment yield models.

Of importance is also the formulation of standardised instrumentation and measurement techniques for assessing soil erosion in different countries. These steps would provide a sound scientific basis for the collection of fresh information to calibrate existing and new soil erosion models.

Bibliography

ANON. (1979) 'Instruction for designing hydrological parameters and their determination for anti-erosion projects in the European USSR'. Leningrad, Gidrometeoizdat, 62 p. (in Russian).

AUTHOR'S CERTIFICATE 886788 (USSR) (1990) 'Method for water flow measurement from slopes'. Invention of Bobrovitskaya. Appl. 25.12.87, N 4349950. Moscow, Publ. in B.I., MKI A 01 B 13/16, 29 p. (in Russian).

BOBROVITSKAYA, N.N. (1979) 'Vorozbitov I.I. Issledovanie vremennoi rucheikovoi seti s ispol'zovaniem aerometodov'. Trudy GGI, vyp. 267, p.53-63

BOBROVITSKAYA, N.N. (1986) 'Methodological recommendations on the use of airborne surveys for investigation and computation of soil erosion characteristics'. In: Y.N. Kornilov (ed.), Leningrad, Gidrometeoizdat, 109 p. (in Russian).

BOBROVITSKAYA, N.N. (1991) 'Metodu issledovaniya, rascheta i kontrolya kharateristic vodnoi erozii pochv' ('The methods for studying, computing and control over the characteristics of soil erosion'). Proc. SHI, Vol. 349, p. 3-18. (in Russian).

BOBROVITSKAYA, N.N., and K.M. ZUBKOVA (1991) 'Vodnoerozionnye prozessy na sklonach I stok nanosov rek Altaiskogo kraya'. Doklady sekzhii ruslovych prozessov Nauchnogo Soveta GKNT, vyp.2 , p. 104-107. (in Russian).

BOGOLUBOVA, I.V., and A.V. KARAUSHEV (1979) 'Problems of ravine formation and evolution'. Trudy GGI, vol. 267, Leningrad, Gidrometeoizdat, p. 5-25 (in Russian).

BORZILOV, V.A.; O.I. VOZZHENNIKOV; I.V. DRAGOLUBOVA and M.A. NOVIZKII (1991) 'Modelirovanie vymyvania radionuklidov iz pochvy dozhdevymi I talymi vodami' ('Modelling of radionuclide wash away from soil by rain and melt waters'). Nauka, p. 103-107. (in Russian).

DOKUCHAEV, V.V. (1888, 1951) Works: 6. 'Preobrazovanie prirody stepei 7. Organizazhiya pochvennych uchrezhdenii I voprosy sel'skogo khozyaistva v Rossii' ('Transformations of steppe environments. 7. Establishing soil institutions and the problems of husbandry in Russia'). Report 1888-1900. Published M., 1951, 596 p. (in Russian).

GARSHINEV, YE. A. and A.T. BARABANOV (1991) 'Metodika polevogo modelirovaniya erozii, rascheta smyva I rasstoyanii mezhdu lesnymi polosami' ('The technique of field erosion modelling, stimating wash away and distances between tree bands') M., All-Union Academy of Agricultural Sciences named after V.I. Lenin, 42 p. (in Russian).

GRIGORJYEV, V.YA. and A.U. SIDORCHUK (1995) 'Prognoz ovrazhnoi erozii tundrovych pochv poluostrova Yamal' ('Forecast of rain erosion of tundra soil on the Yamal Peninsula'). M., Mayak, Nauka, N 3, p. 351-357. (in Russian).

KACHINSKY, N.A. (1963) 'Struktura pochvy. (itogi i perspektivy izucheniya voprosa)'. M.: Izd-vo MGU, 100 p. (in Russian).

KONDRAT'EB, S.A. (1989) ‘Matematicheskoe modelirovanie formirovaniya dozhdevogo stoka I vodnoi erozii na malom sel'skokhozuaistvennom vodosbore // Vodnye resursy’. N 3, p. 14-22. (in Russian).

KORNEV, Ya.V. (1937) ‘Eroziya pozhv kak faktor urozhainosti’ (‘Erosion as a factor of productivity’). /Soil erosion. M., L., p.187-246. (in Russian).

KOSOV, B.F.; E.F. ZORINA; B.P. LYUBIMOV; et al. (1989) ‘Ovrazhnaya eroziya’ (‘Ravine erosion’). In: R.S.Chalov (ed.), MGU Publishing House, 166 p. (in Russian).

KOSTYAKOV, A.N. (1960) *Osnovy melioracii (Bases of amelioration)*. M., 750 p. (in Russian).

KOVDA, V.A. (1985) ‘Biogeokhimiya pochvennogo pokrova’. M.: Nauka, 1985, 263 p.

KOZMENKO, A.S. (1937) ‘Rabotu Novosil'skoi opytno-ovrazhnoi stanzhii po izucheniu priemov bor'by s eroziei’ (‘Studies of Novosil'skoi Experimental Ravine Station on studying the precautions against erosion’). /Soil erosion, M., L., p. 155-185. (in Russian).

KOZMENKO, A.S. (1957) *Bor'ba s eroziei pochv (Struggling with soil erosion)* (*Second Edition*), M., Selkhozgiz, 207 p. (in Russian).

KUZNETSOV, M.S. (1981) *Protivoerosionnaya stoikost' pochv*. M., MGU, 135 p.

LARIONOV, G.A. (1993). *Eroziya I deflyaziya pochv (Soil erosion and deflation)*. M., MGU, p. 200. (in Russian).

NAZAROV, N.A. (1996) ‘Ozhenka erozionnogo smyva pochv I vynosa biogennych veschestv s poverchnocti stokom talych I dozhdebych vod v rechnom bassine’ (‘Assessments of soil erosion wash away and nutrients removal with surface runoff of melt and rain waters in a river basin’). M., MAIK, Nauka, p. 645-652. (in Russian).

POLYAKOV, B.V. (1946) *Hydrological analysis and computations*, Leningrad, Gidrometeoizdat, 480 p.

SACHOK, G.I.; V.V. KAMUSHENKO and G.A., KAMUSHENKO (1994) *Large-scale artographic modelling of soil erosion*. Belorus Academy of Sci., Minsk, 33 p. (in Russian).

SCHEVEBS, G.I. (1981) *Teoreticheskie osnoby erosiovedeniya*. 222 p.

SOBOLEV, S.S. (1970) *Metodika polevogo opyta po bor'be s vodnoi i vetrovoi eroziei pochv*. M., 44 p. (in Russian).

SURMACH, G.P. (1979) ‘Opyt rascheta smyva pochv pri postroenii kompleks protivoerosionnych meropriyatii’. Pochvovedenie, N4, pp.92 - 104.

ZASLAVSKII, M.N. (1979) *Eroziya pochv (Soil erosion)*. M., Mysl', 245 p. (in Russian).

Physically-based erosion and sediment yield modelling: the SHETRAN concept

J.C. Bathurst
Water Resource Systems Research Laboratory,
Department of Civil Engineering, University of Newcastle upon Tyne,
Newcastle upon Tyne NE1 7RU, UK

Introduction

SHETRAN is a physically-based, spatially-distributed, integrated surface/subsurface modelling system for water flow, sediment transport and contaminant migration in river basins, which has been developed at the Water Resource Systems Research Laboratory (WRSRL), Department of Civil Engineering, University of Newcastle upon Tyne. Its original basis was the Système Hydrologique Européen (SHE) hydrological modelling system, conceived in the 1970s by three European research organizations to provide a strong European capability in advanced catchment modelling technology (Abbott et al., 1986a). However, with the addition of sediment transport and contaminant migration components (Bathurst et al., 1995; Ewen, 1995; Wicks and Bathurst, 1996) and extensive revision of numerical solution techniques, SHETRAN has considerably greater capabilities and reliability than the original SHE.

A full description of SHETRAN is given in Ewen et al. (2000). This chapter concentrates on the erosion and sediment yield modelling capability: it describes SHETRAN's distinctive features and reviews a decade of development and application of the sediment component.

Compared with more traditional modelling approaches SHETRAN has particular advantages in representing distributed responses at catchment scales from less than 1 km^2 to 2000 km^2, in predicting the impacts of land use and climate change, in incorporating landslide and gully erosion and in exploring issues such as scale effects and validation techniques which are at the forefront of physically-based modelling research.

There is considerable concern worldwide about the impacts of environmental change induced by human activity. Hydrological issues include the effects of large scale deforestation and climate change on soil erosion and flow regime and the dispersal of contaminants from agricultural and industrial activities. Increasingly, therefore, it is accepted that the development of river basins for economic purposes should be tempered by the maintenance of an acceptable environmental quality. Establishing the necessary trade-off between economic development and environmental quality is a decision-making process involving many elements, one of which is an appreciation of how environmental systems respond to imposed change. In particular, there is a need to assess the impacts of different levels of development on basin hydrology, soil erosion and contaminant concentrations, in advance of any development taking place. Environmental impact and economic return can then be weighed against each other for different levels of development, providing a rational basis for selecting an optimum development strategy.

Mathematical modelling is increasingly relevant to impact assessment but needs to be based on a sound physical understanding of the relevant basin response mechanisms. The task of representing a river basin in a range of possible future altered states is beyond the traditional black box and conceptual hydrological models. These are essentially regression relationships between rainfall and runoff: their parameters have no physical meaning and depend on the availability of sufficiently long meteorological and hydrological records for their calibration. Such records are frequently unavailable but, even when they are available, they refer only to the past state of a basin. Calibration cannot therefore be extended to a future altered state. These models are also spatially lumped, so cannot explicitly account for spatial variation in basin characteristics, rainfall input and hydrological response.

By contrast, physically-based, spatially-distributed modelling systems have particular advantages for the study of basin change impacts and applications to basins with limited records. Their parameters have a physical meaning (e.g., soil conductivity and sediment size distribution) and can be measured in the field. Model validation can therefore be concluded on the basis of a short field survey and a short time series of meteorological and hydrological data. Parameter values can also be specified for a future altered state of the basin, for example a change in vegetation characteristics, thus supporting land use change impact studies. Basin response is represented on both a spatially and a temporally distributed basis and in terms of multiple variable outputs: i.e., rather than providing just one output variable, such as basin discharge, physically-based models provide predictions of all relevant hydrological, sediment and contaminant variables.

Disadvantages of physically-based models include heavy computer requirements, the need to evaluate many parameters (with associated problems of representation at different spatial scales and uncertainty) and a complexity which implies a lengthy training period for new users.

SHETRAN

SHETRAN is a general, physically-based, spatially-distributed modelling system: that is, it can be used to construct and run models of all or any part of the land phase of the hydrological cycle (including sediment and contaminant transport) for any geographical area. It is physically-based in the sense that the various flow and transport processes are modelled either by finite difference representations of the partial differential equations of mass, momentum and energy conservation, or by empirical equations derived from experimental research. The model parameters have a physical meaning and can be evaluated by measurement. Spatial distributions of basin properties, inputs and responses are represented on a three-dimensional, finite-difference mesh. The channel system is represented along the boundaries of the mesh grid squares as viewed in plan.

SHETRAN hydrological component

SHETRAN's hydrological component consists of subcomponents accounting for evapotranspiration and interception, overland and channel flow, subsurface flow, snowmelt and channel/surface aquifer exchange (Figure 1). The component is continually evolving as new process descriptions and solution schemes are introduced. The version used in the case studies described later is Version 3.4. This is similar to the original SHE in that it represents the subsurface as an unconfined aquifer in which a one-dimensional (vertical flow) unsaturated zone overlies a two-dimensional (lateral flow) saturated zone. Integration with the overland flow subcomponent allows overland flow to be generated both by an excess of rainfall over infiltration and by upward saturation of the soil column. Table 1 summarizes the processes modelled and the equations used to describe them. Detailed descriptions of the subcomponents can be found in Abbott et al. (1986b), Bathurst et al. (1995) and Ewen et al. (2000). In Version 4, the latest version of SHETRAN at the time of writing, the subsurface is modelled by a fully three-dimensional variably saturated soil scheme which enables such features as perched water tables and hypodermic flow (i.e., just beneath the soil surface) to be accounted for. Version 5 is currently under development for PC use: until now the model has been run on Unix-based workstations.

Table 1 Processes modelled by the SHETRAN hydrological component, Version 3.4

(1)	Interception of rainfall on vegetation canopy (Rutter storage model)
(2)	Evaporation of intercepted rainfall, ground surface water and channel water; transpiration of water drawn from the root zone (Penman-Monteith equation or the ratio of actual to potential evapotranspiration as a function of soil moisture tension)
(3)	Snowpack development and snowmelt (temperature-based or energy budget methods)
(4)	One-dimensional flow in the unsaturated zone (Richards equation)
(5)	Two-dimensional flow in the saturated zone (Boussinesq equation)
(6)	Two-dimensional overland flow; one-dimensional channel flow (Saint Venant equations)
(7)	Saturated zone/channel interaction, including an allowance for an unsaturated zone below the channel
(8)	Saturated zone/surface water interaction

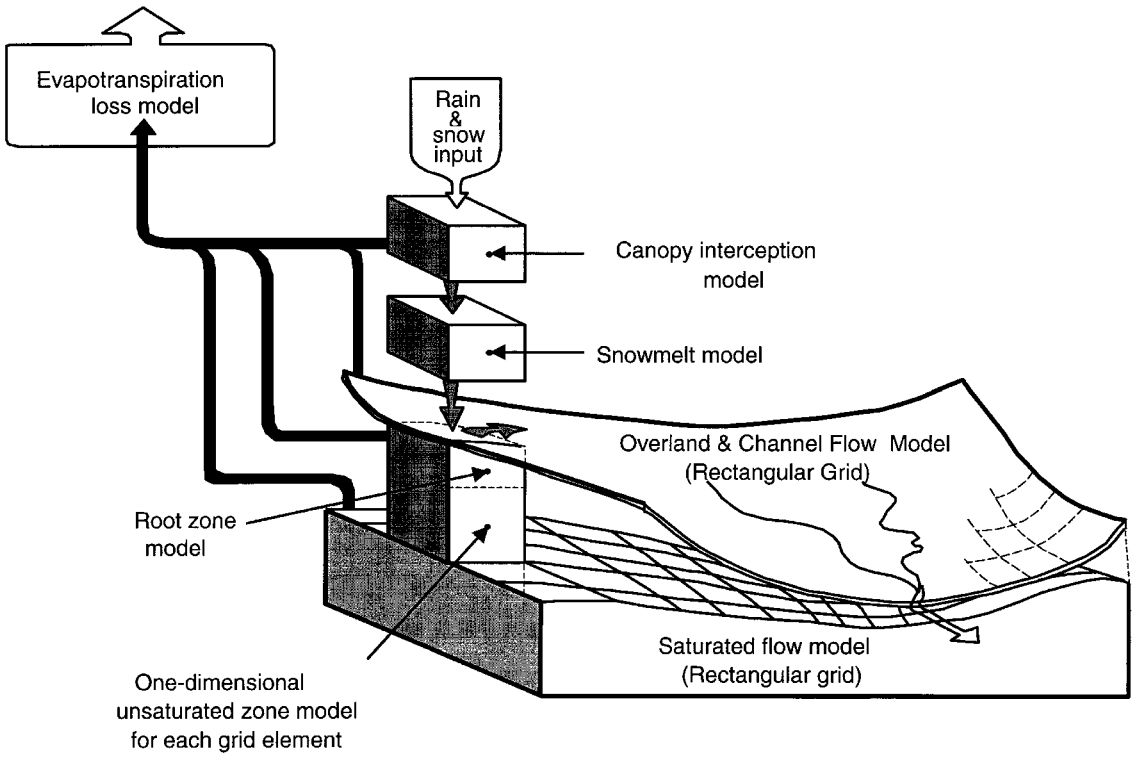

Fig. 1 Schematic diagram of the SHETRAN hydrological component

SHETRAN erosion and sediment yield component

The basic erosion and sediment yield component consists of subcomponents accounting for soil erosion by raindrop impact, leaf drip impact and overland flow, channel bed and bank erosion by channel flow, and sediment transport by overland and channel flow (Figure 2).

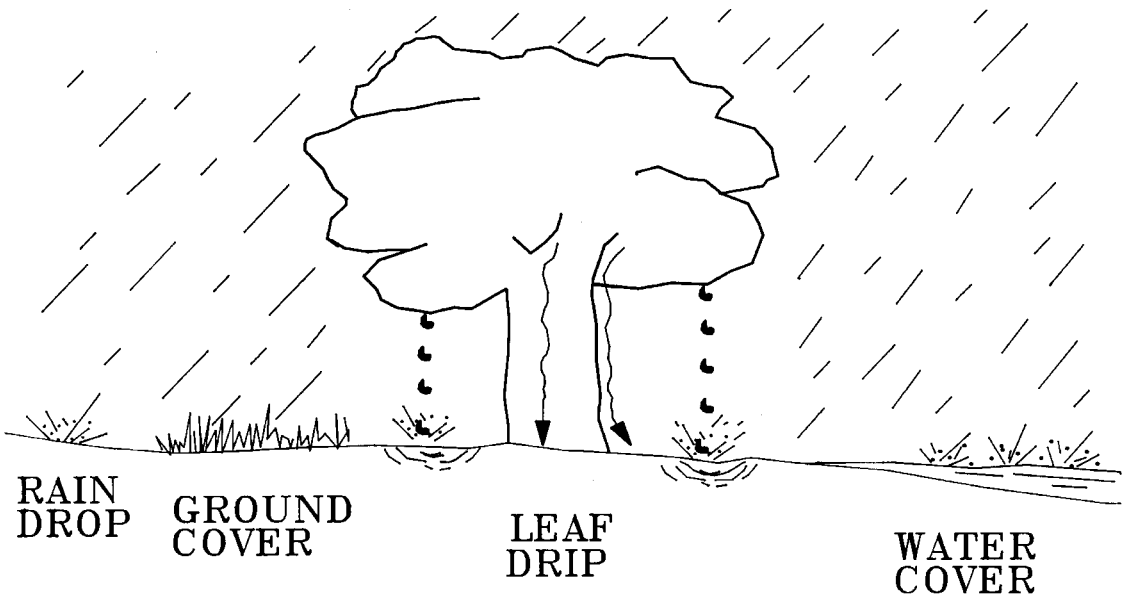

Fig. 2 Soil detachment by raindrop and leaf drip impact, modified by ground cover, canopy cover and surface water layer, as represented in the SHETRAN erosion and sediment yield component (From Bathurst et al., 1995)

The component is driven by inputs from the hydrological (water flow) simulations but feedback to the flow simulations is not modelled as the effects are unlikely to be significant at

the sediment concentrations and relative scales of erosion and deposition typically considered. Table 2 summarizes the processes modelled and the equations used to describe them. More detailed descriptions of the subcomponents can be found in Bathurst et al. (1995), Wicks and Bathurst (1996) and Ewen et al. (2000). However, it will be useful for the reader to know that the equations for determining soil erosion are, for raindrop and leaf drip impact:

$$D_r = k_r F_w (1 - C_g - C_r)(M_r + M_d) \quad (1)$$

and for overland flow:

$$D_f = k_f (1 - C_r)\left(\frac{\tau}{\tau_c} - 1\right) \quad for\ \tau > \tau_c \quad (2a)$$

$$D_f = 0 \quad for\ \tau \le \tau_c \quad (2b)$$

where D_r and D_f = the respective rates of detachment of material per unit area (kg m^{-2} s^{-1}); k_r = raindrop impact soil erodibility coefficient (J^{-1}); k_f = overland flow soil erodibility coefficient (kg m^{-2} s^{-1}); C_g = proportion of ground protected from drop/drip erosion by near ground cover such as low vegetation (range 0-1); C_r = proportion of ground protected against drop/drip erosion and overland flow erosion by, for example, rock cover (range 0-1); M_r = momentum squared for raindrops falling directly on the ground ((kg m s^{-1}) m^{-2} s^{-1}); M_d = momentum squared for leaf drip ((kg m s^{-1}) m^{-2} s^{-1}); F_w accounts for the effect of a surface water layer in protecting the soil from raindrop impact (dimensionless); τ = overland flow shear stress (N m^{-2}); and τ_c = critical shear stress for initiation of soil particle motion (N m^{-2}). The soil erodibility coefficients k_r and k_f increase in value as the soil becomes easier to erode (i.e., sandy soils have larger values than clayey soils). However, they have not yet been quantitatively related to a measurable soil property and must therefore be determined empirically (e.g, Wicks et al., 1992).

Table 2 Processes modelled by the basic SHETRAN erosion and sediment transport component

(1)	Soil erosion by raindrop impact, leaf drip impact and overland flow (see text for equations)
(2)	Two-dimensional total load convection in overland flow by size fraction, including input to the channels; deposition and resuspension of sediments in overland flow (mass conservation equation incorporating Engelund-Hansen total load and Yalin bed load transport capacity equations)
(3)	One-dimensional convection of cohesive and noncohesive sediments in channel flow by size fraction; deposition and resuspension of noncohesive sediments in channel flow; channel bed erosion by channel flow (mass conservation equation incorporating Ackers-White and Engelund-Hansen transport capacity equations)

Landslide erosion and sediment yield component

Through its integrated surface and subsurface representation of river basins, SHETRAN provides not only the overland and channel flows needed for sediment transport modelling but also soil moisture conditions and hence a basis for simulating rain- and snowmelt-triggered landsliding. A component has therefore been developed to simulate the erosion and sediment yield associated with shallow landslides at basin scales of up to about 500 km^2. The occurrence of shallow landslides is determined as a function of the time- and space-varying soil saturation conditions simulated by SHETRAN, using factor of safety analysis. For each landslide the volume of eroded material is determined and routed down the hillslope as a debris flow. Finally the proportion of this material reaching the channel network is

calculated and fed to the SHETRAN sediment transport component for routing to the basin outlet (Bathurst et al., 1997; Burton and Bathurst, 1998). Figure 3 shows an example.

The central feature of the component is a dual resolution approach whereby the basin hydrology is modelled at the SHETRAN grid resolution (which may be as large as 1-2 km) while landslide occurrence and erosion are modelled at a subgrid resolution characteristic of the landslide dimensions (typically 10 - 100 m). A disaggregation technique involving a wetness index is used to link the two scales so that landslide occurrence at the subgrid scale is determined as a function of the soil saturated zone thickness at the SHETRAN grid scale.

The component's applicability at scales ranging from less than a square kilometre to around 500 km^2 and its ability to determine sediment yield distinguish it from other basin scale landslide models which are limited to a few square kilometres or less and provide only the distribution of landslides (e.g., Montgomery and Dietrich, 1994; Wu and Sidle, 1995).

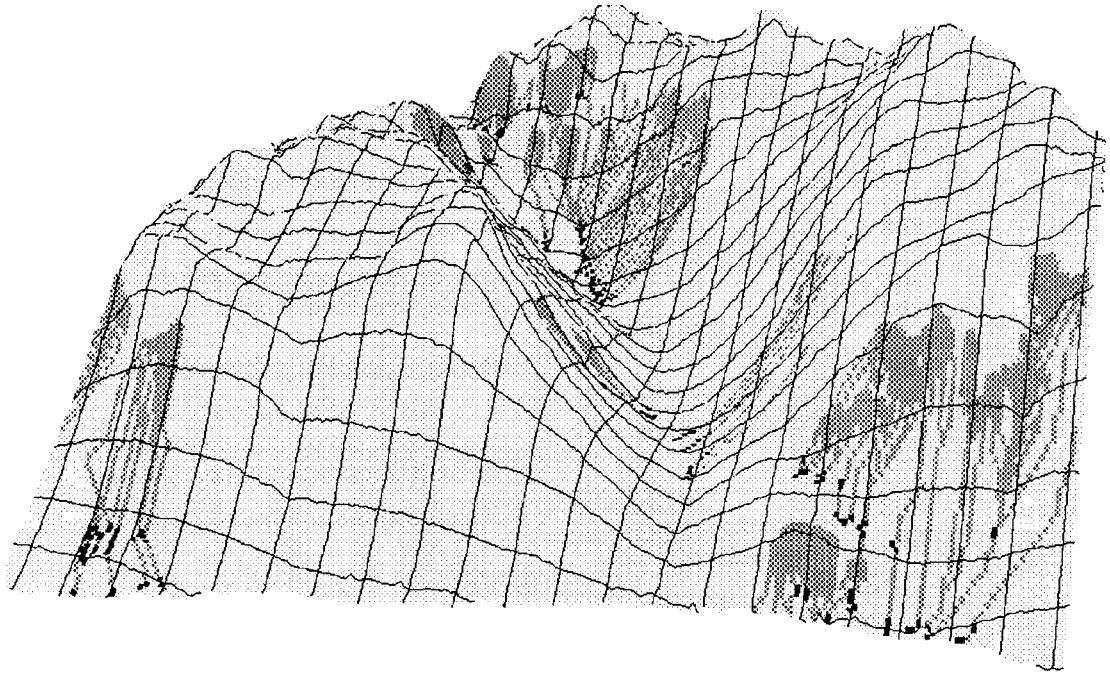

Fig. 3 Simulation of landslide erosion, showing landslide sites, debris flow trajectories and deposition sites

Gully erosion and sediment yield component

The dual resolution approach of the landslide model has also been applied to build a component for modelling the erosion and sediment yield arising from gullying (Bathurst et al., 1998a). In this case the subgrid resolution is around 100 m, typical of gully scales. Sediment discharge from each gully is determined as a function of water discharge (derived by seepage through the gully wall or by local overland flow) and gully properties. The water discharge is determined as a function of phreatic surface elevation and overland flow generation at the subgrid scale, which in turn are related to conditions at the SHETRAN grid resolution using the wetness index. A transfer function is applied to add the gully sediment discharge to the SHETRAN channel network for routing to the basin outlet. This is still a poorly researched area: in this case the proportion of the eroded material transferred to the channel is determined arbitrarily according to the distance of the gully from the channel. Gully growth is simulated by increasing the gully volume in accordance with the amount of sediment discharged. The

component is believed to be the only model of gully sediment yield applicable at basin scales of up to 500 km^2.

SHETRAN data needs

The data required by SHETRAN comprise:

1) Time series of meteorological inputs (precipitation and evapotranspiration) needed to drive the simulation;
2) Time series of output variables (e.g., river discharge and sediment yield records) for validating the model;
3) Property data which characterize the river basin (soil, vegetation, topographic and sediment characteristics).

These data may be based on direct measurements or may be estimated from information in the literature. They may refer to existing basins and conditions or to scenarios of, for example, future altered climates or vegetation covers.

Simulation procedure

A mesh is set up which defines the spatial extent of the basin model and which is used for representing spatial variability in the basin properties. (Computing power is the principal limitation on the number of mesh squares and thence their size for a given basin area. Currently a maximum number of about 400 squares is recommended.) The appropriate

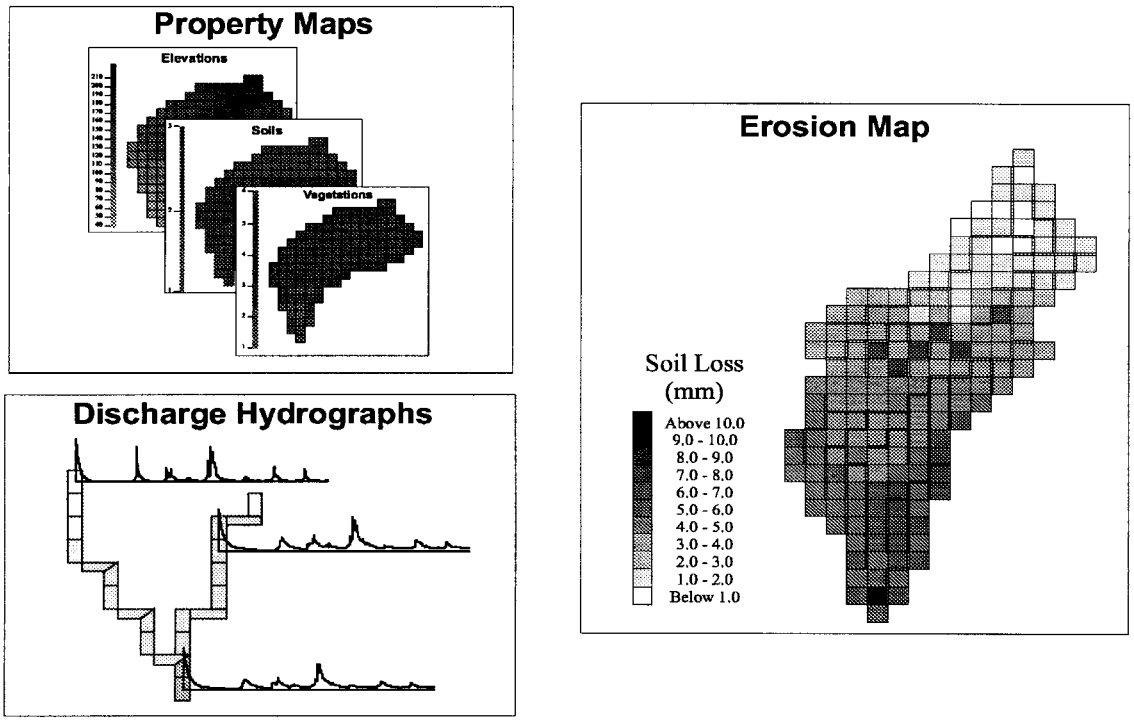

Fig. 4 Examples of SHETRAN data displays: catchment property maps; simulated hydrographs at selected sites along a channel network (represented in plan); and an output map of simulated soil loss across a catchment

meteorological data, spatially and temporally distributed, are fed into the basin model. Each SHETRAN subcomponent is applied at each grid square to generate a response (e.g., overland flow, phreatic surface rise, soil erosion). These responses interact and both surface and subsurface waters, and surface sediments, are routed from square to square. Eventually these products reach the river system and are routed towards the basin outlet. Model outputs may be obtained for any part of this procedure on a spatially and temporally distributed basis. They may include time-varying records of phreatic surface level, snowpack depth, overland flow depth, soil erosion or any other variable at any grid square or channel link within the basin. Alternatively, synoptic views of the spatial distribution of any variable across the basin at any time can be produced (Figure 4).

Parameter uncertainty and model validation

The current physically-based models are subject to a number of important constraints (e.g., Beven, 1989; Grayson et al., 1992), with particular uncertainty in the evaluation of model parameters. It is now generally acknowledged that the uncertainty in model parameterization and its implications for model output should be explicitly recognized in the modelling procedure (e.g., Beven and Binley, 1992; Ewen and Parkin, 1996; Quinton, 1997). The following method of quantifying uncertainty bounds for SHETRAN applications has therefore been adapted from Ewen and Parkin (1996).

Using hydrological judgement, and possibly a degree of calibration, upper and lower bounds are set on the more important model parameters, reflecting uncertainty in the values. A series of simulations is carried out so that each parameter takes the range of values assigned to it. The number of simulations depends on the number of parameters involved, the number of values assigned to each parameter and the number of combinations of different parameter values considered. The simulation outputs are then superimposed in each other and the overall time series of maximum and minimum output bounds extracted. These bounds are typically composed of contributions from several of the simulation outputs. The bounds on the model parameters thus translate into bounds on the model output and conclusions on model performance are drawn according to the width of the resulting output envelope and the extent to which it contains the measured data. This technique considers only the uncertainties associated with parameter evaluation. It does not account for less well understood errors such as the error of approximation implicit in the way SHETRAN represents the complex non-linear physical processes active in a catchment.

The model parameters or functions to which the simulation results are typically most sensitive in full basin simulations are : saturated zone hydraulic conductivity; unsaturated zone hydraulic conductivity; Strickler resistance coefficient for overland flow; soil retention curve (the relationship between tension and moisture content); the relationship between the ratio of actual to potential evapotranspiration and soil moisture tension; and, for sediment simulations using Equations 1 and 2, the soil erodibility coefficients.

Examples of land use and climate change impact simulations

The following examples demonstrate SHETRAN's capabilities for simulating the impacts of land use and climate change on hydrological and sediment yield response. Full details of the applications are in the cited references and only the main points are presented here.

Parameter evaluation for different land covers

The capability of the model to represent the effects of different land managements on erosion and sediment yield was demonstrated by evaluating the erodibility coefficients k_r and k_f (Equations 1 and 2) for erosion plots with different covers. The simulations were carried out with a predecessor of SHETRAN but with essentially the same sediment model. The test data were taken from rainfall-simulator erosion studies carried out at the Reynolds Creek

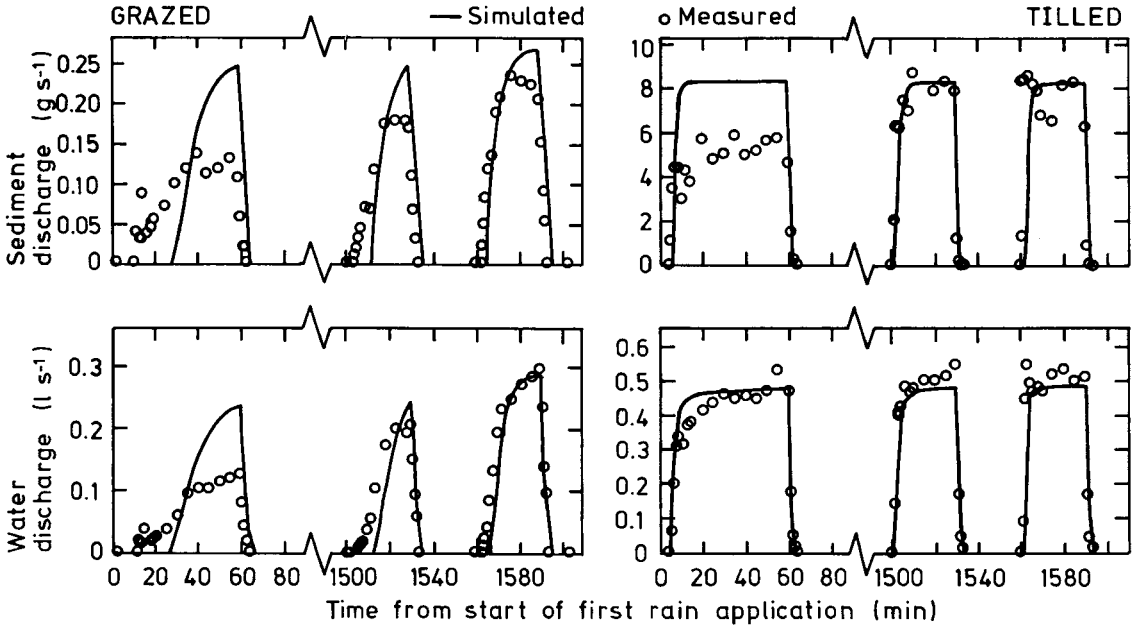

Fig. 5 Comparison of simulated and observed runoff and sediment discharge responses for grazed and tilled plots, Reynolds Creek rangeland research basin, Idaho

rangeland research basin, Idaho, by the Northwest Watershed Research Center of the United States Department of Agriculture's Agricultural Research Service. A full description of the work is provided in Wicks et al. (1982, 1992).

Each erosion plot was 3.05 m wide and 10.67 m long (32.54 m^2 in area). Water was applied from a rotating-boom rainfall simulator at approximately 60 mm h^{-1} in a sequence of three runs : 1) 60-minute application to an initially dry soil; 2) 30-minute application about 24 hours after run (1); 3) 30-minute application 30 minutes after run (2). In this way three different antecedent soil moisture conditions were considered : dry, wet and very wet. The experiments incorporated several ground treatments but the results shown here refer to tilled ground (well pulverized bare soil) and the natural brush and grass cover subjected to cattle grazing.

Each three-event rainfall sequence (over about 26.5 hours) was simulated on a continuous basis. Figure 5 compares the simulated and observed runoff and sediment discharge responses for one of the grazed plots and one of the tilled plots. There is generally good agreement in each case, with the wet and very wet runs being particularly well simulated, indicating the model's ability to link successive rainfall events with appropriate changes in soil-moisture conditions. Just as important, though, is the model's ability to reproduce the broad differences in response between the two land treatments, especially the distinctive hydrograph shapes. This shows also in the significant and physically realistic variations in the calibrated erodibility coefficients: $k_r = 1.3\ J^{-1}$ and $k_f = 0.65$ mg $m^{-2}\ s^{-1}$ for the grazed plots and $k_r = 11.8\ J^{-1}$ and $k_f = 5.9$ mg $m^{-2}\ s^{-1}$ for the more easily eroded tilled plots.

Further plot studies such as this may provide a basis for determining empirical relationships giving the erodibility coefficients as a function of soil properties and land management.

Impact of reforestation on sediment yield

SHETRAN's ability to model the impacts of land use change on sediment yield was investigated using the data from two of the Draix research basins, administered by the French agency CEMAGREF, near Digne in southeast France (Lukey et al., 1995, in press; Bathurst et al., 1998b). A model was first constructed for the 86-ha Laval basin which is severely affected by badlands erosion : vegetation cover is about 32%, the mean annual runoff/rainfall ratio is about 21% and the sediment yield is about 127 t ha^{-1} yr^{-1}. The model was then altered to represent the Laval basin as if it were equivalent to the neighbouring 108-ha Brusquet basin, which was successfully rescued from badlands erosion by reforestation in the early 1990s: its vegetation cover is about 87%, the runoff/rainfall ratio is around 5% and sediment yield is in the range 0.03-2.75 t ha^{-1} yr^{-1}. The aim was to test the ability of SHETRAN to produce hydrological and sediment yield responses similar to those measured in the Brusquet basin, within a quantified representation of parameter uncertainty. Changes in the model parameters to create a reforested Laval basin included : specification of forest vegetation for all model grid squares, with appropriate ground cover and leaf drip parameters; reduction in the Strickler flow resistance coefficient for overland flow from 10 to 3 to simulate the greater resistance of a vegetated ground surface relative to bare soil; and setting the erodibility coefficient for overland flow k_f to zero to represent the protective effect of the vegetation. It was also necessary to replace the Laval rainfall series (mean annual value of 876 mm) with the Brusquet series (767 mm).

Figure 6 compares the simulated and measured sediment yields for 22 measurement periods during 1987-91 for the existing Laval basin. The vertical lines represent the uncertainty range between the upper and lower predictions for each period (derived using the method of Ewen and Parkin (1996) described earlier). The horizontal lines represent the uncertainty range in the measured yields. Bearing in mind the difficulties of simulating the characteristically flashy nature of the Laval response and the complexity of the badlands environment, the comparison is extremely encouraging: there is reasonable overlap of the measured and simulated ranges and the observed variation in sediment yield between measurement periods is mostly well reproduced, as is the long term yield. The model was therefore accepted as the basis for the reforestation study.

Figure 7 compares the simulated yields for the reforested Laval basin with the measured yields for the Brusquet basin (appropriately scaled for basin size). Only three measurements were carried out during 1987-91 as the sediment yield is so low. Again there is good agreement between the simulated and measured yields.

Comparison of Figures 6 and 7 shows that SHETRAN is able to simulate the two orders of magnitude reduction in sediment yield from the Laval to the Brusquet basin as a function of altered vegetation cover and rainfall. The simulated changes are larger that the output uncertainty. These results show how SHETRAN can be used to model land use change impacts but indicate also the need to reduce further the uncertainty in model parameter evaluation.

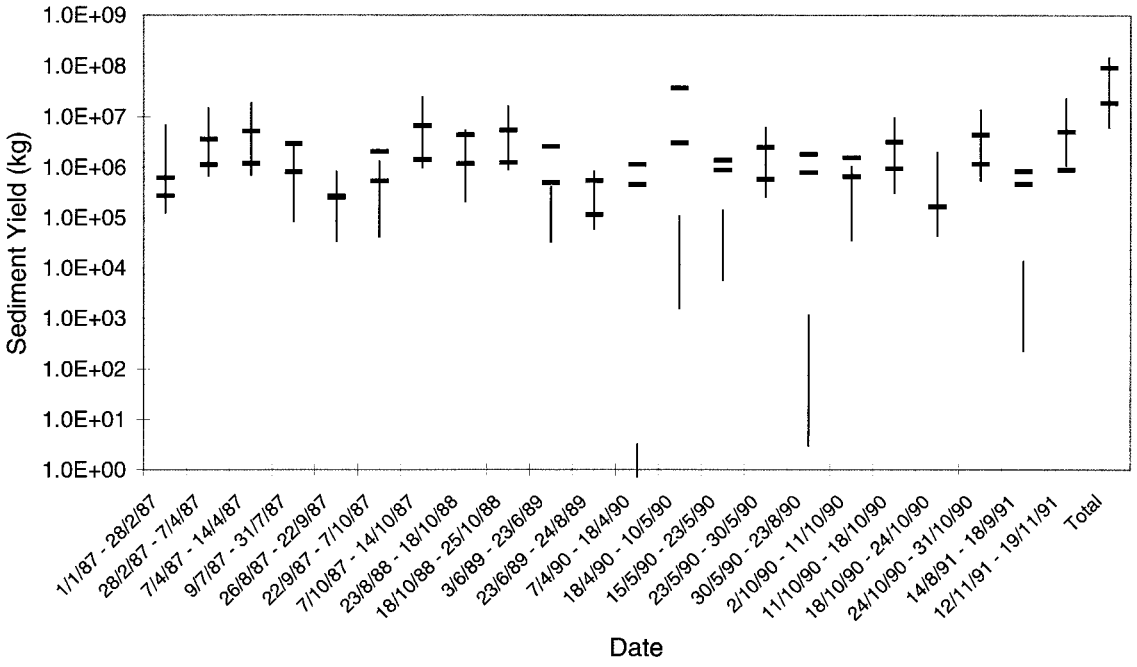

Fig. 6 Comparison of the Laval simulated sediment yield bounds and measured yields for 22 measurement periods and for the combined period during 1987-1991. The vertical lines represent the simulated range, the horizontal lines represent the uncertainty range in the measurements (From Lukey et al., in press)

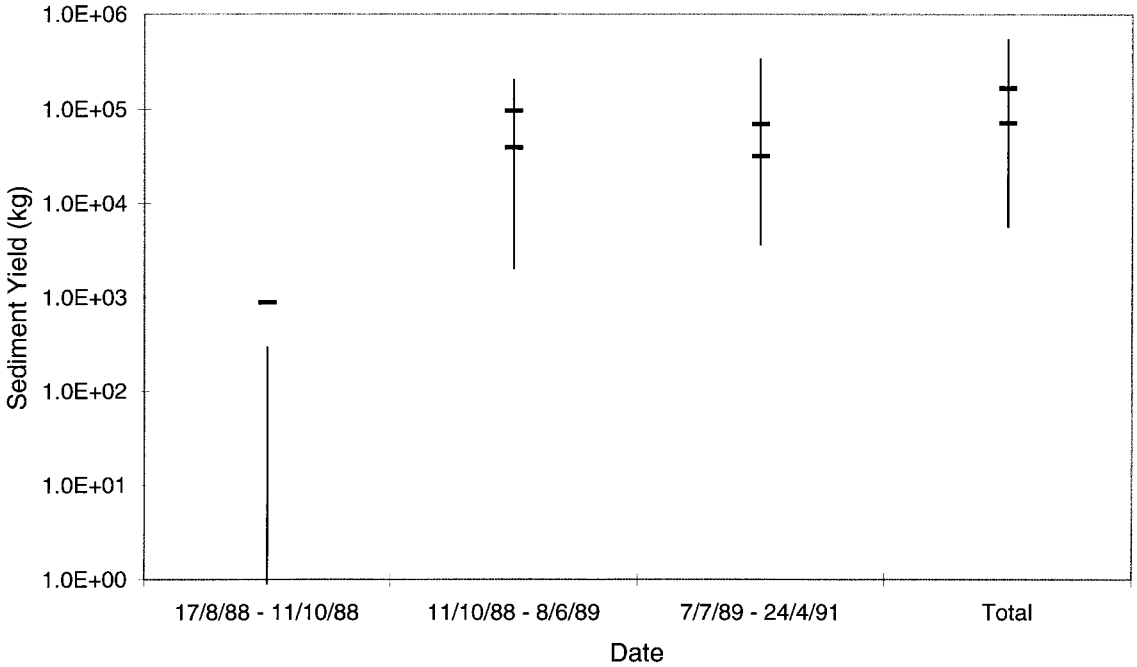

Fig. 7 Comparison of the measured Brusquet sediment yields with the simulated sediment yield bounds for the reforested Laval basin with Brusquet rainfall for three measurement periods and for the combined period within 1988-1991. The vertical lines represent the simulated range, the horizontal lines represent the uncertainty range in the measurements. The horizontal lines coincide for the first period (From Lukey et al., in press)

Table 3 Results of SHETRAN application to the Cobres basin

Simulation	Year[a]	Annual rainfall (mm)	Annual potential evapo-transpiration (mm)	Runoff (mm)		Simulated runoff r^2	Simulated sediment yield[e] (t ha^{-1} $year^{-1}$)	
				Measured	Simulated		Normal	Extreme
Wet	1977-78	657[b]	1362[d]	199	213	-	-	-
(calibration)	1978-79	693[b]	1419[d]	369	370	-	-	-
	1977-79	1350[b]	2781[d]	568	583	0.83	0.28	0.62
Dry	1980-81	250[b]	1525[d]	0	8	-	-	-
(validation)	1981-82	483[b]	1489[d]	86	100	-	-	-
	1980-82	733[b]	3014[d]	86	108	0.81	0.07	0.15
Mean	1983-84	509[b]	1505[d]	124	134	-	-	-
(validation)	1984-85	541[b]	1583[d]	108	120	-	-	-
	1983-85	1050[b]	3088[d]	232	254	0.61	0.09	0.17
1 x CO_2	-	501[c]	1458[c]	-	125	-	0.091	0.14
2 x CO_2	-	414[c]	1720[c]	-	56	-	0.066	0.084

[a] Years are defined October to September.

[b] Basin mean rainfall calculated from measurements at five rain gauges.

[c] Generated from GCM data.

[d] Potential evapotranspiration calculated by Penman combination method from measured data.

[e] Sediment yield simulated using the normal and extreme values of the erodibility coefficients; yields are the mean annual values for the relevant 2-year period.

Climate change impact

SHETRAN's ability to predict the impacts of possible future climate change on runoff and sediment yield was demonstrated in an application to the 701-km^2 Cobres basin in Portugal (Bathurst et al., 1996). The model was first validated for present-day conditions and then run with altered time series of rainfall and potential evapotranspiration. The Cobres basin is relatively homogenous with low relief, uniform soil and extensive wheat production; soil erosion has been a long term problem.

The present-day conditions were represented by three 2-year periods, each beginning in October : 1977-79 (wetter than average), 1980-82 (drier than average) and 1983-85 (average), referred to here as the wet, dry and mean periods. The model was calibrated for the wet period and validated for the dry and mean periods in terms of outlet discharge. Results at the annual level are shown in Table 3 and are generally satisfactory. The validations for the dry and mean periods constitute a rigorous test of the model since the rainfall totals in each were substantially less than in the wet period and the soil conditions antecedent to rainfall might therefore be expected to differ considerably.

Based on local erosion-plot studies, two sets of values were used for the erodibility coefficients. The "normal" values (k_r = 0.13 J^{-1}, k_f = 1.3 mg m^{-2} s^{-1}) accounted for most of the observed plot sediment yields. The "extreme" values (k_r = 2 J^{-1}, k_f = 20 mg m^{-2} s^{-1}) represented large yield events; possibly these involved rill erosion, which is not explicitly described in SHETRAN. However, for both sets the sediment yields simulated for the Cobres basin (Table 3) are at the lower end of the range 0.1 – 10 t ha^{-1} year^{-1} which has been observed for catchments of around 1000 km^2 in area (Walling, 1983).

Data for the future climate conditions were obtained from a General Circulation Model (GCM) which has been used to simulate the climate with current levels of atmospheric carbon dioxide (denoted 1 x CO_2) and a climate represented by doubled carbon dioxide levels (denoted 2 x CO_2). The 2 x CO_2 conditions provided the basis for the future climate, while the 1 x CO_2 conditions provided the control climate. In each case the 12-hour GCM data were disaggregated to give hourly rainfall and daily potential evapotranspiration relevant at the station level for the Cobres region and appropriate time series were generated.

Simulations with the 1 x CO_2 and 2 x CO_2 climates were carried out for 40-year periods. The results are summarized in Table 3, which shows that the 1 x CO_2 condition is representative of present-day conditions and is therefore a suitable control against which to examine the effect of the 2 x CO_2 climate. The reducion in mean annual rainfall from the 1 x CO_2 (501 mm) to the 2 x CO_2 (414 mm) condition is considerable but is still rather less than the natural variability. There is corresponding reduction in mean annual runoff and sediment yield but again there is greater observed variability between, for example, the wet, dry and mean periods. It may therefore be concluded that : a) annual sediment yield is critically dependent on only one or two events in each year; and b) on an annual basis, more significant sediment yield impacts are likely to arise from inter-annual variability than from a shift in climate.

This study demonstrates how SHETRAN can be run with generated climate scenario data to provide predictions of future water and sediment yields. Such predictions are of use in, for example, optimising control strategies for future land management.

Parameter scale effects

Within each model grid square, each physical characteristic is represented by one parameter value. As long as the grid square is small compared with the distances over which there is significant spatial variability in catchment properties and hydrological response, this does not compromise the model's ability to represent local variations in response. However, as grid scales increase, the local spatial variability in properties and response becomes subgrid. There are then difficulties in applying the equations of small scale physics which make up SHETRAN and evaluating their parameters at the grid scale (e.g. Beven, 1989). In particular, the field measurements which form the basis of parameter evaluation are most easily carried out at the point or plot scale, which may not be representative of large grid scales. The solution has been to use "effective" parameter values, which represent the subgrid spatial variability, to give a grid scale response. However, this is a pragmatic approach and it is recognized that the concept may not allow an accurate reproduction of the observed response in all circumstances (as shown for example by Binley et al., 1989). There has also yet been enough research to establish the relationship between the effective parameter value (possibly determined through calibration) and field measurements. However, experience to date suggests that the SHETRAN simulations are robust in this regard and that scale dependency needs to be considered only for the more important parameters. In particular, there is a possibility that the model saturated zone conductivity may increase to compensate for the reduction in simulated groundwater gradients caused by use of large grid squares. Similarly the overland flow resistance might decrease to account for the inclusion of subgrid channel flow within a large grid square or increase to account for the impediments to flow caused by subgrid topography and vegetation distribution.

Studies with SHE, SHETRAN and ANSWERS (another distributed model) suggest that the same model parameter values can be applied at both plot (1-100 m^2) and microbasin (order 1 ha) scales, using small model grid spacings (20 m or less) and with a good availability of field data (Wicks et al., 1988; Connolly and Silburn, 1995; Figueiredo, 1998). For larger basins, scale effects in evaluating saturated zone conductivity appear not to be significant, or at least to be masked by uncertainty in parameter evaluation, as long as basin topography is subdued and there is a general homogeneity of land use, soil characteristics and hydrological response within the basin. Applications of the SHE to large basins in India (area 800-5000 km^2) (Refsgaard et al., 1992; Jain et al., 1992) and to the Cobres basin in Portugal (area 701 km^2) (Bathurst et al., 1996) suggest that conductivities evaluated at the point or small scale can be successfully applied with a model grid spacing of 2 km. Figueiredo (1998) similarly found no evidence of a scale effect when modelling a 137 km^2 basin in northeast Brazil, although in this case the basin did not typically have a saturated zone in the soil column. For the dissected terrain of the Draix basins Bathurst et al. (1998b) concluded that any scale effects which may distinguish simulations at the scales of 0.133 and 86 ha were small enough to be masked by uncertainty in parameter evaluation. However, for basins of 200-2000 km^2 with hilly terrain, unpublished simulation results suggest that the saturated zone conductivity may indeed increase as the grid spacing rises to 1 or 2 km. This dependency has so far been observed empirically and requires closer study.

For overland flow resistance, the picture is less clear. If there is any scale dependency the effect does not appear to be large and other factors such as the type of ground roughness (perhaps determined by land use) may be more important. No scale dependency has yet been observed in the soil erodibility coefficients.

Validation data

A distinguishing feature of physically-based, spatially-distributed sediment yield models is their ability to simulate spatial and temporal variations in erosion and sediment fluxes, enabling, for example, erosion maps to be produced and peak sediment discharges to be predicted. To generate confidence in this ability it is important that it can be validated against measured data. However, the only commonly available data are measurements at the basin outlet. These enable the ability of the model to reproduce the integrated basin response to be tested but are not a basis for indicating whether the simulated responses incorporate a sound representation of the distributed internal basin behaviour. For example, it might be possible to simulate an apparently correct outlet response on the basis of incorrect but compensating internal responses. A model validated in this way could not be applied with confidence to conditions outside the range used for validation. A further limitation is that sediment yield data at basin outlets are often of a bulk, or time-integrated, nature, for example from trap measurements or reservoir sedimentation surveys. These enable the ability to model long term sediment yields to be validated but do not test the ability to represent time-varying sediment discharge at the scale of, for example, a storm event.

Validating the ability to model spatial and temporal variations in erosion and sediment fluxes requires spatially and temporally varied measurements. Over the last decade or so, developments in field instrumentation and advances in data collection techniques have provided the capability for satisfying much of this demand. However, not all these measurements have yet become routine.

1) Time-varying suspended sediment concentration at a site can be measured using turbidity meters and pump samplers (e.g., Gippel, 1995; Morris and Fan, 1997). These are reliable, except in the more extreme environments, but require frequent servicing. Techniques for measuring time-varying bed load discharge are still mainly limited to research studies and include vortex tubes, traps with pressure transducers for measuring accumulating weight and acoustic meters (e.g., Reid et al., 1980; Tacconi and Billi, 1987; Bänziger and Burch, 1990). Long term variations in sediment yield to lakes and reservoirs can be deduced from cores taken from bed sediment deposits (e.g., Walling, 1988). These are particularly useful for describing the effects of land use and climate changes over periods of decades to centuries.
2) Measurements of sediment yield at different spatial scales can be made using a nested basin approach (e.g., Cadier, 1996). However, the resources required to maintain such a measurement campaign limit the approach to research studies. Spatial variation in soil erosion can be determined from the profile of Caesium-137 adsorbed in the soil column (e.g., Walling et al., 1986); such data can be used to validate simulations of spatially distributed erosion (e.g., Ferro et al., 1998; Norouzi Banis, 1998). However, the density of measurements required to depict the pattern of erosion currently limits the technique to areas of a few hectares. Information on sediment sources and long term transport conditions can be inferred from the physical and chemical properties of fine-grained sediment arriving at the basin outlet, a process known as fingerprinting (e.g., Collins et al., 1997).

SHETRAN in the context of other models

To demonstrate SHETRAN's versatility as an erosion and sediment yield modelling system, as well as some of its limitations, comparison is made with four other physically-based models. These are the Areal Non-point Source Watershed Environment Response Simulation

Table 4 Comparison of SHETRAN with four physically-based erosion and sediment yield models

MODEL FEATURE	SHETRAN	ANSWERS	WEPP	EUROSEM	LISEM
Simulation type:					
Continuous	Y	N	Y	N	N
Single event	Y	Y	Y	Y	Y
Basin size	<2000 km^2	<50 km^2	<2.6 km^2	small basin	small basin
Spatial distribution	grid	grid or GIS raster	grid	uniform slope planes	GIS raster
Overland flow:					
Rainfall excess	Y	Y	Y	Y	Y
Upward saturation	Y	N	N	N	Y
Erosion process:					
Raindrop impact/ Overland flow	Y	Y	Y	Y	Y
Rilling	N	N	Y	Y	Y
Crusting	N	Y	N	Y	Y
Channel banks	Y	N	N	Y	N
Gullying	Y	N	N	N	N
Landsliding	Y	N	N	N	N
Output:					
Time-varying sedigraph	Y	Y	N	Y	Y
Time-integrated yield	Y	Y	Y	Y	Y
Erosion map	Y	Y	Y	N	Y
Land use	Most vegetation covers	Mainly agricultural	Wide range of land use	Mainly agricultural	Mainly agricultural

Y = yes; N = no

(ANSWERS) developed in the USA contemporaneously with SHETRAN and subsequently used extensively in a range of countries (Park et al., 1982; Silburn and Connolly, 1995); the more recent United States Department of Agriculture's Water Erosion Prediction Project (WEPP) (Lane et al., 1992); and two recent European developments, the European Soil Erosion Model (EUROSEM) (Morgan et al., 1998) and the Limburg Soil Erosion Model (LISEM) (De Roo et al., 1996). Table 4 summarizes the comparison, based on a number of important model features:

1) Simulation type : can the model simulate continuous periods or is it limited to single rainfall events?
2) Basin size : what is the maximum basin size which can be simulated?
3) Spatial distribution : how is spatial variability represented?
4) Overland flow : is overland flow (important for routing sediment) generated by rainfall excess over infiltration and by upward saturation of the soil column?
5) Erosion process : what processes are included in the model?
6) Output : does the model provide time-varying sediment discharge (a sedigraph), time-integrated (bulk) yield and a spatially distributed erosion map?
7) Land use : what sort of land covers can be simulated?

A further feature, the sediment routing scheme, is not shown since all the models use a similar approach involving a balance between sediment availability and the sediment transport capacity of the flow.

The comparison indicates the basin scale nature of SHETRAN. It can simulate continuous periods (up to several decades) whereas ANSWERS, EUROSEM and LISEM are event models. It can also simulate much larger basins than the others, although the commensurate use of large grid squares (up to 2 km x 2 km) may introduce scaling problems. Because of its integrated surface/subsurface design SHETRAN can simulate runoff generation by both processes, whereas ANSWERS, WEPP and EUROSEM are limited to generation by rainfall excess. All the models can simulate erosion by raindrop impact and overland flow but SHETRAN is the only one which provides a basis for simulating, at a basin scale, the sediment yield arising from gullying and landsliding. SHETRAN is limited in the detail of its process representation as it cannot directly account for rilling or soil crusting. However, these processes are most significant at smaller scales and may merge with a wider range of erosion controls at larger scales. Most of the models can provide time-varying and spatially distributed output. ANSWERS, EUROSEM and LISEM were designed especially to simulate erosion on lands growing crops : however, they could probably be adapted to cover the wider range of covers, including rangeland and forests, which can be simulated by SHETRAN and WEPP. In conclusion, SHETRAN compares favourably with the other models, especially in its ability to simulate erosion and sediment yield at a range of basin scales.

Future directions

SHETRAN is continually evolving as improved process descriptions become available, as more efficient solution schemes are developed and as increasing computing power opens up new opportunities for software development and for the range and scale of model applications. Areas likely to receive attention in the future include:

1) New or improved process models, e.g. for channel bank erosion and infiltration of fine sediments into channel beds of coarser material. Further research is required into the evaluation of the soil erodibility coefficients as a function of measurable soil properties. Overland flow sediment transport is also a poorly researched area where improved process equations are needed.
2) Improved user-friendliness. The current versions of SHETRAN are run on Unix-based workstations. Combined with the model's complexity, this makes it difficult to place the model in the public domain. However, a user-friendly front-end has already been added to help new users and a PC version is under development. In the future SHETRAN will therefore become more generally available.
3) Tests and applications. Each new development requires testing; currently, for example, the landslide and gully erosion and sediment yield components are undergoing validation at test sites. Such tests may require field programmes to provide the necessary data. Future applications are likely to concern the impacts of climate and land use change on erosion and sediment yield. Applications at the larger basin scales will require supporting research on scale dependencies. Related to this, there is a need to investigate, and minimize, the uncertainties in model parameter evaluation. SHETRAN has already been integrated with ecological and economic models within decision support systems and such integration is likely to continue in the future. In particular it enables feedback between the physical and other domains to be accounted for in modelling basin response.

Acknowledgements SHETRAN's development and application at the Water Resource Systems Research Laboratory (WRSRL) has been carried out over many years by a large team of research staff under the overall leadership of Professor P. E. O'Connell (WRSRL Director) and Dr. J. Ewen. Their work forms a basis for some of the discussion in this chapter and its contribution is acknowledged by appropriate references in the text. Particular thanks for help with the diagrams are due to Mr R. Adams, Dr S. J. Birkinshaw, Mr A. Burton and Mr J. Sheffield. Financial support for SHETRAN erosion modelling has been provided by the Commission of the European Communities, UK Nirex Ltd, the UK Department for International Development and the North Atlantic Treaty Organization.

Bibliography

ABBOTT, M.B.; J.C. BATHURST; J.A. CUNGE; P.E. O'CONNELL and J. RASMUSSEN (1986a). 'An introduction to the European Hydrological System - Système Hydrologique Européen, "SHE", 1: history and philosophy of a physically-based, distributed modelling system'. J. Hydrol., 87, p. 45-59.

ABBOTT, M.B.; J.C. BATHURST; J.A. CUNGE; P.E. O'CONNELL and J. RASMUSSEN (1986b) 'An introduction to the European Hydrological System - Système Hydrologique Européen, "SHE", 2: structure of a physically-based, distributed modelling system'. J. Hydrol., 87, p. 61-77.

BÄNZIGER, R. and H. BURCH (1990) 'Acoustic sensors (hydrophones) as indicators for bed load transport in a mountain torrent'. In: H. Lang and A. Musy (eds.), *Hydrology in mountainous regions. I - hydrological measurements; the water cycle*. IAHS Publ. No. 193, p. 207-214.

BATHURST, J.C.; J.M. WICKS and P.E. O'CONNELL (1995) 'The SHE/SHESED basin scale water flow and sediment transport modelling system'. In: V.P. Singh (ed.), *Computer models of watershed hydrology*. Water Resources Publications, Highlands Ranch, Colorado, USA, p. 563-594.

BATHURST, J.C.; C. KILSBY and S. WHITE (1996) 'Modelling the impacts of climate and land-use change on basin hydrology and soil erosion in Mediterranean Europe'. In: C.J. Brandt and J.B Thornes (eds.), *Mediterranean desertification and land use*. Wiley, Chichester, UK, p. 355-387.

BATHURST, J.C.; A. BURTON and T.J. WARD (1997) 'Debris flow run-out and landslide sediment delivery model tests'. Proc. Am. Soc. Civ. Engrs., J. Hydraul. Engrg., 123(5), p. 410-419.

BATHURST, J.C.; E. GONZALEZ and R. SALGADO (1998a) 'Physically based modelling of gully erosion and sediment yield at the basin scale'. In: H. Wheater and C. Kirby (eds.), *Hydrology in a changing environment*, *Vol. III*. Wiley, Chichester, UK, p. 253-259.

BATHURST, J.C.; B. LUKEY; J. SHEFFIELD; R.A. HILEY and N. MATHYS (1998b) 'Modelling badlands erosion with SHETRAN at Draix, south-east France'. In: W. Summer, E. Klaghofer and W. Zhang (eds.), *Modelling soil erosion, sediment transport and closely related hydrological processes*. IAHS Publ. No. 249, p. 129-136.

BEVEN, K. (1989) 'Changing ideas in hydrology - the case of physically-based models'. J. Hydrol., 105, p. 157-172.

BEVEN, K. and A. BINLEY (1992) 'The future of distributed models: model calibration and uncertainty prediction'. Hydrol. Proc., 6 (3), p. 279-298.

BINLEY, A.; K. BEVEN and J. ELGY (1989) 'A physically based model of heterogeneous hillslopes 2. effective hydraulic conductivities'. Wat. Resour. Res., 25, p. 1227-1233.

BURTON, A. and J.C. BATHURST (1998) 'Physically based modelling of shallow landslide sediment yield at a catchment scale'. Environmental Geology, 35(2-3), p. 89-99.

CADIER, E. (1996) 'Hydrologie des petits bassins du Nordeste Brésilien semi-aride : typologie des bassins et transposition écoulements annuels. (Small watershed hydrology in semi-arid north-eastern Brazil : basin typology and transposition of annual runoff data)' (in French). J. Hydrol., 182, p. 117-141.

CONNOLLY, R.D. and D.M. SILBURN (1995) 'Distributed parameter hydrology model (ANSWERS) applied to a range of catchment scales using rainfall simulator data II : Application to spatially uniform catchments'. J. Hydrol., 172, p. 105-125.

COLLINS, A.L.; D.E. WALLING and G.J.L. LEEKS (1997) 'Sediment sources in the Upper Severn catchment : a fingerprinting approach'. Hydrology and Earth System Sciences, 1(3), p. 509-521.

DE ROO, A.P.J.; C.G. WESSELING and C.J. RITSEMA (1996) 'LISEM : A single-event physically based hydrological and soil erosion model for drainage basins. I: theory, input and output'. Hydrol. Proc., 10, p. 1107-1117.

EWEN, J. (1995) 'Contaminant transport component of the catchment modelling system SHETRAN'. In: S.T. Trudgill (ed.), *Solute modelling in catchment systems*. Wiley, Chichester, UK, p. 417-441.

EWEN, J. and G. PARKIN (1996) 'Validation of catchment models for predicting land-use and climate change impacts'. J. Hydrol., 175, p. 583-594.

EWEN, J.; G. PARKIN and P.E. O'CONNELL (2000) 'SHETRAN: Distributed river basin flow and transport modelling system'. Proc. Am. Soc. Civ. Engrs., J. Hydrologic Engrg., 5.

FERRO, V.; C DI STEFANO; G. GIORDANO and S. RIZZO (1998) 'Sediment delivery processes and the spatial distribution of caesium-137 in a small Sicilian basin'. Hydrol. Proc., 12, p. 701-711.

FIGUEIREDO, E. de (1998) *Scale effects and land use change impacts in sediment yield modelling in a semi-arid region of Brazil*. PhD thesis, University of Newcastle upon Tyne, UK.

GIPPEL, C.J. (1995) 'Potential of turbidity monitoring for measuring the transport of suspended solids in streams'. Hydrol. Proc., 9, p. 83-97.

GRAYSON, R.B.; I.D. MOORE and T.A. MCMAHON (1992) 'Physically based hydrologic modeling 2. Is the concept realistic?' Wat. Resour. Res., 28(10), p. 2659-2666.

JAIN, S.K.; B. STORM; J.C. BATHURST; J.C. REFSGAARD and R.D. SINGH (1992) 'Application of the SHE to catchments in India Part 2. Field experiments and simulation studies with the SHE on the Kolar subcatchment of the Narmada River'. J. Hydrol., 140, p. 25-47.

LANE, L.J.; M.A. NEARING; J.M. LAFLEN; G.R. FOSTER and M.H. NICHOLS (1992) 'Description of the US Department of Agriculture water erosion prediction project (WEPP) model'. In: A.J. Parsons and A.D. Abrahams (eds.), *Overland flow: hydraulics and erosion mechanics*. UCL Press, University College, London, p. 377-391.

LUKEY, B.T.; J. SHEFFIELD; J.C. BATHURST; J. LAVABRE; N. MATHYS and C. MARTIN (1995) 'Simulating the effect of vegetation cover on the sediment yield of Mediterranean catchments using SHETRAN'. Phys. Chem. Earth, 20 (3-4), p. 427-432.

LUKEY, B.T.; J. SHEFFIELD; J.C. BATHURST; R.A. HILEY and N. MATHYS (in press) 'Test of the SHETRAN technology for modelling the impact of reforestation on badlands runoff and sediment yield at Draix, France'. J. Hydrol.

MONTGOMERY, D.R. and W.E. DIETRICH (1994) 'A physically based model for the topographic control on shallow landsliding'. Wat. Resour. Res., 30, p. 1153-1171.

MORGAN, R.P.C.; J.N. QUINTON; R.E. SMITH; G. GOVERS; J.W.A. POESEN; K. AUERSWALD; G. CHISCI; D. TORRI and M.E. STYCZEN (1998) 'The European Soil Erosion Model (EUROSEM): a dynamic approach for predicting sediment transport from fields and small catchments'. Earth Surf. Process. Landforms, 23, p. 527-544.

MORRIS, G.L. and FAN, J. (1997) *Reservoir sedimentation handboo*k. McGraw-Hill, New York, p. 8.14-8.23.

NOROUZI BANIS, Y. (1998) *Data provision and parameter evaluation for erosion modelling*. PhD thesis, University of Newcastle upon Tyne, UK.

PARK, S.W.; J.K. MITCHELL and J. N. SCARBOROUGH (1982) 'Soil erosion simulation on small watersheds : a modified ANSWERS model'. Trans. Am. Soc. Agric. Engrs., 25, p. 1581-1588.

QUINTON, J.N. (1997) 'Reducing predictive uncertainty in model simulations: a comparison of two methods using the European Soil Erosion Model (EUROSEM)'. Catena, 30, p. 101-117.

REFSGAARD, J. C.; S.M. SETH; J.C. BATHURST; M. ERLICH; B. STORM; G.H. JØRGENSEN and S. CHANDRA (1992) 'Application of the SHE to catchments in India Part 1. General results'. J. Hydrol., 140, p. 1-23.

REID, I.; J.T. LAYMAN and L.E. FROSTICK (1980) 'The continuous measurement of bedload discharge'. J. Hydraul. Res., 18, p. 243-249.

SILBURN, D.M. and R.D. CONNOLLY (1995) 'Distributed parameter hydrology model (ANSWERS) applied to a range of catchment scales using rainfall simulator data I: infiltration modelling and parameter measurement'. J. Hydrol., 172, p. 87-104.

TACCONI, P. and P. BILLI (1987) 'Bed load transport measurements by the vortex-tube trap on Virginio Creek, Italy'. In: C.R. Thorne, J.C. Bathurst and R.D. Hey (eds.), *Sediment transport in gravel-bed rivers*. Wiley, Chichester, UK, p. 583-606.

WALLING, D. E. (1983) 'The sediment delivery problem'. J. Hydrol., 65, p. 209-237.

WALLING, D. E. (1988) 'Erosion and sediment yield research – some recent perspectives'. J. Hydrol., 100, p. 113-141.

WALLING, D. E.; S. B. BRADLEY and C.J. WILKINSON (1986) 'A Caesium-137 budget approach to the investigation of sediment delivery from a small agricultural drainage basin in Devon, UK'. In: R.F. Hadley (ed.), *Drainage basin sediment delivery*. IAHS Publ. No. 159, p. 423-435.

WICKS, J.M. and BATHURST, J.C. (1996) 'SHESED : a physically based, distributed erosion and sediment yield component for the SHE hydrological modelling system'. J. Hydrol., 175, p. 213-238.

WICKS, J.M.; J.C. BATHURST; C.W. JOHNSON and T.J. WARD (1988) 'Application of two physically-based sediment yield models at plot and field scales'. In: M.P. Bordas and D.E. Walling (eds.), *Sediment budgets*. IAHS Publ. No. 174, p. 583-591.

WICKS, J.M.; J.C. BATHURST and C.W. JOHNSON (1992) 'Calibrating SHE soil-erosion model for different land covers'. Proc. Am. Soc. Civ. Engrs., J. Irrig. Drain. Engrg., 118 (5), p. 708-723.

WU, W. and R.C. SIDLE (1995) 'A distributed slope stability model for steep forested basins'. Wat. Resour. Res., 31, p. 2097-2110.

Multiscale Green's function Monte Carlo approach to erosion modelling and its application to land use optimization

L. Mitas, H. Mitasova
University of Illinois at Urbana-Champaign, Urbana, Illinois, USA

Introduction

Efforts to balance economic development with environmental protection have increased the demand for simulation tools which enable predictions of the human impact on the landscape. In order to prevent irreversible changes and avoid costly, ineffective solutions, the simulation tools should provide detailed spatial and temporal distributions of modeled phenomena. Statistical averages for entire study areas or predictions only for a certain point, such as a watershed outlet, are often insufficient. Effectiveness of land management decisions aimed at preventing negative impacts of soil erosion in complex landscapes can be significantly improved by detailed predictions of erosion and deposition patterns for proposed land use alternatives. Recent advances in Geographic Information Systems (GIS) technology, especially support for modeling with multivariate functions (Mitasova et al., 1995; Mitas et al., 1997), along with the exponential growth in computational power, stimulate the shift from empirical, lumped models to physically-based, distributed ones (Moore et al., 1993; Maidment, 1996; Saghafian et al., 1995).

In spite of a significant progress in this area of research, applications of distributed models are still rather laborious and often results do not have sufficient detail, accuracy and realism for land management purposes. In our research we have tried to address some of these problems by focusing on:

(a) description of processes by 'first principles' relations in a bivariate form allowing us to incorporate impact of spatial variability in rainfall excess, terrain, soil and cover conditions;
(b) use of robust solvers (Green's function Monte Carlo) with multiscale implementation which minimize the preprocessing of input data and support modeling at spatially variable resolution;

(c) investigations of computer simulated land use designs for finding optimal land use patterns with minimized erosion risk;
(d) increase in efficiency by extensive use of GIS for processing, analysis and visualization of the data and results, as described in detail by Mitasova et al. (1995); Mitas et al. (1997).

First, we briefly describe water and sediment flow models based on the solution of bivariate first principles equations by multiscale Monte Carlo method. Then, we illustrate the capabilities of the proposed approach to simulate erosion/deposition patterns for a study area with spatially variable terrain, soil and cover conditions for different land use designs aimed at improving the effectiveness of erosion prevention. Finally, we present an example of water flow simulation with spatially variable resolution using heterogeneous elevation data.

Methods

The methodological framework for the simulation of human impact on erosion/deposition is based upon the description of water flow and sediment transport processes by first principles equations, a concept outlined previously, most often for a one dimensional case, for example, by Bennet, (1974). Within our approach, inputs and outputs of simulations are represented by continuous multivariate functions discretized as grids, as opposed to homogeneous hillslope segments or subwatersheds used in more traditional approaches. To fully incorporate the impact of spatial variability in terrain, soils and cover, we describe the water and sediment flow as bivariate vector fields rather than using a 1D flow routing in the steepest slope direction from a planar hillslope segment common in many distributed models (e.g., Moore et al., 1993; Flacke et al., 1990). Advanced GIS technology is used to support the processing, analysis and visualization of the multiscale data and simulation results (Mitasova et al., 1995; Mitas et al., 1997).

Overland water flow

The model used in this paper is described by Mitas and Mitasova (1998) therefore here we briefly present only its principles. A bivariate shallow water flow continuity equation for a rainfall event (e.g., Saghafian et al. 1995) is given by

$$\frac{\partial h(r,t)}{\partial t} = i_e(r,t) - \nabla.[h(r,t)v(r,t)] \quad (1)$$

where h (r, t) [m] is the depth of overland flow, i_e (r, t) [m/s] is the rainfall excess, v(r,t) is velocity and r = (x, y) [m] is the position. Equation (1) is coupled with the momentum conservation equation (in the diffusive wave approximation) which together with the Manning's relation between the depth and velocity create a closed system of equations. The steady state form of Equation (1) is given by

$$-\frac{\varepsilon}{2}\nabla^2\left[h^{5/3}(r)\right] + \nabla.q(r) = i_e(r) \quad (2)$$

where q(r,t) [m^2/s] is the unit flow discharge (water flow per unit width) and ε is a diffusion coefficient. The diffusive wave effects are incorporated approximately by the term $\nabla^2\left[h^{5/3}(r)\right]$. Such an incorporation of diffusion in the water flow simulation is not new and a similar term has been obtained in derivations of diffusion-advection equations for overland flow, e.g., by Dingman (1984). In our reformulation we use a modified diffusion term, which depends on $h^{5/3}$(r) instead of h(r). Equation (2) has the advantage of being linear in the function $h^{5/3}$(r) which enables us to solve it by means of the Green's function method using stochastic (Monte Carlo) techniques as described later.

The diffusion constant which we have used is rather small (approximately one order of magnitude smaller than the reciprocal Manning's coefficient) and therefore the resulting flow is close to the kinematic regime. However, the diffusion term improves the kinematic solution by filling and overcoming shallow depressions common in digital elevation models (DEM), reducing thus the need for manual modification of a DEM. It also produces smooth flows around slope discontinuities or abrupt changes in land cover which are typical for anthropogenic landscapes.

Sediment transport by overland flow

Overland water flow is the driving force for hillslope erosion which includes sediment entrainment, transport and deposition. The continuity of sediment mass is given by

$$\frac{\partial\left[\rho_s c(r,t)h(r,t)\right]}{\partial t} - \frac{\omega}{2}\nabla^2\left[\rho_s c(r,t)h(r,t)\right] + \nabla.\rho_s(r,t) = sources - \sin ks = D(r,t) \quad (3)$$

where $q_s(r,t)=\rho_s c(r,t)q(r,t)$ [kg/(ms)] is the sediment flow rate per unit width, c(r,t) [particle/m^3] is sediment concentration, p_s [kg/particle] is mass per sediment particle, and ω [m^2/s] characterizes local dissipation (diffusion) processes. For a steady state case the equation is

$$-\frac{\omega}{2}\nabla^2\left[\rho_s c(r)h(r)\right] + \nabla.\rho_s(r) = D(r) \quad (4)$$

The sources/sinks term is derived from the assumption that the detachment and deposition rates are proportional to the difference between the sediment transport capacity and the actual sediment flow rate (Foster and Meyer, 1972):

$$D(r) = \sigma(r)\left[T(r) - \left|q_s(r)\right|\right] \tag{5}$$

where T(r) [kg/(ms)] is the sediment transport capacity, and $\sigma(r)$ [m^{-1}] is the first order reaction term dependent on soil and cover properties. The expression for $\sigma(r) = D_c(r)/T(r)$ is obtained from the following relationship (Foster and Meyer, 1972):

$$D(r) / D_c(r) + \left|q_s(r)\right| / T(r) = 1 \tag{6}$$

which states that the ratio of erosion rate to the detachment capacity $D_c(r)$ [kg/(m^2s)] plus the ratio of the sediment flow to the sediment transport capacity is a conserved quantity (unity)- Equation (6), proposed by Foster and Meyer (1972), is based on observed relationship between soil detachment and transport described e.g., by Meyer and Wischmeier (1969). This concept is used in several erosion models including WEPP (Haan et al., 1994; Flanagan and Nearing, 1995). The qualitative arguments, experimental observations and values for $\sigma(r)$ are discussed by Foster and Meyer, (1972).

The sediment transport capacity T(r) and detachment capacity $D_c(r)$ represent maximum potential sediment flow rate and maximum potential detachment rate, respectively, and are functions of a shear stress (Foster and Meyer, 1972):

$$T(r) = K_{t'}(r)\,[\tau(r)]^{p} = K_t(r)[\rho_\omega\, gh(r)\sin\beta(r)]^{p} \tag{7}$$

$$D_c(r) = K_d(r)\,[\tau(r) - \tau_{cr}(r)]^{q} = K_d(r)\,[\rho_\omega\, gh(r)\sin\beta(r) - \tau_{cr}(r)]^{q} \tag{8}$$

where $\tau(r) = \rho_\omega\, gh(r)\sin\beta(r)$ [*Pa*] is the shear stress, β [*deg]* is the slope angle, *p* and *q* are exponents, $K_{t'}(r)$ [*s*] is the effective transport capacity coefficient, $K_d(r)$ [*s/m*] is the effective erodibility (detachment capacity coefficient), $\rho_\omega\, g$ is the hydrostatic pressure of water with the unit height, $g = 9.81$ [m/s^2] is the gravitational acceleration, $\rho_\omega = 10^3$ [kg/m^3] is the mass density of water, and $\tau_{cr}(r)$ [*Pa*] is the critical shear stress. The parameters and adjustments factors for the estimation of $D_c(r)$, T(r) are functions of soil and cover properties, and their values for a wide range of soils, cover, agricultural and erosion prevention practices are being developed within the WEPP model.

Recently, Nearing et al. (1997) presented an improved fit to several sets of experimental data by relating sediment loads q_s [g/ms] to stream power ω [g/s^2]:

$$\log q_s = A + \frac{Be^{(C+D\log\omega)}}{1+e^{(C+D\log\omega)}} \tag{9}$$

with the constants A = -34.47, B = 38.61, C = 0.845, D = 0.412. Based on the conditions of experiments it was suggested that Equation (9) could be a reasonable estimation of the sediment transport capacity. The Equation (9) can be rewritten to the following form:

$$T(r) \approx |q_s(r)| = a_0 \exp\left[-\frac{b}{1+\left[\omega(r)/\omega_0\right]^d} \right] \tag{10}$$

where a_0 = 1380 [kg/sm], b = 88.90, d = 0.179, ω_0 = 8.89. 10-' [kg/s^3], $\omega = \rho_\omega$,g Iq(r)I sinβ(r) is the stream power [kg/s^3], (note the change of units from gramm to kg for q_s, and ω when compared with Equation (9)). This form of the Equation (9) allows us to define a physical interpretation of the constants, as a_0 represents a saturated sediment load for infinitely large stream power, ω_0 is a 'reference stream power, b = 88.90 and d = 0.179 are dimensionless exponents. Strictly speaking, the choice of the constants corresponds to the experimental results used in the fit and could be different in other cases, e.g., an effective transport capacity coefficient analogous to the one in Equation (7) has to be included for different covers, etc. The important difference between the Equations (7) and (9, 10) is that through the stream power $\omega(r) = \tau(r)$ Iv(r)I the effect of flow velocity is directly incorporated into the transport capacity. For complex terrain and cover conditions, the flow velocity varies and can change dramatically with varying location, so we can expect differences in predicted patterns of erosion/deposition when using Equation (10) for the sediment transport capacity.

Green's function Monte Carlo method

The continuity Equations (1) and (3) are traditionally solved by finite element or finite difference methods. These methods often require special data structures (e.g. meshes for finite element methods) or have problems with numerical stability for complex, spatially variable conditions. As a robust and flexible alternative to these methods we have proposed to use a stochastic approach to the solution, based on Green's function Monte Carlo method. Because of space constraints, we consider only the steady state cases given by Equations (2) and (4), however, methodology is similar also for the time dependent cases. Equations (2), (4) have a general form in which a linear differential operator O acts on a nonnegative function γ(r) (either h(r) or ρsc(r)h(r)), while on the right hand side, there is a source term S(r)

$$O\gamma(r) = S(r) \tag{11}$$

Using the Green's function G(r, r', p) the solution can be expressed as

$$\gamma(r) = \int_0^\infty \int G(r, r', p) S(r')\, dr'\, dp \tag{12}$$

while G(r, r', p) is given by the following equation and an initial condition

$$\frac{\partial G(r,r',p)}{\partial p} = -OG(r,r',p); G(r,r',0) = \delta(r-r') \tag{13}$$

where δ is the Dirac function. In addition, we assume that the spatial region is a delineated drainage basin with zero boundary condition which is fulfilled by G (r, r', p).

Eqsuations (1 to 4) can be interpreted as Fokker-Planck stochastic processes (Gardiner, 1985) with diffusion and drift components. Such an interpretation opens new possibilities to solve these equations through a simulation of the underlying process utilizing stochastic methods (Gardiner, 1985). This type of Monte Caxlo approach is one of the modern alternatives to finite element or finite difference approaches and is being explored in computational fluid dynamics or in quantum Monte Carlo methods for solving the Schrödinger equation (see Mitas, 1996, and references therein). Very briefly, the solution is obtained as follows. A number of sampling points distributed according to the source S(r') is generated. The sampling points are then propagated according to the function G(r, r', p) and averaging of path samples provides an estimation of the actual solution γ(r) with a statistical accuracy proportional to $1/\sqrt{M}$ where M is the number of samples. Figure 1 illustrates the solution with increasing number of walkers (animated illustration of this method can be found in Mitas et al. (1997)).

The Monte Carlo technique has several unique advantages when compared with more traditional methods. It is very robust and enables studies for spatially complex cases with minimum of manual preprocessing of input data. Moreover, rough solutions, which identify the major sediment concentrations and erosion/deposition patterns can be estimated quickly, allowing us to carry out preliminary quantitative studies or to rapidly extract qualitative trends by parameter scans. In addition, Monte Carlo methods are tailored to the new generation of computers as they provide scalability from a single workstation to large parallel machines due to the independence of sampling points. Therefore, the methods are useful both for everyday exploratory work using a desktop computer and for large, cutting-edge applications using high performance computing.

Multiscale implementation for data with spatially variable resolution

With the growing capabilities to collect geospatial data from various sources using different technologies the data set representing the studied landscape can be very heterogeneous with different coverage, resolution, detail and accuracy. To fully exploit the best data available for a given area algorithms should be able to make effective use of these heterogeneous data sets, maximize the accuracy and detail of predictions while performing computations efficiently.

To address this need we have reformulated the solution through the Green's function given by Equation (12) for accommodation of spatially variable accuracy and resolution. The integral (12) can be multiplied by a reweighting function W(r)

$$W(r)\gamma(r) = \int_0^\infty \int W(r)G(r,r',p)S(r')dr'\,dp = \int_0^\infty \int G^*(r,r',p)S(r')dr'\,dp \tag{14}$$

which is equal to the appropriate increase in accuracy (W(r) > 1) in the regions of interest while it is unity elsewhere. The function W(r) can change (abruptly or smoothly) between regions with unequal resolutions and in fact, can be optimally adapted to the quality of input data (terrain, soils, etc) so that the accurate solution is calculated only in the regions with correspondingly accurate inputs. The reweighted Green's function G* (r, r', p), in effect, introduces higher density of sampling points in the region with large W(r). The statistical noise will be spatially variable as $\sim 1/\left[W(r)\sqrt{M}\right]$, where M is the average number of samples resulting in the accuracy increase for the areas with W(r) > 1.

Equations (1 to 4) describe the water and sediment flow at a spatial scale equal or larger than an average distance between rills (i.e., grid cell size $\geq$ 1m) and therefore the presented approach allows us to perform landscape scale simulations at variable spatial resolutions from one to hundreds of meters, depending on the complexity and importance of studied subregions.

Results

High resolution erosion and deposition patterns for spatially complex conditions

We have evaluated the capabilities of the presented model using an ~ 1 km^2 subarea of the Scheyern experimental farm (Auerswald et al., 1996). The measured elevation data were interpolated to a 2m resolution DEM by regularized spline with tension (Mitasova and Mitas, 1993) and land cover and soil data were used to estimate erodibility and transportability parameters based on the literature (Foster and Meyer, 1972; Flanagan and Nearing, 1995).

First, we have applied the model for traditional land use (Figure 1a) for two different situations:

(a) dense grass in the meadow area, baxe soil in the arable area and an extreme storm event;
(b) vegetation cover everywhere and a lower intensity rainfall event.

We compared the results of simulations with spatial distributions of observed colluvial deposits (Figure 1a) and linear erosion features digitized from aerial photographs (Figure 1a). For case (a), prevailing detachment limited erosion ($\sigma \rightarrow 0$) is predicted for the bare soil area, due to the high transporting capacity of fast moving water. The net erosion D(r) ~ D_c(r) and almost all detached sediment is transported to stream while deposition is restricted to small concave areas and channels (Figures 1b,c). This represents a situation close to the one observed after an extreme storm event in 1993 when extensive rilling occurred, with only 7 % of eroded sediment deposited within the area (Auerswald et al. 1996).

For the case (b), with smaller transport capacities and (σ > 1) the erosion process is close to sediment transport capacity limited case when Iq_s (r)I ~ T(r). The erosion rates are lower and the model predicts large extent of areas with deposition (Figures 1b,c). Such a behavior is close to the observed distribution of colluvial deposits (Figure 1a). For this case, the net erosion and deposition can be approximated as

$$D(r) = \nabla.\left|q_s(r)\right| \approx \nabla.\left[T(r)s_0(r)\right] \qquad (15)$$

where $s_0(r)$ is the unit vector in the steepest slope direction and the erosion and deposition pattern is significantly inlfuenced by terrain shape. The impact of topography can be demonstrated by substituing for $T(r) = K_t \rho_\omega g h(r) \sin\beta(r)$ and deriving the net erosion and deposition as a function of water depth and terrain curvatures:

$$D(r) = K_t \rho_\omega g \left\{ [\nabla h(r)].s_0(r) \sin\beta(r) - h(r)\left[\kappa_p(r) + \kappa_t(r)\right] \right\} \qquad (16)$$

where $\kappa_p(r)$ is the profile curvature (curvature in the direction of the steepest slope), $\kappa_t(r)$ is the tangential curvature (curvature in the direction perpendicular to the gradient, i.e., tangential to the terrain surface isoline; for curvature definitions see Mitasova and Hofierka, 1993). Therefore, according to (16) the spatial distribution of erosion/deposition is given by the directional derivative of the overland flow depth (first term) and by the local geometry of terrain (second term), including both profile and tangential curvatures (Figure 2).

The commonly used univaxiate formulations of erosion models neglect the influence of tangential curvature (Figure 2) underestimating thus the deposition in areas with $\kappa_t(r) < 0$ (tangential concavity) and underestimating erosion in areas with $\kappa_t(r) > 0$ (tangential convexity) as demonstrated by Mitas and Mitasova (1998). Although the above analysis strictly applies to the case when p = 1 in Equation (7), it is possible to derive similar expression with a general exponent p not equal to 1 and the qualitative conclusions remain the same.

From the point of view of land use management, it is important to note that for both simulations (a), (b) the highest rates of net erosion as well as net deposition were predicted in hollows with high concentrated sediment flow (Figures 1b,c). Field measurements confirm that this area has the thickest layers of colluvial deposits but also large linear erosion features were observed here after a strong storm (Auerswald et al., 1996). The second highest erosion is predicted on upper convex parts of hillslopes where the highest loss of radio-tracers and the lowest yields were observed (Auerswald, personal communication). Increased erosion is predicted also for bare narrow stripes below the grass areas, where water accelerates after depositing the sediment. The major difference in spatial patterns between the two modeled cases is the spatial extent of erosion/deposition. In the simulation (a) 93% of the area experienced erosion while simulation (b) predicted erosion only for 70% of the area, with extent of deposition close to the observed spatial distributions of colluvial deposits. Deposition was also predicted at upper edges of meadows, where the rills follow the borderline between the grass and bare soil areas and where deposits were found in the upper convex part of the grass hillslope (Figure 1).

Land use design for improved erosion prevention

The presented bivariate erosion model can be used for analyzing and designing the placement of selected erosion protection measures based on land cover, as illustrated by the following simple example. First, we used the model to identify locations with the highest erosion risk, assuming a uniform land use. Then, the protective grass cover was distributed to the high risk areas while preserving the extent of grass cover at the original 30% of the area (Figure 3). We performed a simulation with the new land use to evaluate its effectiveness. The results

demonstrate that the new design has a potential to dramatically reduce soil loss and sediment loads in the ephemeral streams (Figure 3). The crest in sediment flow in the valley disappears and is replaced by light deposition within the grassways, while the maximum and total rates of erosion are significantly reduced. We have found, that the effectiveness of this design depends on differences in roughness, combination of very smooth bare soil and very dense grassway resulted in predictions of higher erosion along the borders of the grass waterway. It is interesting to note, that the land use design obtained by this rather simple computational procedure, using only the elevation data, had several common features with the sustainable land use design proposed and implemented in 1993 at the farm, based on extensive experimental work (Auerswald et al., 1996). The design uses significantly higher proportion of permanent grass cover and fallow and increases cover/roughness in the hop field in the center of the valley. The results show that this design keeps increased amounts of soil moisture and, at higher cost, reduces the net erosion even further.

Simulations with spatially variable resolution and accuracy

The necessity for spatially heterogeneous modeling of fluxes can arise due to various reasons, for example, when the modeled region is represented by vaxious data sets at different resolutions or when the region is very large with spatially variable complexity and only a subarea of high spatial variability needs to be simulated at high resolution while for the rest of the reagion lower resolution is sufficient.

We illustrate the concept of multiscale modeling using a 16 km^2 region represented by a 10m resolution DEM (400c x 400r) with a smaller 1 km^2 subregion mapped with more detail and represented by a 2m resolution DEM (680c x 395r). Resampling the DEM for entire region to 2m resolution would lead to 4 million grid cell DEM requiring substantial increase in computational requirements with little gain in detail for low resolution area. With spatially variable resolution we simulate the water flow at 10m resolution for the entire area and save the walkers entering the high resolution subregion. Water flow for the subregion is then simulated at 2 m resolution using the saved resampled walkers as inputs, as illustrated by Figure 4. Probably the most significant research and application potential of this approach is in multiscale/multiprocess simulations which would allow us to run simulations using the models which axe the most appropriate for the given scale. For example, by transfering the water and sediment from average overland flow model for low resolution area to rill-interril-channel model for subregion represented at high, submeter resolution.

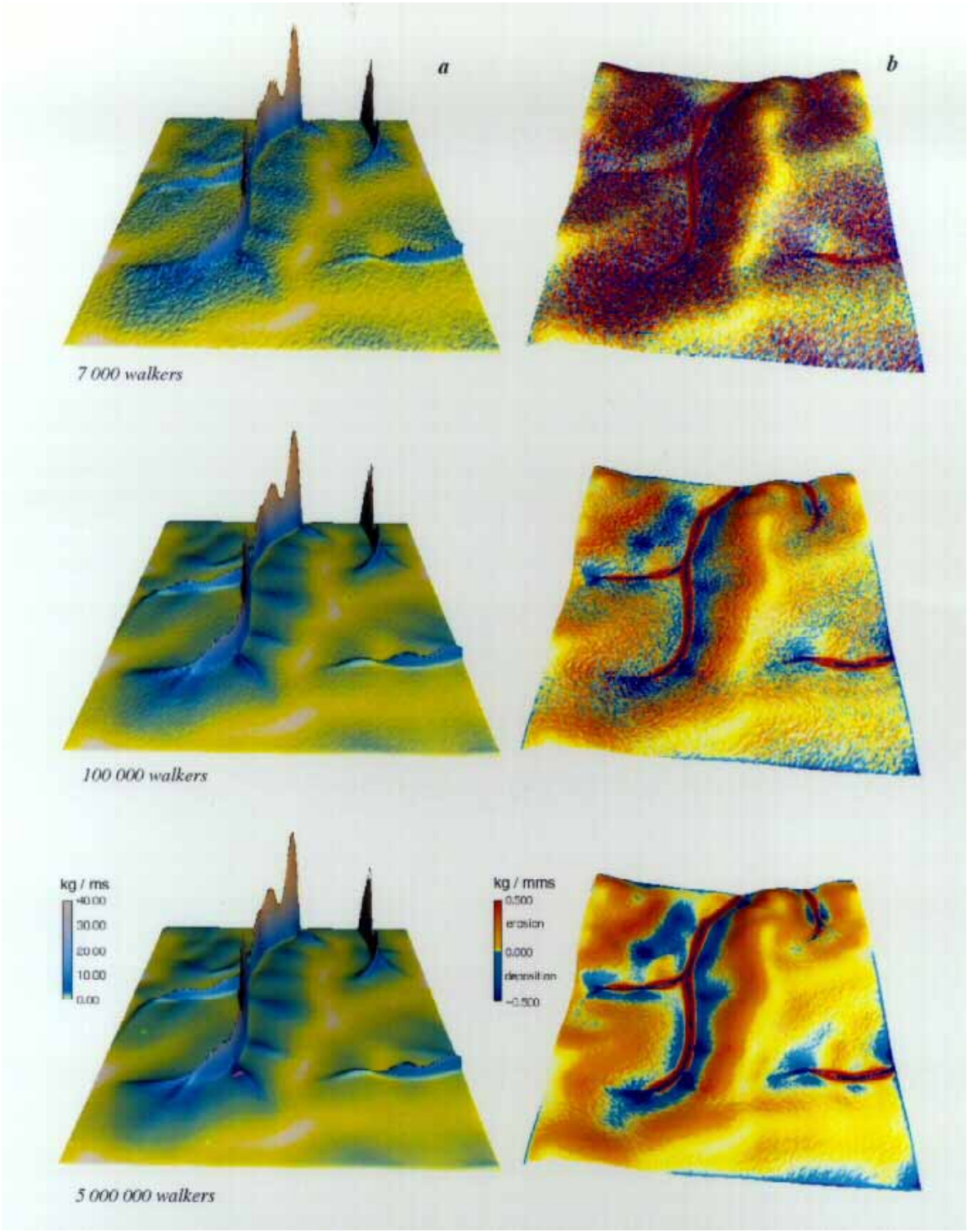

Fig. 1 Monte Carlo solution of sediment transport equation using increasing number of walkers: (a) sediment flow rate, (b) net erosion and deposition

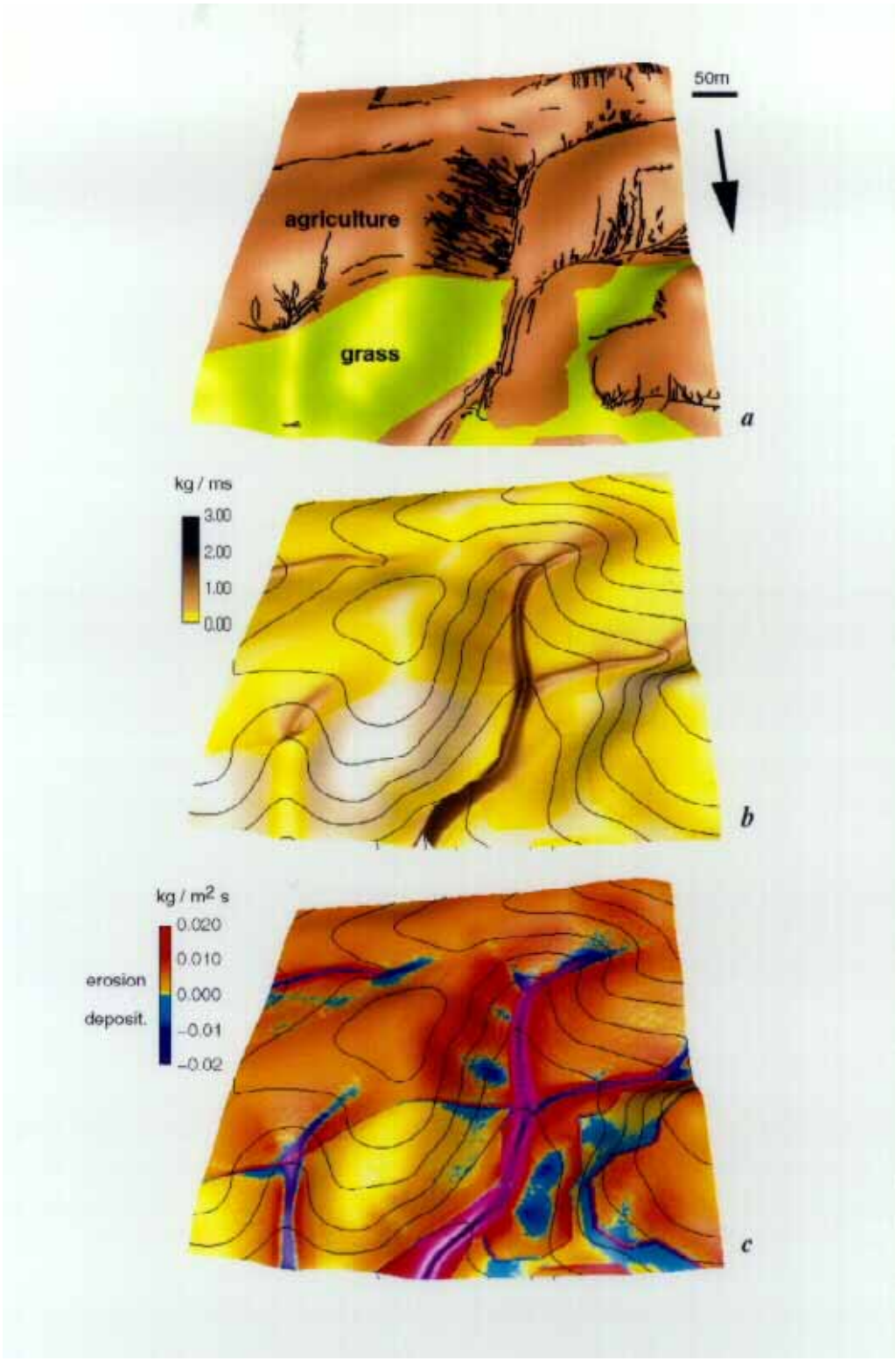

Fig. 2 Terrain model with (a) traditional land use and observed rills and gullies, (b) simulated sediment flow, (c) erosion and deposition pattern for 70 mm/hr rainfall excess and bare soil in the agricultural field

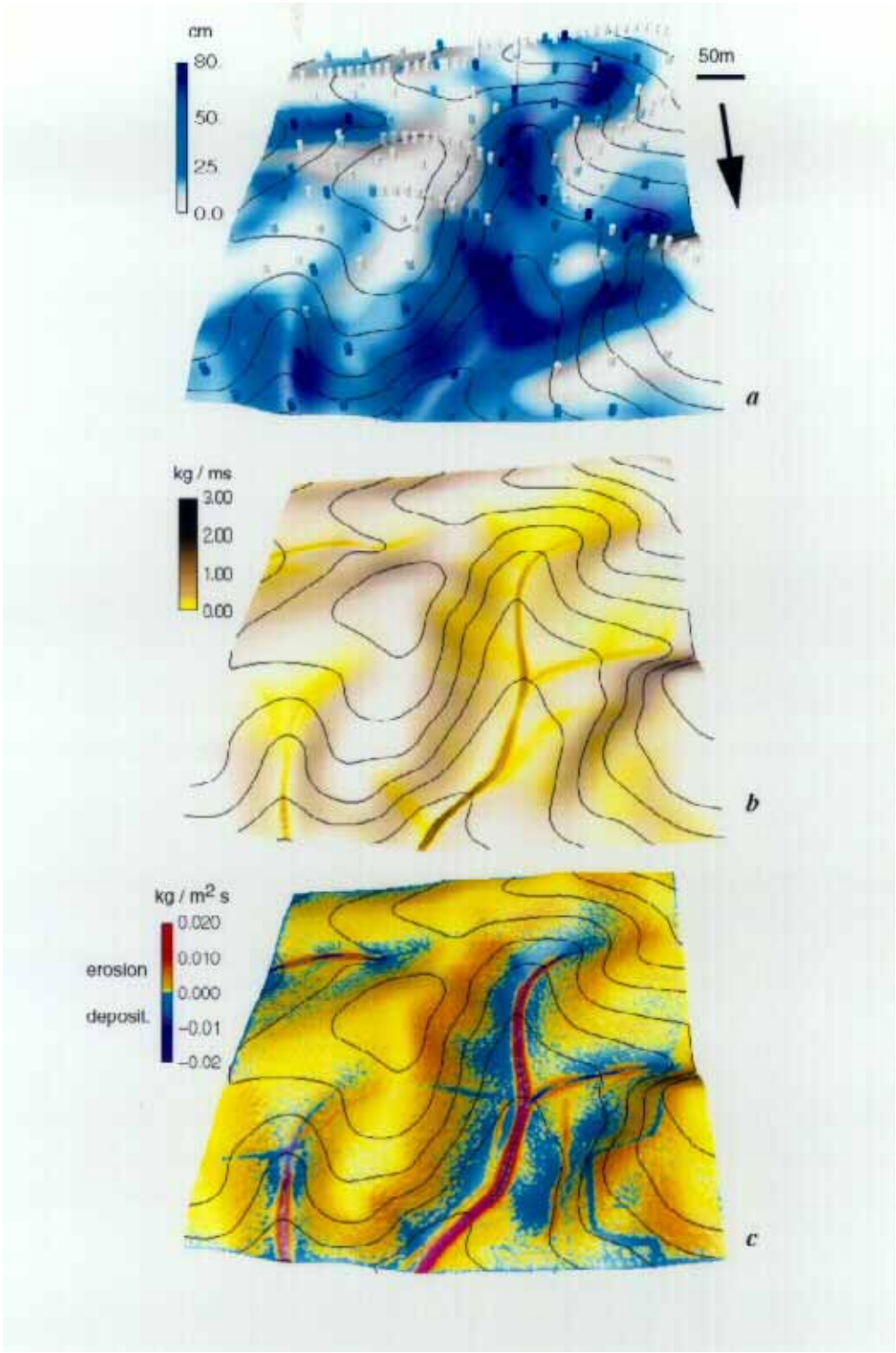

Fig. 3 Terrain model with (a) observed depths of colluvial deposits, (b) simulated sediment flow, (c) erosion and deposition pattern for 20 mm/hr rainfall excess and vegetative cover in the agricultural field

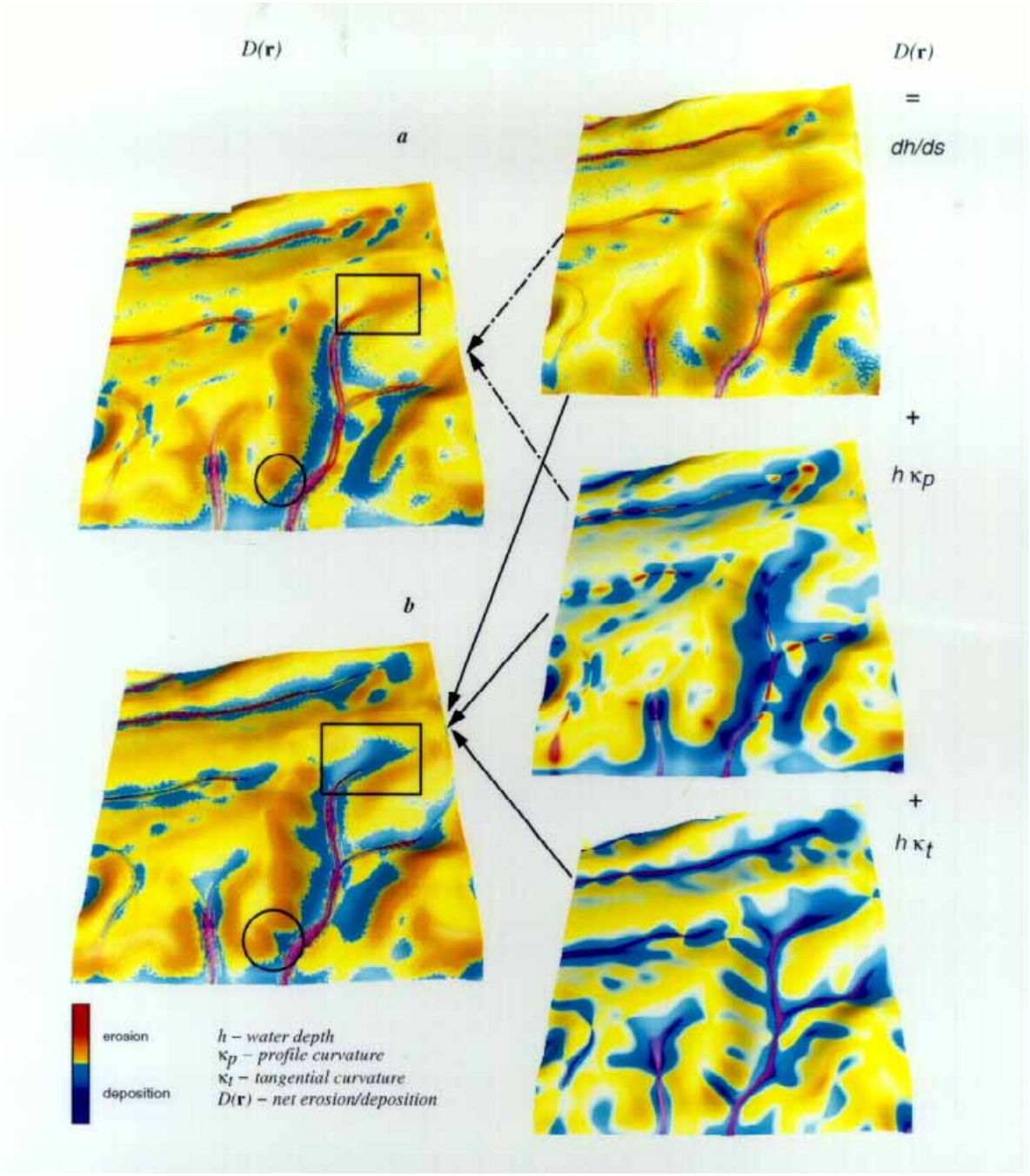

Fig. 4 Univariate and bivariate computation of net erosion and deposition for transport capacity limiting case: (a) erosion and deposition as a change of 1D sediment flow along flow line: d lqsl / ds, (b) erosion and deposition as a divergence of 2D vector field representing sediment flow: div qs

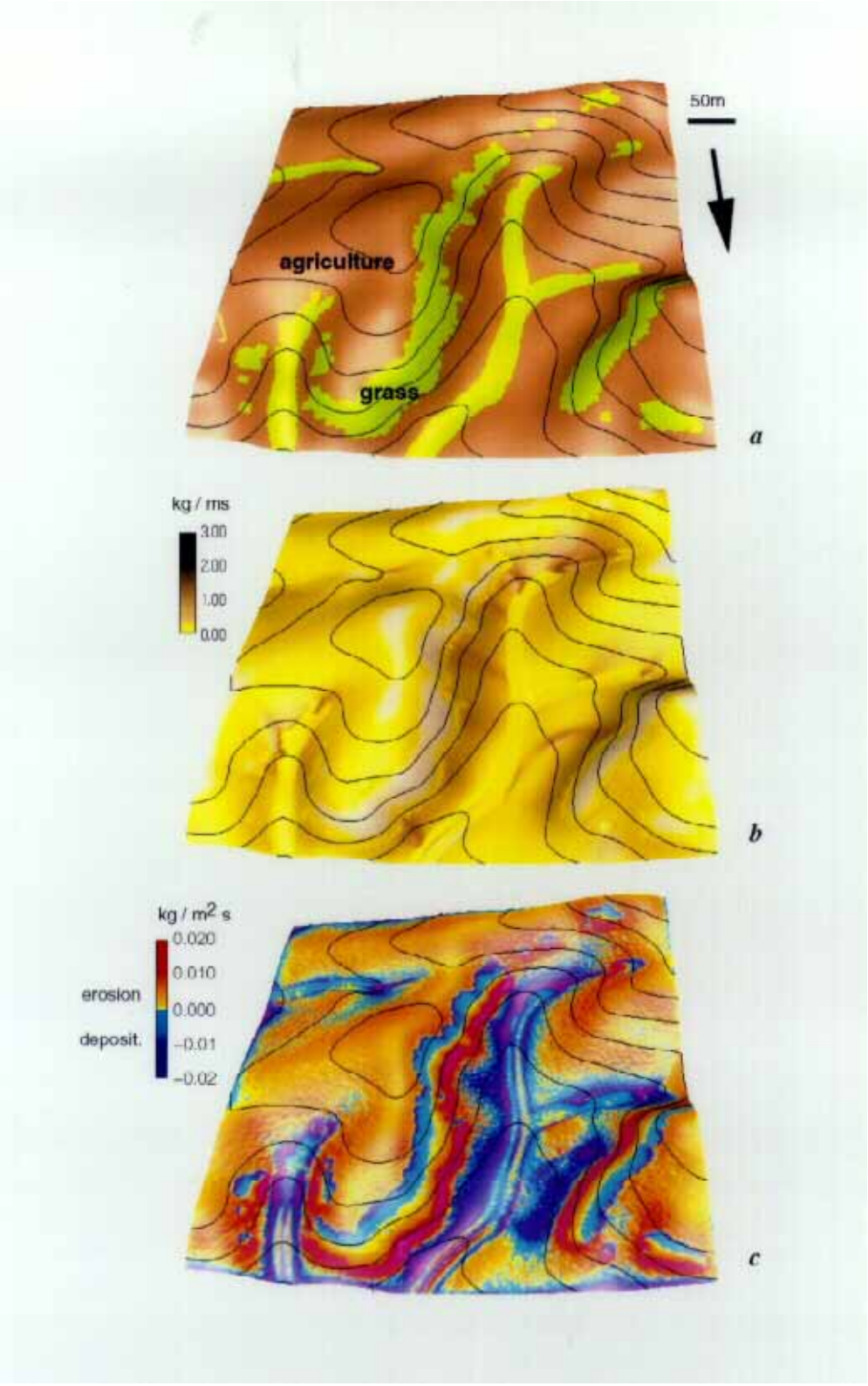

Fig. 5 Terrain model with (a) computer designed land use, (b) simulated sediment flow, (c) erosion and deposition pattern for 70 mm/hr rainfall excess and bare soil in the agricultural field

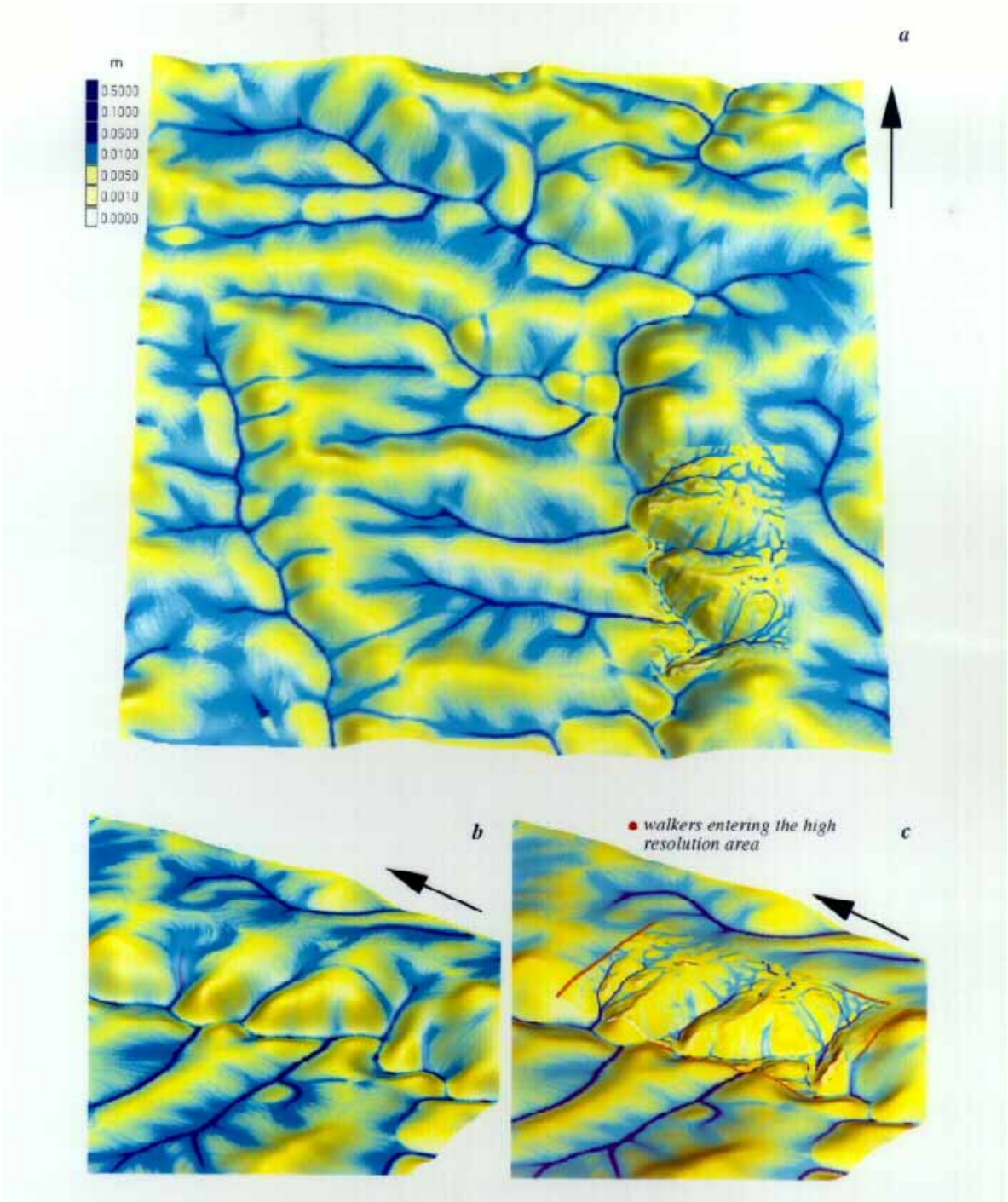

Fig. 6 Multi-scale simulation of steady state water depth: (a) water depth at combined 10m and 2m resolution for the entire study area, (b) selected subarea at 10m resolution, (c) the same selected subarea at 2m resolution

Conclusions

The stochastic method of solving the first principles equations using Green's function Monte Carlo technique provided us with a valuable research tool of a much needed robustness and flexibility. It enabled us to investigate several important issues such as impact of complex terrain on spatial patterns of erosion/deposition under different regimes of sediment transport, impact of land use design on effective erosion prevention and the possibility to simulate flow at spatially variable resolution.

Comparisons of simulation results with field data indicate that the study area at Scheyern experimental farm exhibits colluvial deposition patterns consistent with prevailing transport capacity limited regime, modeled for the conditions with vegetative cover and small event. On the other hand, as we conjecture from our preliminary investigations, the detachment limited case seems to dominate the creation of short term erosion features, such as rilling and gully formation, which are related to large rainstorm events, bare soil conditions and high transport capacities concentrated to short time intervals. The bivariate model was also capable to predict the location of thalweg erosion by simulating high rates of both erosion and deposition in valleys.

A suggestion of Nearing at al. (1997) that the sediment loads from rills may be more strongly influenced by a sediment transport limit rather than by the soil detachment, in general, agrees with our results. This seems to be true especially in complex terrain conditions where transport capacity changes significantly due to variations in terrain shape and cover affecting significantly the distribution and amplitudes of the water flow field. Our calculations and analysis also suggest that the sediment transport capacity plays a more important role than anticipated by the previous research which focused on erodibility as the key control quantity. Obviously, a subtle and spatially variable interplay between erodibility and transport capacity can influence the processes in a profound way. We believe that this complexity clearly points out towards the importance of the high resolution 2D simulations.

The presented model enabled us to study the impact of different land cover designs on the erosion processes and estimate their effectivenes for erosion protection, demonstrating the possibilities to create powerful tools for computer aided sustainable land use design.

The presented model was implemented as an independent computational module named SIMWE (Simulation of Water Erosion) and linked to the Geographic Resources Analysis System (GRASS).

Acknowledgments We would like to express our gratitude to K. Auerswald from the Technical University Muenchen, Germany, and to S. Warren from the USA Construction Engineering Research Laboratory (USA CERL) for providing the experimental data used in this paper and for valuable discussions. We acknowledge the support by the Strategic Environmental Research and Development Program (SERDP) and the USA CERL. We thank Douglas Johnston from the GMS Laboratory at the University of Illinois for his support and discussions, and to William Brown for his contribution to the new GRASS tools used in this paper.

Bibliography

AUERSWALD, K.; A. EICHER; J. FILSER; A. KAMMERER; M. KAINZ; R. RACKWITZ; J. SCHULEIN; H. WOMMER; S. WEIGLAND and K. WEINFURTNER (1996) 'The Scheyern project of the FAM. In: H. Stanjek (ed.), *Development and implementation of soil conservation strategies for sustainable land use*, Technische Universitaet Muenchen, F'reising-Weihenstephan, Germany, Int. Congress of ESSC, Tour Guide II p.25-68.

BENNET, J. P., (1974) Concepts of mathematical modeling of sediment yield. Water Resources Research 10, p.485-496.

DINGMAN, S. L. (1984) *Fluvial hydrology*. Freeman, New York.

FLACKE, W.; K. AUERSWALD and L. NEUFANG (1990) Combining a modified USLE with a digital terrain model for computing high resolution maps of soil loss resulting from rain wash. Catena 17, p.383-397.

FLANAGAN, D.C. and M.A. NEARING (eds.) (1995) *Water Erosion Prediction Project*. Report No. 10, National Soil Erosion Lab., USDA ARS, West Laffayette, Indiana, USA.

FOSTER, G. R. and L. D. MEYER (1972) „A closed-form erosion equation for upland areas." In: H.W. Shen (ed.), *Sedimentation*. Symposium to honor Prof H. A. Einstein 12.1-12.19, Colorado State University, Ft. Collins, USA.

GARDINER, C. W. (1985) *Handbook of stochastic methods for physics, chemistry, and the natural sciences*. Springer, Berlin.

HAAN, C. T.; B. J. BARFIELD and J. C. HAYES (1994) *Design hydrology and sedimentology for small catchments*. Academic Press, p. 242-243,

MAIDMENT, D. R. (1996) Environmental modeling within GIS. In: M. F Goodchild, L. T. Steyaert and B. 0. Parks (eds.), *GIS and environmental modeling: progress and research issues*. GIS World, Inc., Ft. Collins, USA. p.315-324,

MEYER, L.D., and W. H. WISCHMEIER (1969) Mathematical simulation of the process of soil erosion by water. Transactions of the ASAE, Vol.12, p.754-758.

MITAS, L. (1996) Electronic structure by Quantum Monte Carlo: atoms, molecules and solids. Computer Physics Communications 97, p.107-117.

MITAS, L. and H. MITASOVA (1998) Distributed soil erosion simulations for effective landuse managment. Water Resources Research 23, p.505-516.

MITAS, L.; W. M. BROWN and H. MITASOVA (1997) Role of dynamic cartography in simulations of landscape processes based on multi-variate fields. Computers and Geosciences Vol.23, p.437-446.

MITASOVA, H. and L. MITAS (1993) Interpolation by regularized spline with tension: I. theory and implementation. Mathematical Geology Vol.25, p.641-655.

MITASOVA, H. and J. HOFIERKA (1993) Interpolation by regularized spline with tension: 11. Applicationto terrain modeling and surface geometry analysis.“ Mathematical Geology Vol.25, p.657-669.

MITASOVA, H.; L. MITAS; W. M. BROWN; D. P. GERDES; I. KOSINOVSKY and T. BAKER (1995) Modelling spatially and temporally distributed phenomena: new methods and tools for GRASS GIS. Int. Journal of Geographical Information Systems Vol.9, p.433-446.

MOORE, I. D.; A. K. TURNER; J. P. WILSON; S. K. JENSEN and L. E. BAND (1993) GIS and land surface-subsurface process modeling. In: M. F Goodchild, L. T. Steyaert and B. 0. Parks (eds.), *Geographic Information Systems and environmental modeling*. Oxford University Press, New York. p.196-230

NEARING M.A.; L.D. NORTON; D.A. BULGAKOV; G.A. LARIONOV; L.T. WEST and K.M. DONTSOVA (1997) Hydraulics and erosion in eroding rills. Water Resources Research Vol.33, p.865-876.

SAGHAFIAN, B.; P. Y. JULIEN and F. L. OGDEN (1995) Similarity in catchment response 1. stationary rainstorms. Water Resources Research Vol.31(6), p.1533-1541.

Developments in physically-based overland flow modelling

W. Summer
Chartered Engineering Consultant for Hydraulic Engineering and Water Management,
Brennleitenstrasse 59-61/3, A-2202 Hagenbrunn, Austria

Introduction

The hydrologic component represents a major part within the integrated watershed management approach, considering, assessing and combining the complex relationships between environmental features as well as the cumulative effects of disturbances on environmental quality across complex landscapes. Therefore, the requirements for hydrologic models simulating overland flow and related transport processes on a physical basis, by using mathematical algorithm, increased significantly in the same way as the demand for higher modelling precision has risen. Although, new tools such as Geographic Information Systems have been developed to enable the assess of spatial heterogeneity, present physical modelling of surface transport processes still requires assumptions of spatial homogeneity. The justified degree of simplification is determined by model scale, data requirements, availability and processing of data as well as by expenses for man-power and instrumentation involved in the overall watershed management task.

Due to the difficulties of quantitative estimates on surface transport processes by physically-based modelling approaches, simulations were done on the basis of conceptual models. As they combine the simplicity of an empirical concept with the wider applicability of the more rigorous physically-based approach, their advantage lies in the representation of the significant features of a physical process in mathematical terms. Although several decades have elapsed since these methods were introduced, they still play a major role in computer based complex hydrologic models where, in addition, the movement of nutrients, chemicals and pesticides is estimated and predicted. Their predictive capabilities are limited however to the simulation of various simple scenarios, as well as the evaluation of the resulting consequences as only a limited understanding of the underlying physical process is reflected by the conceptual approach.

Over the last few decades hydrologists constantly decreased the lack of physical basis of mathematical models. But simulating overland flow by a fully dynamic, two-dimensional model accounting for microtopographic flow characteristics (Zhang and Cundy, 1989) will hardly be feasible if a considered catchment exceeds a certain size. A first practical solving technique for the conservation equations was based on the approximate kinematic wave theory (Lighthill and Whitham, 1955; Iwagaki, 1955). It was then first introduced to the modelling of watershed flow problems by Henderson and Wooding (1964) who considered in theory the runoff from a V-shaped catchment (Wooding, 1965a, 1965b, 1966) (Figure 1a). A detailed analysis on the kinematic wave criteria was then published by Woolhiser and Liggett (1967). The practical validity of the kinematic model has to be judged by direct reference to the physics of the processes involved e.g. by considering more accurate differential equations of higher order (Morris and Woolhiser, 1980; Viera, 1983).

The concept of kinematic cascades (Figure 1b) was introduced by Brakensiek in 1967. Based on the kinematic wave theory it helped to overcome geometric landscape restrictions in modelling complete watersheds. This type of model represents the first of its kind to combine a physically-based approach with an operational method as well as offering a certain flexibility to varying hillslope shapes.

Due to increased computer power over the years a big effort was also put into mathematical models coping with the spatially highly variable overland flow phenomena, as well as surface transport processes by using a fully dynamic two-dimensional approach (Abbott et al., 1986a and 1986b; Bathurst, 1986; Lane and Nearing, 1989; Nearing et al., 1989). Aiming at considering microtopographic characteristics, a grid-based approach as well as the use of the point-scale technology poses the problem of estimating local friction and local x- and y-direction slope values at multiple single/nodal points of a computational network over a watershed due to the two-dimensional solution of the point-scale overland flow equations (Figure 1c). In practice, this results in a very substantial parameter estimation problem. To overcome grid-based routing disadvantages as well as the difficulties of flow division and convergence in one-dimensional kinematic routing on a grid basis, an improved two-dimensional kinematic routing concept on a triangular irregular network was developed by Goodrich et al. (1991).

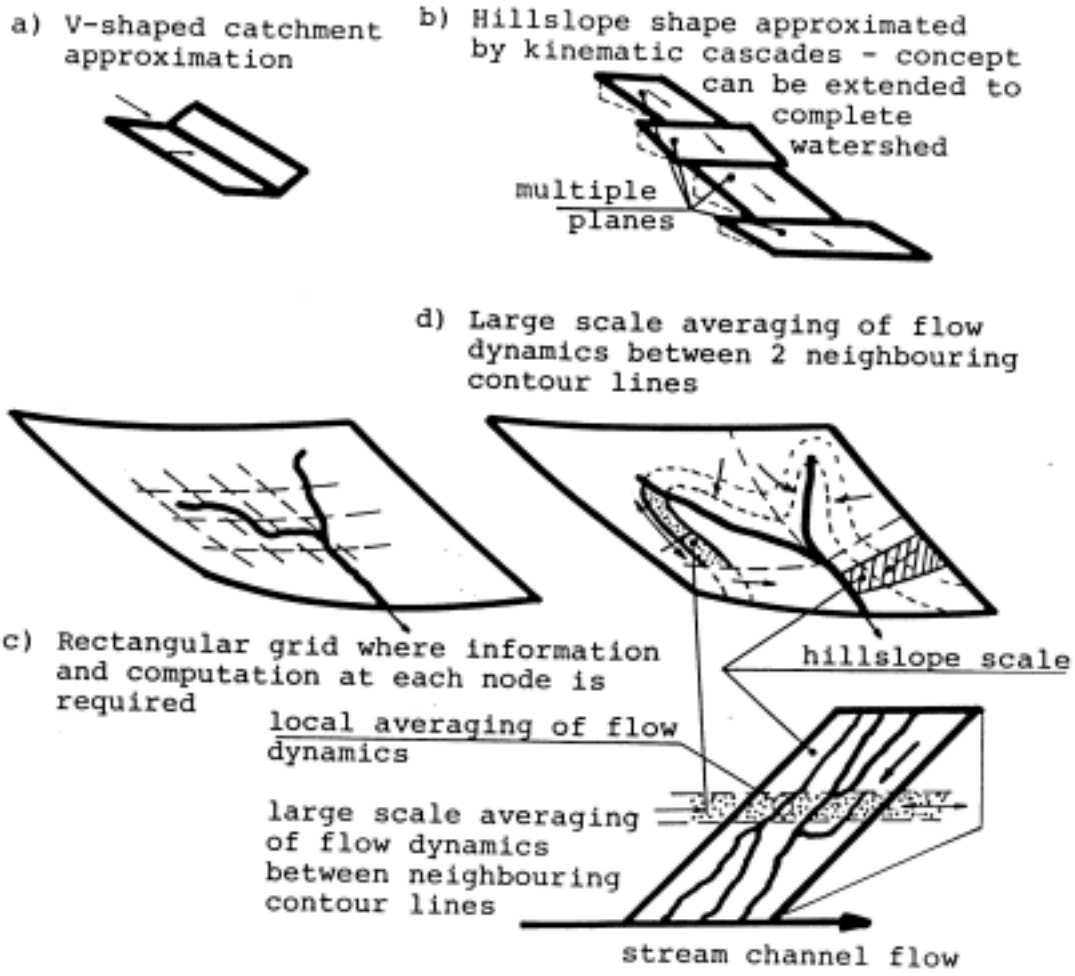

Fig. 1 Schematic representations of shape approximations of watersheds in overland flow modelling: a) V-shaped catchment, b) Kinematic cascades - KINEROS, c) Rectangular grids -SHE model, etc., d) spatially averaging technique of flow dynamics

These and other physically-based models are essential in highlighting the physical processes involved. But in general, they are confronted with difficulties in estimating overland flow parameters due to the heterogeneity of the land surface microtopography. In addition they also have difficulties in computing overland flows at small grid spacing in order to gain realistic results. All recent models are based on a dynamic approach in one or another way, considering point-scale overland flow equations. But their correct solutions require gradually varied flow. Therefore in the case of a rapidly changing microtopography on a hillslope, it is not possible to use the point-scale equations, unless one smoothes the natural surface microtopography (Tayfur et al., 1993). To account for a realistic overland flow situation, the importance of the natural hillslope system, broken into rill and interrill processes (Emmett, 1978; Meyer et al., 1975), has to be understood and then considered.

A mathematical overland flow model

A physically-based modelling technique represents a major advance in understanding and predicting overland flow on complex hillslope profiles. Based on the derivation of spatially averaged conservation equations for interacting rill and interrill area overland flows (Tayfur and Kavvas, 1994), this chapter will show ways to overcome the common difficulties in

- estimating overland flow parameters of heterogeneous surfaces, considering the microtopography of the surface at the same time.
- representing the flow over complex landscape surfaces.
- computing overland flows at small grid spacing for realistic results by

In real life situations, overland flow, over land surfaces, is characterised by flow on interrill areas as well as flow in rills discharging into the stream channel network of a catchment (Fig. 1 d). Hence, a good hydrologic model not only has to assume the occurrence of surface flow as sheet flow, it also has to consider the influence of rills on the flow dynamics to avoid serious misinterpretation of results and finally has to have the capability to express the combined flow dynamics over the landscape forming hillslopes.

Kavvas and Govindaraju (1992) combined in a simple, and strictly one-dimensional way - no interaction between flows in parallel rills and neighbouring interrill areas - the rill flow dynamics. As interrill areas always contribute a certain amount of flow towards rills, which in a realistic approach therefore can't be assumed as straight and parallel, a two-dimensional expansion of the combined flow dynamics was then developed by Tayfur and Kavvas (1994), where flow interaction between interrill areas and rills exists.

The interrill area flow is conceptualised as a two-dimensional sheet flow and a one-dimensional channel flow is assigned to the rills. The overland flow dynamic is simulated by a kinematic wave approximation of the St. Venant equations as this is a very practicable approach (Govindaraju et al., 1992; Woolhiser, 1974). The kinematic wave arises out of a continuity equation,

$$\frac{\partial A}{\partial t} + \frac{\partial Q}{\partial x} = R \tag{1}$$

e.g. with A as the cross-sectional area of flow, Q as the discharge and R as a source/sink term as well as an unique relationship of the form

$$Q = Q(A; x, t) \tag{2}$$

For the case of two-dimensional overland flow over a plane of constant width this results in

$$\frac{\partial h_o}{\partial t} = i_e(x, y, t) - \frac{\partial q_x}{\partial x} + \frac{\partial q_y}{\partial y} \tag{3}$$

and

$$q_x = q_x(h_o; x, t) \tag{4a}$$

$$q_y = q_y(h_o; y, t) \tag{4b}$$

where q_x and q_y denote the discharge per unit width in x-direction respectively in y-direction, $h_o(x,y,z)$ the interrill area sheet flow depth and i_e the rate of rainfall excess. In most situations of hydrologic relevance an explicit independence of q on t can be assumed leading to $q_x = q_x(h_o; x)$ respectively $q_y = q_y(h_o; y)$. It can be expressed in power law form $q = ch^m$ with c and m as parameters giving q_x and q_y as

$$q_x = C_x h_o^{5/3} = \frac{\sqrt{S_{ox}}}{n\sqrt{1+\sqrt{\frac{S_{oy}}{S_{ox}}}}} h_o^{5/3} \tag{5a}$$

and

$$q_y = C_y h_o^{5/3} = \frac{\sqrt{S_{oy}}}{n\sqrt{1+\sqrt{\frac{S_{ox}}{S_{oy}}}}} h_o^{5/3} \tag{5b}$$

where n denotes Manning's roughness coefficient, S_{ox} the bed slope in x-direction ($S_{ox}=\tan\theta_x$) and S_{oy} the bed slope in y-direction ($S_{oy}=\tan\theta_y$) (Figure 2).

As Equation (3) represents an equation conserving mass at a single point, its practical application will be impracticable as each model parameter has to be monitored at every single node/point location on the hillslopes. Therefore Equation (1) is locally averaged over an individual interrill area having a width (Figures 1d and 3) to obtain the locally averaged sheet flow equation

$$\frac{\partial \bar{h}_o}{\partial t} = \bar{i}_e - \frac{\partial}{\partial x}(C_x \bar{h}_o^{5/3}) - \frac{1}{2}\pi^{5/3}\frac{C_y}{l} h_o^{5/3} = f_o(\bar{h}_o; x, y, t) \tag{6}$$

where $\bar{h}_o$ and $\bar{i}_e$ denote the averaged parameter values. Although Equation. (6) is one-dimensional, it contains two-dimensional properties as the second term on the right hand side of the equation represents the water flux discharging from the interrill area section into the rill.

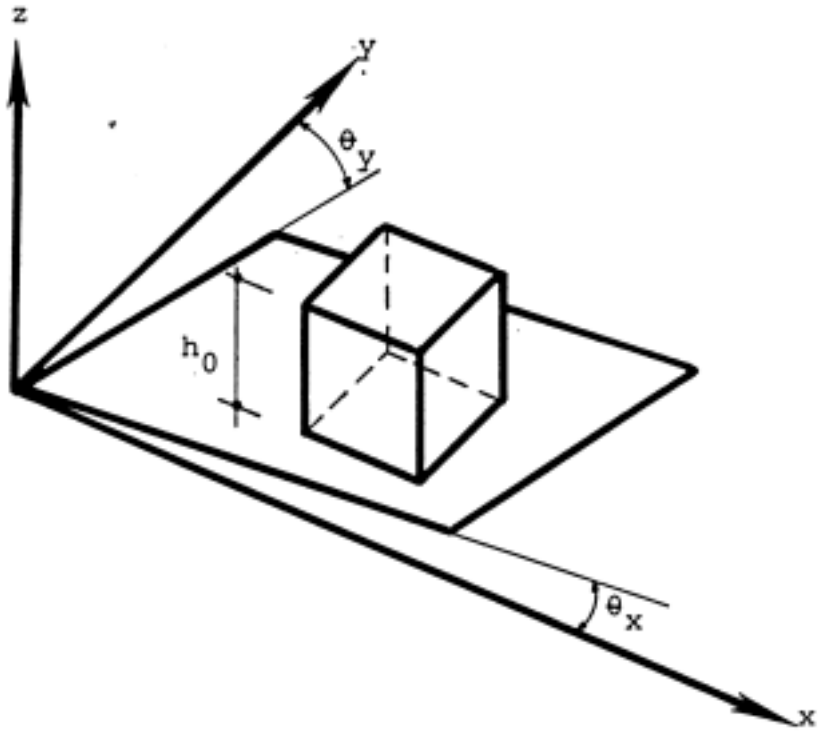

Fig. 2 Schematic flow element representing the sheet flow dynamics on an interrill area

The locally averaged one-dimensional equation for rill flow is similar to the overland flow equation. For rectangular rill cross-section as well as under the kinematic wave assumption, the flow equation can be stated as

$$\frac{\partial h_r}{\partial t} = i_e + q_l - \frac{\sqrt{S_{ox}}}{n}\frac{1}{b_r}\frac{\partial}{\partial x}\frac{(bh_r)^{3/2}}{\sqrt{b+2h_r}} = f_r(h_r, b; x, t) \tag{7}$$

where b denotes the rill width, h_r the rill flow depth, S_{ox} the bed slope of the rill and q_l the net lateral inflow from the interrill area section into the rill - q_l can then be separated into a rill inflow component from the right hand side of the rill as well as the left hand side and can be estimated according to Equations (5a) and (5b).

But as natural landscapes consist of hillslopes with microtopographic surface structures characterised by a large number of rills and interrill areas, it is unrealistic to evaluate the physical and hydraulic properties of each rill and interrill section in order to avoid gross errors in the flow predictions. Therefore the locally averaged flow Equations (6) and (7) have to be averaged along the transect and/or contour lines of the watershed representing hillslopes (Figures 1 and 3). This large scale averaging is based on the stochastic averaging theory. Its application to the overall overland flow dynamics (combined averaged interrill and rill flow) over a certain length L results in an equation for an overall mean flow depth $\bar{h}$ (Govindaraju et al., 1992).

$$\frac{\partial \bar{h}}{\partial t} = \langle f_r(h_r, b; x, t) \rangle . \lambda(x, y, t) + \langle f_o(h_o; x, y, t) \rangle . [1 - \lambda(x, y, t)] \qquad (8)$$

Equation (8) reflects the distribution of the rills over a hillslope through the parameter λ *(x,y,t)* as well as the fact that any stochastic parameter such as the rill widths and depths etc. have to be averaged which is expressed by < >. The multiple solution of Equation (8) for various hillslope transects respectively watershed contour lines leads then to averaged flow velocities and discharges. Overland flow towards the draining watershed channels can then be computed.

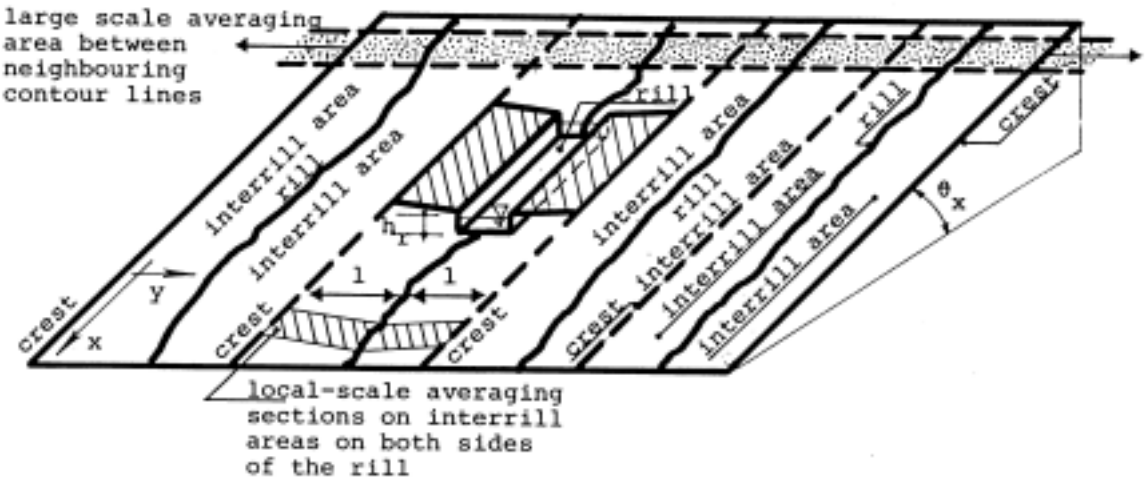

Fig. 3 Schematic landscape representation of a part of a watershed with a local-scale averaging rill and interrill section as well as with a large-scale averaging area between two neighbouring contour lines

The overland flow model within a watershed framework

The spatially averaged conservation equations for overland flow with interacting rill and interrill dynamics represent the innovative component of the new watershed modelling system for the transport over complex surfaces. Other presently available process components incorporated into the expending system are rainfall, infiltration and channel flow. The system, expendable for soil erosion, nutrient transport etc., allows for spatial and temporal variability of the relevant parameters. The watershed is subdivided by contour lines where the controlling parameters are averaged over the area within neighbouring contours. The input file is structured in such a manner that the relevant simulation parameters for the estimation of the flow dynamics along chosen streamlines are provided for each area between neighbouring contour lines. Consequently the

resulting overland flow discharges from the hillslopes, which finally drain into the channel network of the watershed, are computed. However, due to the splitting of the basin by contour lines as well as stream line,s spatial variability is considered. For every time increment during the simulation of a rainstorm a relevant input file has to be prepared. Thus, the system not only allows for areal variability but also considers the temporal variations within a storm event.

Monitored rainfall data is gathered from various rain gauges representing the rainfall characteristics of the catchment. It is planned to provide pattern of rainfall intensities as simulation input for a situation of a moving thunderstorm over a research area.

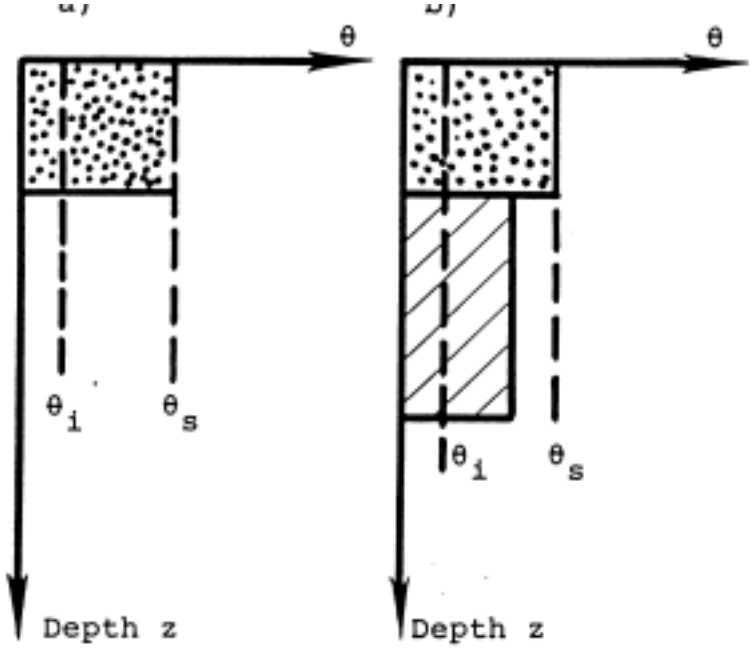

Fig. 4 Schematic representation of a soil water infiltration front at a precipitation event with a rainfall intensity a) constant in time as well as b) varying in time

The infiltration is simulated on the basis of the Green and Ampt (1911) parameters. Due to its simplicity as well as widely available parameters this model is very popular in large scale watershed modelling. Using an approximative procedure, certain assumptions regarding the hydraulic properties of the soil have to be considered:

- Homogeneous soil profile
- Infiltration only occurs in vertical direction
- Infiltration through macropores is neglected
- Shrinking and expansion of the soil is neglectable
- No incrustation on the soil surface occurs during rainfall

As the Green and Ampt model was used for the ponded infiltration into a homogeneous soil with initial uniform water content (Figure 4) the infiltration rate is given by

$$f = K + K\frac{n\psi_f}{F} \tag{9}$$

and its integration leads to

$$Kt = F - n\psi_f \ln(1 + \frac{F}{n\psi_f}) \tag{10}$$

with $n = \phi_e - \theta_i$ denoting the available porosity, $\phi_e = \phi - \phi_r$ the effective porosity, ϕ_r the residual saturation, θ_i the initial soil water content, ψ_f the wetting front capillary pressure head [cm], t the time [h], F the total amount of infiltrated water [cm], f the infiltration rate [cm/h] and K the hydraulic conductivity [cm/h]. These parameters can be estimated on the basis of soil texture classes (Rawls et al., 1983).

The runoff produced on the hillslopes form small stream channels where it is finally transported through the stream channel network towards the outlet of the watershed. Considering a complex 4th order dendritic channel structure on the basin scale (Figure 5) Rajbhandari (1989) applied an efficient method for the solution of the two partial differential equations representing the conservation of mass and momentum to simulate the network's flow dynamics. For the computational improvement the overlapping Y-segment (Sevuk, 1973) and/or sequential routing technique (Yen and Akan, 1976) is used as well as a sparse matrix solution technique based on a special Gauss elimination technique (Gupta and Tanji, 1977) to gain a fast solvable matrix of banded structure of the dynamic equations. An implicit weighted four-point finite-difference scheme (Fread, 1978) is used for the solution of the unsteady flow equations, besides the Newton-Raphson iterative procedure (Amein and Fang, 1970) for their sequential solving. The same solving technique is applied to the overland flow part. For the channel flow, the dynamic wave model, the diffusion wave model as well as the kinematic wave model can be applied as a solution method of the St. Venant equations.

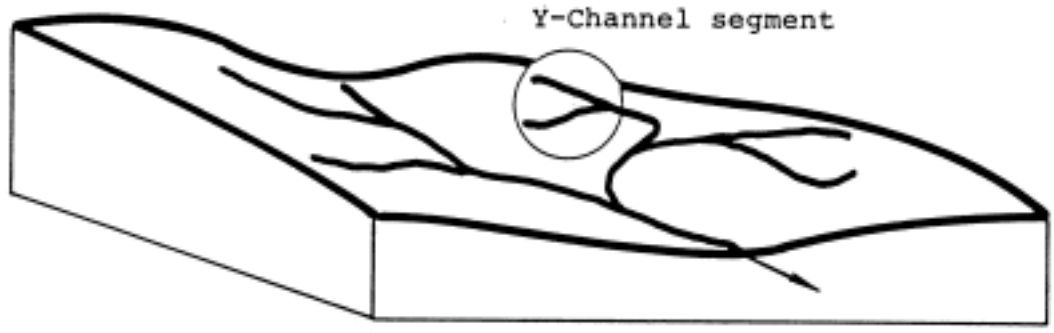

Fig. 5 Schematic representation of a 4th order stream channel network of a watershed which can efficiently be solved either by the overlapping of Y-segments which stepwise substitute for the complete network or by sequential and separate routing in each channel from the most upstream branch towards downstream, satisfying the continuity requirements at each junctions

Concluding summary

The most powerful developments in rainfall-runoff modelling refer to a physically-based approach to allow for spatial variations as well as impacts, nowadays caused by man induced land use changes. With increased computer power, two-dimensional overland flow modelling became the State-of-the Art. But due to highly varying flow characteristics over complex surfaces, the use of point equations for the detailed description of spatially occurring processes rapidly leads to a data deficit in the requirements. In addition, the assumptions of gradually varied flow in the used point-scale technology do not hold, unless one smoothes the important microtopographic surface structure. To overcome these deficiencies spatially averaged conservation equations for interacting rill and interrill area overland flows are introduced. On the basis of the kinematic wave approximation the combined rill (channel) and interrill (sheet) flow is treated as one-dimensional flow with an additional interaction term. The overland flow part with the quasi-two dimensional conservation equations of the presented catchment modelling system is then linked to the flow in the channel network. It is routed by the fully dynamic St. Venant equations.

Current research aims at representing complex landscape surfaces and the flow over those surfaces. The concept of the stochastically averaged flow dynamics, leading to extended overland flow equations based on the kinematic wave approximation for sheet flow and rill flow, characterises the controlling surface geometry in terms of a limited number of parameters, besides the approach to combine rill flow dynamics with sheet flow dynamics. A first time application of this technique within a watershed modelling system was performed on a small alpine watershed basin with complex landsurface geometry. In point scale technology, by avoiding the intensive data requirements as well as the time consuming data processing, the spatially averaged conservation equation technology uses significantly less information about the landsurface microtopography, while the computation is simplier, hence, faster. The plausibility of this technology is also shown by the fact that in practice one never has all the necessary information for each point of a detailed numerical scheme laid over a watershed. Estimations of slope gradients for hillslopes by the use of GIS storing DTM information with a resolution of 30x30m represents the common data availability in practical hydrologic engineering. Based on such a data base, a comparison of the new spatially averaged conservation equations with two other popular watershed models (EPIC and AGNPS), which are based on simple but very practical and powerful approaches (SCS-method in the EPIC model and mass balance between neighbouring cells - continuity equation considering steady overland flow dynamics - in the AGNPS model), is currently being validated in an alpine catchment.

The new averaged equations representing the overland flow dynamics are the major component within a newly developed hydrologic system for the modelling of transport processes over complex landscape surfaces. Just considering the flow processes within a watershed, the overland flow part was linked to the Green and Ampt based infiltration component as well as to a component simulating the unsteady flow dynamics in a dendritic stream channel system draining the basin.

Critically analysing the equation for the overland flow dynamics as well as the approximate procedure for the infiltration simulation, the physically-based concept will more efficiently produce results of sufficient precision in hydrologic engineering applications in

comparison to other physically-based approaches. Merely the simulation of rainstorms characterised by several peaks with significant drying periods in-between (also consider large variation in intensities), limits the application of this concept. The assumption of a rigid wetting front in the case of a Hortonian overland flow situation (storm intensity > vertical infiltration rate at saturated soil conditions) is valid. But the concept shows deficiencies during single storm situations where the rainfall intensity of a later peak is smaller than the one of a previous peak and/or the vertical infiltration rate of the saturated soil. In such situations a significant hysteretic effect regarding the pF-curve can occur, strongly depending on the soils. However, dealing with storm events of strongly varying intensities an adapted infiltration approach has to be considered.

The flow dynamics in the channel network are substituted by Y-segments. The diffusion wave approximation of the St. Venant equations can result in less precision near the junction of the Y-system, as the effect of local and convective acceleration due to interacting channels can't be considered by this type of model. The kinematic wave approximation shows the inability to account for backwater effects from the downstream. Only the full dynamic wave model accounts for the complete flow dynamics. However, reasonable results combined with efficient computation needs the correct evaluation of the expected flow situation in the stream channel network.

In general it can be stated that models based on the spatially averaging technology of conservation equations offers a powerful and versatile hydrologic tool. Although an erosion as well as a nutrient transport component for the presented watershed system based on the same averaging principles has recently been developed, the potential of the new technology has not been yet fully exploited. In particular climatic and/or groundwater modelling may prove a promising field for further developments and applications.

Acknowledgments Max Kade Foundation Inc. supported a one-year sabbatical visit of the author at the civil and environmental engineering department of the University of California Davis to work on physical-based soil erosion modelling.

Bibliography

ABBOTT, M.B.; J.C. BATHURST; J.A. CUNGE; P.E. O'CONNELL and J.R. RASMUSSEN (1986a) 'An introduction to the European Hydrological System - Système Hydrologique Européen, 'SHE', 1: History and philosophy of a physically-based, distributed modelling system.' J. Hydrol., Vol.87, p. 45-59.

ABBOTT, M.B.; J.C. BATHURST; J.A. CUNGE; P.E. O'CONNEL and J.R. RASMUSSEN (1986b) 'An introduction to the European Hydrological System - Système Hydrologique Européen, 'SHE', 2: Structure of a physically-based modelling system.' J. Hydrol., Vol.87, p. 61-77.

AMEIN, M. and C.S. FANG (1970) 'Implicit flood routing in natural channels.' J. Hydraul. Engr., ASCE, Vol.96, No.12, p. 2481-2500.

BATHURST, J.C. (1986) 'Physically-based distributed modelling of an upland catchment using the Système Hydrologique Européen'. J. Hydrol., 87, p. 79-102

BRAKENSIEK, D.L. (1967) 'Simulated watershed flow system for hydrograph prediction: A kinematic application.' Proc. Int. Hydrol. Symp., Pap. No. 3, Fort Collins, Colorado.

EMMETT, W.W. (1978) 'Overland flow.' In: M.J. Kirkby (ed.), *Hillslope hydrology*. John Wiley and Sons, New York, pp. 145-176.

FREAD, D.L. (1978) 'NWS operational dynamic wave model.' In: *Proceedings verification of math. and phys. models. 26th annual hydraul. div. spec. conf.*, ASCE, College Park, Maryland, pp. 455-464.

GOODRICH, D.C.; D.A. WOOLHISER and T.O. KEEFER (1991) 'Kinematic routing using finite elements on a triangular irregular network.' Water Resour. Res., 27, No.6, p.995-1003.

GOVINDARAJU, R.S.; M.L. KAVVAS and G. TAYFUR (1992) 'A simplified model for two-dimensional overland flows.' Adv. in Water Res., 15, p.133-141.

GREEN, W.H. and G.A. AMPT (1911) 'Studies on soil physics. I: the flow of air and water through soils'. J. Agric. Sci. 4, p.1-24.

GUPTA, S.K. and K.K. TANJI (1977) 'Computer program for solution of large, sparse, unsymmetric systems of linear equations.' J. Numerical Meth. in Engr., Vol.11, p. 1251-1259.

HENDERSON, F.M. and R.A. WOODING (1964) 'Overland flow and groundwater flow from a steady rainfall of finite duration.' J. Geophys. Res.,Vol.69 No.8, p.1531-1540.

IWAGAKI, Y. (1955) 'Fundamental studies of the runoff analysis by characteristics.' Disaster Prevention Research Institute, Bulletin No. 10, Kyoto University, Kyoto.

KAVVAS, M.L. and R.S. GOVINDARAJU (1992) 'Hydrodynamic averaging of overland flow and soil erosion over rilled hillslopes.' In: *Erosion, debris flows and environment in mountain regions.* (Proc. of the Chengdu Symp.), IAHS Publ. No. 209, p.101-111.

LANE, L.J. and M.A. NEARING (1989) *Water Erosion Prediction Project landscape profile model documentation*. NSERL Rep. No. 2, NSERL, ARS, USDA, Purdue Univ., West Lafayette.

LIGHTHILL, M.L. and G.B. WHITHAM (1955) 'On kinematic waves, I. Flood movement in long rivers.' Proc. Roy. Soc., A229, p. 281-316.

MEYER, L.D.; G.R. FOSTER and M.J.M. ROMHENS (1975) 'Sources of soil eroded from upland slopes.' In: *Proc. 1972 sediment yield workshop*. USDA Sediment Lab., ARS, Oxford, Mississippi, pp. 177-189.

MORRIS, E.M. and D.A. WOOLHISER (1980) 'Unsteady one-dimensional flow over a plane: Partial equilibrium and recession hydrographs.' Water Resour. Res., Vol.16, No.2, p. 355-360.

NEARING, M.A.; G.R. FOSTER; L.J. LANE and S.C. FINKNER (1989) 'A process-based soil erosion model for USDA-Water Erosion Prediciton Project technology.' Transact. Amer. Soc. Agr. Eng.

RAJBHANDARI, H. (1989) *Dynamics of flow in channel networks*. M.Sc. Thesis submitted to Dept. Civil and Env. Engr., Univ. California, Davis.

RAWLS, W.J.; D.L. BRAKENSIEK and MILLER, N. (1983) 'Green-Ampt infiltration parameters from soils data.' J. Hydraul. Engr., ASCE, 109, No.1.

SEVUK, A.S. (1973) *Unsteady flow in sewer networks*. PhD Thesis submitted to Dept. Civil. Engr., Univ. Illinois, Urbana-Champaign.

TAYFUR, G. and M.L. KAVVAS (1994) 'Spatially averaged conservation equations for interacting rill-interrill area overland flows.' J. Hydraul. Engr., ASCE, 120 No.12, p. 1426-1448.

TAYFUR, G.; M.L. KAVVAS; R.S. GOVINDARAJU and D.E. STORM (1993) 'Applicability of St. Venant equations for two-dimensional overland flows over rough infiltrating surfaces.' J. Hydraul., ASCE, 119 No.1, p. 51-63.

VIERA, J.H.D. (1983) 'Conditions governing the use of approximations for the St. Venant equations for shallow water surface flow.' J. Hydrol., No.60, p. 43-58.

WOODING, R.A. (1965a) 'A hydraulic model for the catchment-stream problem. I, kinematic wave theory.' J. Hydrol., No.3, p. 254-267.

WOODING, R.A. (1965b) 'A hydraulic model for the catchment-stream problem. II, numerical solutions.' J. Hydrol., No.3, p. 268-282.

WOODING, R.A. (1966) 'A hydraulic model for the catchment-stream problem. III, comparison with runoff observations.' J. Hydrol., No 4, p. 21-37.

WOOLHISER, D.A. (1975) 'Simulation of unsteady overland flow.' In: K. Mahmood and V. Yevjevich (ed.), *Unsteady flow in open channels*. Water Res. Publ., Fort Collins, Colorado, No.2, p. 485-508.

WOOLHISER, D.A. and J.A. LIGGETT (1967) 'Unstead one-dimensional flow over a plane - the rising hydrograph.' Water Resour. Res. 3, No 3, p. 753-771.

WOOLHISER, D.A.; R.E. SMITH and D.E. GOODRICH (1990). KINEROS, 'A kinematic runoff and erosion model: Documentation and user manual.' USDA, ARS-77.

YEN, B.C. and A.O. AKAN (1976) 'Flood routing through river junctions.' Proc. Symp. of Waterways. Rivers 1976. ASCE 1, p. 212-231.

ZHANG, W. and T.W. CUNDY (1989) 'Modelling of two-dimensional overland flow.' Water Resour. Res. 25, No 9, p. 2019-2035.

Sediment transport modelling - combination of theoretical concepts and practical approach

C. T. Yang
U.S. Bureau of Reclamation Technical Service Center, Denver, Colorado USA

Introduction

The processes of sediment transport, scour, and deposition in an alluvial channel are extremely complex. Theoretical developments of sediment transport functions for different flow and sediment conditions were based on assumptions of different degrees of complexity. Some of the simplified assumptions are based on idealized laboratory conditions that may not be true for the much more complicated natural river systems. Many of the more sophisticated theoretical solutions require a large number of parameters that are difficult or impossible to obtain from most natural rivers. Empirical solutions based on site-specific observations and data may be useful for a particular site where the data were collected. Application of these solutions to any other sites should be conducted with extreme caution. Some experienced hydraulic engineers with a good theoretical background in fluvial hydraulics and sediment transport are able to strike a balance between theoretical concepts and a practical approach for solving engineering problems. Their solutions help improve our understanding of the river morphologic processes.

The advancement of computer technology and capability enables engineers to analyze or simulate fluvial processes of different degrees of complexity. Complex computer models not only require a longer amount of computational time and computer capacity, most of them also need a large amount of field data for calibration and testing. From an engineering point of view, a good engineer should select the simplest model possible that can simulate the phenomena that are important to achieve the study objectives. There is no lack of computer models for engineers to choose from. The success of a study depends, to a large degree, on the engineer's understanding of fluvial processes, associated theories, and the capabilities and limitations of computer models. In many cases, the selection of a modeler is more important than the selection of computer models. A good modeler should have the ability to make necessary modifications to an existing general model for solving site-specific problems.

This report provides a general description of theoretical concepts used in the development of sediment transport computer models. The U.S. Bureau of Reclamation=s Generalized Stream Tube model for Alluvial River Simulation, version 2.0 (GSTARS 2.0), by Yang et al. (1998) is used as an example model for solving practical engineering problems. Current and future enhancements of GSTARS 2.0 are summarized in this report to indicate a trend of future model development.

Model dimension

Three-dimensional model

Flow phenomena in natural rivers are three dimensional, especially those at or near a meander bend, local expansion and contraction, or a hydraulic structure. Sophisticated numerical schemes have been developed to solve truly three-dimensional flow phenomena. Three-dimensional models need three-dimensional field data for testing and calibration. The collection of such data is not only costly but also time consuming. Certain assumptions need to be made before a sediment transport formula developed for one-dimensional flows can be applied to a truly three-dimensional model. With the exception of detailed simulation of flow in an estuary area, secondary current, or flow near a hydraulic structure, truly three-dimensional models are seldom used, and especially not for long-term simulations.

Two-dimensional model

Two-dimensional models can be classified into two-dimensional vertically averaged and two-dimensional horizontally averaged models. The former scheme is used where depth-averaged velocity or other hydraulic parameters can adequately describe the variation of hydraulic conditions across a channel. The latter scheme is used where width- or length-averaged hydraulic parameters can adequately describe the variation of hydraulic conditions in the vertical direction. Most two-dimensional sediment transport models are depth-averaged models. The width- or length-averaged two-dimensional models are usually used for modelling helicaldal flows.

One-dimensional model

Most sediment transport models are one-dimensional, especially those used for long-term simulation of a long river reach. One dimensional models require the least amount of field data for calibration and testing. The numerical solutions are more stable and require the least amount of computer time and capacity. However, one-dimensional models are not suitable for simulating truly two- or three-dimensional local phenomena.

Semi-two-dimensional model

A truly one-dimensional model cannot simulate the lateral variation of hydraulic and sediment conditions at a given river station. Engineers often take advantage of the non-uniform hydraulic and sediment conditions across a channel in their hydraulic design. For example, a water intake structure should be located on the concave side of a meandering bend, where the water is deep and sediment deposition is minimal. There are three types of semi-two-dimensional models.

Strip model

A strip model divides a channel into longitudinal strips of equal width or non-uniform width. Many modelers treat the main channel as the center strip and represent the flood plain as the left and right strips. There is no lateral variation of hydraulic and sediment parameters within each strip. The movement of water and sediment between strips is governed by diffusion equations. Many modelers assume that the diffusion coefficient is a constant in a diffusion equation. In reality, the diffusion coefficient varies with changing channel geometry, which is part of the unknown a computer model is trying to predict. Consequently, from a theoretical point of view, predicting the variation of the diffusion coefficient is difficult and may be impossible.

Stream tube model

Stream tubes are conceptual tubes whose walls are defined by streamlines. A streamline is a conceptual line to which the velocity vector of the fluid is tangent at each and every point, at each instant in time. A study reach is divided into stream tubes of equal discharge based on equal conveyance. Water and sediment cannot cross the boundary of stream tubes. Consequently, there is no need for solving diffusion equations and the difficulties of determining diffusion coefficients can be avoided. The velocity and sediment concentration distributions in a stream tube are assumed to be uniform across the tube. However, because the stream tube width and location can change with respect to time across a given station, water and sediment can move with stream tubes implicitly across a channel. Yotsukura and Sayre (1976) combined the stream function with transverse diffusivity to explain the movement of tracer in a natural channel.

Composite model

A composite model superimposes lateral movement of water and sediment on a one-dimensional model. The knowledge of variation of shear stress, or other parameters, is often required in the development of a composite model. For example, Song et al. (1995) superimposed the lateral sediment transport across GSTARS (Molinas and Yang, 1986) stream tubes due to secondary current and lateral shear stress. This composite model enabled them to more accurately simulate sediment transport near a meandering bend.

Fixed and variable width model

Fixed width model

Open-channel hydraulic problems can be solved only if the channel width is fixed or can be assumed. With the exception of empirical relationships, conventional open-channel hydraulics cannot provide theoretical solutions for the determination of channel width. Consequently, most sediment transport models assume that the channel width is given and would not adjust with changing flow and sediment conditions. This assumption can cause significant errors in the prediction of variation of channel geometry and profile, especially for alluvial rivers, where the width change may be more significant than the depth change during a flood.

Variable width model

The concept of threshold tractive force on channel perimeter and the theory of minimum energy dissipation rate (Yang and Song, 1986) or its simplified minimum stream power theory (Yang, 1992) can be used as a theoretical basis for the determination of optimum channel geometry and width.

Threshold tractive force approach

Lane (1955) applied the threshold tractive force concept to determine the stable channel geometry of a straight channel of noncohesive materials, where the effects of secondary flow can be neglected. A threshold channel is based on the flow condition at incipient motion of sediment particles. It cannot be used to determine stable channel geometry and width in an area of active sediment transport. Parker (1978) employed the momentum balance of Lundgren and Jonsson (1964) to account for lateral turbulent diffusion of downstream momentum. Due to the complexity of the corresponding differential equation, Parker's solution was limited to the flat bed region. The bank geometry was solved as a first-order solution, yielding a cosine profile. More recent modifications and improvements of Parker's approach were made by Vigilar and Diplas (1994, 1997). The stable channel dimensions and bed-load transporting capacity can be determined by these modified methods for known local bed slope, sediment size and shape, critical Shields parameter, and water discharge. However, for a width-depth ratio greater than 12, which is typical of natural streams, the bank profile remains constant.

Minimum energy dissipation rate or minimum stream power approach

The theory of minimum energy dissipation (Yang and Song, 1986) states that for a closed and dissipative system at dynamic equilibrium, the energy dissipation rate of the system must be at a minimum value subject to the constraints applied to the system. If the system is not at its dynamic equilibrium condition, its energy dissipation rate is not at minimum. However, the system will adjust itself in such a manner that its energy dissipation rate can be reduced to a minimum and regain equilibrium. For open-channel flows where the energy dissipation rate due to sediment transport is small, compared with that for water transport, the minimum energy dissipation rate theory can be reduced and simplified to the minimization of stream

power. Stream power is the product of discharge Q and energy slope S. Chang (1988) considered Q a constant within a time step of computation. In this case, minimization of stream power QS would be equivalent to minimization of slope S. Chang further stated that channel width adjustment at all cross sections should be such that the spatial distribution of stream power along the study reach moves toward uniformity. Because the spatial variation of Q is small, uniform QS is equivalent to uniform slope S in the longitudinal direction. To determine whether the width should increase or decrease, the energy or water-surface slope S_i at station i is compared with the weighted average slope $\bar{s}_i$, i.e.,

$$\overline{S_i} = \frac{S_{i+1}\Delta X_{i-1} + S_{i-1}\Delta X_i}{\Delta X_i + \Delta X_{i-1}} \tag{1}$$

where S_{i-1} and S_{i+1} = slope at stations $i - 1$ and $i + 1$, respectively; ΔX_{i-1} and ΔX_i = reach length between stations $i - 1$ and i, and between stations i and $i + 1$, respectively. If S_i is greater than S_i, channel width at station i will be reduced to reduce S_i. If S_i is less than S_i, channel width will be increased to increase S_i. The use of uniform slope by Chang has a computational advantage of being simple and straightforward. However, uniform slope is not equivalent to minimum stream power in many cases. Uniform slope exists in a relative short reach at a high flow or channel-forming discharge. At medium or low flows, slope varies between pools and riffles, and uniform slope does not exist anymore. Yang and Molinas (1988) explained this phenomenon from a theoretical point of view and supported it with field data and computed profiles to show that Chang's method is valid at high or channel-forming discharge.

The method used in computer models GSTARS (Molinas and Yang, 1986) and GSTARS 2.0 (Yang et al., 1998) is based on the minimization of total stream power in a study reach, i.e.,

$$\Phi = \gamma \sum_{i=1}^{N-1} \left(\frac{Q_i S_i + Q_{i+1} S_{i+1}}{2} \right) \Delta X_i = a\ minimum \tag{2}$$

where Φ= rate of energy dissipation; $Q_i S_i$ and $Q_{i+1} S_{i+1}$ = stream power at station i and $i+1$, respectively; ΔX_i = reach length between station i and $i + 1$; and N = total number of stations.

It should be pointed out that even though Q_i is considered a constant during a computational time step, Q_i cannot be taken out of the minimization process without going through the channel geometry adjustment process first. In the minimization process, Q_i is related to water conveyance at station i, which is a function of channel geometry and energy slope. Thus the adjustment of channel geometry and width is implicitly included in the minimization of stream power. This approach is valid for high, medium, and low flows.

Computer model classification

Sediment routing models can be classified as steady or unsteady, coupled or uncoupled, equilibrium or non-equilibrium, and uniform or non-uniform sediment models.

Steady or unsteady model

If the flow and sediment conditions in a model vary over time, it is an unsteady model. Otherwise, it is a steady model. Strictly speaking, flow and sediment conditions in most natural rivers are unsteady due to the changing hydrologic conditions over time. However, a hydrograph may be approximated by a series of constant discharge bursts, and the steady-flow techniques can be used for these quasi-steady-flow computations. The basic governing equations for a one-dimensional unsteady flow are:
Water continuity equation

$$\frac{\partial A}{\partial t} + \frac{\partial Q}{\partial x} + p_s \frac{\partial A_s}{\partial t} - q_l = 0 \tag{3}$$

Water momentum equation

$$\frac{\partial(\rho Q)}{\partial t} + \frac{\partial}{\partial x}\left(\rho \frac{Q^2}{A}\right) + g\rho A \frac{\partial z}{\partial x} + \rho g A S_f = 0 \tag{4}$$

Sediment continuity equation

$$\frac{\partial(C_v A)}{\partial t} + (1 - p_s)\frac{\partial A_s}{\partial t} + \frac{\partial Q_s}{\partial x} + C_l q_l = 0 \tag{5}$$

where A = cross-sectional area of flow; A_s = cross-sectional area of river bed; C_v = suspended load concentration by volume; C_l = concentration of lateral flow by volume; g = gravitational acceleration; p_s = bed sediment porosity; Q = water discharge; Q_s = volumetric total sediment discharge; q_l = lateral inflow per unit length x; S_f = energy or friction slope; t = time; x = distance along the channel; z = water surface elevation; and ρ = density of water.
For steady flow, Equations (3), (4), and (5) can be reduced to

$$\frac{\partial Q}{\partial x} - q_l = 0 \tag{6}$$

$$\frac{\partial}{\partial x}\left(\frac{Q^2}{A}\right) + gA\frac{\partial z}{\partial x} + gAS_f = 0 \tag{7}$$

$$(1 - p_s)\frac{\partial A_s}{\partial t} + \frac{\partial Q_s}{\partial x} + C_l\, q_l = 0 \tag{8}$$

The friction or energy slope S_f is related to sediment particle size, flow discharge, sediment load or concentration, bed forms, channel geometry and pattern, growth of vegetation, etc. Strictly speaking, S_f should be treated as an unknown variable. In practice, S_f is treated as a constant and is computed from a resistance function such as the Manning, Chezy, or the Darcy-Weisbach's formula, i.e.,

$$S_f = \frac{Q\,|\,Q\,|}{K^2} \tag{9}$$

$$K = \sum_{j=1}^{m} K_j \tag{10}$$

$$K_j = \frac{1}{n_j} A_j R_j^{2/3} \tag{11}$$

where K = total conveyance; K_j = conveyance of subsection j; A_j = cross sectional area of subsection j; R_j = hydraulic radius of subsection j; n_j = Manning's roughness coefficient of subsection j; and m = total number of sections. If the English unit is used, 1 should be replaced by 1.486 in Equation (11).

Coupled or uncoupled model

A coupled model solves the water continuity equation, water momentum equation, and sediment continuity equation simultaneously. If the change of A_s in Equations (3) and (5)

within a short period of time is much smaller than the change of cross-sectional area *A,* the solution can be uncoupled by solving the water continuity and momentum equations first. The solutions thus obtained are then used to solve the sediment continuity equation. Uncoupled models solve the water and sediment routings separately to simplify the numerical solution. Generally speaking, a coupled model is more stable than an uncoupled model. The stability of uncoupled and coupled models can be improved by using a smaller time step of computation.

Equilibrium or non-equilibrium model

If we assume that there is an instantaneous exchange of sediments in transportation and those on an alluvial channel bed when and where there is a difference between sediment supply and a river's sediment transport capacity, the model is an equilibrium model. This assumption is valid if sediments are transported mainly as bed load or if the sediments are coarse. For fine sediments, the assumption of instantaneous exchange may not be valid and there is a lag between the time when the imbalance occurs and the time sediments are actually deposited or scoured from the bed. A model that takes this phenomenon into consideration is a non-equilibrium model. Usually a decay function is applied in a non-equilibrium model to reflect the non-instantaneous exchange of sediments.

Uniform or non-uniform model

A uniform model uses a representative particle size for sediment routing. A non-uniform model routes sediment by size fraction to more realistically reflect the phenomenon of sediment sorting and the formation and destruction of an armour layer on a river bed.

Numerical solution

Finite element and finite difference methods

Most of the sediment-transport models use the finite difference method for solving partial differential equations. Consequently the finite element method will not be discussed in this section. Martin and McCutcheon (1999) and Abbott and Basco (1989), among others, gave detailed descriptions of numerical methods commonly used in hydrodynamic computer models. Wu and Molinas (1996) gave a comprehensive presentation of different techniques, which can be used for solving Equations (3), (4), and (5). The general approach is to replace the partial derivatives in Equations (3), (4), and (5) with quotients of finite differences by using explicit or implicit finite difference methods. The choice of numerical techniques for a particular situation should be based on its accuracy, stability, and convenience to use. Amein and Fang (1970), among others, found that the implicit method is unconditionally stable. This method is also faster and more accurate than other finite-difference methods when applied to open channel flood routing. The finite-difference method formulated by Amein

and Fang solves nonlinear algebraic equations by iteration, which is time consuming. Preissman (1960) developed a more efficient implicit finite-difference scheme to approximate a function *f (x, t)* and its derivatives of *Mf/Mx* and *Mf/Mt* at point *P* using the following equations:

$$f_p(x,t) \cong \lambda \frac{f_i^{j+1} + f_{i+1}^{j+1}}{2} + (1 - \lambda)\frac{f_i^{j} + f_{i+1}^{j}}{2} \tag{12}$$

$$\frac{\partial f}{\partial x}\Big|_p \cong \lambda \frac{f_{i+1}^{j+1} - f_i^{j+1}}{\Delta x} + (1 - \lambda)\frac{f_{i+1}^{j} - f_i^{j}}{\Delta x} \tag{13}$$

$$\frac{\partial f}{\partial t}\Big|_p \cong \frac{1}{2}\left(\frac{f_i^{j+1} - f_i^{j}}{\Delta t} + \frac{f_{i+1}^{j+1} - f_{i+1}^{j}}{\Delta t}\right) \tag{14}$$

where $f_i^j = f(x_i, t^j)$; $\lambda = \delta t/\Delta t$; δt = distance of point *P* on the time axis for the old time line t^j; and Δt = distance of the time axis between t^j and t^{j+1}. If $\lambda = 2$, the scheme is called center-implicit. If $\lambda = 1$ the scheme is called fully implicit. If $\lambda = 0$, the scheme is called fully explicit. The Preissman's finite difference scheme is shown in Figure 1. Four commonly used methods of solution are the complete solution, the uncoupled unsteady solution, the known discharge solution, and the uncoupled steady solution. These methods can be categorized into the coupled method of complete solution with known discharge and the uncoupled method of unsteady and steady solutions. Wu and Molinas (1996) made the following comments of the advantages and disadvantages of different methods:

(1) The coupled method can better account for the continuous interaction between the hydraulic and sediment transport phases.
(2) The coupled method can be used with a longer time increment.
(3) The formulation of the complete solution of a coupled method is the most elaborate among the four methods.

The known-discharge solution is developed solely for sediment routing.

The uncoupled method is simpler to formulate than the coupled method.

The length of time increment of an uncoupled solution is restricted in that the bed elevation change over one time increment must be small.

For a stable channel with mild changes, the uncoupled method should be used for water and sediment routing.

Under constant flow conditions, the uncoupled steady method should be used for sediment routing.

If the channel is very active, the coupled method is most suitable.

The coupled method is desirable for routing both water and sediment.

The known discharge solution can be utilized to simulate sediment transients.

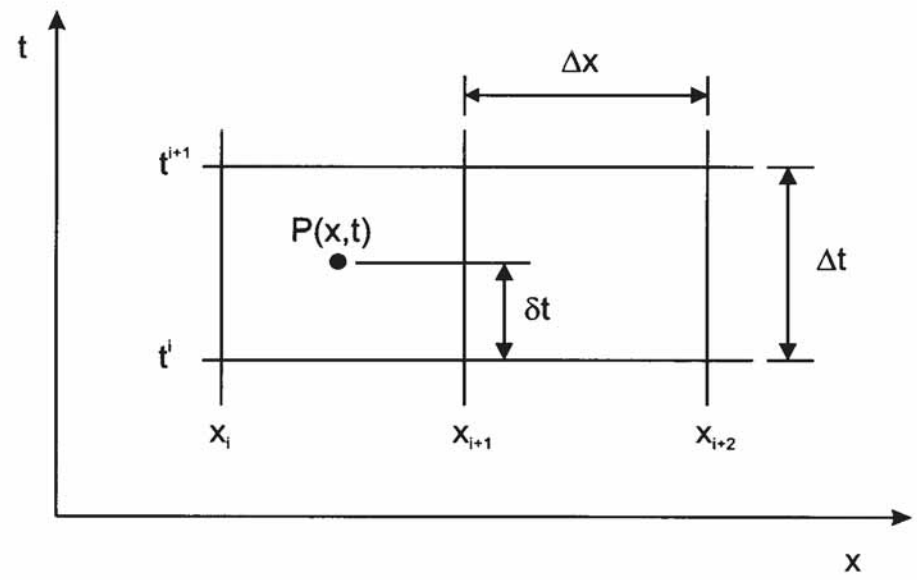

Fig. 1 Represantation of Preissman's finite difference scheme

Stability and accuracy

If small numerical truncation and other errors introduced at a given time in the numerical procedure do not amplify during successive applications of the procedure, the finite difference procedure is stable. The stability of a numerical solution may be improved by reducing the size of the space and time intervals. Implicit methods of finite differences are generally unconditionally stable for linear problems. The maximum allowable time step is limited by the required accuracy (Fread, 1974; Liggett and Lunge, 1975). The stability of an explicit method is governed by the Courant condition $\Delta t \leq \frac{\Delta x}{C}$ where Δx = distance between x_i and x_{1+t}; Δt = time difference between t^j and t^{j+1}; C = wave celerity = $\sqrt{gy} + V$; y = water depth; and V = mean flow velocity. For explicit schemes the Courant Number should not exceed 1; i.e., $C\Delta t/\Delta x$ *#1* for stability reasons.

Accuracy is a measure of the discrepancy between the computed and observed results. Liggett and Cunge (1975) gave the following reasons for possible discrepancies between a mathematical model and the prototype:

1. Inaccurate simplification and approximation of the basic equations to simulate a complex prototype.
2. Inaccurate measuring techniques, such as survey errors and badly located gaging stations.
3. Insufficient field data, such as unknown tributary discharges, seepage flow, etc.
4. Phenomena such as the variations of roughness coefficient with varying bed forms and channel geometry and pattern are not fully understood and their impacts on computed results are ignored.
5. Inaccurate or inadequate schematization of topographic features.

Model components

A sediment routing model that can simulate the dynamic adjustments of channel geometry, shape, and longitudinal profile should consist of the components or modules listed below. The GSTARS 2.0 (Yang et al., 1998) terminology is used in the following descriptions.

Geometric component

A geometric component includes basic data used to describe or compute channel geometry, slope and reach length. Geometric computations include the computations of cross-sectional areas, wetted perimeter, hydraulic radius, centroid of a cross-section or subsection, top width of a cross-section or subsection. Information between the selected stations is generally interpolated linearly. The selection of representative cross-sections and study reach length may affect the accuracy of simulated or predicted results.

Hydraulic component

A hydraulic component utilizes geometric and hydrologic information for backwater surface profile computations to determine flow velocity, depth, slope, total energy loss through the study reach, and local energy loss due to channel expansion and contraction. The energy equation for subcritical water surface profile computation is

$$Z_1 + Y_1 + \alpha_1 \frac{V_1^2}{2g} = Z_2 + Y_2 + \alpha_2 \frac{V_2^2}{2g} + H_t \tag{15}$$

where Z = bed elevation; Y = water depth; V = velocity; V = velocity distribution coefficient; H_t = total energy loss between sections 1 and 2; g = gravitational acceleration; and subscripts 1 and 2 denote sections 1 and 2, respectively. The total conveyance, K, is used to determine the friction slope, S_f, for a specified discharge:

$$S_f = \left(\frac{Q}{K}\right)^2 \tag{16}$$

The formulas by Manning, Chezy, or Darcy-Weisbach are generally used for the computation of conveyance:

Manning's formula:

$$Q = KS_f^{1/2} = \left(\frac{1.49}{n} AR^{2/3}\right) S_f^{1/2} \tag{17}$$

Chezy's formula

$$Q = KS_f^{1/2} = (CAR^{1/2}) S_f^{1/2} \tag{18}$$

Darcy-Weisbach's formula:

$$Q = KS_f^{1/2} = \left[\left(\frac{8gR}{f}\right)^{1/2} A\right] S_f^{1/2} \tag{19}$$

where n, C, and f = roughness coefficients in Manning, Chezy, and Darcy-Weisbach's formulas, respectively; g = acceleration due to gravity; A = cross-sectional area; and R = hydraulic radius. The friction loss, h_f, through each reach is the product of friction slope and the reach length, L. The friction loss at the cross section in GSTARS 2.0 (Yang et al., 1998) can be determined from one of the following four choices:

from the average friction slope of the adjacent reaches:

$$h_f = \left[\frac{(S_f)_1 + (S_f)_2}{2}\right] L \tag{20}$$

from the geometric mean:

$$h_f = L\sqrt{(S_f)_1 (S_f)_2} \tag{21}$$

from the harmonic mean:

$$h_f = \left(\frac{2(S_f)_1 (S_f)_2}{(S_f)_1 + (S_f)_2}\right) L \tag{22}$$

or from the average conveyance:

$$h_f = \left(\frac{2Q}{K_1 + K_2} \right)^2 L \tag{23}$$

The local loss caused by channel expansion and contraction, h_E, is computed from:

$$h_E = C_E \left| \frac{V_1^2}{2g} - \frac{V_2^2}{2g} \right| \tag{24}$$

where C_E = energy loss coefficient.

Other local losses, such as losses due to channel bends or manmade construction, are computed from:

$$h_B = C_b \frac{V_2^2}{2g} \tag{25}$$

where C_b = an energy loss coefficient supplied by the user. For most natural rivers, C_b values are assumed to be zero. The total energy loss, H_t in Equation (15), is the sum of friction loss and the local losses.

The energy equation is applied if there is no change of flow regime throughout the study reach. If there are changes in flow regime (i.e., if the flow changes from subcritical to supercritical or vice versa), the momentum equation is used. For the reaches where flow regime changes are detected (i.e., in hydraulic jumps), the momentum equation is used:

$$\frac{Q\gamma}{g}(\beta_2 V_2 - \beta_1 V_1) = p_1 - p_2 + W \sin \theta F_f \tag{26}$$

where γ = unit weight of water; β = momentum coefficient; p = pressure acting on a given cross section; W = weight of water enclosed between section 1 and 2; θ = angle of inclination of channel; and F_f = total external friction force acting along the channel boundary. If the value of θ is small, $\sin \theta \approx .0$ and $\beta_1 = \beta_2 = 1$, and Equation (26) becomes

$$\frac{Q^2}{A_1 g} + A_1 \overline{y_1} = \frac{Q^2}{A_2 g} + A_2 \overline{y_2} \quad (27)$$

where $\overline{y}$ = depth measured from water surface to the centroid of cross section A containing flow.

Sediment component

Basic equations

The basis for sediment-routing computations in one-dimensional unsteady flow is the sediment continuity equation, Equation (5), which can be rewritten as:

$$\frac{\partial Q_s}{\partial x} + \eta \frac{\partial A_d}{\partial t} + \frac{\partial A_s}{\partial t} - q_s = 0 \quad (28)$$

where η = volume of sediment in a unit bed layer volume (one minus porosity); A_d = volume of bed sediment per unit length; A_s = volume of sediment in suspension at the cross section per unit length; Q_s = volumetric sediment discharge; and q_s = lateral sediment inflow. A number of
assumptions are often made to simplify Equation (28). First, it is assumed that the change in suspended sediment concentration in a cross section is much smaller than the change of the river bed, i.e.:

$$\frac{\partial A_s}{\partial t} \ll \eta \frac{\partial A_d}{\partial t} \quad (29)$$

Second, during a time step, the parameters in the sediment-transport function for a cross section are assumed to remain constant:

$$\frac{\partial Q_s}{\partial t} = 0 \text{ or } \frac{\partial Q_s}{\partial x} = \frac{dQ_s}{dx} \quad (30)$$

This assumption is valid only if there is little variation of the cross-sectional geometry, i.e., if not much erosion and/or deposition occurs in a time step. This assumption allows the decoupling of water and sediment routing computations. In practice, this condition can be met by using a small enough time step.

Finally, if there are no lateral inflows, the $q_s = 0$, and the final form of the sediment continuity equation used is:

$$\eta \frac{\partial A_d}{\partial t} + \frac{dQ_s}{dx} = 0 \tag{31}$$

In order to solve Equation (31) numerically, a discretization process must be adopted. First, the change in the volume of bed sediment due to deposition or scour, ΔA_d , is written as:

$$\Delta A_d = (aP_{i-1} + bP_i + cP_{i+1})\Delta Z_i \tag{32}$$

where P = wetted perimeter; ΔZ = change in bed elevation (positive for aggradation, negative for scour); i = cross section index; and *a, b,* and *c* are weight factors that must satisfy:

$$a + b + c = 1 \tag{33}$$

Using expression (31) and (32), the partial derivative terms are approximated as follows:

$$\frac{dQ_s}{dx} \approx \frac{Q_{s_i} - Q_{s_{i-1}}}{‰(\Delta x_i + \Delta x_{i-1})} \tag{34}$$

$$\frac{\partial A_d}{\partial t} \approx \frac{(aP_{i-1} + bP_i + cP_{i+1})\Delta Z_i}{\Delta t} \tag{35}$$

$$\Delta Z_{i,k} = \frac{2\Delta t(Q_{s_{i-1,k}} - Q_{s_{i,k}})}{\eta_i(aP_{i-1} + bP_i + cP_{i+1})(\Delta X_i + \Delta X_{i-1})} \tag{36}$$

where k = size fraction index; η_i = volume of sediment in a unit bed layer at cross section i; and
$Q_{si,k}$ = computed volumetric sediment discharge for size k at cross section i. The total bed elevation change for a stream tube at cross section i, ΔZ_i, is computed from

$$\Delta Z_i = \sum_{k=1}^{nsize} \Delta Z_{i,k} \tag{37}$$

where *n size* = total number of size fractions present in cross section i. The new channel cross section at station i, to be used at the next time iteration, is determined by adding the bed elevation change to the old bed elevation.

Bed sorting and armouring

If a model computes sediment transport by size fraction, it will show particles of different sizes being transported at different rates. Depending on the hydraulic parameters, the incoming sediment distribution, and the bed composition, some particle sizes may be eroded, while others may be deposited or may be immovable. A model computes the carrying capacity for each size fraction present in the bed, but the amount of material actually moved is computed by the sediment routing equation. Consequently, several different processes may take place. For example, all the finer particles may be eroded, leaving a layer of coarser particles for which there is no carrying capacity. No more erosion may occur under these hydraulic conditions, and the bed is said to be armoured. This armour layer prevents the scour of the underlying materials and the sediment available for transport becomes limited to the amount of sediment entering the reach. However, hydraulic events, such as an increase of flow velocity, may increase the flow carrying capacity, causing the armour layer to break and restart the erosion processes in the reach.

Many different processes may occur simultaneously within the same channel reach. These depend not only on the composition of the supplied sediment, i.e., the sediment entering the reach, but also on bed composition within that reach. The bed composition may vary within the reach both in space and time. The concept of active and inactive layers is used in most sediment routing models. The active layer is the top layer on the bed, which contains the bed materials available for transport. The inactive layer is the layer beneath the active layer used for storage. Below these two layers is the undisturbed bed with the initial bed material composition.

Sediment transport formulas

There are many sediment transport formulas in the literature for a user to choose. Some of them are intended for bed load, some for suspended load, and some for total bed-material load. There is no universal formula that can be applied to all flow and sediment conditions. Depending on the selection of transport formulas, simulated and predicted results from a computer model may vary significantly from each other and from observation. Systematic and detailed evaluations of sediment transport formulas were presented by Yang (1996) that include recommendations on the selection of formulas for engineering applications.

Sediment transport formulas are developed for one-dimensional steady uniform flows under equilibrium conditions. When a formula is applied to a sediment routing model, we usually assume that there is an instantaneous exchange of sediments in motion, including those in suspension, with those on the bed. This assumption is valid if sediment particles are transported mainly as bed load or if the difference between the sediment supply from upstream and a river's transport capacity is small. Otherwise, a decay function may be needed for non-equilibrium sediment transport, especially for fine sediment transport. The spatial-delay and/or time-delay decay function can be expressed as a function of sediment particle fall velocity and a recovery factor for deposition and/or entrainment. For example, Han (1980) developed the following decay function for non-equilibrium sediment transport based on analytical solution of the convection-diffusion equation:

$$C_i = C_i^* + (C_{i-1} - C_{i-1}^*) \exp\left(-\frac{\alpha \omega_s \Delta x}{q}\right) + (C_{i-1}^* - C_i^*)\left(\frac{q}{\alpha \omega_s \Delta x}\right)\left[1 - \exp\left(-\frac{\alpha \omega_s \Delta x}{q}\right)\right] \quad (38)$$

where C_i = sediment concentrationat cross-section i; C_i^* = sediment carrying capacity at cross section i; q = discharge of flow per unit width; Δx = reach length; ω_s = sediment fall velocity; i = cross-section index (increasing from upstream to downstream); and α= recovery factor. The α value can vary widely from case to case. Han and He (1990) recommended a value of 0.25 for deposition and 1.0 for entrainment.

Width adjustment component

Most sediment transport models do not have a width adjustment component. These models assume that the channel width is fixed and cannot be changed or adjusted. However, except for reaches in which the channel width is confined by levees or canyon walls, the width adjustment of an alluvial river during a flood may be much larger than the depth adjustment. Consequently, a sediment transport model without the width adjustment component may give inaccurate and sometimes erroneous results.

FLUVIAL-12 (Chang, 1990) and GSTARS 2.0 (Yang et al., 1998) are two recent models that include the width adjustment component. The width adjustments of these two models are based on minimum stream power. However, Chang used uniform slope as specified by Equation (1), whereas Yang et al. used minimum total stream power as specified by Equation (2), for the determination of optimum channel width. Equation (1) is valid for channel forming discharge or high flows. Equation (2) is valid regardless of whether the flow is high, medium, or low.

GSTARS 2.0 model

There are many sediment transport models having various degrees of complexity. Some models were developed for solving site-specific problems. Some models are very sophisticated and have a sound theoretical basis but require extensive field data for testing and calibration. Some models are based on simplified assumptions, which may or may not be substantiated by field observations. A general sediment transport model, which can be used for solving practical river engineering problems should have the following characteristics:

1. The mathematical formulation is based on well-established theories applicable to field conditions.
2. The model can be applied to open channels with fixed as well as alluvial boundaries.
3. The model can be applied to subcritical, critical, or supercritical flows or to a combination of them without interruption.
4. The model can compute and simulate hydraulic and sediment conditions in both the longitudinally and laterally.
5. The model can route sediment by size fraction to simulate the formation and destruction of an armour layer for long-term simulation of river morphologic processes.
6. The model can simulate and predict channel geometry change in depth as well as in width.
7. The model can simulate equilibrium as well as non-equilibrium sediment transport.
8. The model can incorporate site-specific conditions such as channel side stability and erosion limits.
9. The model does not require extensive field data, which can be difficult or impossible to obtain.

GSTARS 2.0 (Yang et al., 1998) is a generalized stream tube model developed by the U.S. Bureau of Reclamation for solving practical river engineering and sedimentation problems. GSTARS 2.0 has the characteristics listed above. This model is used herein to illustrate how some of the basic theoretical concepts can be incorporated in a sediment transport model for solving practical engineering problems.

General description of GSTARS 2.0

The Generalized Stream Tube model for Alluvial River Simulation (GSTARS) was developed by the U.S. Bureau of Reclamation (Molinas and Yang, 1986) as a generalized water and sediment-routing computer model for solving complex river engineering problems. Since then, GSTARS has been applied by many investigators to simulate and predict river morphologic changes caused by manmade and natural events. As a result of these applications, GSTARS has been revised and enhanced. An enhanced and improved model, GSTARS version 2.0 (GSTARS 2.0) developed for PC applications has been released recently (Yang et al., 1998) to replace GSTARS.

Improvements and revisions made in GSTARS 2.0 over GSTARS include, but are not limited to the following (Yang and Simões, 1998):

- Number of user-selected sediment transport functions increased from 4 to 13.

- Cohesive sediment transport capabilities.
- Side stability subroutine based on the angle of repose.
- Nonequilibrium sediment transport based on the decay function of Han (1980).
- Transport function for sediment-laden flows by Yang et al. (1996).
- Mass balance check and many debugging features.
- Subroutine that adds points to enable continued accurate modeling of cross sections that have an insufficient number of measured points in any given stream tube.
- Increased the number of cross sections and cross-section points that can be put to describe the study reach.
- Original CYBER mainframe version of GSTARS modified to operate on a PC using FORTRAN 77 and FORTRAN 90 in syntax in GSTARS 2.0.
- Error checking of input data file.
- Output plotting options, including graphic display capability for cross sections and water surface profiles (program GSPLOT).
- Extensive revision of computer codes and functions, even though some of the input record names may be the same in GSTARS and GSTARS 2.0.
- Data input using either U.S. or metric units.

Among the 49 data records used in GSTARS and GSTARS 2.0, only 14 remain the same in both versions.

GSTARS is no longer supported by the U.S. Bureau of Reclamation and no longer available to the public. The complete GSTARS 2.0 user's manual and the program can be obtained by registering at www.usbr.gov/srhg/gstars/2.0. The following brief descriptions are limited to GSTARS 2.0 only. Some of the important features of GSTARS 2.0 are:

- The use of the stream tube concept to simulate the longitudinal and lateral variations of flow and sediment conditions in a semi-two-dimensional manner. The variation of bed elevation due to scour and deposition constitute the variation in the third dimension. Thus a one-dimensional numerical solution along stream tubes can simulate river morphologic changes in a semi-three-dimensional manner.
- The conjunctive use of energy and momentum equations can compute water surface profiles through subcritical, critical, and supercritical flows without interruption.
- The minimum energy dissipation rate theory or its simplified total stream power minimization provides the theoretical basis for determining channel width and depth adjustments at each time step of computation.
- The model consists of independent but mutually connected components or modules for easy modification and improvement to meet specific project needs in the future.

Basic computations

Geometric computation

$$A_i = 0.5(y_i + y_{i+1})dx_i \tag{39}$$

For natural channels or irregular cross sections, the channel can be divided into subchannels. In GSTARS 2.0, the variables related to the cross-sectional geometry (area, wetted perimeter, hydraulic radius, channel's top width) are computed for each subchannel. These values are summed to obtain the total values for the cross section. The relationships used are well known in the literature and are the following (Yang et al., 1998):

$$R_i = \frac{A_i}{P_i} \tag{40}$$

$$A_t = \sum_{i=1}^{m} A_i \tag{41}$$

$$P_t = \sum_{i=1}^{m} P_i \tag{42}$$

$$\bar{y} = \frac{1}{3} y_i \text{ if adjacent to channel wall} \tag{43}$$

$$\bar{y}_i = 0.25(y_i + y_{i+1}) \text{ if not adjacent to channel wall} \tag{44}$$

$$R = \frac{A_t}{P_t} \tag{45}$$

$$P_i = [dx_i^2 + (y_i - y_{i+1})^2]^{1/2} \tag{46}$$

$$T = \sum_{i=1}^{N} T_i \tag{47}$$

$$\bar{y} = \frac{\sum_{i=1}^{m} A_i \bar{y}_i}{A_t} \tag{48}$$

where A_i, P_i, R_i, $\underline{y}_i$ = area, wetted perimeter, hydraulic radius, and centroid of a subsection, respectively; T_i = top width of a subchannel; A_t, P_t, R, and $\underline{y}$ = area, wetted perimeter, hydraulic radius, top width, and centroid of the whole cross section, respectively; m = number of subsections; and N = number of computed subchannels.

Backwater surface profile computation

For most of the water profile computations, GSTARS 2.0 uses the energy equation:

$$Z_1 + Y_1 + \alpha_1 \frac{V_1^2}{2g} = Z_2 + Y_2 + \alpha_2 \frac{V_2^2}{2g} + H_t \quad (49)$$

where Z = bed elevation; Y = water depth; V = velocity; α= velocity distribution coefficient; H_t = total energy loss between sections 1 and 2; g = gravitational acceleration; and subscripts 1 and 2 denote sections 1 and 2, respectively. The energy loss can be computed by the Manning, Chezy, or the Darcy-Weisbach formula.

The energy equation is applied if there is no change of flow regime throughout the study reach. If there are changes in flow regime (i.e., if the flow changes from subcritical to supercritical or vice versa), the momentum equation is used, i.e.:

$$\frac{Q\gamma}{g}(\beta_2 V_2 - \beta_1 V_1) = p_1 - p_2 + W \sin\theta - F_f \quad (50)$$

where γ = unit weight of water; β= momentum coefficient; p = pressure acting on a given cross section; W = weight of water enclosed between sections 1 and 2; θ = channel angle of inclination; and F_f = total external friction force acting along the channel boundary. If the

$$\frac{Q_2}{A_1 g} + A_1 \overline{y_1} = \frac{Q^2}{A_2 g} + A_2 \overline{y_2} \quad (51)$$

value of θ is small, sin $\theta \approx .0$ and $\beta_1 = \beta_2 = 1$, and Equation (51) becomes:
where $\underline{y}$ = depth measured from water surface to the centroid of cross section A containing flow. In GSTARS 2.0, $\underline{y}$ is computed by dividing the irregular cross sections into m subsections (m = 10) and using the relation:

$$\bar{y} = \frac{\sum_{i=1}^{m} A_i \overline{y_i}}{A} \quad (52)$$

Stream tube computation

The water surface profiles are computed first, as described above. The channel is then divided into a selected number of stream tubes with the following characteristics: (1) the total discharge carried by the channel is distributed equally among the stream tubes; (2) stream tubes are bounded by channel boundaries and by imaginary vertical walls; (3) the discharge along a stream tube is constant; and (4) there is no exchange of water or sediments through stream tube boundaries.

Due to the nature of the backwater computations, the water surface elevation is assumed to be horizontal across each cross section. The lateral locations of the stream tubes are computed at each time step from the channel conveyance; i.e., stream tube boundaries are set to provide equal conveyance.

Stream tube widths and locations are computed for each time step; therefore, they are allowed to vary with time. Sediment routing is carried out independently for each stream tube and for each time step. Bed material composition is computed for each tube at the beginning of the time step, and bed sorting and armouring computations are also done separately for each stream tube. In GSTARS 2.0, lateral variations of bed material composition are accounted for, and this variation is included in the computations of the bed material composition and sorting for each stream tube. Therefore, although no material is allowed to cross stream tube boundaries during a time step, lateral movement of sediment is accomplished by the lateral variation of the stream tube boundaries from time step to time step.

Sediment transport computation

The basic sediment transport continuity equation and equations governing channel geometry adjustment are given in Equations (28) through to (37). GSTARS 2.0 has the following 13 sediment transport formulas from which a user may choose:

- Meyer-Peter and Müller's 1948 formula
- Laursen's 1958 formula
- Toffaleti's 1969 method
- Engelund and Hansen's 1972 method
- Ackers and White's 1973 method
- Revised Ackers and White's 1990 method
- Yang's 1973 sand and 1984 gravel transport formulas
- Yang's 1979 sand and 1984 gravel transport formulas
- Yang's 1996 modified formula for sediment-laden flow with a high concentration of wash load
- Krone's 1962 and Ariathurai and Krone's 1976 methods for cohesive sediment transport
- Parker's 1990 method

Most sediment transport formulas were developed for computing the total load without breaking it into load by size fraction. In GSTARS 2.0, these formulas have been modified to account for transport by size fraction. The total carrying capacity or sediment concentration for a particular river section, C_t, is computed by using the formula:

$$C_t = \sum_{I=1}^{N} p_i C_i \quad (53)$$

where p_i = percentage of material of size fraction i available in the bed; C_i = sediment concentration or carrying capacity for each size fraction; and N = number of size fractions.

Han's (1980) decay function, as shown in Equation (38), can be used in conjunction with one of the above formulas for non-equilibrium sediment transport. GSTARS 2.0 adopts the method proposed by Bennett and Nordin (1977) to simulate the bed sorting and armouring processes.

Minimization computation

The minimization computation is based on Equation (2) for every station. GSTARS 2.0 channel geometry adjustments can be vertical, lateral, or both. GSTARS 2.0 selects the adjustment that results in the minimum total stream power for the study reach. Channel width and depth adjustments can take place only at the stream tubes adjacent to the banks. For interior tubes, bed adjustments can only be made in the vertical direction.

Channel side slope computation

GSTARS 2.0 offers the user the option of checking whether the angle of repose exceeds a known critical slope. If this option is chosen, the user must then supply the critical angle. The user is also allowed the option of specifying one critical angle above the water surface, and a different critical angle for submerged points. GSTARS 2.0 scans each cross section at the end of each time step to determine if any vertical or horizontal adjustments have caused the banks to become too steep. If any violations occur, the two points adjacent to the segment are adjusted vertically until the slope equals the user-provided critical slope.

Examples of application

The examples below illustrate various capabilities of the GSTARS 2.0. Yang's 1973 and 1984 formulas for sand and gravel transport, respectively, are used for the first two examples. For the Rio Grande study, the Laursen (1958) formula was used because it is more suitable for fine sediment transport. One stream tube was used for Figure 2 and Figure 3, three stream tubes were used for the computations for Figure 4 through to Figure 7.

Bed material sorting and bed degradation

Yang and Simões (1998) used the physical model study results by Ashida and Michiue (1971) to demonstrate the capabilities of GSTARS 2.0 in predicting bed-material size change and river bed profile adjustment below a dam. Figure 2 shows that the bed material median size d_{50} increased from 1.7 to 5.1 mm, which is in close agreement with the physical model

results. Figure 3 shows that the predicted bed profile is also in good agreement with the experimental results.

Channel profile and geometry adjustments

Figure 4 shows the predicted longitudinal bed profile variations along the unlined channel downstream of the emergency spillway of the Willow Creek Dam in Montana (Yang et al., 1998). The computed profiles consist of combinations of subcritical and supercritical bed profiles. Figure 4 shows that an initially fairly symmetrical cross section can become one with a point bar on the left side and a deep channel on the right, which is typical of the cross-section at a meander bend. Figure 5 also shows that non-uniform channel geometry adjustment can be predicted by the use of minimum total stream power. Figure 6 shows the comparison between the predicted and measured cross-section downstream of the unlined emergency spillway at Lake Mescalero, New Mexico (Yang et al., 1998). It is apparent that the predicted cross-section with the minimization computation is closer to the measurement than is the one without the minimization.

Equilibrium and non-equilibrium sediment transport

Figure 7 compares the longitudinal profiles along the Rio Grande where it flows into the Elephant Butte Reservoir, New Mexico (Yang et al., 1998). The Rio Grande sediment has a high concentration of fine materials and wash load. Figure 7 shows that the non-equilibrium sediment transport computation simulates the variation of bed profile more accurately than the equilibrium computation. The profile based on equilibrium sediment transport overestimates the amount of sediment deposition at the upstream end of the study reach near the entrance of the Elephant Butte Reservoir. Figure 6 also shows that the use of three stream tubes can more accurately simulate the thalweg profile than the use of only one stream tube.

Limits of application

GSTARS 2.0 is a general numerical model developed for a personal computer to simulate and predict river morphologic changes caused by natural and engineering events. Although GSTARS 2.0 is intended to be used as a general engineering tool for solving fluvial hydraulic problems, it does have the following limitations from a theoretical point of view:

GSTARS 2.0 is a quasi-steady flow model. Water discharge hydrographs are approximated by bursts of constant discharges. Consequently, GSTARS 2.0 should not be applied to rapid, varied, unsteady flow conditions.

GSTARS 2.0 is a semi-two-dimensional model for flow simulation and a semi-three-dimensional model for simulation of channel geometry change. It should not be applied to situations where a truly two-dimensional or truly three-dimensional model is needed for detailed simulation of local conditions. However, GSTARS 2.0 should be adequate for solving many river engineering problems.

GSTARS 2.0 is based on the stream tube concept. The phenomena of secondary current, diffusion, and super elevation are ignored.

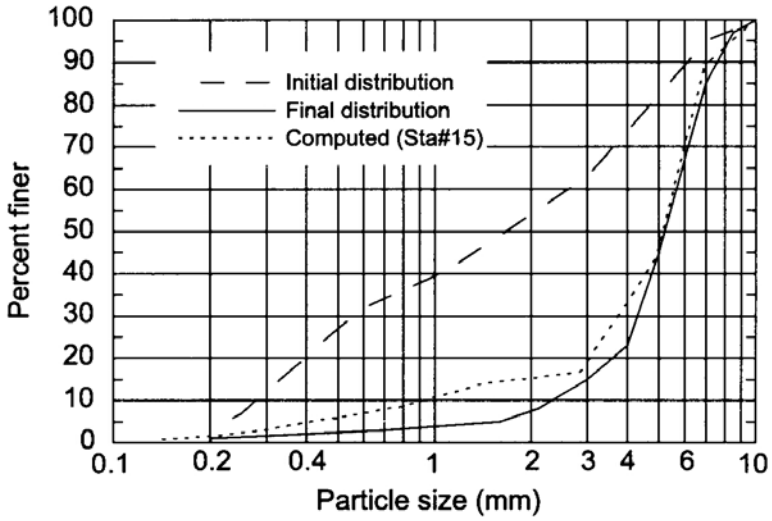

Fig. 2 Comparison between computed versus physical model results of bed-material coarsening resulting from bed degradation below a dam (Yang and Simões, 1998)

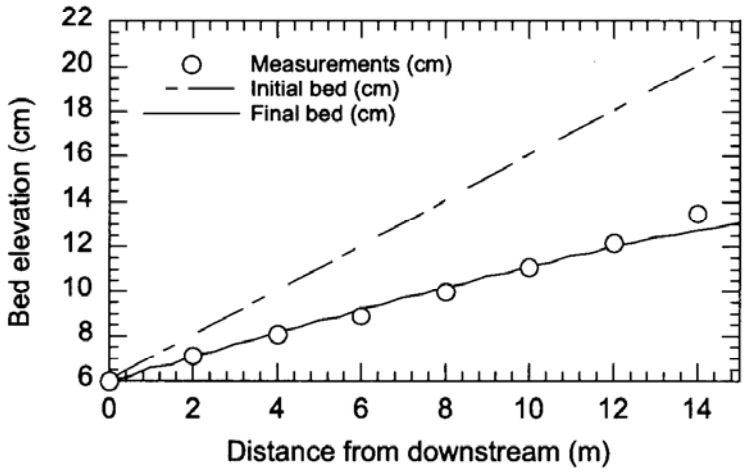

Fig. 3 Comparison between computed versus physical model results of bed degradation due to depletion of sediment supply below a dam (Yang and Simões, 1998)

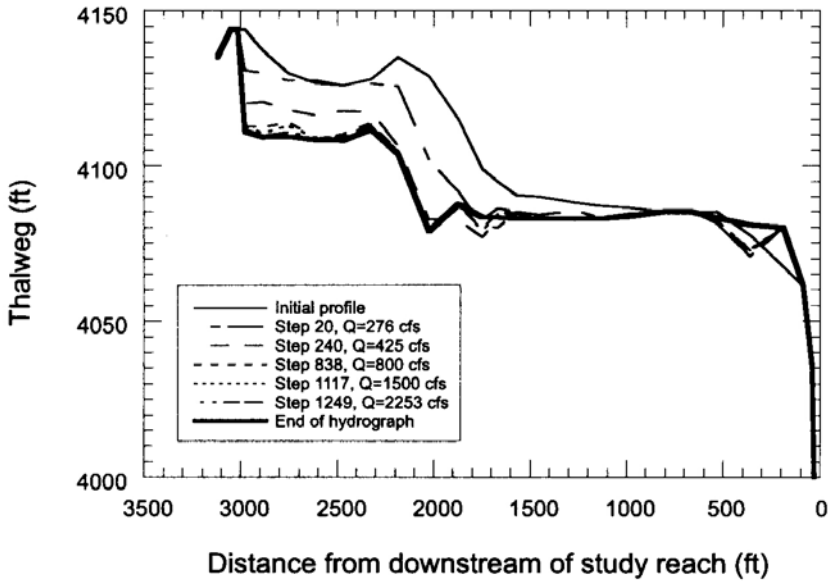

Fig. 4 Simulated longitudinal bed profiles along the Willow Creek Dam unlined emergency spillway (Yang et al., 1998)

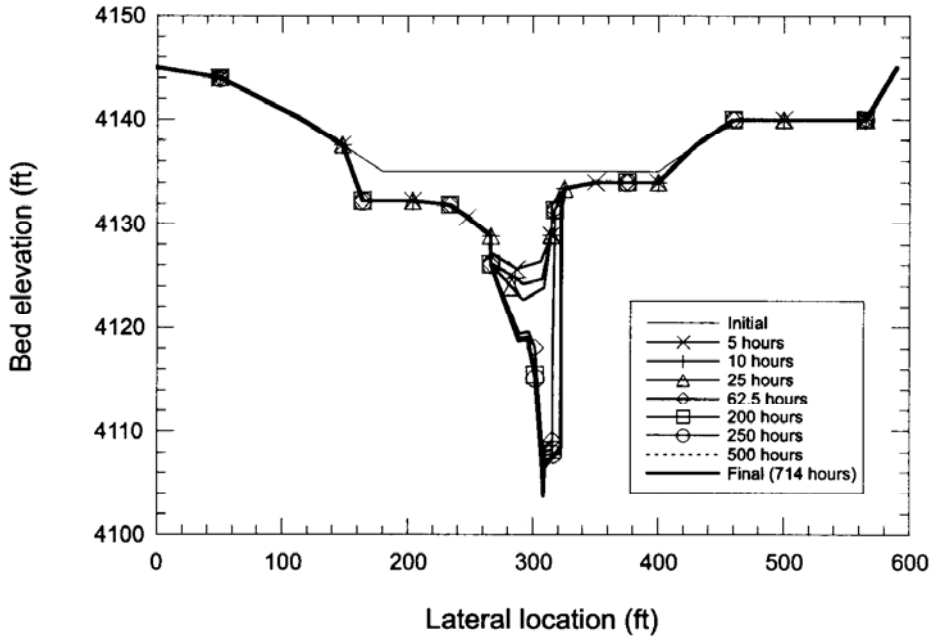

Fig. 5 Variation of the simulated cross sections at 2185 ft downstream of the Willow Creek Dam emergency spillway (Yang et al., 1998)

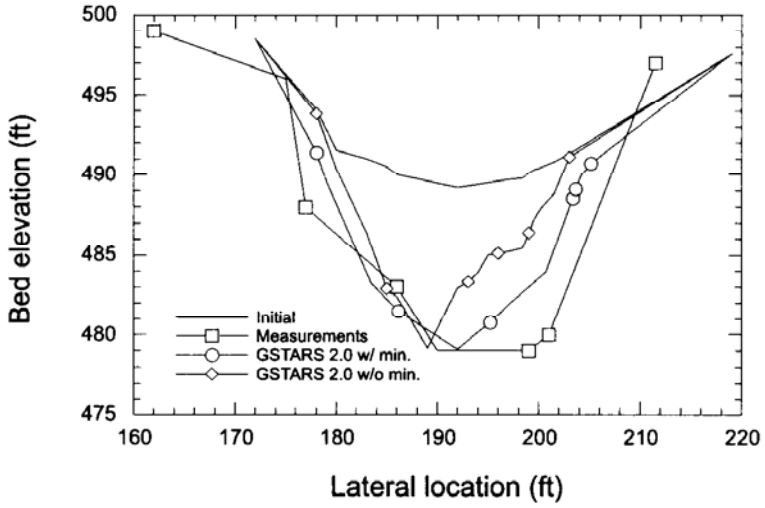

Fig. 6 Measured and simulated cross-sectional geometry at station 0+60 downstream of the Lake Mescalero emergency spillway (Yang et al., 1998)

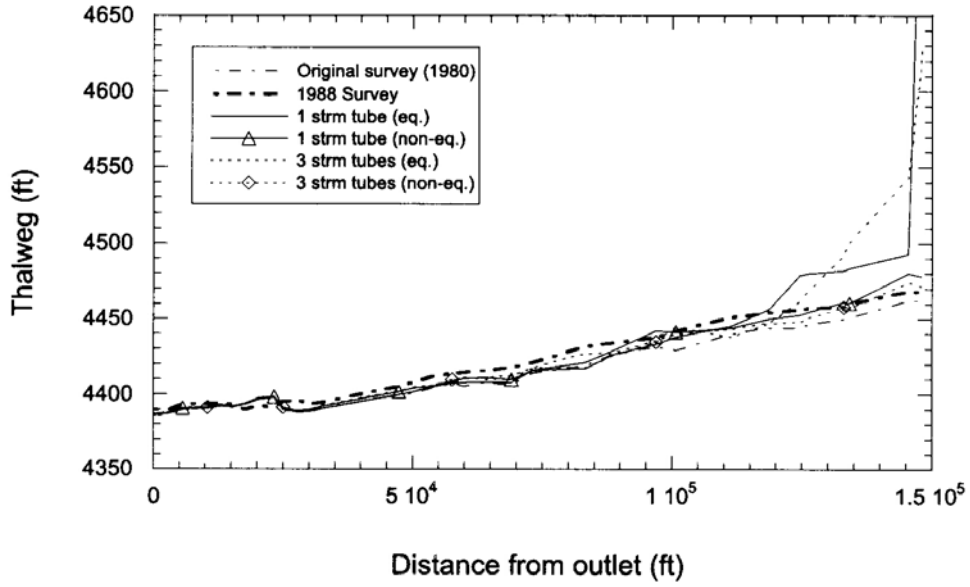

Fig. 7 Simulated thalweg elevations for the Rio Grande at the upper reach of the Elephant Butte Reservoir (Yang et al., 1998)

Current and future developments based on GSTARS 2.0

GSTARS 2.0 consists of independent but interrelated components or modules. Such modules can be easily modified to accommodate future developments, revisions, and improvements. Some of the current and future Bureau of Reclamation sediment model developments are summarized in this section.

GSTARS 2.1 model

GSTARS 2.0 is written for DOS PC application. GSTARS 2.1 is being developed for Windows and will have an extensive graphical interface. GSTARS 2.1 will be able to handle water and sediment inputs from tributaries. It will also include some useful engineering applications such as dredging. GSTARS 2.1 should become available by the end of 1999.

GSTARS 3.0 model

GSTARS 2.0 is intended mainly for rivers. The U.S. Bureau of Reclamation has now begun a 3-year effort to develop and test GSTARS 3.0 for reservoir sedimentation. GSTARS 3.0 will be able to simulate density current, reservoir routing, delta and channel formation, and sluicing and flushing under certain reservoir operation rules. GSTARS 3.0 should have the ability to simulate and assess the impacts of different reservoir operation criteria on reservoir sedimentation and hydraulic flushing and sluicing.

NETSTARS model

Lee et al. (1997, 1998) developed a quasi-two-dimensional NETSTARS model for alluvial river network systems. NETSTARS expanded GSTARS and GSTARS 2.0 capabilities for channel network application. NETSTARS has the option to treat bed load and suspended load separately or treat them as total bed-material load. The model solves the Saint Venant equation and thus can be applied to steady and unsteady flow conditions. However, NETSTARS does not have a width adjustment component and cannot be applied to situations where the width adjustment is important.

FLDSTARS model

The U.S. National Weather Service's FLDWAV (Fread and Lewis, 1988) is a truly unsteady one-dimensional fixed boundary flood wave routing model. FLDWAV replaced DAMBRK (Fread, 1984) as a standard model for flood routing due to dam failure in the United States. DAMBRK and FLDWAV do not consider the effects of sediment transport, scour, and deposition on the change of channel geometry and slope. In the event of a dam failure, channel depth, width, and slope are all subject to change. Field data indicate that the observed flood stages are often lower than those predicted by DAMBRK or FLDWAV due mainly to the change of channel width and local restriction. The U.S. Bureau of Reclamation began a 3-year cooperative effort with the U.S. National Weather Service in 1998 to combine FLDWAV and GSTARS 2.0 into FLDSTARS to include the effects of sediment transport, scour, deposition, channel geometry and profile changes on flood routing.

Model comparison

There are many sediment transport models, and each has its strengths and weaknesses Comprehensive reviews of the capabilities and performance of these models are provided in reports by the National Research Council (1983), and Fan (1988), among others. Fifteen U.S. Federal agencies participated in a Federal Interagency Stream Restoration Working Group (1998) to produce a handbook on *Stream Corridor Restoration Principles, Processes, and Practices.* They selected the following eight models for comparison: CHARIMA (Holly, et al., 1990), FLUVIAL-12 (Chang, 1990), HEC-6 (U.S. Army Corps of Engineers, 1993), TAS-2 (McAnally and Thomas, 1985) MEANDER (Johannesson and Parker, 1985), USGS (Nelson and Smith, 1989), D-O-T (Darby and Thorne 1996, and Osman and Thorne, 1988), and GSTARS (Molinas and Yang, 1986). Table 1 summarized the comparisons of these eight models. Since the U.S. Bureau of Reclamation has now replaced GSTARS with GSTARS 2.0 (Yang et al., 1998), the new version GSTARS 2.0 is included in Table 1. HEC-6, TABS-2, USGS, and GSTARS 2.0 are Federal models in the public domain; CHARIMA, FLUVIAL-12, MEANDER, and D-O-T are academic or privately owned models.

Table1 Comparison of sediment transport models (Y = yes; N = no)

Model	CHARIMA	Fluvial-12	HEC-6	TABS-2	Meander	USGS	D-O-T	GSTARS 2.0
Discretization and formulation:								
Unsteady flow | stepped hydrograph	Y|Y	Y|Y	N|Y	Y|Y	N|Y	Y|Y	N|Y	N|Y
One-dimensional | quasi two-dimensional	Y|N	Y|Y	Y|N	N|N	N|N	N	Y|Y	Y|Y
Two-dimensional | depth-average flow	N	N	N	Y|Y	Y|Y	Y|Y	N	N|Y
Deformable bed | banks	Y|N	Y|Y	Y|N	Y|N	Y|N	Y|N	Y|Y	Y|Y
Graded sediment load	Y	Y	Y	Y	Y	N	Y	Y
Nonuniform grid	Y	Y	Y	Y	Y	Y	Y	Y
Variable time stepping	Y	N	Y	N	N	N	N	Y
Numerical solution scheme:								
Standard step method	N	Y	Y	N	N	N	Y	Y
Finite difference	Y	N	Y	N	Y	Y	Y	Y
Finite element	N	N	N	Y	N	N	N	N
Modeling capabilities:								
Upstream water & sediment hydrographs	Y	Y	Y	Y	Y	Y	Y	Y
Downstream stage specification	Y	Y	Y	Y	Y	N	Y	Y
Floodplain sedimentation	N	N	N	Y	N	N	N	N
Suspended | total sediment transport	Y|N	Y|N	N|Y	Y|N	N|N	N|Y	N|Y	N|Y
Bedload transport	Y	Y	Y	N	Y	N	N	Y
Cohesive sediments	N	N	Y	Y	N	Y	N	Y
Bed armouring	Y	Y	Y	N	N	N	Y	Y
Hydraulic sorting of substrate material	Y	Y	Y	N	N	N	Y	Y
Fluvial erosion of streambanks	N	Y	N	N	N	N	Y	Y
Bank mass failure under gravity	N	N	N	N	N	N	Y	N
Straight | irregular nonprismatic reaches	Y|N	Y|N	Y|N	Y|Y	N|N	N|N	Y|Y	Y|Y
Branched | looped channel network	Y|Y	Y|N	Y|N	Y|Y	N|N	N|N	N|N	N|N
Channel beds	N	Y	N	Y	Y	N	Y	Y
Meandering belts	N	N	N	N	N	Y	N	N
Rivers	Y	Y	Y	Y	Y	Y	Y	Y
Bridge crossings	N	N	N	Y	N	N	N	N
Reservoirs	N	Y	Y	N	N	N	N	Y
User support:								
Model documentation	Y	Y	Y	Y	Y	Y	Y	Y
User guide | hot-line support	N|N	Y|N	Y|Y	Y|N	N|N	Y|N	N|N	Y|N

Summary and conclusions

Sediment transport computer models have been increasingly used as study tools for solving practical engineering problems. These models are also used to improve our understanding of river morphological processes. This paper provides a brief review and evaluation of basic theoretical concepts used in developing models and some of the practical approaches used for solving engineering problems. The study reached the following conclusions:

(1) Strictly speaking, river hydraulics and sediment transport in natural rivers are three-dimensional. Truly two- or three-dimensional models may be needed for solving localized problems, using detailed, site-specific field data for testing and calibration. One-dimensional models are more suitable for long-term simulation of a long river reach, where the lateral variation of hydraulic and sediment conditions can be ignored. From a practical point of view, a semi-two-dimensional model may be adequate for solving many river engineering problems.

(2) Due to the changing hydrologic conditions of a river, hydraulic conditions in a river are unsteady from a theoretical point of view. However, with the possible exception of routing during a flood near its peak, most river hydraulic conditions can be approximated by a semi-steady hydrograph using constant-discharge bursts of short durations.

(3) There are many well-established numerical schemes for solving sediment transport model governing equations. The one-dimensional finite difference uncoupled method is the one most commonly used in practice.

(4) The simulated results from a sediment transport computer model are sensitive to the selection of sediment transport formulas in the model. The user of a model should have a good understanding of sediment transport theories and the limits of application of different sediment transport formulas.

(5) Most sediment transport models assume that channel width is a constant and cannot be adjusted. This unrealistic assumption can lead to erroneous results when applied to an alluvial river.

(6) The GSTARS 2.0 model is based on the stream tube concept and the minimum stream power theory. Both the energy and momentum equations are used for water surface profile computation. GSTARS 2.0 incorporates the concepts of sediment routing by size fraction, formation and destruction of an armor layer, channel width adjust, channel side stability, among other things, to simulate site-specific conditions. GSTARS 2.0 should be adequate for solving many semi-two-dimensional, quasi-steady river engineering problems with a minimum amount of field data required for calibration and testing.

(7) A generalized computer model for sediment transport should be a PC-based model consisting of independent and iterative components or modules. These types of models can easily accommodate future modifications and improvements.

Main symbols

A	cross-sectional area
A_d	volume of bed sediment per unit length
A_s	volume of suspended sediment or cross-sectional area of river bed per unit length
C	wave velocity, sediment concentration, or Chezy's roughness coefficient
C_E, C_b	energy loss coefficient
C_l	concentration of lateral flow by volume
C_v	suspended load concentration by volume
C*	sediment carrying capacity
f	Darcy-Weisbach's roughness coefficient
F_f	total external friction force
g	gravitational acceleration
h_B, h_E	local energy loss
h_f	friction loss
H_t	total energy loss
K	conveyance
n	Manning's roughness coefficient
N	total number of stations
p	pressure
p_i	percentage of sediment in size fraction i
p_s	bed sediment porosity
P	wetted perimeter
q_l	lateral water inflow per unit channel length
q_s	later sediment inflow per unit channel length
Q, Q_s	water discharge and sediment discharge, respectively
R	hydraulic radius
S	slope
S_f	energy or friction slope
t	time
Δt	time difference
T	channel top width
V	average flow velocity
ω_s	sediment fall velocity
x	distance along the channel
Δx	reach length
y	water depth
$\bar{y}$	water depth to the centroid of a cross section
z	water surface elevation
Z	river bed elevation
α	velocity distribution coefficient or recovery factor
β	momentum coefficient
η	one minus porosity
ρ	density of water
θ	channel angle of inclination

Φ	rate of energy dissipation
γ	specific weight of water

Bibliography

ABBOTT, M. and D. BASCO (1989) *Computational fluid dynamics - an introduction for engineers.* Longman Scientific & Technical, Essex, UK.

ACKERS, P. and W.R. WHITE (1973) 'A sediment transport: new approach and analysis.' ASCE Journal of the Hydraulics Division, Vol. 99, No. HY11, p.2041-2060.

AMEIN, M. and C. S. FANG (1970) 'A implicit flood routing in natural channels.' ASCE Journal of the Hydraulics Division, Vol. 96, No. HY12, p.2481-2500.

ARIATHURAI, R. and R. B. KRONE (1976) 'A finite element model for cohesive sediment transport.' ASCE Journal of the Hydraulics Division, Vol. 102, No. HY3.

ASHIDA, K. and M. MICHIUE (1971) 'An investigation of river bed degradation downstream of a dam.' In: *Proceedings 14th Congress of IAHR,* Vol. 3.

BENNETT, J. P. and C. F. NORDIN (1977) *A simulation of sediment transport and armouring*. Hydrological Sciences Bulletin, XXII.

CHANG, H. H. (1988) *Fluvial processes in river engineering*. John Wiley & Sons, Inc.

CHANG, H. H. (1990) *Generalized computer program FLUVIAL-12, mathematical model for erodible channels: user's manual*.

DARBY, S. E. and C. R. THORNE (1996) 'A development and testing of riverbank stability.' ASCE Journal of Hydraulic Engineering, Vol. 122, No. 8, p.443-454.

ENGELUND, F. and E. HANSEN (1972) *A monograph on sediment transport in alluvial streams*. Teknisk, Forlag, Copenhagen.

FAN, S. S. ED. (1988) 'A twelve selected computer stream sedimentation models developed in the United States.' In: *Proceedings of the interagency symposium on computer stream sedimentation model*, Denver, Colorado. Published by the Federal Energy Regulatory Commission, Washington, DC.

FEDERAL INTERAGENCY STREAM RESTORATION WORKING GROUP (1998) *Stream corridor restoration principles, processes, and practice*. Washington, DC.

FREAD, D. L. (1974) *Numerical properties of implicit four-point finite difference equations of unsteady flow*. NOAA Technical Memorandum NMS HYDRO-18.

FREAD, D. L. (1984). *ADAMBRK - The NWS Dam-Break Flood Forecasting Model* National Weather Service Hydrologic Research Laboratory, Silver Spring, Maryland.

FREAD, D. L. and J. M. LEWIS (1988) 'AFLDWAV - A generalized flood routing model.' In: *ASCE Proceedings of national conference on hydraulic engineering,* Colorado Springs, Colorado, p.668-673.

HAN, Q. (1980) 'A Study on the Nonequilibrium Transportation of Suspended Load.' In: *Proceedings of the international symposium on river sedimentation*, (in Chinese) Beijing, China, p.793-802.

HAN, Q. and M. HE (1990) 'A mathematical model for reservoir sedimentation and fluvial processes.' International Journal of Sediment Research, Vol. 5, No. 2, p.43-84.

HOLLY, M. F.; J. C. YANG; P. SCHWARZ; J. SCHAEFER; S. H. SU and R. EINHELLING (1990) *CHARIMA - Numerical Simulation of Unsteady Water and Sediment Movement in Multiply Connected Networks of Mobile-Bed Channels*.' IIHR Research Report No. 343, Iowa Institute of Hydraulic Research, The University of Iowa, Iowa City, Iowa.

JOHNNESSON, H. and G. PARKER (1985) *Computer simulated migration of meandering rivers in Minnesota*. Project Report No. 242, St. Anthony Falls Hydraulic Laboratory, University of Minnesota.

KRONE, R. B. (1962) *Flume studies of the transport of sediment in estuarial processes*. Hydraulic Engineering Laboratory and Sanitary Engineering Research Laboratory, University of California, Berkeley, California.

LANE, E. W. (1955) 'A design of stable channels.' Transactions of ASCE, Vol. 120, p.1234-1260.

LAURSEN, E. M. (1958) 'The total sediment load of streams.' ASCE Journal of the Hydraulics Division, Vol. 84, No. HY1.

LEE, H. Y.; H. M. HSIEH; J. C. YANG and C. T. YANG (1997) 'A quasi-two-dimensional simulation of scour and deposition in alluvial channels.' ASCE Journal of Hydraulic Engineering, Vol. 123, No. 7, p.600-609.

LEE, H. Y.; H. M. HSIEH; S. Y. LEE; J. C. YANG and C. T. YANG (1998) 'Numerical simulations of scour and deposition in a channel network.' In: *Proceedings 1st federal interagency hydrologic modelling conference*, Vol. 1, Las Vegas, Nevada, p.3-94.

LIGGETT, J. A. and J. A. CUNGE (1975) 'Numerical Methods of Solution of the Unsteady Flow Equations.' Chapter 4, Vol..1, In: K. Mahmad and V. Yevjevich (eds.), *Unsteady flow in open channels*, Water Resources Publications, Fort Collins, Colorado, USA.

LUNDGREN, H. and I. G. JONSSON (1964) 'Shear and velocity distribution in shallow channels.' ASCE Journal of the Hydraulics Division, Vol. 90, No. HY1, p.1-21.

MARTIN, J. L. and S. C. MCCUTCHEON (1999) *Hydrodynamics and transport for water quality modeling*. Lewis Publishers, New York.

MCANALLY, W. H. and W. A. THOMAS (1985) *User's manual for the generalized computer program system, open-channel flow and sedimentation, TABS-2, main text.* U. S. Army Corps of Engineers, Waterways Experiment Station, Vicksburg, Mississippi.

MEYER-PETER, E. and R. MÜLLER (1948) 'A formula for bed-load transport.' In: *Proceedings of international association for hydraulic research,* 2nd Meeting, Stockholm.

MOLINAS A. and C. T. YANG (1986) *Computer program user's manual for GSTARS Generalized Stream Tube model for Alluvial River Simulation*. U.S. Bureau of Reclamation Engineering and Research Center, Denver, Colorado, USA.

NATIONAL RESEARCH COUNCIL (1983) *An evaluation of flood-level prediction using alluvial river models*. National Academy Press, Washington, DC.

NELSON, J. M. and J. D. SMITH (1989) 'Evolution and stability of erodible channel beds.' In: S. Ikeda and G. Parker (eds.), *River meandering*. Water Resources Monograph 12, American Geophysical Union, Washington, D.C.

OSMAN, A. M. and C. R. THORNE (1988) 'Riverbank stability analysis; I: theory.' ASCE Journal of Hydraulic Engineering, Vol. 114, No. 2, p.134-150.

PARKER, G. (1978) 'Self-formed straight rivers with equilibrium banks and mobile bed. part 1: the sand-silt river.' Journal of Fluid Mechanics, Vol. 89, No. 1, p.109-125.

PARKER, G. (1990) ‘A surface-based bedload transport relation for gravel rivers.’ Journal of Hydraulic Research, Vol. 28, No. 4, p.417-436.

PREISSMAN, A. (1960) ‘A Propagation des intumescences dans les cannaux et riviers.’ 1st Congres de l’Acesoc. Francaise de Calcul, Grenoble, France, p.433-442.

SONG, C. C. S.; Y. ZHENG and C. T. YANG (1995) ‘Modeling of river morphologic changes.’ International Journal of Sediment Research, Vol. 10, No. 2, p.1-20.

TOFFALETI, F. B. (1969) ‘Definitive computations of sand discharge in rivers.’ ASCE Journal of the Hydraulics Division, Vol. 95, No. HY1, p.225-246.

U.S. ARMY CORPS OF ENGINEERS (1993) *HEC-6 Scour and deposition in rivers and reservoirs user’s manual*. Hydrologic Engineering Center, Davis, California.

VIGILAR, G. G. and P. DIPLAS (1997) ‘Stable channels with mobile bed: formulation and numerical solution.’ ASCE Journal of Hydraulic Engineering, Vol. 123, No. 3, p.189-199.

VIGILAR, G. G. and P. DIPLAS (1994) ‘Determination of geometry and stress distribution of an optimal channel.’ In: G.V. Cotreano and R.R. Rumer (eds.), *Proceedings ASCE hydraulic engineering*, p.959-968.

WU, B. and A. MOLINAS (1996) ‘Modeling of alluvial river sediment transport.’ In: *Proceedings international conference on reservoir sedimentation, Vol. 1*, Chapter 4.4, Colorado State University, Fort Collins, Colorado, USA.

YANG, C. T. (1973) ‘Incipient motion and sediment transport.’ ASCE Journal of the Hydraulics Division, Vol. 99, No. HY10, p.1679-1704.

YANG, C. T. (1979) ‘Unit stream power equations for total load.’ Journal of Hydrology, Vol. 40, p.123-138.

YANG, C. T. (1984) ‘A unit stream power equation for gravel.’ ASCE Journal of Hydraulic Engineering, Vol. 110, No. 12, p.1783-1797.

YANG, C. T. (1992) ‘A Force, Energy, Entropy, and Energy Dissipation Rate.’ In: V. P. Sing and M. Fiorentin (eds.), *Entropy and energy dissipation in water resources*. Kluwer Academic Publishers, London, 63-89.

YANG, C. T. (1996) *Sediment transport theory and practice*. McGraw-Hill Book Company, New York.

YANG, C. T. and C. C. S. SONG (1986) ‘A Theory of Minimum Energy and Energy Dissipation Rate.’ In: *Encyclopaedia of fluid mechanics*, *chapter 11*, Gulf Publishing Company, Houston, Texas, p.353-399.

YANG, C. T. and A. MOLINAS (1988) ‘Dynamic adjustments of channel width and slope.’ In: W.R. White (ed.), *International conference on river regimes*. John Wiley & Sons, Inc.

YANG, C. T. and F. J. M. SIMÕES (1998) ‘Simulation and prediction of river morphologic changes using GSTARS 2.0.’ In: *Proceedings third international conference on hydro-science and engineering*, Cottbus/Berlin, Germany, 1-8.

YANG, C. T; A. MOLINAS and B. WU (1996) ‘Sediment transport in the Yellow River.’ ASCE Journal of Hydraulic Engineering, Vol. 122, No. 5, p.237-244.

YANG, C. T.; M. A. TREVIÑO and F. J. M. SIMÕES (1998) *User’s Manual for GSTARS 2.0 (Generalized Stream Tube model for Alluvial River Simulation Version 2.0)*. Technical Service Center, U.S. Bureau of Reclamation, Denver, Colorado. USA.

YOTSUKURA, N. and W. W. SAYRE (1976) ‘Transverse mixing in national channels.’ Water Resources Research, Vol. 12, p.695-704.

Sediment transport analysed by energy derived concepts

W. Zhang[1], W. Summer[2]
[1]Hohai University, College of Harbour, Waterway and Coastal Engineering,
Xikang Road 1, 210024 Nanjing, China
[2]Chartered Engineering Consultant for Hydraulic Engineering and Water Management,
Brennleitenstrasse 59-61/3, A-2202 Hagenbrunn, Austria

Introduction

Often the profitability of the investments into a reservoir for single or multiple water management purposes depends on the correct prediction of the life time of the reservoir. Hence, it is an essential task in hydrological engineering simulating sediment transport. The sediment originating in the drainage basin will be transported in the river courses as the bed and suspended load including the wash load. Solids moving in suspension represent the major component of the above mentioned silting processes. Therefore any accurate estimation of the relevant particle transport is of great importance in applied engineering practices.

Developed transport formulas present a relationship between sediment discharge and hydrological as well as hydraulic factors, such as flow discharge, slope, river morphometry, sediment characteristics, etc. As these sediment formulas were often gained from laboratory investigations under steady flow condition, their basic applicability is usually limited to these flow conditions. But, in natural rivers most of the sediment displacement takes place during floods which represent unsteady flow. Hence, one should be aware of conceptual formula limitations and possible prediction errors.

This paper demonstrates how the sediment transport is derived from the physical principle of the Power Theories. Their applicability to the sediment prediction under unsteady open channel flow is discussed.

Carrying capacity for sediment laden flow

In open channel flow the establishment of a relationship between the available potential energy, respectively the energy dissipation rate, and the sediment transport, is a very reasonable approach to this hydrodynamic process. Such a relation, describing the sediment transport in open-channel flow, can be derived on the physical basis of a power concept. These concepts are listed in the following three paragraphs. They are described on their theoretical basis, including their derivation, as well as their linkage towards a new conceptual approach, which is briefly explained.

Stream power

This concept was introduced and developed by Bagnold (1966, 1973). It is based on general physical principles arguing that the transport of grains depends on the efficiency of the available power. This concept was also firstly applied by Bagnold for the description of the bed load transport, wherein he related the total power supply P

$$P = \vartheta \bar{u} = \Delta g S_f h \bar{u} \tag{1}$$

(Δ = density of the fluid-sediment mixture, g = gravity, S_f = energy slope, h = water depth, $\bar{u}$ = mean flow velocity, ϑ = shearing stress of the fluid on the river bed) to the unit bed area. In other words, it states that the rate of energy dissipation, used in grain transport, should be related to the rate of materials being transported.

Unit stream power

If Equation (1) is divided by (gh), the unit stream power (Yang, 1971, 1972) can be derived from the stream power. This slightly different theory relates the rate of potential energy dissipation to the unit weight of water. It can be defined as

$$\frac{dY}{dt} = \frac{dx}{dt}\frac{dY}{dx} = \bar{u}S \tag{2}$$

where Y denotes the potential energy per unit weight of water, x the longitudinal distance, t the time and S the energy or water surface slope. Based on this concept, Yang (1979) developed several sediment transport by the analysis of relevant laboratory data as well as field observations in natural streams.

Gravitational power

In addition to the previous two theories, the gravitational power theory (Velikanov, 1954) suggests that the energy dissipation rate for the transport of the fluid-sediment mixture can be divided into

- the power required to overcome the transport resistance and
- the power necessary to keep sediment particles in suspension.

Based on this Velikanov understands that energy allowances for the sediments transport have to be made in an energy balance. In terms of the solid friction of an entire volume of a disperse medium, the sediment concentration is given by Velikanov as

$$C_V = K\frac{\bar{u}^3}{\rho h \omega} \tag{3}$$

where C_V denotes the volumetric concentration, K represents a coefficient related to the energy dissipation rate assigned to the sediment transport and T is the fall velocity of the sediment particle. These last two parameters result from laboratory investigations with limited natural conditions.

Power concept for the sediment concentration and transport capacity

Under the assumptions of energy separation and potential sediment transport, a suitable equation can be gained on the basis of the available power, explaining the linkage between a Power Concept and the sediment transport rate. The relevant theory for the derivation of this concept can be expressed as following, where the left hand side of Equation (4) represents the energy dissipation for suspended sediment transport and the right hand side, the Stream Power:

$$(\rho_s - \rho_w) g C_v \omega = \eta \rho_w g \bar{u} S \tag{4}$$

where ρ_s and ρ_w denote the gravity of the grains respectively of the water and η denotes a coefficient that describes the actual portion of energy dissipation used for sediment transport. It is similar to Velikanov´s *K*-value. Rearranging Equation (4) leads finally to Equation (5) which is the basis for the discussion on the sediment transport analysis under steady as well as unsteady flow conditions in open channels:

$$C_v = \eta \frac{\rho_w \bar{u} S}{\omega(1 - \frac{\rho_w}{\rho_s})} \tag{5}$$

The latter Equation (5) shows that the sediment concentration depends directly on the available stream power ($\bar{u}S$) as well as on a factor determining the energy dissipating

proportion for different flow and transport characteristics such as turbulence, river bed roughness, sediment properties, etc.

Transport analysis under steady flowconditions

The potential energy as the only source for work performance drives the flow of the water-sediment mixture from a location of higher altitude to a lower situated location, overcoming all transport, respectively, fluid shear resistance. It is a turbulent flow situation where the intensity of the turbulence depends strongly on hydraulical and geometrical parameters such as the river bed friction, as well as the overall river morphology. The internal forces of the turbulence themselves also use up a certain amount of the available potential energy so that the effective power available to transport is reduced.

Assume that the considered water volume consists of a mixture of water and suspended sediment particles as well as bed load grains. The internal portion of the energy dissipation rate causes the continuous chaotic displacement of these particles. Nevertheless repeating turbulence pattern related to the flow characteristics can be observed by the visualisation of moving particles. The referring eddy structures develop on the river bed. In this area, close to the viscous sub-layer, turbulent motion is manifested in the form of sweep and burst events. They consequently spread periodically all over the flow field as large scale turbulent eddies. The turbulence structures keep sediment particles in suspension as well as force bed load grains into a part time movement such as

- an occasional rolling motion which includes the rarely observed sliding motion,
- or a saltating motion, which comprises a series of ballistics hops or jumps

characterised by ascent from the river bed to a height of a few grain diameters.

The turbulent transport of the fluid-sediment mixture is therefore characterised by an intensive collision between grains as well as the disintegration of eddies. During all these processes, a certain amount of the dissipated kinetic energy is also transformed into another stage of energy, such as heat and sound. Therefore the physical background of the power concept allows the consideration of, and consequently, the integration of different energy consuming processes into a simple formula, i.e. by the introduction of the already listed coefficients *K* and/or *0* which vary due to overall changing flow characteristics.

Nevertheless, the gravitational power concept, as the theoretical basis for the derivation of sediment transport formulas, probably was only thought for steady flow situations. Under steady uniform flow ($v_{av} = \frac{1}{n} R_h^{2/3} S^{1/2}$) Equation (5) leads to

$$C_v = \eta \frac{\rho_w}{\omega(1 - \frac{\rho_w}{\rho_s})} \frac{\bar{u}^3 n^2}{R_h^{4/3}} \tag{6}$$

and under the assumption of a wide river ($R_h = h$) Equation (6) becomes

$$C_v = \eta \frac{\rho_w \bar{u}^3 n^2}{\omega \rho h^{4/3}} \tag{7}$$

Introducing the coefficient > instead of *0* Equation (7) leads to

$$C_v = \xi \frac{\bar{u}^3}{\omega \rho h} \tag{8}$$

This last Equation (8) is now identical to the Velikanov's equation, where > is an empirical coefficient, identical to *K*.

Depending on the internal available transport energy as well as on sedimentologic factors (grain size, Δ_s) the sediment transport takes place in suspension and as bed material transport. The physical process behind Equation (8) postulates that a certain amount of the available energy dissipates due to the transport of grains, others due to friction forces. However, the total transport capacity concentration is related to the energy dissipation as well as the intensity of the turbulence in the following manner:

- More available energy increases the rate of energy dissipation.
- An increased energy dissipation is directly related to a higher turbulence intensity as well as an increase in the sediment transport capacity.
- A certain amount of available energy can be dissipated in a variable portion - an increase in the turbulence intensity (i.e. increase in the bed roughness) means a decrease in the sediment concentration and vice versa; Equation (8) follows this principle: an increased friction factor causes a decrease in the flow velocity and an increase in the water depth. They lead to a reduction in the sediment concentration. Whereas Celik and Rodi (1991) explain this phenomenon in such a way that the turbulence energy produced in the separated shear layers behind the roughness elements, needs to be convicted and diffused first to the region above the bed, and that during this process, energy is dissipated so that more energy is dissipated directly and a smaller part of the energy produced is available for suspension.

Transport analysis under unsteady flowconditions

The following discussion refers to the assumption that the conceptional structure of Equation (8) can also be applied to the estimation of the sediment transport capacity under unsteady flow conditions. But under natural conditions they cause most of the sediment displacement (Summer and Zhang, 1994) therefore unsteady processes are rather relevant in engineering practices than in steady situations. Unsteady flow in an open channel is often modelled by the one-dimensional St. Venant equations. The dynamic equation of these may be written as follows (Cunge et al., 1980):

$$\frac{\partial Q}{\partial t} + \frac{\partial}{\partial x}\left(\frac{Q^2}{A}\right) + gA\left(\frac{\partial h}{\partial x} - S_0\right) + gAS_f = 0 \tag{9}$$

Rearranging Equation (9) after substituting $\frac{Q}{A}$ by $\bar{u}$ leads to

$$S_f - S_0 = -\frac{\partial h}{\partial x} - \frac{1}{g}\left[\frac{\partial \bar{u}}{\partial t} + \bar{u}\frac{\partial \bar{u}}{\partial x}\right] \tag{10}$$

where S_0 and S_f denotes the bed slope and the energy slope respectively, A the cross sectional area and Q the discharge. According to the magnitude on the right hand side of equation (10) the flood wave can be classified either as kinematic wave ($S_0 = S_f$) or diffusion/dynamic wave (Ponce, 1989).

Due to $S_0 = S_f$, the sediment transport for a kinematic wave situation can be expressed by Equation (8). This has been proven by Suszka and Graf (1987) on the basis of laboratory investigations as well as by Nouh (1988) who monitored and analysed suspended sediment transport in ephemeral channels. Therefore, for rivers where the kinematic wave assumptions are valid, formulas obtained from steady flow can also be applied without additional errors due to hydraulic unsteadiness.

Looking at a diffusion/dynamic wave, where the right hand side of (10) cannot be neglected, the energy slope at the rising stage of the flood is greater than the bed slope but smaller at the tail end. This has been indicated by Tu and Graf (1992), who compared the friction velocity under steady, uniform flow u_{*S}

$$u_{*S} = \sqrt{ghS} \tag{11}$$

with the friction velocity $u_* S\bar{u}$

$$u_* S\bar{u} = \{gh\,(S_0 - \frac{\partial h}{\partial x} - \frac{\bar{u}}{g}\frac{\partial \bar{u}}{\partial x} - \frac{1}{g}\frac{\partial \bar{u}}{\partial t})\} \tag{12}$$

gained from the St. Venant equation of motion. Figure 1 shows one of several relevant hydrograph investigations, indicating the true value of the friction velocity $u_* S\bar{u}$ during the passage of the hydrograph as well as the apparent friction velocity u_{*S} under the assumption that S_f equals S_0.

From these as well as from other investigations (e.g. Walling and Webb, 1988), it can be concluded that the maximum value for S_f occurs at the rising stage of the discharge response during a storm event, so that the stream power should have a maximum before the discharge peak. In detail, the concentration peak will be situated between the point of inflection on the rising side of the hydrograph, where the increase in the water table starts to decrease again, and between the peak discharge (Thomas and Lewis, 1993). In this case the application of the sediment transport Equation (8) might lead to an increased error in the prediction - therefore an improvement in the formula concept is advisable.

Concluding summary

The sediment transport in natural rivers may be estimated on the basis of the stream power concept. The rate of energy dissipation derives from an energy balance which adjusts to the river bed's roughness, sediment discharge, channel geometry and cross section. Under these assumptions the sediment transport is analysed under various flow conditions as well as changing turbulent kinetic energy. It is shown and discussed under what assumptions the concept of energy dissipation rate for sediment transport can be extended from steady open channel flow to unsteady flow conditions.

An alluvial channel has the tendency to create a balance between flow controlling factors in order to adjust the sediment transport rate to the rate of potential energy expenditure. Such a concept is based on the power theory, which can be expressed as stream power, unit stream power and/or gravitational power. These approaches to an understanding of the sediment transport process, reject the concept that the rate of sediment transport depends mainly on one independent variable, such as discharge, average flow velocity, energy slope or shear stress. Based on these power concepts - their linkage is shown in this study - several suspended sediment transport equations were derived by different researchers (Shen and Hung, 1972; Yang, 1972; Ackers and White, 1993). The procedure of the derivation of such a sediment transport equation based on the gravitational power theory is presented. Its basic idea focuses on the energy balance of sediment transport, considering the fluid and sediment grains separately, where two forces occur namely gravity (transporting the fluid along the slope) and resistance forces (tending to retard the flow movement). The relevant equation corresponds to a transport equation for steady open channel flow given by Velikanov, gained in a simple way.

According to Equation (8) it can be concluded that increased friction forces (i.e. increase in the river bed roughness causing higher turbulence) decrease the transport potential of particles. Therefore the coefficients ξ or K denoting the energy dissipation ratio between sediment transport and friction resistances - i.e. turbulent eddy structures cause them; they have their origin on the river bed and gain their characteristics by the bed structure/roughness.

However, Equation (8) can be extended to express the relationship between the sediment transport rate and unsteady open channel flow. Considering flood discharges, their hydrographs can either rise slowly or rapidly. Consequently, this leads to two typical unsteady flow situations, which on one hand can be classified as kinematic wave and on the other as diffusion and/or dynamic wave. With Equation (8) it can easily be shown that during unsteady flow situations and under certain assumptions (sufficient suspended sediment supply, regular cross-section, etc.)

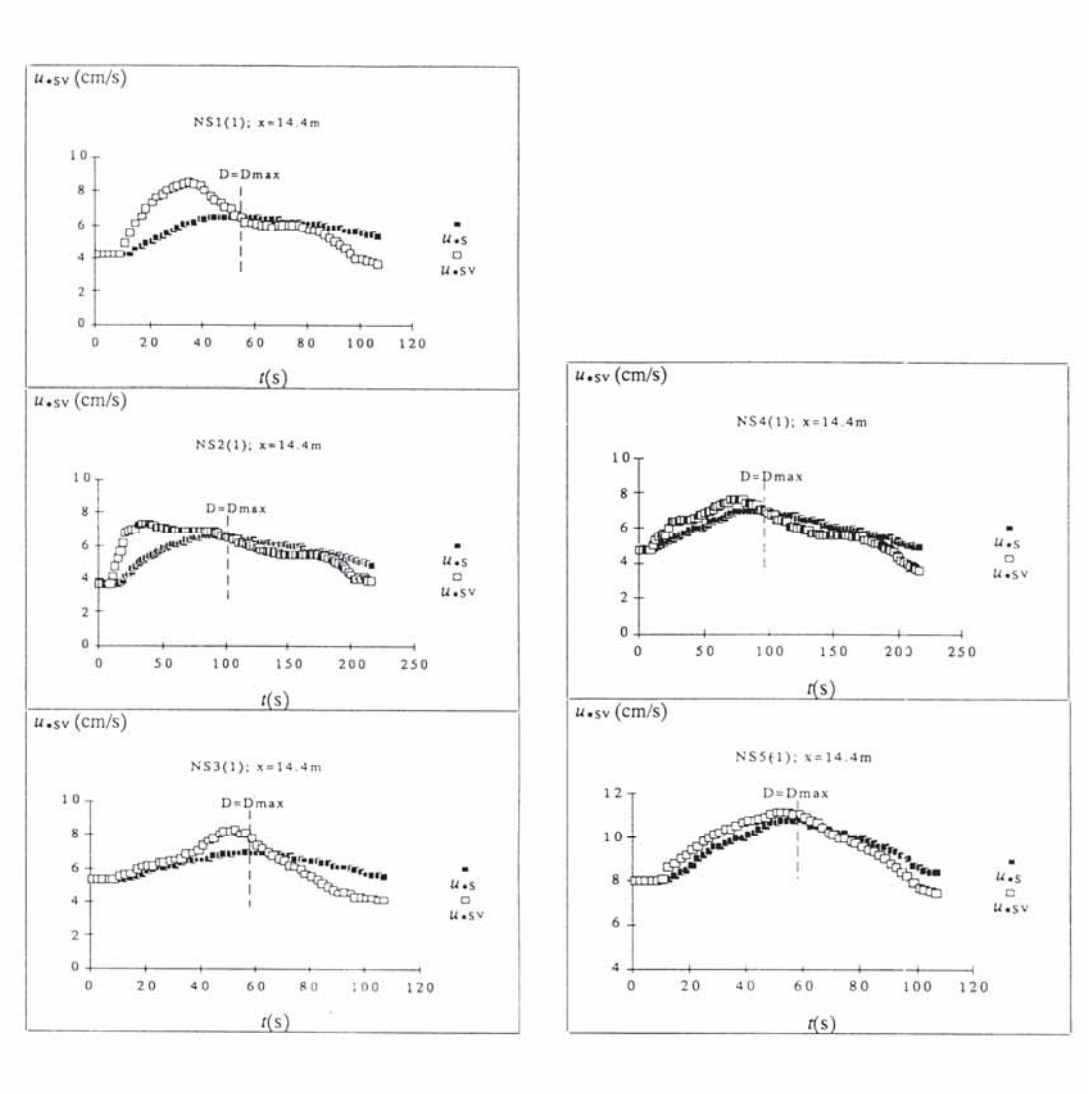

Fig.1 Friction velocity u^*_S and $u^* S\overline{u}$ for a hydrograph (Tu and Graf, 1992)

- the max. suspended sediment concentration occurs at the rising stage of the hydrograph in the case of a dynamic wave,
- in the less common case of a kinematic wave (which in nature could be assumed only for floods in big rivers) the concentration peak corresponds to the discharge peak.

When comparing equal discharges of a flood wave (diffusion/dynamic wave) it can be stated that more energy is available during the rise of a flood than during its decrease. This hydraulic principle leads to an energetic maximum at the rising branch of the storm flow, which also means that under the assumption of a direct relation between power and total sediment transport capacity the sediment concentration peak occurs on the rising flood stage. This physical/hydraulical phenomenon is one of the reasons for the hysteretic effect in a sediment discharge rating curve; hydrological factors have the second major impact on the creation of a looped rating curve.

Bibliography

ACKERS, P. and W.R. WHITE (1973) 'Sediment transport: new approaches and analysis.' J. Hydraul. Div., ASCE, vol. 99, p.2041-2060.

BAGNOLD, R.A. (1966) *An approach to the sediment transport problem from general physics*. USGS Prof. Pap., No. 422-I.

BAGNOLD, R.A. (1977) 'Bedload transport by natural rivers.' Water Resour. Res., 13, p.303-312.

CELIK, I. and W. RODI (1991) 'Suspended sediment transport capacity for open channel flow.' J. Hydraul. Eng., ASCE, vol. 117, no.2, p.191-204.

CUNGE, J.A.; F.M. HOLLY JR. and VERWEY, A. (1980) *Practical aspects of computational river hydraulics*. Pitman Advanced Publishing Program, London.

NOUH, M. (1989) 'Transport of suspended sediment in ephemeral channels.' IAHS Publ. No. 174, p.97-106.

PONCE, V.M. (1989) *Engineering hydrology - principles and practices*. Prentice Hall, London.

SHEN, H.W. and C.S. HUNG (1972) 'An engineering approach to total bed-material load by regression analysis.' In: H.W. Shen (ed.), *Sedimentation*. Symposium to honour Professor H.A. Einstein, Colorado State University, Fort Collins, Colo., 14/1-14/7.

SUMMER, W. and W. ZHANG (1994) 'An impact analysis of hydraulical and hydrological changes on the suspended sediment transport in the Austrian Danube' Proc. XVII Donauländerkonferenz, Budapest.

SUSZKA, L. and W. GRAF (1978) 'Sediment transport in steep channels at unsteady flow.' In: *22nd IAHR congress: topics in fluvial hydraulics*, Lausanne, Switzerland, p.166-170.

THOMAS, R.B. and J. LEWIS (1993) 'A comparison of selection at list and time-stratified sampling for estimating Suspended sediment loads.' Water Resour. Res., 29, p.1247-1256.

TU, H. and W. GRAF (1992.) 'Friction in unsteady open-channel flow over gravel beds.' J. Hydraul. Res., 31, p.99-110.

VELIKANOV, M.A. (1954) 'Perenos vzveshennykh nanosov turbulentnym potokom.' Izd. AN SSSR, OTN no. 3.

WALLING D.E. and B.W. WEBB (1988) 'The reliability of rating curve estimates of suspended sediment yield: some further comments.' IAHS Publ. No. 174, p.337-350.

YANG, C.T. 1971. 'Potential energy and sediment transport.' Water Resour. Res., 7, p.312-322.

YANG, C.T. (1972) 'Unit stream power and sediment transport.' J. Hydraul. Div., ASCE, vol. 98, no.10, p.1805-1826.

YANG, C.T. (1979) ‘Unit stream power equations for total load.’ J. Hydrology, vol. 40, No.1/2, p.123-138.

The linkage between hydrological processes and sediment transport at the river basin scale – a modelling study

V. Krysanova, J. Williams, G. Bürger and H.Österle
Potsdam Institute for Climate Impact Research, Department of Natural Systems,
P.O. Box 601203 Telegrafenberg, D-14412 Potsdam, Germany

Introduction

Soil erosion is a major type of land degradation induced by human population. Erosion by water is a widespread, global problem. The Global Change and Terrestrial Ecosystems Project (GCTE) assigned erosion as a first priority within the task 'Soil Degradation under Global Change' (Ingram et al., 1996). For that the GCTE Soil Erosion Network was created recently. The use of water erosion models in global change studies requires that the model (a) has already been validated in several watersheds or regions, (b) uses readily available input data, (c) is transferable to other regions/conditions. For that, the models need to be validated in different environmental conditions in order to evaluate their robustness for global change studies.

Erosion processes are very complex, and there are a number of modelling tools developed for different spatial scales and using different concepts. Three model categories are used for the assessment of water erosion: (a) fully empirical models like USLE (Wischmeier and Smith, 1978) and RUSLE (Renard et al., 1991); (b) models largely based on mathematical descriptions of physical processes like WEPP (Nearing et al., 1989) and EUROSEM (Morgan et al., 1992); and (c) intermediate models combining mathematical process description with some empirical relationships like ANSWERS (Beasley et al., 1980), EPIC (Williams, 1984), GLEAMS (Leonard et al., 1987) and AGNPS (Young et al., 1989). Most of these models can be used only at the field scale or in small homogeneous watersheds. The water erosion models usually include a hydrological module, except the fully empirical ones, which can calculate sediment yield using some rainfall or runoff factor. An overview about erosion model validation for global change studies is given in Favis-Mortlock et al. (1996).

One of the models intensively used for coupled hydrological / crop / erosion simulations, with an objective to determine the effect of management strategies on crop yield, soil and water resources, is EPIC. The EPIC model has been used in several impact studies in

the United States, including those described in Robertson et al. (1987; 1990) and Easterling et al., (1993). The model was investigated specifically for its applicability for the assessment of global change impacts (Williams et al., 1996). In the framework of global change studies it was suggested to use the simulation results of complex process-based models for developing simplified reduced-form models that capture the main features of the response to changing conditions, like it was already done with EPIC (Ingram et al., 1996).

The availability of GIS (Geographic Information System) tools and more powerful computing facilities makes it possible to overcome many difficulties and limitations and to develop distributed continuous time basin-scale models, based on available regional information. Recent development provides a few models, which allow evaluation of erosion processes at the basin scale, among them SWRRB (Arnold et al., 1990), SWAT (Arnold et al., 1993 and 1994), and SWIM (Krysanova et al., 1996 and 1998a). Usually, the basin-scale model includes a version of a field-scale model as a module, plus a parametrization of the routing processes. Thus a simplified version of EPIC (Williams et al., 1984) is included in SWAT and SWIM for simulation of crop growth and sediment yield processes.

This paper demonstrates the ability of the SWIM model to evaluate sediment yield and transport at the basin scale. SWIM was first applied for the larger Mulde river basin (6171 km^2), and then for the mesoscale Glonn river basin (392 km^2) with the objectives

- to validate basin-scale sediment transport modelling;
- to investigate scaling issues by subdividing the basin into sub-basins in three different ways; and
- to study the linkage between hydrological processes, on the one hand, and sediment yield and transport, on the other.

Modelling approach

General model description

SWIM (Soil and Water Integrated Model) is a continuous-time spatially distributed model, simulating hydrology, vegetation, erosion and nutrients (nitrogen, N, and phosphorus, P) at the river basin scale. The model is described in detail in Krysanova et al., 1998a.

SWIM is based mainly on two previously developed tools: SWAT (Arnold et al., 1993) and MATSALU (Krysanova et al., 1989), and includes some new modules (e.g. the Muskingum-Cunge method for river routing, and a new approach for the CO_2 fertilisation effect). The new model SWIM was developed with an intention to incorporate the best features of both tools, like coupled hydrological/crop modules and GIS interface from SWAT, and three-level disaggregation scheme from MATSALU. The other objective was to arrange data input in agreement with data formats available in Europe and in this way to ensure that the model is transferable to other European river basins. The both SWAT and SWIM run with the daily time step, but only SWIM was validated hydrologically with the daily time step in a number of basins, while SWAT as a long-term predictor was always validated only with monthly and annual time steps.

SWIM can be applied to river basins with the area from 100 to 10,000 km^2. A three-level disaggregation scheme 'basin – sub-basins – hydrotopes' plus a vertical subdivision into a maximum of 10 soil layers are implemented in SWIM for mesoscale basins. A mesoscale basin has firstly to be subdivided into sub-basins of a reasonable average area. After that hydrotopes are delineated within every sub-basin, based on land use and soil types. A

hydrotope is a set of elementary units in the sub-basin, which have the same land use and soil type. The sub-basin area should not exceed 10 – 100 km^2 (depending on the basin area) to ensure that the surface runoff reaches the sub-basin outlet within one day. Climate is homogeneous at the second level of disaggregation - for sub-basins.

SWIM has interface to the GIS GRASS (Geographic Resources Analysis Support System, US Army, 1988), which was modified from the SWAT/GRASS interface (Srinivasan and Arnold, 1993) to extract spatially distributed parameters of elevation, land use, soil types, and groundwater table.

During the last three years SWIM was extensively tested and validated in a number of mesoscale basins in Germany (mainly belonging to the Elbe drainage basin) regarding different processes – hydrological, vegetation growth, nutrient cycling and erosion (Krysanova et al., 1996, 1998a, b, 1999a). Besides, the model was validated regionally for crop yield in the state of Brandenburg, Germany (Krysanova et al., 1999b).

Hydrological processes and vegetation

The simulated hydrological system consists of four control volumes: the soil surface, the root zone, the shallow aquifer, and the deep aquifer. The soil column is subdivided into several layers in accordance with the soil database. The water balance equation for the soil column includes precipitation, surface runoff, evapotranspiration, percolation to groundwater and subsurface lateral flow. The water balance for the shallow aquifer includes groundwater recharge from the soil profile, capillary rise back to the soil profile, lateral return flow (contribution to stream flow), and percolation to the deep aquifer.

Surface runoff is estimated as a non-linear function of precipitation and a retention coefficient, which depends on soil water content, land use and soil type (modification of the Soil Conservation Service (SCS) curve number method described in Arnold et al., 1990). The method was adapted to German conditions by validation in seven mesoscale river basins of different size (all in the Elbe drainage area) and with different climatic conditions, land use and soils. Besides, it is possible to exclude the dependency on curve number in SWIM and to use the retention coefficients as dependent only on soil saturation.

Lateral subsurface flow (or interflow) is calculated simultaneously with percolation. It appears when the storage in any soil layer exceeds field capacity after percolation and is especially important for soils having impermeable or less permeable layer below several permeable ones. Potential evapotranspiration is estimated using the method of Priestley-Taylor. Actual evaporation from soil and actual transpiration by plants are calculated separately.

The module representing crop and natural vegetation is an important interface between hydrology and erosion. A simplified EPIC approach is included in SWIM (as well as in SWAT) for simulating arable crops (e.g. wheat, barley, rye, maize, potatoes) and aggregated vegetation types (e.g. 'grass', 'pasture', 'forest'), using specific parameter values for each crop/vegetation type. It is simplified mainly in the description of phenological processes in order to decrease the requirements on input information. This enables crop growth to be simulated in a distributed modelling framework at the regional scale.

Different vegetation types affect the hydrological cycle by the cover-specific retention coefficient, which influences runoff, and indirectly - the amount of evapotranspiration (ET), which is simulated as a function of potential evapotranspiration and leaf area index.

Sediment yield in sub-basins

Sediment yield Y (in t) is calculated for each sub-basin with the Modified Universal Soil Loss Equation (MUSLE, Williams and Berndt, 1977), practically the same as in SWAT (Arnold et al., 1994):

$$Y = 11.8 \cdot (Q \cdot q_p)^{0.56} \cdot (K) \cdot (C) \cdot (ECP) \cdot (LS), \tag{1}$$

where Q is the surface runoff for the sub-basin in m^3, q_p is the peak runoff rate for the sub-basin in m^3s^{-1}, K is the soil erodibility factor for soil, C is the crop management factor, ECP is the erosion control practice factor, and LS is the slope length and steepness factor. The only difference is that in SWIM the surface runoff, the soil erodibility factor K and the crop management factor C are estimated for every hydrotope, and then averaged for the sub-basin (weighted areal average), while in SWAT there are two options: a) based on two-level disaggregation 'basin – sub-basins', when the above mentioned factors are first estimated for the sub-basins, and b) similar to that of SWIM, when the factors are estimated first for HRUs (Hydrologic Response Units) – similar as hydrotopes.

The surface runoff and the peak runoff rate from (1) are estimated in the hydrological module. The peak runoff rate (Arnold et al., 1994) is calculated as

$$q_p = \frac{\alpha \cdot Q \cdot A}{3.6 \cdot t_c}, \tag{2}$$

where A is the drainage area in km^2, t_c is the basin's time of concentration in h, and α is a dimentionless parameter expressing the proportion of total rainfall that occurs during t_c.

The stochastic parameter α is taken from gamma-distribution, which is parametrized using monthly rainfall intensity. This stochastic element is included to allow realistic representation of peak flow rates, given only daily rainfall and monthly rainfall intensity. The time of concentration is calculated as a sum of the surface and the stream flow times, which are estimated from the slope (or channel) length, the slope (or channel) steepness, and the Manning's n coefficients for the sub-basin (or channel), respectively (Arnold et al., 1994). Here the channel is a part of the river network belonging to the sub-basin.

The soil erodibility factor K is estimated from the texture of the upper soil layer or is taken form a database.

The crop management factor C is estimated for all days when runoff occurs as

$$C = \exp[(-a_1 - CVM) \cdot \exp(-a_2 \cdot CV) + CVM], \tag{3}$$

where CV is the above-ground biomass in kg ha^{-1}, CVM is the minimum value of C for crop, a_1 = -0.2231, a_2 = -0.00115.

The erosion control practice is estimated as default value of 0.5, if no other data are available.

The slope length and steepness factor LS is estimated as

$$LS = \left(\frac{L}{b_1}\right)^{\xi} (b_2 \cdot S^2 + b_3 \cdot S + b_4), \tag{4}$$

$$\xi = b_5 \cdot \left[1 - \exp\left(b_6 \cdot S\right)\right], \tag{5}$$

where the slope length L and the slope steepness S for the sub-basins are estimated from the Digital Elevation Model (DEM) of the basin, and the constants b_1 = 22.1, b_2 = 65.41, b_3 = 4.565, b_4 = 0.065, b_5 = 0.6, b_6 = -35.835.

Sediment routing in streams

The sediment routing model consists of two components operating simultaneously – deposition and degradation in the streams. Deposition in the stream channel is based on the stream velocity in the channel V_c (in m s^{-1}), which is estimated as a function of the peak flow rate *PR* (in m^3 s^{-1}), the flow depth *D* (in m), and the average channel width *CHW* (in m)

$$V_c = \frac{PR}{D \cdot CHW}. \tag{6}$$

The flow depth is calculated using the Manning's formula as

$$D = \left(\frac{PR \cdot CHN}{CHW \cdot (CHS)^{0.5}} \right)^{0.6}, \tag{7}$$

where CHN is the channel n, and CHS is the channel slope (m m^{-1}).

The sediment delivery ratio *DR* through the reach is defined in accordance with the latest modification by J.Williams as

$$DR = \frac{Q}{Y_{in}} \cdot SPCON \cdot (V_c)^{sp\exp}, \tag{8}$$

where Y_{in} is the sediment amount entering the reach, and the parameters SPCON (between 0.0001 and 0.01) and SPEXP (between 1.0 and 1.5) can be used for calibration.

If DR < 1.0, the deposition is

$$DEP = Y_{in} \cdot (1. - DR), \tag{9}$$

and degradation is zero. Otherwise, the deposition is zero, and the degradation is calculated as

$$DEG = Y \cdot (DR - 1.) \cdot CHK \cdot CHC, \tag{10}$$

where CHK is the channel K factor, and CHC is the channel C factor.
And finally, the amount of sediment reaching the sub-basin outlet, Y_{out}, is

$$Y_{out} = Y_{in} - DEP + DEG \tag{11}$$

Case study river basins

The modelling study was done in two river basins – the Mulde basin, gauge station Bad Düben, 6171 km^2, located in Saxony (Figure 1), and the Glonn basin, gauge station Hohenkammer, 392 km^2, located in Bavaria (Figure 2). The first application was performed for the Mulde basin, using a DEM with rough 1000 m resolution, and measurements of suspended solids with rather low frequency. A more thorough validation of the model was performed for the Glonn basin, where better DEM and daily measurements of suspended sediments (SS) in the river outlet were available

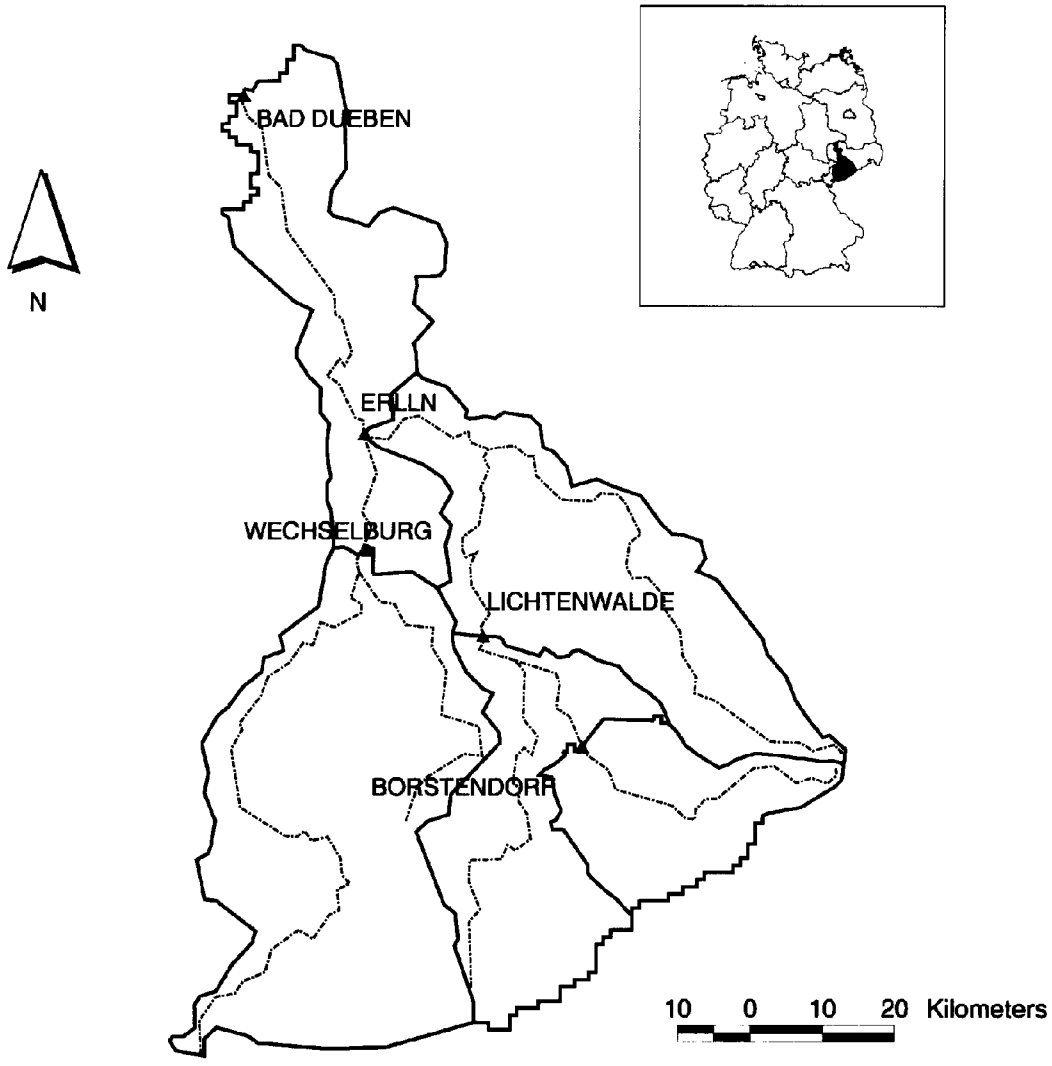

Fig. 1 The Mulde basin (6171 km^2) located in Saxony, Germany and its subdivision into 5 sub-basins with the corresponding gauge stations

The Mulde basin

The Mulde river basin (Figure 1 and Table 1) is located in the south of the German part of the Elbe drainage basin. The Elbe is one of the most heavily contaminated water courses in Europe, due to ineffective sewage water treatment and lack of diffuse source pollution control (agricultural areas cover about 56% of the total drainage area). Erosion is more pronounced in the southern and western part of the Elbe basin (including the Mulde basin) due to the mountainous or hilly relief and occurrence of loess soils.

Elevation in the Mulde basin increases southward from 80 to 1229 m above sea level. Different soil types occur in the basin: from sandy soils with different percentages of loam (38.5 %), to loamy and loess soils (32.3%), and loamy-clay and clay soils (28.7 %). The soil erodibility factor K was estimated from the texture of the upper soil layer, it varies from 0.19 to 0.66. The area is dominated by cropland (58%) and forest (29.6%). Forested areas are located predominantly in the mountainous southern part of the basin. Average precipitation in the period 1981 – 1995 was 783 mm per year, and the runoff coefficient was 0.42.

Table 1 General characteristics of two investigated river basins: the Glonn and the Mulde

	Glonn / gauge Hohenkammer	Mulde gauge Bad Düben
Area, km^2	392	6171
Elevation, m a.s.l.	450 to 559	80 to 1229
Land use: cropland	73 %	58 %
pasture	6.5 %	3 %
forest	16.5 %	29.6 %
Soil types: sandy and loamy-sandy soils	9.8 %	19.1 %
sandy-loamy and sandy loess soils	23.0 %	19.4 %
loamy and loess soil	60.3 %	32.3 %
loamy-clay and clay soils	4.5 %	28.7 %
peat soil	2.4 %	0.5 %
Precipitation, long-term average, mm/yr	~ 880	~ 783
Runoff coefficient*	0.30	0.42
Specific runoff: min, $l/s/km^2$	3.24	2.38
average, $l/s/km^2$	8.24	10.3
max, $l/s/km^2$	121	75

* Runoff coefficient as a long-term characteristic is a proportion of the volume of total runoff in the river to the volume of precipitation in the corresponding river basin taken for a period of 20-30 years

The Glonn basin

The Glonn river (Figure 2 and Table 1) is a tributary of Amper, which is a tributary of Isar. The basin is located to the north of München in the loess region. Elevation in the Glonn basin (gauge Hohenkammer) is between 450 to 559 m above sea level. Loamy and loess soils dominate in the basin area: 60.3 %. The soil erodibility factor K, defined in accordance with the soil database presented in Schmidt et al. (1992), varies from 0.12 to 0.55. The area is clearly dominated by arable cropland (73%), forest occupies only 16.5 % of the drainage area. Average long-term precipitation is 880 mm per year, and the runoff coefficient is 0.30.

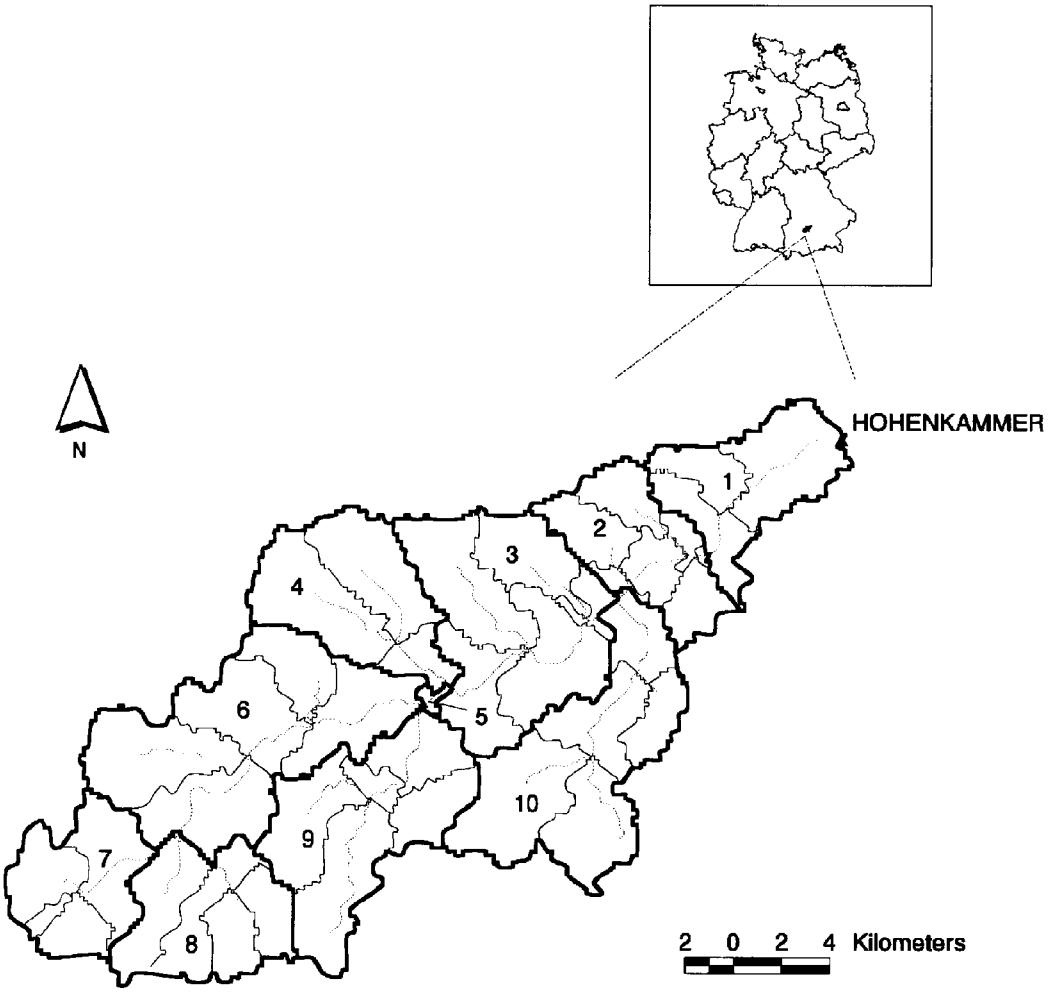

Fig. 2 The Glonn basin (392 km^2) with the gauge station Hohenkammer located in Bavaria, Germany and its subdivision into 10 and 42 sub-basins

Input data and transformation methods

Input data requirements for SWIM

The SWIM/GRASS interface was used to extract spatially distributed parameters of elevation, land use, soil types, and groundwater table. The interface creates a number of input files for the basin and sub-basins, including the hydrotope structure file and the routing structure file. To start the interface, the user must have at least four map layers for a basin: the elevation map (Digital Elevation Model), the land use, the soil, and the sub-basin maps. The fourth, sub-basin map can be created using the *r.watershed* program of GRASS (or by subdividing the basin in any other way).

The weather parameters necessary to drive the model are daily precipitation, air temperature (average, minimum and maximum), and solar radiation. Weather data can be taken from meteorological stations or produced using a weather generator based on monthly statistical data. One set of weather parameters may be used for the entire basin, or they can be specified for each sub-basin separately. In addition, a soil data base and a crop management data base have to be provided. River discharge, concentrations of nutrients and suspended sediments in the basin outlet are needed for model validation.

Spatial data and soil parameters

A DEM with 1000 m resolution provided by the 'Institut für Angewandte Geodäsie IFAG, Frankfurt-am-Main' was used for the simulations in the Mulde basin. For the Glonn basin a DEM with 160 m resolution provided by the Technical University of Darmstadt, Department of Meteorology, was used.

A land use map with 500 x 500 m horizontal resolution, provided by the 'Statistische Bundesamt, Wiesbaden', with 44 land use categories, was used in the both cases. It was reclassified to a new map with the following categories: 1) water, 2) settlement, 3) industry, 4) road, 5) cropland, 6) perennial grass, 7) pasture, 8) fallow, 9) forest, 10) sand or dunes, 11) bare soil, 12) wetland.

The digital soil map of Germany, 'Bodenübersichtskarte der Bundesrepublik Deutschland' 1:1,000,000, BÜK-1000, generated by the 'Bundesanstalt für Geowissenschaften und Rohstoffe, Hannover', was used for the Mulde basin. It provides parameters for 72 soil types, characterised through a 'leading profile'. For each horizon of every soil profile, 8 attributes are specified: depth, texture class, clay content, humus content, carbon content, nitrogen content, field capacity, and available field capacity.

For the Glonn basin the soil map 'Konzeptbodenkarte 1:25,000', generated by the 'Bayerische Geologische Landesamt', was used. The following parameters for several soil horizons (Schmidt et al., 1992) were used for the modelling: depth; sand, silt and clay content; bulk density; porosity; field capacity and available field capacity; carbon and nitrogen content; effective root depth; and soil erodibility. The saturated conductivity was estimated from porosity, sand and clay content in the horizon using the method of Rawls and Brakensiek (Smith, 1992).

The Mulde basin was subdivided for modelling into 62 sub-basins (average sub-basin area was 99.5 km^2). In the Glonn basin three different disaggregation schemes were applied in order to study the scaling effects: into 10, 42 and 162 sub-basins. Two of them, with 10 and 42 sub-basins are shown in Figure 2.

Relational data

Actual weather data obtained from German Weather Service (Deutsche Wetter Dienst, DWD) were used for simulations. In the case of Mulde, daily temperature (minimum, average and maximum), and sunshine duration from four climate stations (Oschatz, altitude 150 m; Chemnitz, 263 m; Zinnwald, 877 m; and Fichtelberg, 1213 m), and daily precipitation from 72 precipitation stations were used. The multivariate regression method described was used to estimate global radiation for these four stations. An altitude-correction coefficient was used to estimate temperature in the sub-basins.

In the case of Glonn, daily minimum, average and maximum temperatures from station 4116 Altomünster, located in the centre of the basin, and daily sunshine duration from station 4117 Weihenstephan were used. The regression method described was used to estimate global radiation for the Glonn basin from sunshine duration. Precipitation data from nine precipitation stations located in the basin, were used.

Data on water discharge were available for five gauge stations indicated on Figure 1 for the period 1981 – 1995. The measurements of suspended solids ('abfiltrierbare Stoffe') in the river were only available for these five stations for the period 1993 - 1995, with the frequency 14 -15 measurements a year (source: Sächsisches Landesamt für Umwelt und Geologie).

Daily water discharge and suspended sediment ('Schwebstoff') measurements available for 15 years from 1981 to 1995 for the gauge station Hohenkammer on the Glonn river were used for model validation in this basin. The longer time series, starting from 1971, were used for the double mass plot analysis described below. The data were obtained from the Bayerisches Landesamt für Wasserwirtschaft, München.

Methods to estimate solar radiation

Multivariate regression on the normals

Daily variations of sunshine duration and radiation show strong correlation of more than 0.9; this is true even with seasonal variations removed. Therefore, a simple linear regression model promises good results in expressing them through one another. Both quantities are, however, strongly non-normal in distribution, hence a linear model might nevertheless not be an optimum. On the other hand, daily radiation depends on more than just sunshine duration, for example, on humidity, hence further improvement might be achieved by using multivariate regression. Note that such improvements are minor since the original high correlation to sunshine duration already guarantees sound results. This might change if one considers more extreme climates.

We used a multivariate non-linear regression approach, whose parameters were calibrated using 30 years of daily measurements, between 1961 and 1990, at the station Potsdam, Germany. The following Table 2 summarizes the set of variables used for the regression model, together with the respective regression model coefficients. Here we see that besides sunshine duration, vapour pressure deficit plays a major role in the regression model. Note that the vapor pressure deficit and the relative humidity interact in such a way in this multivariate regression model that contribution of the latter one is rather low.

Table 2 Regression coefficients for the estimation of global radiation using the multivariate regression method described

Variable	Model coefficient
Temperature (mean)	0.03
Temperature (max)	0.05
Temperature (min)	-0.10
Precipitation	-0.02
Wind speed	-0.06
Rel. humidity	-0.03
Air pressure	0.01
Vapor pressure	-0.05
Sunshine	0.57
Cloudiness	-0.08
Snow height	0.03
Fog	0.01
Vapor pressure deficit (vpd)	0.22

As mentioned, many of the variables, especially those related to humidity, are strongly non-normal in distribution, thus disturbing linear regression relationships. To establish such relations, we first transformed each of the variables to one which is normally distributed, using the generic probit scheme as described, e.g., in Bürger (1996). This renders, in a 1-1 fashion, for any (continuous) variable X another variable Y, which is normally distributed. Formally, there exists a 1-1 mappings, ψ, with the following properties:

$$Y = \Psi(X) = \Phi^{-1}(F(X)) \tag{12}$$

$$X = \Psi^{-1}(Y) = \Phi(F^{-1}(Y)) \tag{13}$$

where F denotes the cumulative distribution function of X, and ϕ the cumulative normal distribution function.

Using the normalized variables, a 13-dimensional regression model was fitted which calculates daily normalized radiation. Again formally:

$$Y_{14} = \mathbf{L} Y_{1:13} \tag{14}$$

Having established the regression, a link is created via (12) $\rightarrow$ (13) $\rightarrow$ (14) between the 13 predictor variables and radiation in physical (non-normal) units.

Monthly regression on sunshine duration

In the second method the reconstruction of daily values of global radiation was done on the basis of sunshine duration and other meteorological parameters from seven synoptical stations located at different altitudes in different sub-regions in Germany: Schleswig, 43 m; Braunschweig, 81 m; Potsdam, 81 m; Lindenberg, 98 m; Passau, 409 m; Konstanz, 443 m; and Hohepeisenberg, 986 m.

The monthly correlation coefficients between the global radiation and other parameters measured at these meteorological stations have a maximum in summer and a minimum in winter. The sunshine duration showed the highest correlation with the global radiation (0.9 in winter to 0.95 in summer). Lower values were obtained for the relative humidity (0.6 to 0.85), the cloudiness (0.7 to 0.8), and the daily amplitude in temperatures (0.5 to 0.8).

After that, based on the results of the correlation analysis, daily global radiation was calculated in two different ways. In the first case, it was calculated on the basis of an unconditioned one-dimensional regression equation

$$Y_i = a \cdot X_i + b \tag{15}$$

where Y represents the global radiation, X stands for the sunshine duration, and i - the day number.

In the second case, an additional information about the second best predictor, the relative humidity, was used. For that, all days were divided into 5 clusters with different relative humidity: below 60%, between 60 and 70%, between 70 and 80%, between 80 and 90%, and between 90 and 100%. A specific regression equation

$$Y_i = a_k \cdot X_i + b_k \tag{16}$$

was calculated for every cluster K. The regression equations were estimated separately for every month on the basis of data from seven above mentioned synoptical stations.

The mean relative error (relative to mean standard deviation per month) in the estimation of global radiation was 0.41 when applying the unconditional regression equation (15), and 0.39 when applying the conditional Equation (16). This small difference confirms that the unconditional regression, applied on the monthly basis, can be used to estimate global daily radiation from sunshine duration using the monthly coefficients (Table 3).

Table 3 Monthly coefficients of the unconditional regression equation to estimate global radiation (Kj/cm^2) as a linear function of sunshine duration (h)

Month	a	b	Month	A	B
I	0.068	0.173	*VII*	0.146	0.797
II	0.093	0.301	*VIII*	0.133	0.691
III	0.126	0.456	*IX*	0.129	0.473
IV	0.140	0.645	*X*	0.102	0.321
V	0.152	0.762	*XI*	0.074	0.191
VI	0.151	0.851	*XII*	0.061	0.148

Table 4 Average annual sediment yield, t ha^{-1} for selected sub-basins 2, 4, 36, and 45 (see their location in Figure 4b) of the Mulde basin in 1993 and 1994

Sub-basin	Average annual sediment yield in sub-basins, t ha^{-1}	
	1993	1994
2	0.2	0.4
4	0.9	1.2
36	1.8	2.4
45	2.6	2.8

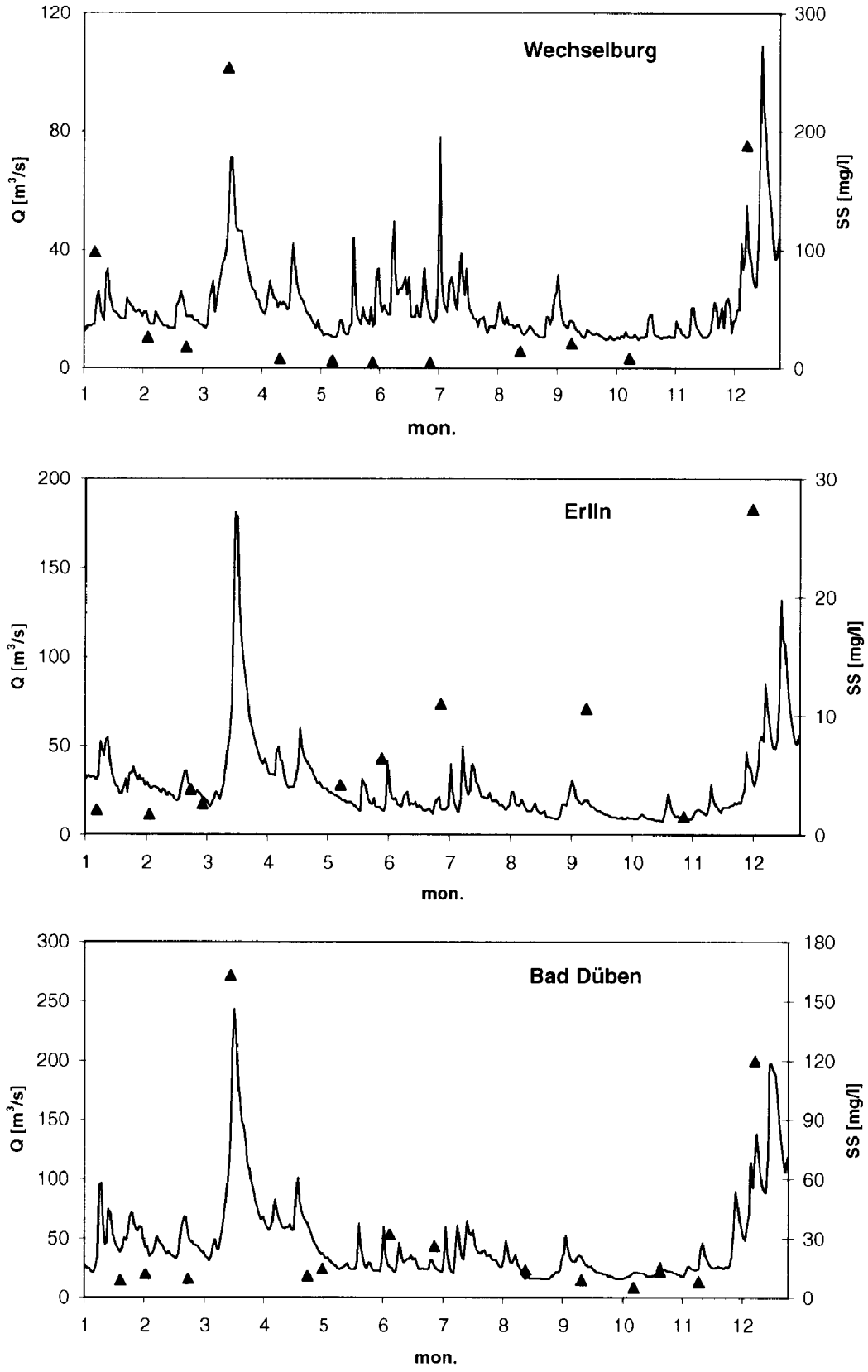

Fig. 3 The daily discharge (—) and suspended solids (Δ) in the river Mulde, gauge stations Wechselburg, Erlln, and Bad Düben in 1993

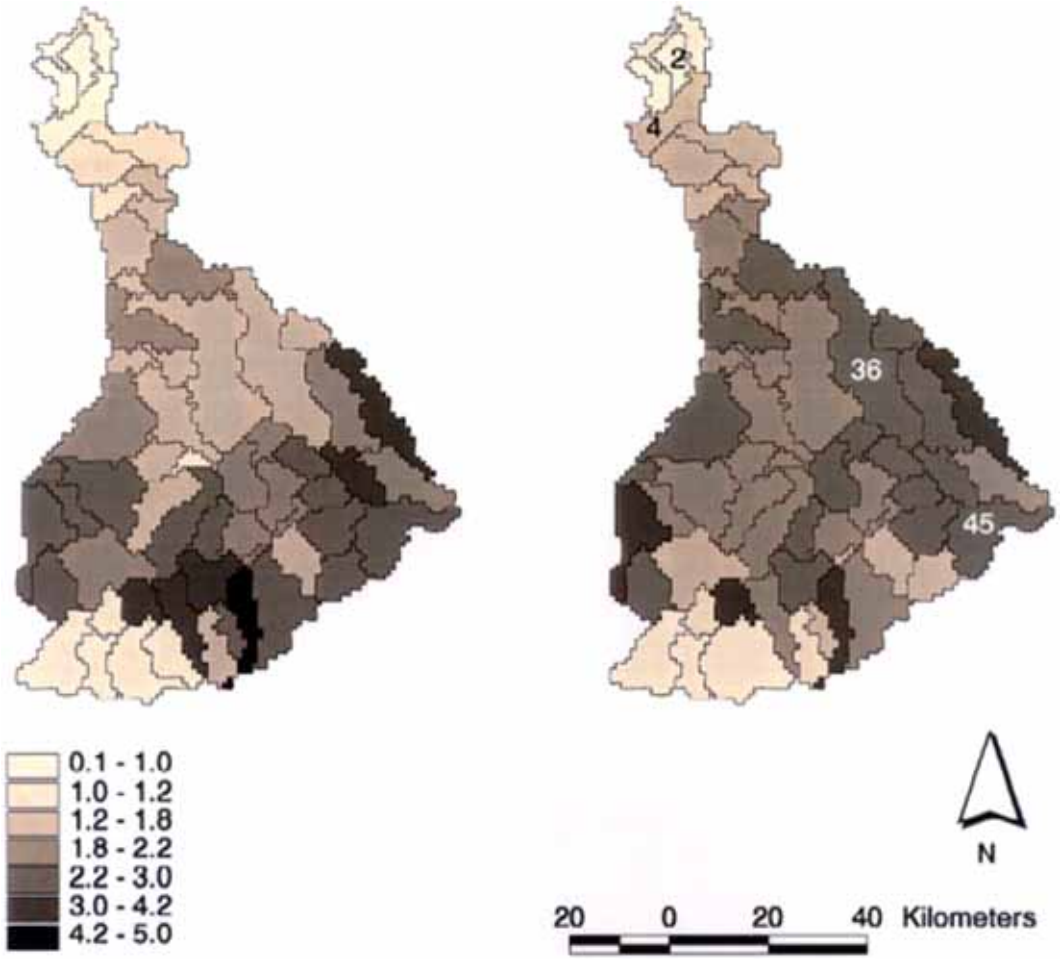

Fig. 4 Spatial patterns of the total annual sediment yield for 62 subbasins of the Mulde in 1993 (left) and 1994 (right)

Model application in the Mulde basin

Preparatory steps

Firstly, the simulation results for hydrology were compared with measured data for the periods 1981 - 1983 and 1993 - 1995. Statistical evaluation of results was performed by (a) analysing the simulated annual water balance, and (b) applying the common efficiency criterion after Nash and Sutcliffe (1970). The flood events were represented quite satisfactorily, and the efficiency of runoff simulation was in the range 0.68 - 0.72.

Unfortunately, the frequency of suspended sediment measurements was not sufficient for proper validation of the model. As we can see in Figure 3 the peaks of suspended solid concentrations usually occur during flood events in spring and autumn. Also, it is clear that there is a high probability that one peak at the station Erlln was ‘missed’ during the spring flood.

Spatial patterns

After the hydrological validation, the sediment yield for sub-basins and sediment transport were analysed for three subsequent years 1993 - 1995, for which the measured data on sediments were available.

Spatial patterns of sediment yield in 62 sub-basins are shown in Figure 4 for 1993 and 1994. The maximum values reach 4-5 t ha^{-1} yr^{-1}, corresponding to a moderate level of erosion. The highest surface runoff rates are observed in the south of the basin due to a mountainous landscape and higher precipitation. The highest soil erodibility occurs in the middle and northern parts of the basin (loess region). The forested areas are concentrated mainly in the south, and arable land occupies the lower northern part of the drainage basin. According to the modelling results, sub-basins with the highest sediment yield rates are located in the lower middle part of the basin (Figure 4). This is probably the result of several contributing factors - hydrological processes, soil erodibility, and land use.

Linkage between hydrological processes and sediment yield

The average annual sediment yield differs significantly between sub-basins of the Mulde. An example is given in Table 4 showing average annual sediment yields in 1993 and 1994 for sub-basins 2, 4, 36 and 45, located in different parts of the basin (see Figure 4 right).

Figure 5 depicts time series of simulated surface runoff (negative values, up) and sediment yield (positive values, down) for sub-basins 2, 4, 36, and 45, which have different sedimentation rates. As one can see, there are 2 - 3 peaks of sediment yield in spring in sub-basins 2, 4 and 36, and there are 5 spring and 2 autumn peaks in sub-basin 45. Practically all the peaks correspond to the runoff peaks. This confirms the strong linkage between hydrological processes (surface runoff) and sediment yield. The maximum daily sediment yield increases clearly from sub-basin 2 (lower than 40 kg ha^{-1}), located in lowland, to sub-basin 45 (more than 500 kg ha^{-1}), located in the mountainous part of the basin.

And finally, an attempt of model validation is presented in Figure 6 where the measured and simulated suspended solids can be compared for the river outlet in 1994. As one can see, there are two flood events in spring, and two corresponding peaks in the simulated suspended sediments. Only the first peak (day 76) is represented in the time series of measured data, and the concentrations are very close in both cases. Unfortunately, there were no measurements of suspended solids during the second flood event (days 103 - 106).

More thorough model validation was possible in the second basin, the Glonn.

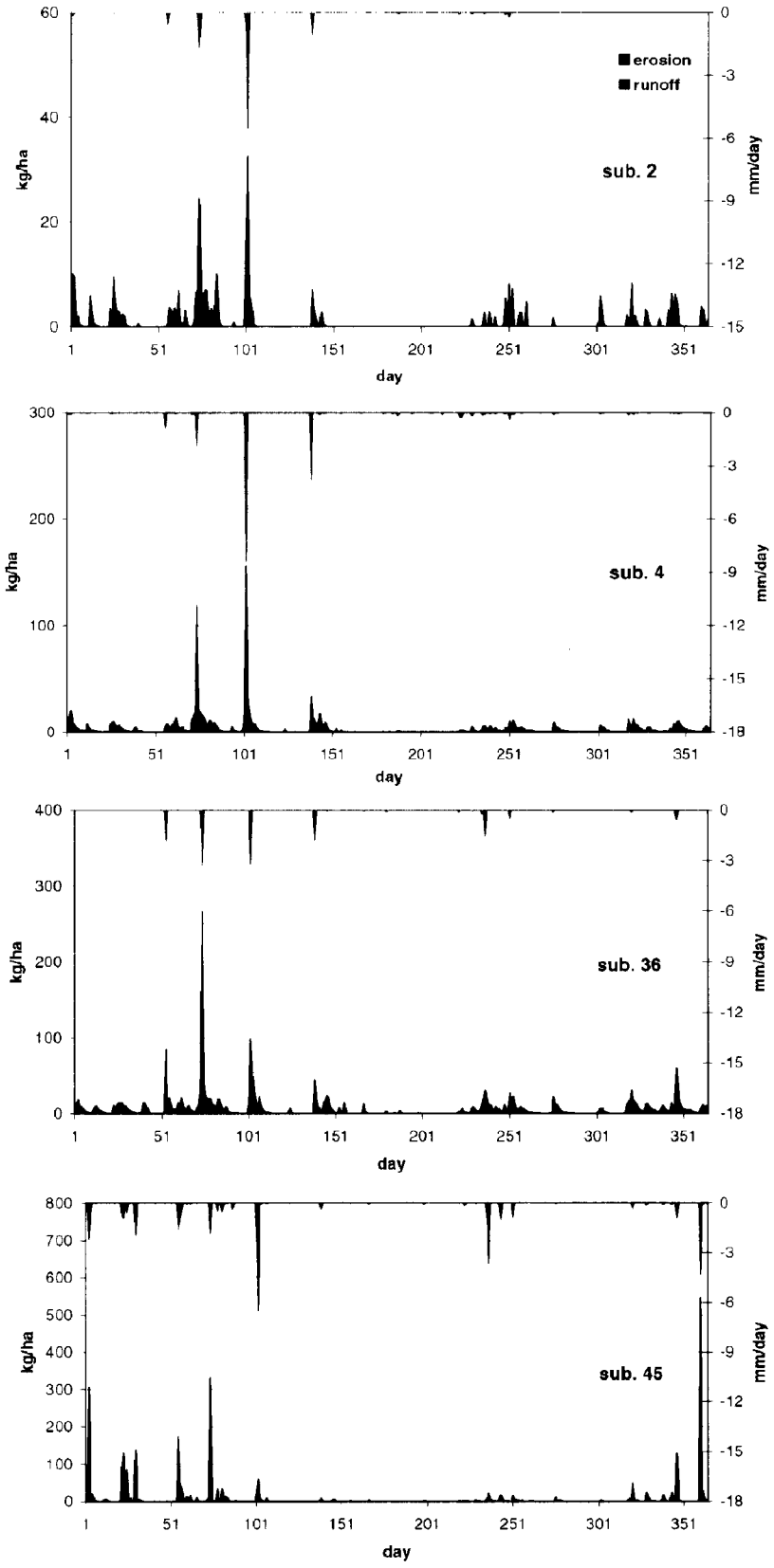

Fig. 5 Time series of simulated surface runoff (mm/day, grey, negative Y axis) and sediment yield (kg/ha, black, positive Y axis) for subbasins 2, 4, 36 and 45 of the Mulde basin in 1994

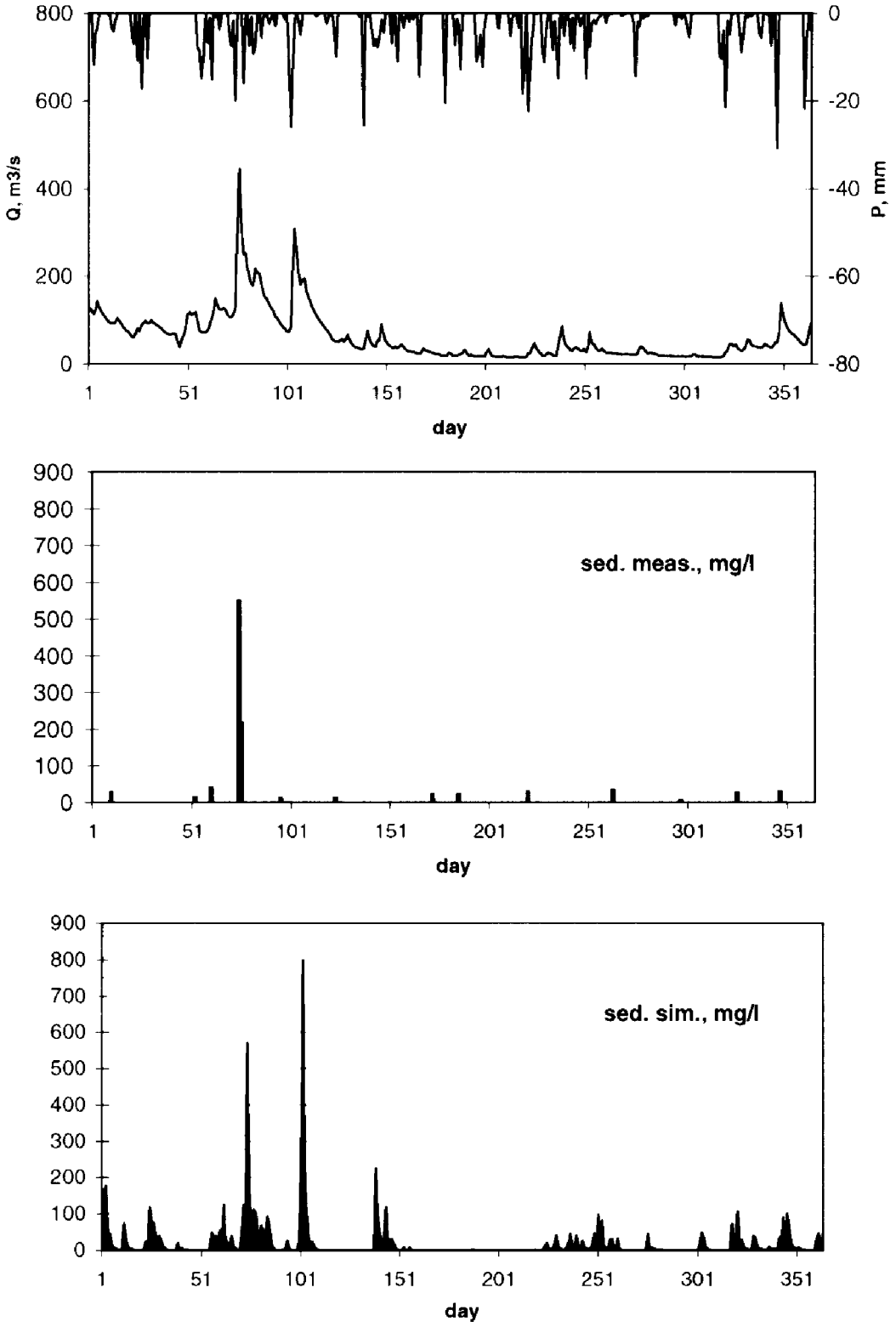

Fig. 6 An example of model validation in the Mulde, gauge station Bad Düben in 1994: time series of precipitation (P, mm), water discharge (Q, m^3/s), measured (sed. meas.), and simulated (sed. sim.) suspended solids

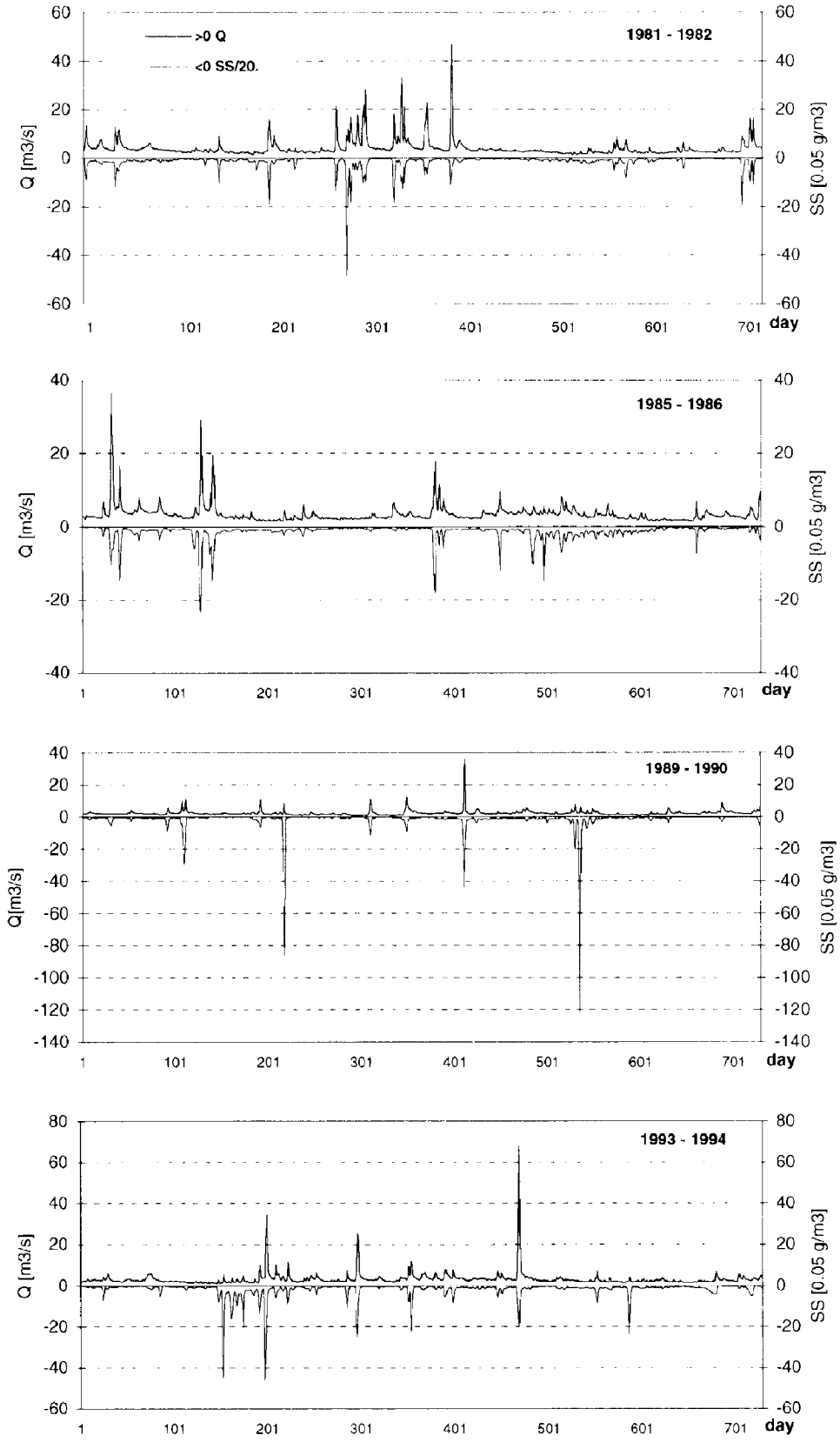

Fig. 7 Time series of measured river discharge (positive values, Q, m^3/s) and suspended sediment concentration (negative values, SS, 0.05 g/m^3) for eight years in the Hohenkammer gauge station of the Glonn basin

Model validation in the Glonn basin

Analysis of time series

Daily river discharge and daily concentrations of suspended sediments measured in the Hohenkammer gauge station of the Glonn river (period 1981 – 1995) were used for this case study. Figure 7 shows time series of river discharge (as positive values) and suspended sediments (as negative values) for selected eight years in this period. In order to compare the both time series, the concentrations of suspended sediments were recalculated with the coefficient 0.05, so the units are 0.05 g m^{-3}.

As we can see, in most cases the peaks of SS correspond clearly to the peaks of water discharge ('mirror-patterns'). Nevertheless, there are some peaks of suspended sediment concentration, which appear not during flood events, for example two very large peaks, one of 1732 g m^{-3} on the 7th of August 1989, and second of 2439 g m^{-3} on 20th of June 1990 (shown after days 201 and 501 on the graph). In both cases river discharge was lower than 10 m^3 s^{-1}. Note that there were no significant peaks of suspended sediments in other river in this region (Große Vils/Vilsburg, Rott/Ruhstorf, Mindel/Offingen, Regen/Regenstauf) in these periods of time.

In order to investigate whether there are any trends in the sediment transport, the double mass plot of sediment yield versus runoff was built (Figure 8), considering the longer period, from 1971 to 1995. This figure shows that there is no clear trend and little evidence of changing sediment loads over the period of 25 years, though during three years 1984 to 1986 the observed sediment load was lower.

We can compare this result with a more extended analysis of trends in sediment yields due to land use change in several rivers of the world performed by Walling (1999). This study included also two rivers in Germany. He found a significant reduction in sediment yield over the period 1960 – 1990 for the river Isar at München, Bavaria, and no trends in the sediment records over 60 years for the river Lech above Füssen in Bavaria. The reduction for the Isar was explained by the construction of storage reservoirs for hydropower stations on this river. In this respect the basin of Glonn behaves similarly to the Lech, both showing little evidence of changes in sediment transport despite of changes in both land use and land management practices over the last decades.

Hydrological validation

The basin boundaries of the Glonn, gauge Hohenkammer were delineated using the *r.watershed* program of GRASS (US Army, 1988). The area of the basin in GRASS was 392.9 km^2 – very close to that indicated in the statistical yearbook (Deutsches Gewässerkundliches Jahrbuch), 392 km^2.

Three different disaggregation schemes DS1, DS2 and DS3 were applied in the Glonn basin in order to study the scaling effects: into 10, 42 and 162 sub-basins, respectively. Two of them, with 10 and 42 sub-basins, are shown in Fig. 2. The average sub-basin areas were 39.2, 9.3, and 2.4 km^2 for DS1, DS2 and DS3 respectively. The corresponding numbers of hydrotopes in the whole basin were 479, 1088 and 2115, and the average hydrotope areas were 0.82, 0.36 and 0.19 km^2.

Hydrological validation in the Glonn basin was performed for the whole period 1981 – 1995, considering the first four years as calibration period. The same as in the case of Mulde,

statistical evaluation of results was performed by analysing the simulated annual water balance, runoff coefficients, and applying the efficiency criterion after Nash and Sutcliffe (1970). The largest uncertainty involved was that of land use and land cover, because the current land use map was used over the whole period (no other maps were available), and no data were available on crop rotation in the area.

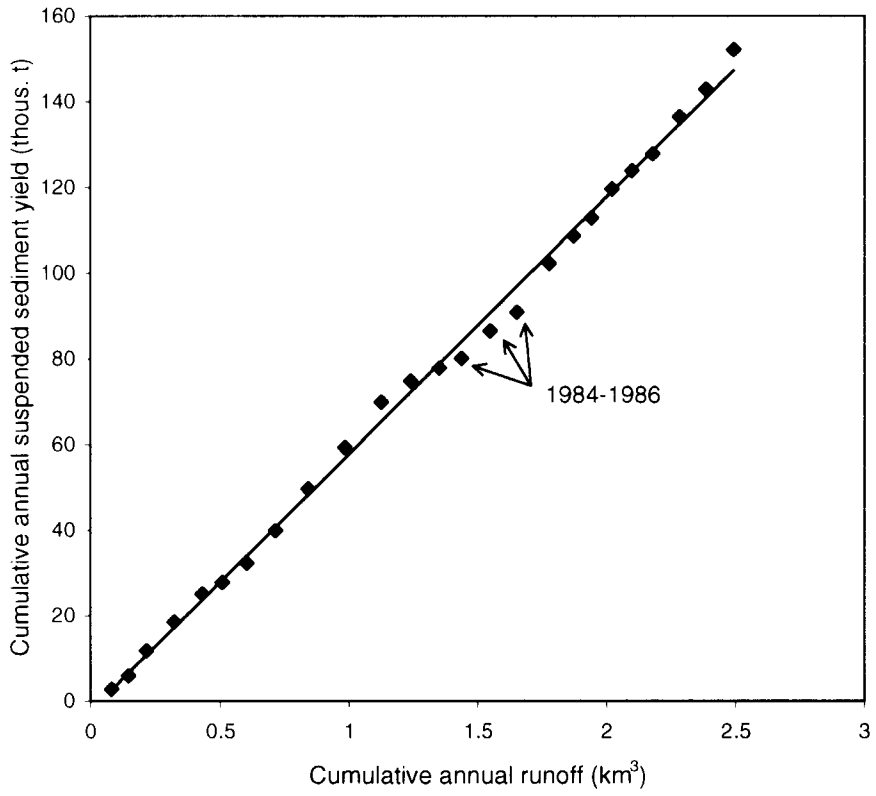

Fig. 8 The double mass plot of sediment yield versus river discharge in the Hohenkammer gauge station, the Glonn basin for 1971 – 1995

Nevertheless, the flood events are represented quite good, the low flow is also on appropriate level, and the efficiency of runoff simulation is in the range 0.66 - 0.80. The satisfactory results of hydrological validation were obtained using the first disaggregation scheme DS1, and they were only slightly different when using the more detailed schemes DS2 and DS3. An example of the model validation is shown in Figure 9 for the validation period 1990 – 1995.

Validation of sediment transport modelling and scaling issues

Scaling effects were much more important for the modelling of sediment transport than for hydrology. When the first disaggregation scheme DS1 was used, the most of large peaks of suspended sediment load appeared simultaneously with the measured peaks of SS load, but the total annual load was overestimated.

This resulted from the fact that sediment transport is simulated as a three-stage process in SWIM: at first the surface runoff and the factors C and K are estimated for hydrotopes, then sediment yield is calculated for sub-basins using (1), and after that sediments are routed in the streams following (11). However, if the number of sub-basins is small, the stream network may be underrepresented. This leads to the lower deposition in river network, and to the overestimation of the total annual sediment load.

When the second scheme DS2 was used, the results were improved: both the peaks of the SS load and the total annual balance were close to the measured ones. The application of the third scheme DS3 resulted in underestimation of the total annual loads (due to the too dense river network).

The other possible solution of this problem, in our opinion, would be to introduce one more step in the sediment transport modelling, namely, the sediment delivery ratio for sub-basins in order to take into account the sub-basin area.

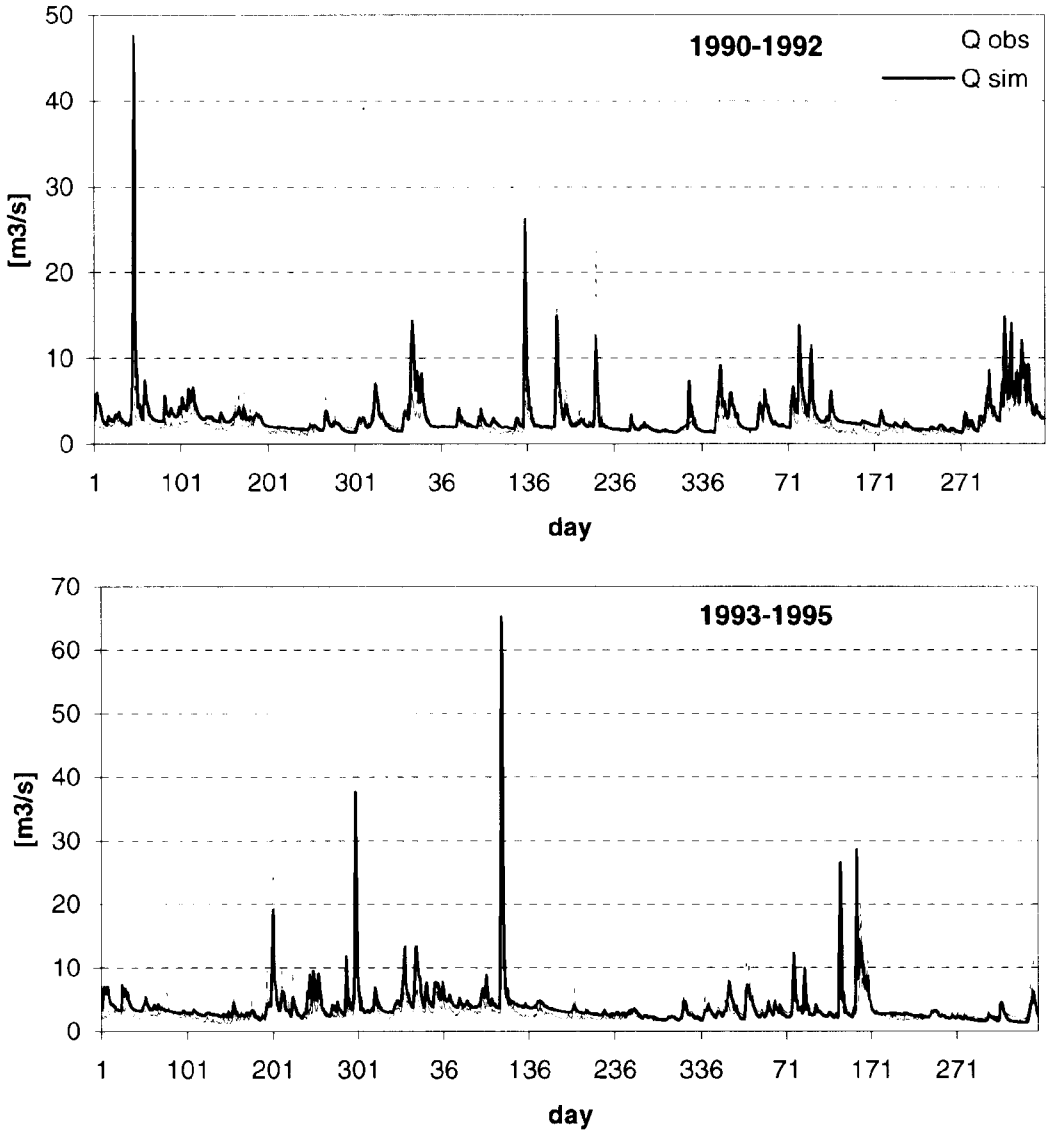

Fig. 9 Hydrological validation: simulated and observed river discharge for the Glonn basin, gauge Hohenkammer in 1990 – 1995

Another factor, which influenced the results, was the vegetation cover. For example, the absence of vegetation cover in winter resulted in higher sediment load during winter time. We compared three options: summer crop, winter crop, and summer crop in combination with cover crop during winter time. Among those, the best results were obtained assuming that the cover crop is following the summer crop. Here, we could not proceed with our analysis due to missing detailed data on crop rotation in the basin.

Three different disaggregation schemes influenced sediment transport, but not sediment yield in sub-basins. Let us look at some results on sediment yield for ten sub-basins (scheme DS1). The average annual sediment yield in the whole investigated period 1981 – 1995 varied from 0.1 t ha^{-1} yr^{-1} to 3.4 t ha^{-1} yr^{-1}. The difference between sub-basins can be explained mainly by the topography (LS factor), because there are no significant differences in land use and soil erodibility between sub-basins. Regarding temporal dynamics, the average annual simulated sediment yield in the Glonn basin of about 0.2 – 0.3 t ha^{-1} yr^{-1} was the smallest in 1984, 1986 and 1989, and the largest of 6.8 t ha^{-1} yr^{-1} in 1981 (see Fig. 11a).

The following results on sediment transport (Figures 10 and 11b) are presented for the case when the DS2 scheme was used, subdividing the basin into 42 sub-basins. Figure 10 depicts daily dynamics of simulated and measured suspended sediment load (in t) for eight years of simulation (the same years as in Figure 7). Most of the peaks in both time series appear simultaneously, though some of them are under- or overestimated. As could be expected, the two peaks corresponding to very high measured concentrations of SS in 1989 and 1990 in the period of low flow (see Figure 8) do not appear in the simulated time series. The reason is clear – the low flow cannot create high peaks of sediments in the model because of low surface runoff. The correlation coefficients calculated considering the full sets of measured and simulated load with daily time step were 0.68 for the whole period, 0.62 for nine years 1981 – 1989, and 0.71 for the first six years.

And finally, the annual amounts of simulated and measured sediment loads were compared (Figure 11b). The comparison is not bad, especially for the first six years. The correlation coefficients between these time series were 0.66 for the whole period, 0.77 for nine years 1981 – 1989, and 0.97 for the first six years. We can conclude that the validation results are satisfactory.

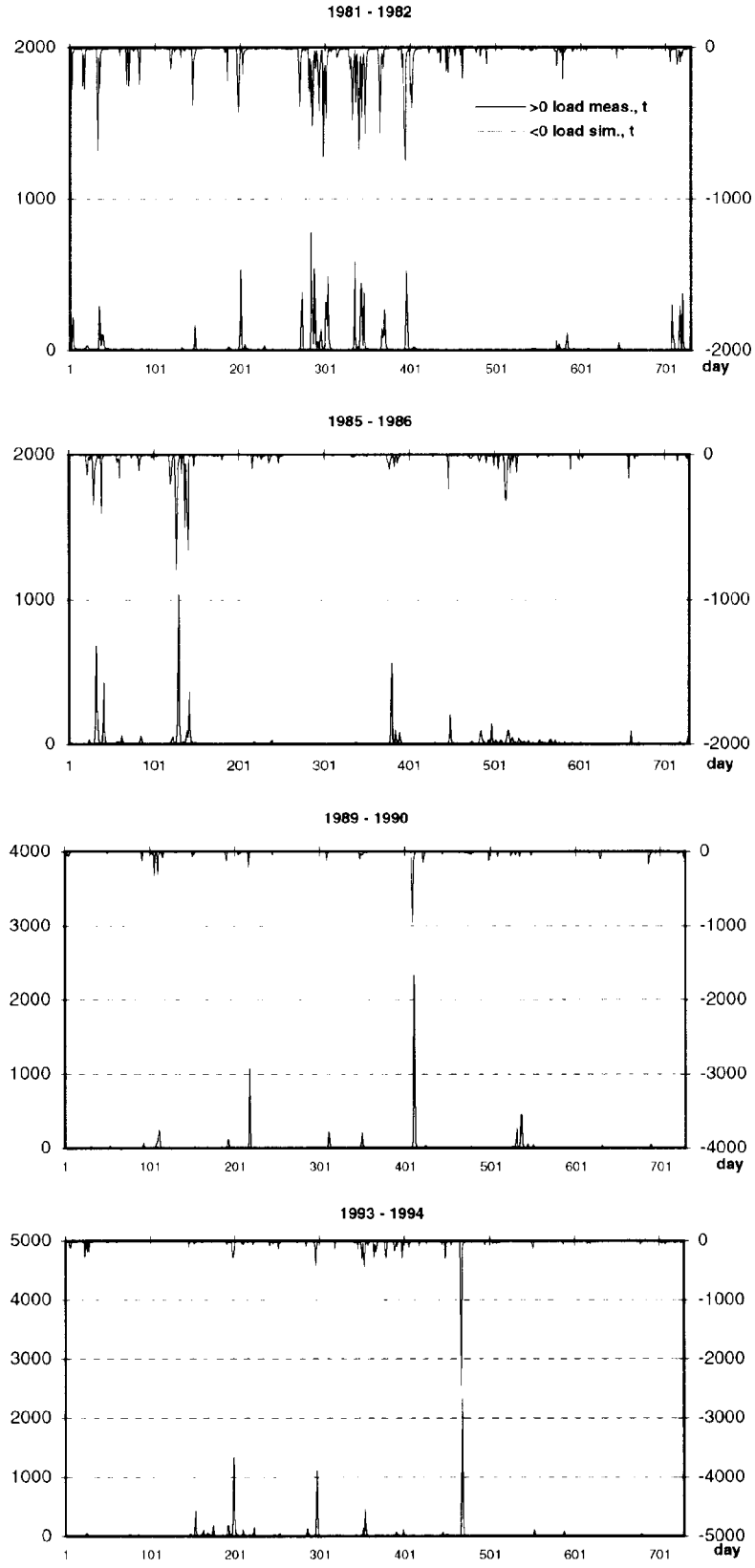

Fig. 10 Daily dynamics of simulated (negative values from the top of the diagram) and measured sediment load (positive values) for eight years in the period 1981 – 1994

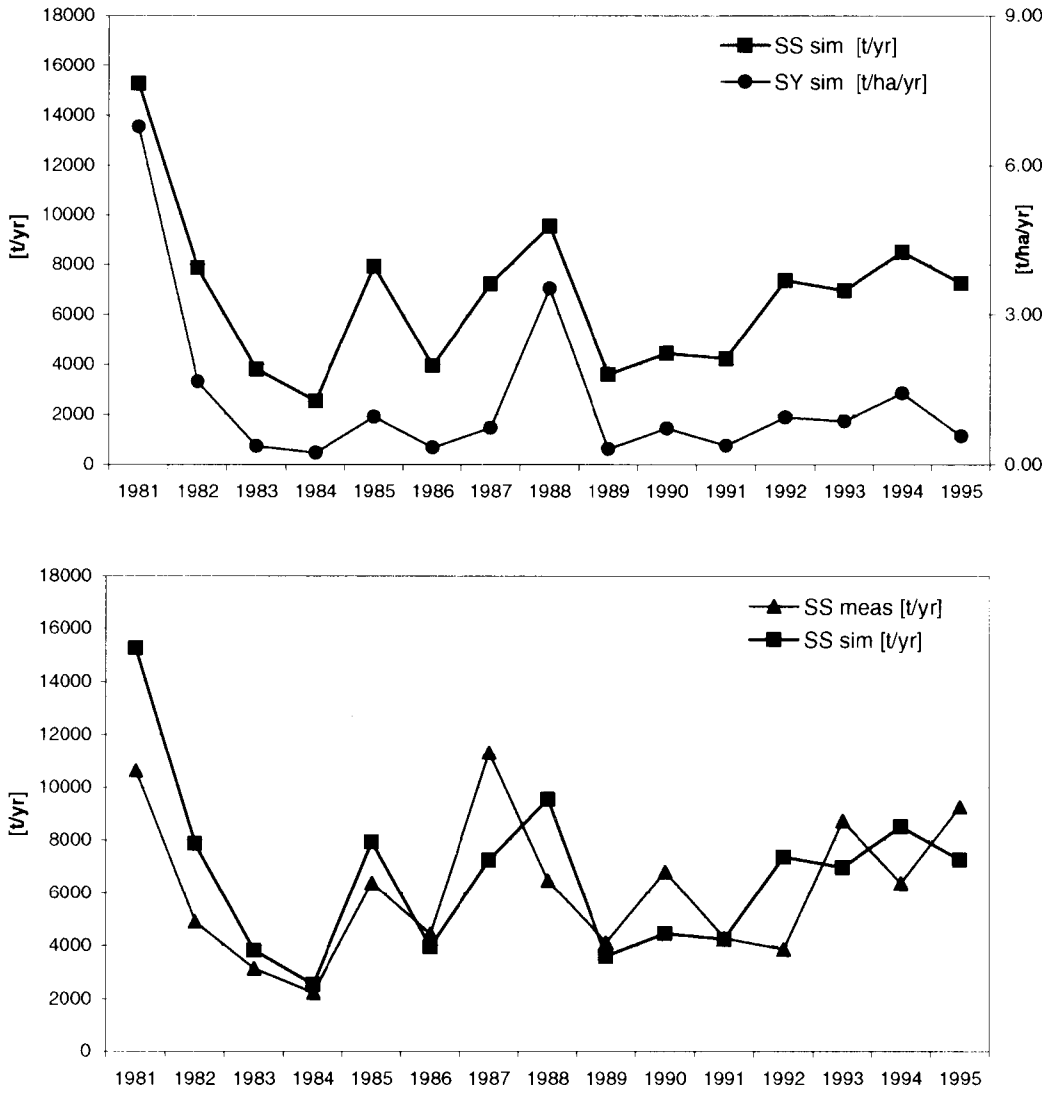

Fig. 11 The average annual simulated sediment yield (SY sim, t ha^{-1} yr^{-1}) in the Glonn basin, gauge Hohenkammer and the annual simulated sediment load (SS sim, t yr^{-1}) (a); and the comparison of the annual amounts of simulated (SS sim) and measured (SS meas) sediment loads (b)

Discussion and conclusions

The validation of the erosion module demonstrated the ability of SWIM model to simulate sediment yield and transport at the river basin scale with daily time step using regionally-available information. The model can be used for other regions/conditions, as soon as data requirements are modest.

Our study confirmed the importance of scaling effects for erosion modelling at the basin scale. They have to be taken into account by applying an appropriate disaggregation scheme for the studied basin, or by introducing additional sediment delivery ratios within sub-basins.

It was shown that hydrological processes play a dominant role in controlling sediment yield and transport, because most of the sediment yield is produced during a few high flow events in a year, usually in spring and autumn. Also, the soil erodibility and land use/land

cover are important factors determining spatial patterns of sediment yield. We can conclude that the linkage between hydrological processes and erosion is even stronger in the model than in reality, as soon as the model cannot reproduce some observed high concentrations of suspended sediments occurring during low flow periods.

The model can be used for climate impact studies, because both hydrology and erosion processes respond correctly to the changing weather conditions. In order to use the model for land use change studies, an additional analysis of interrelations between vegetation cover and erosion should be done with SWIM, using better land cover data.

Acknowledgements The authors are grateful to Claus Rachimow and Sibyll Shaphoff for their help in data aquisition and processing and preparation of some graphs. Thanks to the German Federal Ministry for Research and Technology (BMBF) for providing the funding for this research (project 'Elbe Ecology').

Bibliography

ARNOLD, J.G.; J.R. WILLIAMS; A.D. NICKS and N.B. SAMMONS (1990) *SWRRB - a basin scale simulation model for soil and water resources management*. Texas A&M University Press, College Station.

ARNOLD, J.G.; P.M. ALLEN and G. BERNHARDT (1993) 'A comprehensive surface-groundwater flow model.' J. Hydrol., 142, p. 47-69.

ARNOLD, J.G.; J.R. WILLIAMS; R. SRINIVASAN; K.W. KING and R.H. GRIGGS (1994) *SWAT, Soil and Water Assessment Tool*. USDA, ARS, 808 East Blackland Road, Temple, TX 76502.

BEASLEY, D.B.; L.F. HUGGINS and E.J. MONKE (1980) 'ANSWERS: A model for watershed planning.' Trans. ASAE 23, No.4, p. 938-944.

BÜRGER, G. (1996) 'Expanded downscaling for generating local weather scenarios.' Clim. Res. 7, p. 111-128.

EASTERLING, W.E.; P.R. CROSSON; N.J. ROSENBERG; M.S. MCKENNEY; L. KATZ and K. LEMON (1993) 'Agricultural impact of and responses to climate change in the Missouri-Iowa-Nebraska-Kansas (MINK) Region.' Climatic Change 24 (1-2), p. 23-62.

FAVIS-MORTLOCK, D.T.; J.N. QUINTON and W.T. DICKINSON (1996) 'The GCTE validation of soil erosion models for global change studies.' J. Soil and Wat. Conserv., 51, No.5, p. 397-402.

INGRAM, J.; J. LEE and C. VALENTIN (1996) 'The GCTE Soil Erosion Network: A multi-participatory research program.' J. Soil and Wat. Conserv. 51, No.5, p. 377 – 380.

KRYSANOVA, V.; A. MEINER; J. ROOSAARE and A. VASILYEV (1989) 'Simulation modelling of the coastal waters pollution from agricultural watershed.' Ecol. Modelling, 49, p. 7-29.

KRYSANOVA, V.; D.I. MÜLLER-WOHLFEIL and A. BECKER (1996) *Integrated modelling of hydrology and water quality in mesoscale watersheds*. PIK Report No. 18, Potsdam Institute for Climate Impact Research, Germany, 32 pp.

KRYSANOVA, V.; D.I. MÜLLER-WOHLFEIL and A. BECKER (1998a) 'Development and test of a spatially distributed hydrological / water quality model for mesoscale watersheds.' Ecological Modelling, 106 (1-2) p.261-289.

KRYSANOVA, V.; A. BECKER and B. KLÖCKING (1998b) 'The linkage between hydrological processes and sediment transport at the river basin scale.' In: W. Summer, E. Klaghofer and W. Zhang (eds.), *Modelling soil erosion, sediment transport and closely related hydrological processes*' IAHS Publication No. 249, 13-20.

KRYSANOVA, V. and A. BECKER (1999a) 'Integrated modelling of hydrological processes and nutrient dynamics at the river basin scale.' Hydrobiologia (in press).

KRYSANOVA, V.; F. WECHSUNG; A. BECKER; W. POSCHENRIEDER and J. GRÄFE (1999b) 'Mesoscale ecohydrological modelling to analyse regional effects of climate change', Environmental Modelling and Assessment (in press)

LEONARD, R.A.; W.G. KNISEL and D.A. STILL (1987) 'GLEAMS: Groundwater Loading Effects of Agricultural Management Systems.' Trans. of the American Society of Agricultural Engineers 30, No.5, p. 1403-1418.

MORGAN, R.P.C.; J.N. QUINTON and R.J. RICKSON (1992) *EUROSEM documentation manual*. Silsoe College, Silsoe, Bedford, UK.

NASH, J.E. and J.V. SUTCLIFFE (1979) 'River flow forecasting through conceptional models. 1. A discussion of principles.' J. Hydrol., 10, p. 282-290.

NEARING, M.A.; G.R. FOSTER; L.J. LANE and S.C. FINCKNER (1989) 'A process-based soil erosion model for USDA – Water Erosion Prediction Project Technology.' Trans. of the American Society of Agricultural Engineers 32, p. 1587-1593.

RENARD, K.G.; G.R. FOSTER; G.A. WEESIES and J.P. PORTER (1991) 'RUSLE – Revised Universal Soil Loss Equation.' Journal Soil and Wat. Conserv. 46, No.1, p. 30-33.

ROBERTSON, T.; V.W. BENSON; J.R. WILLIAMS; C.A. JONES and J.R. KINIRY (1987) 'The impact of climate change on yields and erosion for selected crops in the southern United States.' In: *Proceedings symposium on climate change in the southern United States: future impacts and present policy issues*. New Orleans, Louisiana: Science and Public Policy Program, p. 89-134.

ROBERTSON, T., C. ROZENZWEIG, V. BENSON and J.R. WILLIAMS (1990) 'Projected impacts of carbon dioxide and climate change on agriculture in the Great Plains.' In: P.W. Unger, T.V. Sneed, W.R. Jordan and R. Jenson (eds.), *Proceedings international conference on dryland farming, challenges in dryland agriculture – a global perspective*, August 1988, Amarillo/Bushland, Texas. Texas Agric. Exp. Stn., pp. 675-677.

SCHMIDT, F.; A. BÖHM; J. HAMMERL; B. HOFMANN; G. HOLZNER; R. JOCHUM; X. KELLER; C. MAHLER; W. MARTIN; A. PETSCHL; R. PRINZ; B. SCHILLING; E.-D. SPIES; G. STIMMELMEIER and O. WITTMANN (1992) 'Die Böden Bayerns. Datenbuch für die Böden des Tertiärhügellandes, der Iller-Lech-Platter und des Donautales.' Bayerisches Geologisches Landesamt, München, pp. 527

SMITH, R.E. (1992) *Opus, an integrated simulation model for transport of nonpoint-source pollutants at the field scale, vols. 1 and 2*. US Department of Agriculture, ARS-98, Springfield, VA.

SRINIVASAN, R., and J.G. ARNOLD (1993) 'Basin scale water quality modelling using GIS.' In: Applic. of Adv. Inform. Techn. for Manag. of Nat. Res., Spokane, WA, USA, p. 475-484.

U.S. ARMY (1988) *GRASS reference manual*. USA CER, Champaign, IL.

WALLING, D.E. (1999) 'Linking land use, erosion and sediment yields in river basins.' Hydrolobiogia (in press)

WILLIAMS, J.R. and H.D. BERNDT (1977) 'Sediment yield prediction based on watershed hydrology.' Trans. ASAE, 20, No.6, p. 1100-1104.

WILLIAMS, J.R.; K.G. RENARD and P.T. DYKE (1984) 'EPIC - a new model for assessing erosion's effect on soil productivity.' J. of Soil and Water Conservation 38, No.5, p. 381-383.

WILLIAMS, J.; M. NEARING; A. NICKS; E. SKIDMORE; C. VALENTIN; K.KING and R. SAVABI (1996) 'Using soil erosion models for global change studies.' J. Soil and Wat. Conserv. 51, No.5, p. 381-385.

WISCHMEIER, W.H., and D.D. SMITH (1978) *Predicting rainfall erosion losses*. U.S. Department of Agriculture, Agricultural Research Service, Handbook No. 537, 58 pp.

YOUNG, R.A., C.A. ONSTAD, D.D. BOSCH and W.P. ANDERSON (1989) 'AGNPS: a nonpoint source pollution model for evaluating agricultural watersheds.' J. Soil and Wat. Conserv., 44, No.2, p. 168-173.

Essai de modélisation du risque d´érosion hydrique utilisant des paramètres socio-économiques. Cas d´ une zone rurale sénégalaise

A. Thioubou, M. W. Ostrowski
TU-Darmstadt, Institute for Hydrology,
Petersenstrasse 13, D-64287 Darmstadt, Germany

Introduction

La dégradation des sols par l´érosion hydrique constitue une menace permanente à la désertification dans les pays sahéliens. Si les causes sont en général bien connues – agressivité des pluies, techniques de mise en valeur inappropriées... -, il n'en demeure pas moins que les techniques de contrôle n'ont connu jusqu'à présent que peu de succès. Cela tient d'une part au privilège accordé aux démarches sectorielles qui dissocient les interventions des techniciens de diverses branches: agriculture, foresterie... D'autre part, les recherches menées dans le domaine de l´érosion hydrique, du fait qu´elles mobilisent des moyens financiers importants, font souvent défaut. La mise en place de démarches simples qui présentent le triple avantage d´exiger des coûts peu élevés, de fournir des résultats probants et d´assister les planificateurs à tous les niveaux de leurs interventions doit être conçue comme une priorité. Par ailleurs, le souci de favoriser des méthodes préventives au détriment des méthodes correctives est à mettre en avant.

Dans cet article, est présenté un modèle d´évaluation du risque d´érosion hydrique basé sur l´utilisation de Systèmes d´Informations Géographiques dans une zone rurale située à l´Ouest du Sénégal. Il a la particularité d'aller au delà de l'aspect purement physique dans le schéma causal de l´erosion et de prendre en charge l'aspect socio-économique qui joue ici le rôle de catalyseur dans le processus de dégradation des terres au Sahel. En outre, l´approche participative est de mise. Cette première étape doit aboutir à la conception et à la mise en place d´un plan d´aménagement.

Matériel et méthode

Matériel

Le Tableau 1 présente la liste des données cartographiques utilisées dans ce travail. Comme autre type de paramètres, on peut noter d'une part des statistiques de population et de précipitation à diverses dates et de l'autre les résultats des enquêtes sur le foncier et sur les comportements environnementaux, qui sont présentés sous forme de tableaux.

Tableau 1 Données cartographiques utilisées

Type de données	échelle	Source
Cartes topographiques : feuilles de Diass, Thicky, Sindia et Kirène.	1/10.000ème	(IGN, 1974)
Carte topographique : feuille de Thiès 3a	1/50.000ème	JICA, METL, 1991
Carte topographique : feuille de bargny sud-est	1/50.000ème	IGN, 1983
Carte hydrogéologique du horst de Diass	1/50.000ème	Martin, 1967
Carte pédologique de la presqu'île du Cap-Vert: feuille Sud-est	1/50.000ème	Maignien, 1959
Photographies aériennes. Missions 1954, 1978 et 1989	1/60.000ème	IGN France
Images satellitaires TM	30 * 30 m	CSE, 1994
Images satellitaires SPOT	20 * 20 m	CSE, 1988

Méthodologie

Dans les régions sahéliennes, le manque et parfois la quasi absence de suivi et de contrôle réguliers des bassins versants constitue un obstacle de taille dans la simulation des processus d´érosion hydrique. Or, la qualité des résultats générés par tout modèle dépend en grande partie de la fiabilité des paramètres d´entrée (Von Werner, 1995). Pour pallier à cet obstacle, un Système d´Information Géographique (SIG) est mis en place. Un SIG, tel que défini par Strobl (dans Blaschke, 1997) est „ un système informatique destiné à la saisie, au stockage, à la vérification, à la manipulation, à l´intégration, à l´analyse et à la représentation de données spatialisées. ". Avec ce système, de nouvelles informations peuvent être générées à partir de celles déjà disponibles. IDRISI. C'est un SIG de type raster composé de plus de 150 modules. Cette construction modulaire a pour avantage de faciliter la représentation graphique et l´analyse de données spatialisées.

La démarche suivie repose sur trois étapes : l´identification des facteurs participant à l´explication des phénomènes en cours, la transformation de données brutes et l´élaboration de modèles partiels, la conception du modèle définitif et la vérification de celui-ci.

L´identification des facteurs

L´érosion comprise comme le résultat de l´interaction des trois processus suivants – détachement des particules, transport par le ruissellement et enfin déposition (Schramm, 1994) – fait intervenir deux types de facteurs : les facteurs d´ordre physique et les facteurs d´ordre socio-économique (Figure 1).

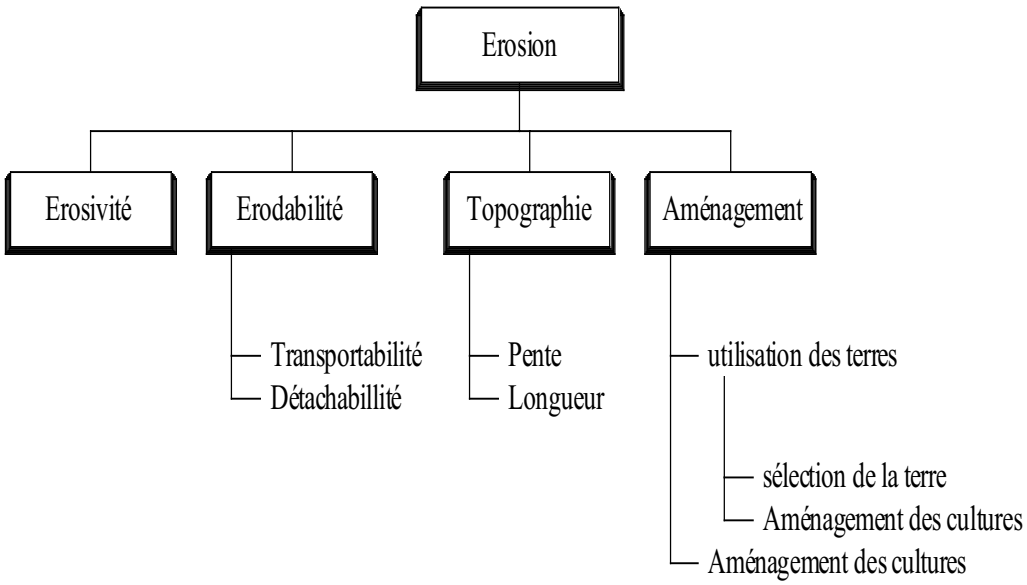

Fig. 1 Facteurs influant sur l´érosion [Source : F.A.O., 1986 (modifié)]

Le premier facteur est constitué par le climat. Les climats sahéliens sont caractérisés par la grande variabilité interannuelle des pluies, la durée raccourcie de la saison pluvieuse, des températures et des valeurs d´ Evapotranspiration élevées toute l'année (Riou, 1990). Plusieurs recherches menées sous ce climat tendent à démontrer que l´érosivité des pluies constitue ici le facteur décisif de l´érosion hydrique (Roose, 1978). La chute d'une goutte de pluie à la surface terrestre s´accompagne de la libération d´énergie cinétique qui entraîne la désagrégation des matériaux superficiels. Il existe plusieurs méthodes qui permettent de déterminer l´érosivité à partir d´ indices (Wischmeier et Smith, Fournier).

Le second facteur est de nature pédologique. L´érodabilité exprime la susceptibilité d´un sol face à l´érosion. Elle traduit aussi la capacité de leur résistance face à l´érosion (Poesen J, 1995). C'est pourquoi, les propriétés du sol, à la fois physiques et chimiques - l´infiltrabillité, la teneur en eau, le taux de couverture végétale mais aussi la teneur en matière organique, la Capacité d´Echanges Cationiques (CEC) - sont déterminants dans le cours des processus de ruissellement et d´érosion.

La pente est le troisième facteur. Même s´il est clair que la pente joue un rôle crucial dans les processus d´erosion, il n'en demeure pas moins qu'il y a plusieurs théories discutant de son effet réel (Tauer et Humborg, 1993). Pour certains auteurs, l´écoulement est accéléré

dans le cas d´un bassin versant escarpé tandis que l´infiltration est minime. Pour d´autres par contre, l´infiltration augmenterait avec la rugosité ainsi occasionnée.

Enfin le dernier facteur est constitué par la végétation qui joue le rôle de protection du sol et atténue par conséquent les effets du splash. Le Tableau 2 permet de constater que le taux de couverture du sol est déterminant dans le processus de splash. Ainsi pour des sols couverts de résidus végétaux, les pertes en terre sont insignifiantes contrairement au sol nu ou mis en culture dans le cas de plantes non couvrantes.

Tableau 2 Pertes de sols en fonction de différents systèmes par rapport à un sol nu.

Systèmes	Perte relative
Sol nu	1
Jachère buissonnante	0.004
Jachère herbeuse mal développée	0.09
Paillis à 20 %	0.2
Paillis à 40 %	0.04
Paillis à 60 %	0.008
Semis directs sans résidus végétaux	0.01 - 0.3
Semis directs avec résidus végétaux	0.0001 - 0.0003
Mais	0.4 - 0.8
Manioc	0.4 - 0.9
Arachide	0.3 – 0.8

Source : Nill, 1993 (in Steiner, 1996)

Cependant, l'action anthropogénique reflétée par les systèmes de mise en valeur, la pression sur les ressources liée à une démographie galopante, les types de plantes cultivées, la politique foncière appliquée ne peut être négligée dans l´appréhension des processus en jeu.

Les facteurs ainsi déterminés, il est procédé à la transformation des données brutes et à l´élaboration de modèles partiels.

La transformation des données brutes et l´élaboration de modèles partiels

L´intégration des données fournies par les cartes thématiques exige la transformation de celles-ci sous forme numérisée : vectoriel et/ou raster. Ainsi, les cartes topographiques servent de base à la construction du modèle numérique de terrain à partir duquel la carte des pentes est produite. La carte pédologique fournit les informations servant à la détermination de l´érodabilité des sols. L´érosivité est obtenue à partir de la transformation des séries pluviométriques et du calcul d´un index d´érosivité. L´interprétation des photographies aériennes et des images satellitaires fournit les renseignements sur la répartition et la nature de la couverture végétale. Les statistiques de population servent à la détermination de la

densité réelle et de la pression sur l´espace et sur les ressources.

Conception du modèle définitif et la vérification de celui-ci

Les deux sous-modèles (physique et socio-économique) sont séparément vérifiés sur le terrain et si possible rectifiés. Il s´agira ensuite de les superposer pour concevoir le modèle définitif qui permettra de retracer l´evolution spatio-temporelle du risque d´érosion anthropique pour un espace déterminé. L´objectif est d´identifier dans de brefs délais et à moindre coût les zones prioritaires à l´aménagement. Egalement, cela permettra aussi bien d´améliorer les connaissances sur le rôle des facteurs pris séparément dans le processus de dégradation des terres. Les planificateurs pourront mieux orienter leurs interventions qu´elles soient de nature préventive ou curative. La sensibilisation des acteurs est ainsi renforcée.

Des unités homogènes du point de vue de leur comportement face à l´érosion sont définies et des plans d´aménagement fonctionnels incluant toutes les composantes à la fois naturelles et anthropiques conçues dans le but d'une gestion durable des ressources. En somme, il s´agira de définir le cadre optimal de l´utilisation de celles-ci. Par conséquent, la participation et l´approbation des populations à tous les niveaux du processus est indispensable dans la mesure où ils en sont non seulement les premiers bénéficiaires mais aussi les garants les plus sûrs de l'application de techniques de gestion environnementales adéquates.

Pour l'instant le test d'application est effectué à Diass mais il est également prévu de l´étendre à d´autres bassins sahéliens.

Application

Site de recherches

Le site se trouve à près de 70 km à l´ouest de la région de Dakar, précisément entre les latitudes 14°45 Nord et 14° 32 Nord et les longitudes 17° 10 et 16° 55 Ouest (Figure 2).

Il se présente sous la forme d´un Horst sur lequel affleurent dans la partie centrale des formations du Maestrichtien composé essentiellement de sables et de grès. On distingue trois faciès principaux: une série sableuse en profondeur, une série gréso-calcaire que l'on retrouve à Popenguine et enfin la série dite 'Cap–rouge/cap de Naze'. En outre, on note quelques affleurements datant du Paléocène composé de formations carbonées pour l´essentiel avec des niveaux calcaro-marneux et marneux à N´dayane et des calcaires zoogènes karstiques que l'on rencontre à l´Est vers Bandia (Martin, 1970). Le Quaternaire est, quant à lui, marqué par des phases de cuirassement à la faveur de changements climatiques importants. Les témoins de ces formations se retrouvent au sommet des massifs de Thicky (Nahon, 1970).

Cette structure influence fortement le modelé dominé par un ensemble de bas plateaux, de glacis et de collines qui culminent à 104 m à Thicky. Mais dans l'ensemble la moyenne des altitudes ne dépasse pas 50 m. Cette structure vallonnée est réalisée grâce à un réseau de drainage caractérisé par son intermittence.

Le climat est de type sahélien avec une saison des pluies qui s´étend de Juin à Octobre. Des tendances à la sécheresse marquées par la baisse des débits précipités sont aussi observées (Figure 3). Par exemple, à la station de Mbour, la moyenne pluvieuse est passée de 747 mm pour la période comprise entre 1920 et 1966 à seulement 495 mm entre 1985 et 1994 (Thioubou, 1996).

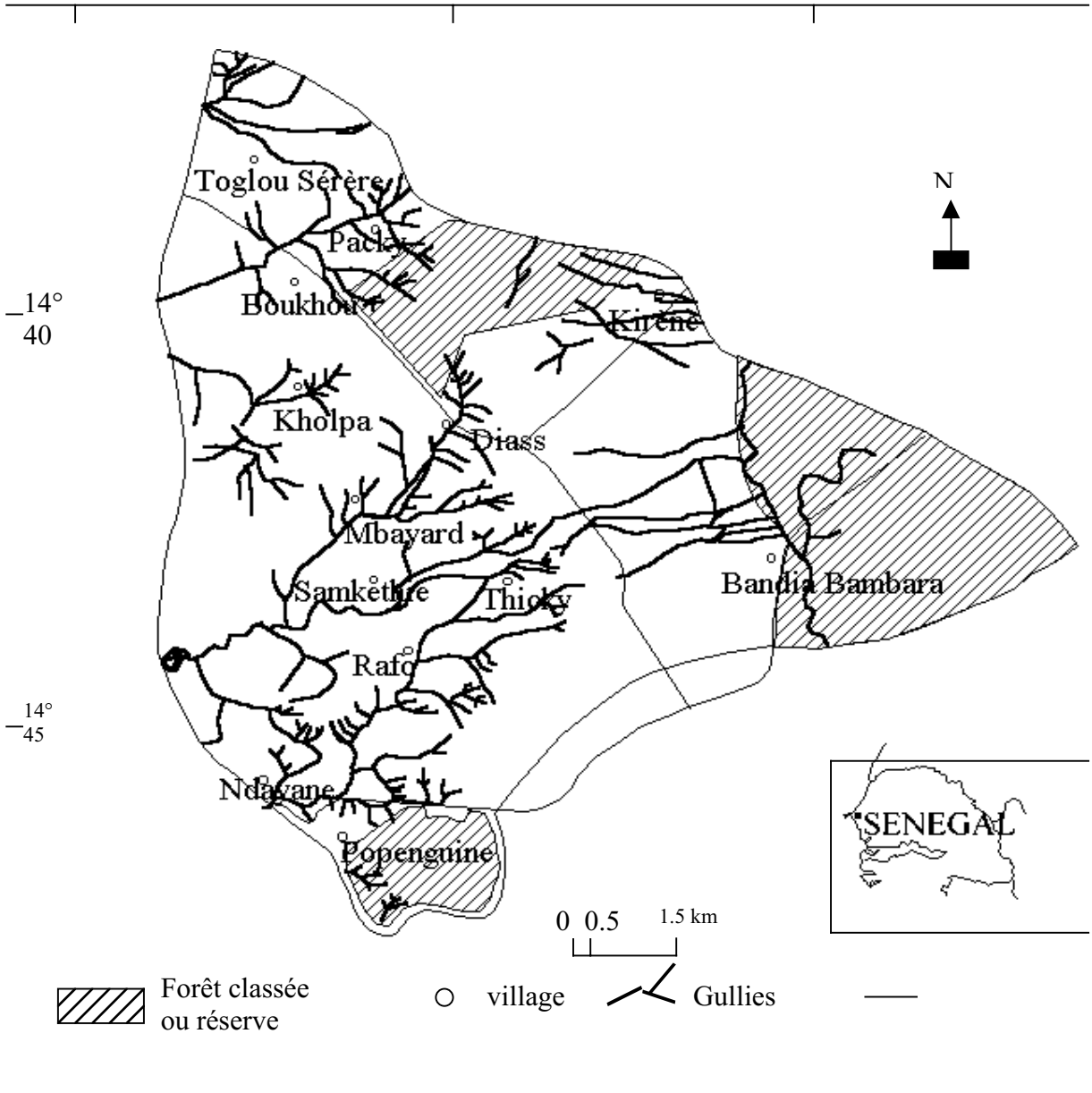

Fig. 2 Situation de la zone d´étude

Les sols sont répartis en quatre groupes selon les études de Maignien en 1959: dans les zones basses prédominent les sols ferrugineux tropicaux peu lessivés appelés 'joor' dans la terminologie locale. Ils sont caractérisés par leur texture sableuse et leur pauvreté en matière organique. Ils couvrent 23 % de la zone d´étude et portent les cultures d´ arachide et de mil. Au sommet des collines recouvertes parfois de blocs et de gravillons, l´on retrouve les sols minéraux bruts d´érosion sur plus de la moitié de la superficie totale. On ne leur prête aucun intérêt agricole. Dans les bas-fonds inondables se forment les sols hydromorphes, le plus souvent à pseudo-gley, très profonds et de texture fine. Ils représentent 14 % de la superficie totale de la Communauté Rurale. En bordure de mer, près de Ndayane, l'on retrouve des sols halomorphes de faible étendue et un peu plus loin sur le continent, les vertisols lithomorphes.

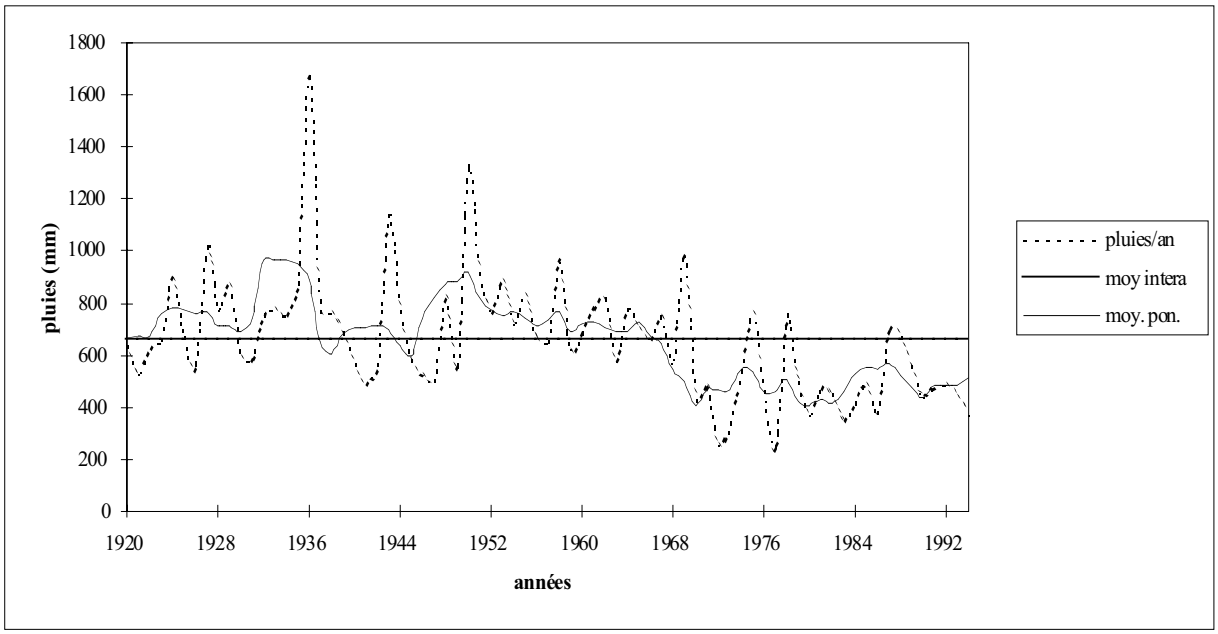

Fig. 3 Pluie moyenne, moyenne interannuelle (moy. Intera.) et moyenne mobile pondérée(moy. Pon.) à la station de Mbour (1920-1994)

La végétation naturelle est une savane arbustive qui résulte de la dégradation de la forêt originelle de type soudano-guinéen (SDSU, RSI, 1986). En fonction du relief, l'on distingue sur les buttes et collines du massif un peuplement de buissons épineux parfois dense et impénétrable à *Acacia ataxacantha*. Néanmoins, on compte dans la strate ligneuse, des mimosaceae (*Acacia seyal*), des capparidaceae (*Boscia senegalensis*) et notamment des combretaceae (*Combretum micranthum, Combretum glutinosum*) (Barambirwa, 1979).

Dans les zones basses et les dépressions, subsistent encore quelques individus d´espèces reliques tels *Borassus aethiopum,* aujourd'hui menacé de disparition mais aussi Ziziphus mauritiana, Sterculia serinera...Ce couvert végétal est durement affecté par la dégradation du climat mais aussi les actions anthropiques.

La population composée en majorité de l´éthnie saafen dont le massif de Diass est le berceau de la civilisation est passée de 13 445 en 1970 à 25 067 âmes en 1992. Elle vit essentiellement d´activités agricoles qui ont connu de grandes mutations depuis l´introduction de l´arboriculture dans les années 1960 dont le but est de pallier au déficit des ressources financières provenant de l´agriculture. Mais cela a aussi en même temps impliqué des changements notables sur le plan de l´organisation de l´espace passant ainsi d´un mode d´exploitation en Openfield au bocage.

La sévérité de la dégradation des sols lisible directement dans le paysage se traduit par l'existence de nombreux ravins et ravines – *xulup* dans la terminologie locale. Cependant la hiérarchisation du réseau n'est pas très nette. Il présente le plus souvent un caractère endoréique. Les principales rivières sont le Ndougoumou, le Ngaba et la Somone.

Le Ndougoumou draine toutes les eaux de ruissellement en provenance des reliefs de Diass et à travers la zone de Samkéthie. Il est fonctionnel dans sa zone aval jusque tard dans la saison sèche.

La Somone coule dans le sens nord-sud avant de se jeter dans l´océan au sud de la Communauté Rurale. Comme le Ndougoumou, elle n'est permanente que dans sa partie aval.

Le Ngaba quant à lui est alimenté par une multitude de petits bras descendant des collines voisines de Thicky et de Popenguine.

Ce réseau est caractérisé par son aspect peu hiérarchisé. Il se développe rapidement en raison de l'importance de l´érosion régressive (Thioubou, 1996). Les dégâts matériels et

parfois humains sont assez importants. Des haies à moitié emportées par les flots, des pans de maisons détruits témoignent du calvaire vécu par ces populations qui le plus souvent sont obligées de faire face seuls à la menace.

Modélisation du risque d´érosion naturelle à Diass

Quatre étapes sont identifiées : la détermination de L´érodabilité des sols, le calcul des pentes, la prise en compte de l ´érosivité des pluies et enfin la végétation.

La carte de L´érodabilité des sols

Le procédé le plus commun de la prise en considération de L´érodabilité est le calcul de l´indice K tel que stipulé dans l´équation universelle des pertes en terre de Wischmeier et Smith et modifié par Schwertmann et al. L´équation s´écrit de la forme suivante :

$$K = 2.77 \times 10^{-6} \times M^{1.14} \times (12 - OS) + 0.043 \times (A - 2) + 0.033 \times (4 - D) \qquad (1)$$

avec : K = indice d´érodabilité

M : (% teneur en limon et sable fin) * (% teneur en limon et sable)

OS : % en matières organiques (= 4 si OS > 4)

A : classe d´agrégat

D : classe de perméabilité

L'application de cette formule es t pour l'instant impossible à cause de l´absence d´analyses pédologiques détaillées.

Dans le cadre de ce travail, il est proposé une autre méthode simple permettant de faire un diagnostic rapide de la capacité de résistance des sols. La carte pédologique au 1/50.000ème établie par Maignien (1959) a été digitalisée et rastérisée. Cependant une légère modification a été apportée en vue de limiter le nombre de classes. Quant aux propriétés des sols, elles ont été déterminées sur la base des résultats publiés par le groupe SDSU/RSI/USAID/DAT (1986). Quatre paramètres, estimés déterminants ont été choisis :

i. La texture

La sensibilité à l´érosion est étroitement dépendante de la composition granulométrique (CTFT).Les sols sableux avec une faible stabilité structurale se révèlent moins résistants que les sols argileux par exemple qui sont caractérisés par une plus grande cohésion.

ii. La pierrosité

Les fragments grossiers absorbent l´ énergie cinétique des gouttes de pluie et réduisent ainsi le détachement des particules.

iii. La perméabilité

Un sol perméable est plus sujet à l´infiltration qu´au ruissellement et donc à l´erosion.

iv. La teneur en matières organiques

Les matières organiques ont la propriété d´accroître la stabilité des sols et augmentent leur capacité de résistance.

Pour chacun de ces paramètres, une comparaison qualitative est effectuée entre les divers types de sols. En reclassifiant la carte des sols, quatre cartes ont ainsi pu être extraites. Le module *Image Calculator* de IDRISI a permis de superposer celles-ci. Les valeurs obtenues varient entre 1, qui signifie une faible sensibilité à l´érosion et 5, valeur maximale traduisant des conditions pédologiques favorables à l´érosion.

Le calcul des pentes

Pour le calcul des pentes, les courbes de niveaux de la carte topographique au 1/50.000ème ont été digitalisées. Un modèle numérique de terrain avec une résolution de 90 m * 90 m fut généré. Les pentes ont été calculées en %. Les résultats montrent que dans 65 % de la zone d´étude les pentes ont une valeur inférieure à 5 %. Les valeurs maximales se situent autour de 30 %, sur la bordure ouest du massif de Thicky. Enfin cinq classes ont été définies comme suit (Tableau 3).

Tableau 3 Répartition des pentes dans la zone d´étude

Classe	Pente (%)	Surface (km_)	% de la surface totale
1	0 - 5	133	65
2	5 - 10	70	29
3	10 - 15	11	5
4	15 - 20	3	4.5
5	20 - 25	1	0.5

Détermination de l´indice d´érosivité

En l´absence de pluviographes installés, il demeure très difficile d´avoir une idée sur l´intensité des précipitations. En outre, la station équipée la plus proche est Dakar-yoff qui ne reflète point les conditions locales. Ainsi pour pallier à cet obstacle, la pluie maximale journalière a été prise en considération. L´analyse statistique de plusieurs stations de la zone de même que les données de la littérature ont permis de faire les observations suivantes qui justifient son choix.

D'abord, ce sont les événements pluvieux qui présentent les plus grandes intensités et les plus grosses quantités de pluie qui causent les dégâts les plus importants (Ferro et al., 1999).

De plus, ces événements s´observent le plus souvent au milieu ou à la fin de la saison des pluies c'est-à-dire au moment où les sols sont saturés, l´infiltration moindre et le ruissellement élevé. Nills et al. (1996) citent à ce propos les travaux de Temple qui a observé des taux de ruissellement 8 fois plus élevés en fin de saison des pluies qu´au début Cette valeur s´observe aussi pour l´essentiel au cours du mois le plus pluvieux, ce qui vient confirmer la deuxième hypothèse émise.

A la station pluviométrique de Diass, les données journalières de la période étalées sur les dix dernières années (1989-1998) sont disponibles. La valeur recherchée atteint 75 mm. Afin de déterminer la valeur correspondante à chaque situation au niveau local, des sous bassins ont été tracés et le coefficient d´abattement K calculé. Il permet de passer de la pluie ponctuelle d'une station donnée par la pluie moyenne d´un bassin versant voisin. La formule utilisée est celle modifiée par Vuillaume. Elle s´écrit comme suit :

$$K = 1 - (9 - 42.10^{-3} P + 152)\ 10^{-3} \log S \quad (2)$$

Avec P = pluie moyenne annuelle (mm)

S = Superficie du bassin versant (km^2)

La pluie reçue au niveau de chaque sous bassin est ainsi obtenue :

$$P_{max} = K * P_{maxd} \quad (3)$$

Avec P_{maxd} = pluie à la station de Diass = 75 mm

La dernière étape a concerné la reclassification de la carte des bassins et la détermination de quatre classes.

La végétation

Trois séries de photos aériennes ont été utilisées dans ce travail : 1954, 1978, 1989. Avec l´aide d´un stéréoscope, les diverses unités taxonomiques ont été identifiées : la forêt claire, les zones de reboisement, la savane arborée et la savane dégradée (comprenant aussi les jachères car les tons à cette échelle du 1/60.000éme ne permettent pas de les différencier. De toute façon, ces surfaces sont négligeables car cette pratique n'est pas courante dans la région) et les surfaces cultivées.

Après la géocodification avec la carte topographique comme base, ces données ont été vectorisées et rasterisées à une échelle de 1/50.000ème. Quatre classes ont été définies en fonction de l´appréciation du taux de couverture des sols. Les valeurs affectées varient entre 1 pour une couverture jugée relativement élevée et 4 qui désigne ici les surfaces cultivées. Les zones de reboisement ont été classées comme des savanes arborées et ont donc été notées 2. Les résultats obtenus montrent ainsi le rythme de dégradation à Diass au cours de ces 35 dernières années. On note simplement que malgré la protection sous forme de forêts classées et de réserves dont font l'objet les sommets de versant, le processus de dégradation ne s´en est pas moins poursuivi, surtout durant la période entre 1978 et 1989. Ces effets ne manqueront pas d'être visibles sur la carte du risque d´érosion.

Tableau 4 Répartition des diverses strates de végétation en 1954, 1978 et 1989

Année	forêt claire	savanne arborée	savanne dégradée	cultures
1954	42	31	0	27
1978	0	56	15	29
1989	0	20	47	33

Résultats et discussions

L´objectif poursuivi est la représentation spatio-temporelle de l'évolution de l´érosion sur la période 1954-1989. La méthode utilisée est celle du SIG. Les quatre facteurs choisis ont été

superposés par multiplication et un premier scénario développé. L´équation s´écrit comme suit :

$$REH = plufac \times solfac \times pfac \times vegfac \quad (4)$$

avec: REH: risque d´érosion hydrique

plufac: facteur pluviométrique

solfac: érodabilité des sols

pfac: facteur pente

vegfac: facteur végétation

Cependant ce modèle présente des insuffisances dans la mesure où à chaque paramètre d´entrée est affecté un coefficient égal à 1, qui traduit dans la réalité le caractère équilibré de l´impact de ces facteurs dans le processus d´érosion. Cela pose problème. Or, l´optimisation de la description de la réalité est nécessaire afin de ne pas biaiser les résultats définitifs. En outre, l´approche participative qui permet de faire intervenir le savoir paysan dans l´élaboration du modèle se justifie à plus d´un titre.

La méthode utilisée s´articule autour de trois points: l´affectation de valeurs aux paramètres respectifs en fonction de leur incidence réelle, le calcul des coefficients et la modélisation.

La première étape de l´affectation des valeurs aux facteurs a été réalisée directement sur le terrain. Un groupe composé de natifs de la région et d´un agronome a été formé et initié aux principes de la méthode. Elle consiste à construire une diagonale de comparaison des paramètres deux à deux avec des valeurs évoluant entre 1/9ème qui traduit une très faible influence par rapport au rôle joué dans l´occurence de l´érosion et 9 qui désigne une importance suprême. Grâce au module *WEIGHT* de IDRISI, ces valeurs ont été recherchées de façon automatique et rectifiées au fur et à mesure, jusqu'à ce que le meilleur résultat soit obtenu : il s'agit d'arriver à un rapport inférieur à 0.1.

Les coefficients suivants ont été en fonction de leur influence sur le cours de l´érosion attribués :

Pluie (plufac): 0.2307

Sol (solfac): 0.0678

Pente (pfac) : 0.1624

Végétation (vegfac) : 0.5390

Au vue de ces résultats, l'on se rend compte que dans la mentalité paysanne, le risque d´érosion dépend beaucoup moins des facteurs naturels que sont le sol, la pluie et la pente que de l'existence ou de l´absence de végétation qui joue ici un rôle catalyseur. En fait, ce qu'il faut voir au-delà, c'est tout le changement intervenu aussi bien au niveau climatique avec des tendances accentuées à la sécheresse qu´au niveau anthropique avec des méthodes de gestion de l´espace peu soucieuses de la durabilité des ressources.

L´équation du modèle enfin adopté s´intitule comme suit :

$$REH=(0.2307 \text{ X } plufac)+(0.5390 \text{ X } vegfac)+(0.1624 \text{ X } slofac)+(0.0678 \text{ X } solfac) \quad (5)$$

Les cartes générées sont présentées à la Fig. 5 ***Schéma d´utilisation de l´espace rural à Paki***. Elles montrent l'évolution du risque d´erosion à Diass entre 1954 et 1989. La portée des résultats a été discutée avec les paysans. Dans l'ensemble, le modèle restitue bien le degré d´affectation des terres par l´érosion hydrique. Sept classes (Fi) ont été retenues qui permettent de voir dans le détail comment le processus de dégradation s'est effectué au cours de ces dernières années.

D'une façon générale, on remarque que la destruction de la couverture végétale au niveau des massifs a joué un rôle très important. L´extension du risque d´érosion s'est d'abord faite autour des régions agricoles plus sensibles avant de s´étendre vers les massifs dont la dénudation s´est accélérée durant la deuxième période. Cela s'explique par l'effet accumulé et menaçant de la sécheresse et par l´exploitation abusive. Le Tableau 5 montre ainsi que 31 % de la superficie sont enregistrés en classe 2 en 1954 contre seulement 9 % en 1989 alors que pendant ce temps la classe 4 passait de 6 à 30 %. En général seules les zones bien protégées n'ont pas connu de grandes évolutions. C'est le cas de la forêt classée de Bandia .

En outre, les zones cultivées ont toujours été marquées par un risque élevé dû à l'effet conjugué de la nature des sols joor qui sont meubles et très sensibles à la dégradation mais aussi des conditions d´exploitation. Elles sont représentées dans la classe 6.

Tableau 5 Chronologie de l'évolution du risque d´érosion hydrique à Diass

1		Classe	2		3		4		5		6		7	
Km^2	%	Surface	km^2	%	km^2	%	km^2	%	km^2	%	km^2	%	km^2	%
41	19	1954	67	31	38	17	13	6	9	4	37	17	12	6
1	1	1978	52	24	43	20	42	19	25	11	41	19	13	6
1	1	1989	20	9	21	10	66	30	43	20	50	23	16	7

Il est par ailleurs prévu d´améliorer les performances du modèle grâce à l´augmentation de la fiabilité des données d´entrée. Ainsi l´interprétation d´images satellitaires prises à une date récente permettra d'obtenir plus de détails. Il en est aussi du calcul de l´érodibilité tenant compte des résultats d´analyse au laboratoire des échantillons de sols.

Le modèle socio-économique

Il est en cours de conception. Comme le modèle physique, il doit permettre de donner un aperçu sur l'évolution du risque d´érosion vu sous l´angle socio-économique. Quatre paramètres d´entrée ont été ciblés :

Le facteur démographique

L'aspect population constitue dans les pays sahéliens le facteur moteur du changement des paysages. Son rôle peut s´apprecier à un triple point de vue : du point de vue de l'évolution démographique, de la dynamique temporelle et des densités.

Du point de vue de l'évolution démographique, le calcul du taux d´accroissement naturel moyen permet d´apprécier le rythme de la croissance. A Diass la population est passée de 13445 habitants en 1970 à 21117 habitants en 1988. En fait, ce chiffre n'est pas très élevé comparé aux régions agricoles du Nord du Sénégal qui accueillent un nombre élevé de migrants. A Diass, les contraintes environnementales obligent plutôt les jeunes à migrer vers les villes proches comme Dakar ou Rufisque afin de trouver un travail rémunérateur. Une enquête détaillée aurait certainement permis de situer ce problème de façon plus exacte. Par ailleurs, d´un village à l'autre, des disparités énormes apparaissent : Kirène qui en son temps a abrité le projet maraîcher de BUD SENEGAL puis de SENPRIM ou Ndayane situé sur la façade atlantique et donc propice à la pêche attirent plus de migrants que Mbouroukh Bambara par exemple qui présente un solde migratoire négatif.

La dynamique spatiale de l´occupation est parfois aussi révélatrice des potentialités et aussi des contraintes en matière de disponibilité des ressources à l´echelle du terroir. Par exemple, les dégâts occasionnés par l'eau peuvent contribuer au déplacement des populations jadis installées au bas des collines vers les régions avales. De même l´étroitesse du milieu peut expliquer que des espaces peu viables parce que non aménagés (bas fonds, sommets de collines) soient utilisés comme habitat.

La densité de population est aussi un indicateur du niveau de pression sur l´espace et donc sur les ressources naturelles. Il va de soi qu'un surpeuplement entraînera un déséquilibre marqué entre la disponibilité de celles-ci et les besoins de la consommation et se soldera par une crise écologique. A Diass, la densité est en moyenne de 99 habitants au km_ (recensement de 1988). Cependant, à y voir de près, on s´aperçoit que l´espace n'est occupé que partiellement à cause des contraintes topomorphologiques. Donc ce chiffre rend très mal compte de la pression sur le milieu. Ceci justifie le recours à la densité utile, qui est le rapport entre population et surface cultivée. Ainsi on en arrive à des chiffres de 309 habitants au km_. Cette procédure sera utilisée à l´echelle des sous-bassins afin de faire ressortir l´essentiel des disparités spatiales. La cartographie sur les trois périodes permettra de suivre l'évolution de l´impact démographique réel. Quatre classes vont être déterminées, qui vont traduire les divers niveaux du risque de dégradation.

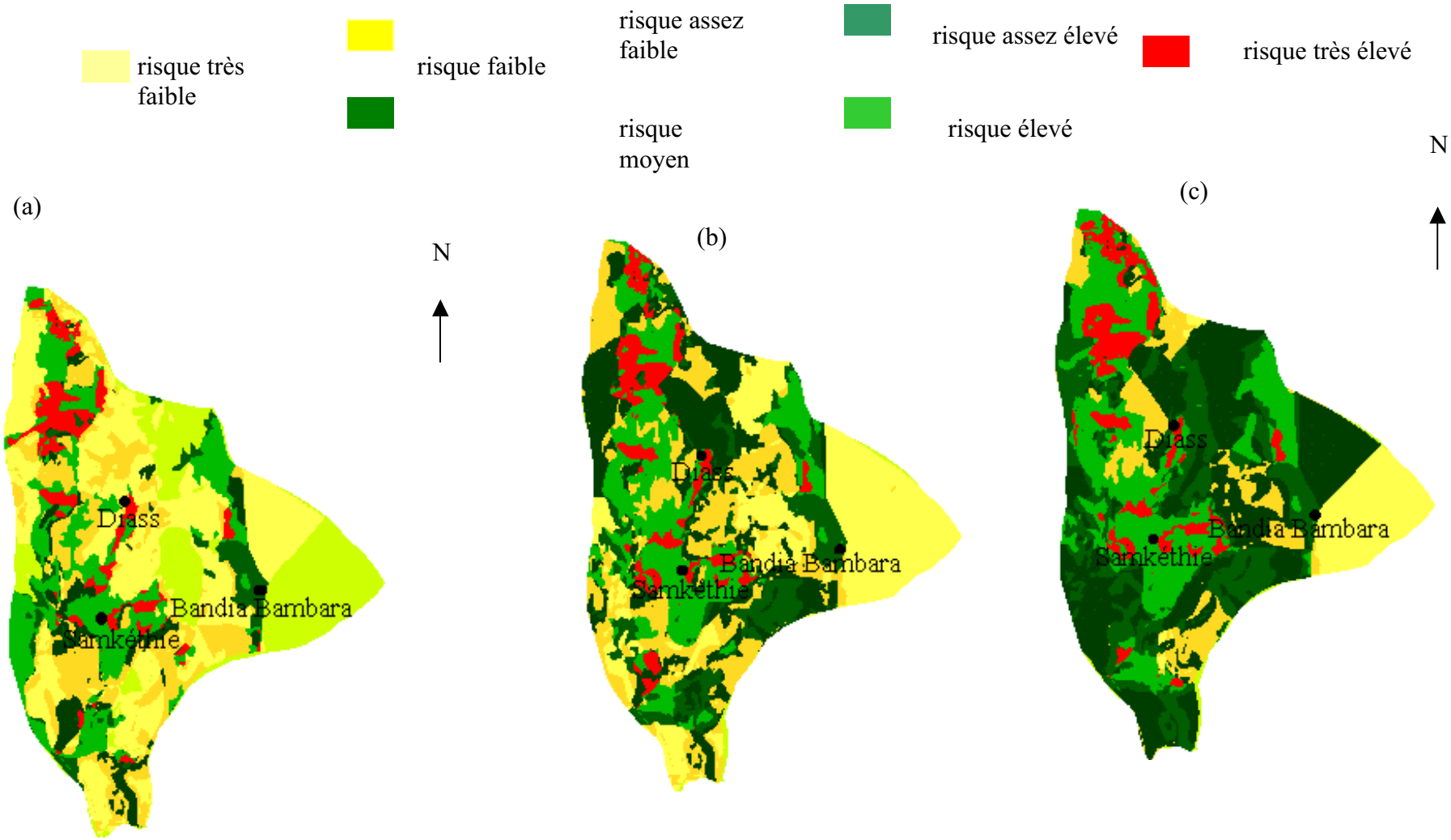

Fig. 4 Modélisation de l'évolution du risque d'érosion hydrique à Diass en 1954 (a), 1978 (b) et 1989 (c)

Structure de l´espace

L´analyse de l´organisation d´un espace donné fournit beaucoup de renseignements. Elément essentiel de la civilisation locale, elle constitue un moyen d´adaptation aux conditions naturelles du milieu de vie et établit donc un lien fondamental entre l'Homme et son environnement, si bien que les changements qui interviennent à un niveau sont ressentis à un autre.

La société saafen traditionnelle utilisait un schéma d´organisation de l´espace tel que les champs de culture formaient une auréole autour des habitations. Cet espace ouvert était semé de mil, de sorgho, d´arachide (*Arachis hypogea*) et de niébé (*Vigna unguiculata*) destinés à l´autoconsommation. L´élevage pratiqué consistait à amener les animaux en brousse pendant la saison des pluies et à les laisser paître dans les champs en saison sèche pour les fumer. Tant que les conditions démographiques étaient favorables et la production céréalière maintenue à un niveau acceptable, ce schéma pouvait subsister. Mais au milieu des années 1960 qui ont marqué le point de début de la sécheresse, l'on assista à l´introduction des cultures fruitières devant procurer des revenus monétaires devenues nécessaires pour l´achat de céréales en période de soudure. Ainsi le choix fut porté sur le manguier (*Manguifera indica*) dont c'est la zone de prédilection. Cependant, devant le manque d´espaces cultivables, la stratégie nouvelle fut l´introduction de cultures mixtes : arboriculture et céréaliculture. Les espaces entre les arbres accueillent le mil ou le sorgho. Ce type d´organisation existe encore mais on assiste aussi à l´érection de plusieurs vergers à but essentiellement commercial.

La Figure 5 montre l'évolution de l´organisation de l´espace du village de Packy. : les quartiers traditionnels (Filène, Mboynak, Pouranké) ont conservé la structure d´antan alors que dans les nouveaux quartiers domine la nouvelle forme. L'importance de ces mutations dans le cadre de l´analyse de l´érosion anthropique n'est pas à négliger. En effet, le système de verger qui met en avant la propriété individuelle nie l'existence d´Openfield qui est l´émanation de la propriété collective. En outre, l´extension de l´agriculture colonisatrice ne laisse aucune place aux pâturages qui sont désormais inexistants. A partir de ce moment, la clôture des champs est de mise afin de les protéger de la divagation du bétail. Or, cela a pour inconvénient de canaliser les voies d'eau qui coïncident justement avec les pistes et sentiers. Ces derniers à la fois pistes de production et voies piétonnières sont aussi fréquentés en plus par le bétail dont les parcours sont supprimés faute d´espace, ce qui ameublit davantage les terrains et les rendent encore plus sensibles à l´érosion.

Cet aspect sera modélisé grâce à la cartographie de la structure spatiale : l´interprétation de photos aériennes de 1954 agrandies au 1/10.000ème permettra de dessiner la structure spatiale. Une situation plus récente (1974) est obtenue à partir d'une carte topographique au 1/10.000ème qui restitue le détail du parcellaire de même que nos récentes observations sur le terrain. De la comparaison entre ces deux situations sera déduite l'évolution de la structure et son impact sur l'évolution de l´érosion (par exemple superposition avec la topographie, le réseau hydrographique...).

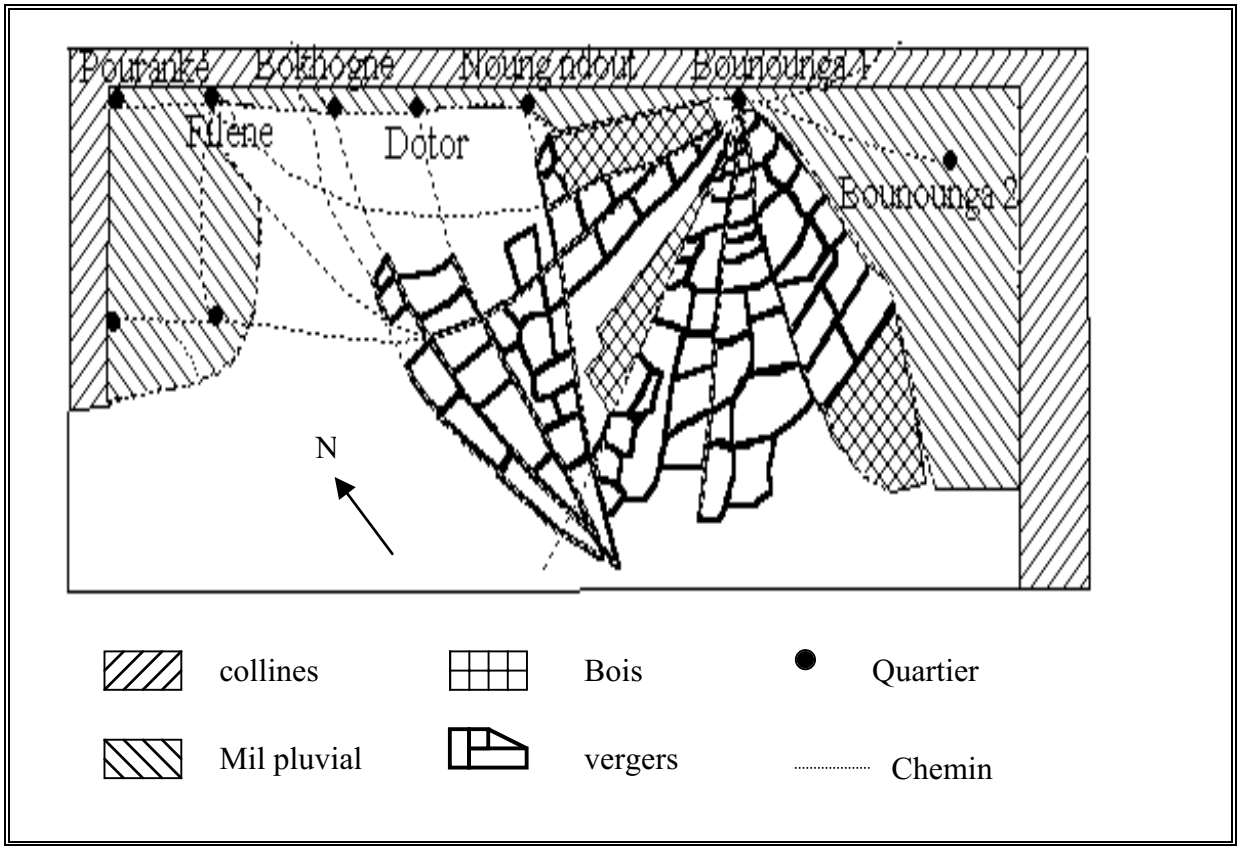

Fig. 5 Schéma d´utilisation de l´espace rural à Paki

Le foncier

Les relations entre foncier et dégradation des sols sont très étroites dans la mesure où le système de propriété influence l´utilisation de techniques durables de conservation du sol (Steiner, 1996) car il est vrai que les « paysans du dimanche » motivés uniquement par l´appât du gain sont moins portés en général vers les méthodes de conservation que les propriétaires natifs du terroir que des liens affectifs unissent à la terre.

En milieu *saafen*, la terre d´un point de vue traditionnel appartenait au « maître du feu », le lamane dans la terminologie locale à qui revenait le droit d´attribuer des terres. Par ailleurs, il était possible d´en hériter selon le droit successoral musulman ou traditionnel.

L´adaptation de la loi 64-46 sur le domaine national qui fait de l´Etat le propriétaire de toutes les terres vient basculer cette donne. Désormais, la terre appartient à celui qui la met en valeur et le conseil rural est chargé des affectations en matière foncière. Les nombreuses spéculations font que beaucoup de terres tombent entre les mains d´ « étrangers », venant ainsi aggraver la situation foncière.

L´analyse de la répartition du type de propriété mais aussi du comportement des uns et des autres en matière de conservation des sols et en général des ressources naturelles permettra de voir dans quel sens le foncier peut favoriser ou contraindre la dégradation des sols et quelles sont les solutions foncières à mettre en œuvre pour y remédier.

La dynamique de lutte contre l´érosion

L'action anthropique sur le paysage ne peut se résumer simplement à la dégradation du milieu. Parallèlement de nombreuses actions de lutte sont entreprises au niveau local ou régional pour au moins limiter les pertes et dégâts dus á l´érosion. Les moyens déployés sont diversifiés et englobent aussi bien des actions spontanées comme la pose de radiers en sable en saison des pluies afin de bloquer la progression des xulup ou alors ce sont de véritables organisations structurées qui sont créées dans l´objectif de défense du terroir. Dans ce cadre, le rôle pionnier des femmes est à souligner. Si dans certains villages ce type de mouvement fonctionne bien et aboutit à des résultats probants, dans d´autres par contre, des blocages de diverses natures sont enregistrés et ceci entraîne l´éclosion d'action individualisées qui ont une faible portée par rapport à l´objectif visé.

La prise en considération de ce paramètre dans la modélisation de l´érosion anthropique qui compte plutôt comme une contrainte à l´érosion, permettra de rétablir la balance entre le poids des actions en faveur et contre la dégradation des sols.

Le modèle utilise aussi un SIG. La superposition des cartes dressées selon un schéma logique permettra de définir l'importance du facteur social dans le processus d´érosion hydrique.

Conclusion

L´évaluation du risque d´érosion hydrique dans cette zone rurale du Sénégal a été abordée à deux points de vue : physique mais aussi socio-économique. Le modèle physique, avec comme paramètres d´entrée des données climatiques, topographiques, bioclimatiques et pédologiques a permis de situer l´évolution chronologique du phénomène calée sur trois dates repères: 1954 choisie dans la première phase considérée comme pluvieuse si l´on se refère à l´analyse climatique de la station de Mbour ; 1978 choisie comme faisant partie de la période après sécheresse avec toutes les conséquences sur la réduction du couvert végétal. Enfin 1989 qui illustre la sévérité de la dégradation des ressources naturelles à tous les points de vue.

Les résultats permettent de voir quelles sont les zones les plus affectées par l´érosion. Ce sont en général celles surexploitées par la mise en culture et qui servent en même temps d´habitat, ce qui aggrave la concentration des écoulements dans les espaces libres devenus rares ou le long des voies de communication.

Quant au modèle socio-économique, il tient en compte des facteurs liés à la densité de population (qui exprime le niveau de surexploitation des ressources), la structure de l´espace, le foncier et la dynamique collective de lutte contre l´érosion hydrique. En cours de conception, il permettra d´aborder tous les aspects socio-économiques qui justifient l´accélération du processus de dégradation. Une enquête déjà réalisée permettra de rassembler les données qui vont servir de paramètres d´entrée.

D´une facon générale, l´obstacle majeur à la modélisation réside dans le manque notoire de données fiables dans cette région qui n´a fait l´objet d´aucune étude récente allant dans le sens d´actualiser et de compléter les informations disponibles. Ceci contribuerait grandement à l´amélioration de la qualités des résultats.

Remerciements Les auteurs remercient particulièrement Monsieur Honoré Dacosta dont les observations et les remarques ont permis la réalisation de cet article.

Liste des abbréviations

CSE : centre de suivi écologique

DAT : direction de l´aménagement du territoire

IGN : institut géographique national

JICA : japan international cooperation agency

MET : ministère de l´équipement et des transports terrestres du Sénégal

ORSTOM : office français pour le développement en coopération

RSI : remote sensing institute

SDSU : south Dakota state university

USAID: agency for international development

Bibliographie

BLASCHKE, T. (1997) 'Landschaftanalyse-und bewertung mit GIS. Methodische Untersuchungen zur Ökosystemforschung und Naturschutz am Beispiel der bayerischen Salzachauen. ' Deutsche Akademie für Landeskunde, Trier Band 243, 320 S.

CTFT (Centre Technique Forestier tropical) Conservation des sols au sud du Sahara." 2ème ed., *collection techniques rurales en Afrique*, 296 p.

EASTMAN, J. R. (1992) *IDRISI Version 2 user´s guide*. Clark University USA.

ESTEVES, M. et A. THIOUBOU (1996) *Etude des causes de l´érosion hydrique sur le territoire de la Communauté Rurale de Diass*. Rapport final d´étude Communauté Rurale de Diass, 23 p. et annexes, multigr.

FAO (1986) *La conservation et l'aménagement des sols dans les pays en développement*. bulletin pédologique de la FAO n° 33, Rome.

FERRO, V. et P. PORTO (1999) 'A comparative study of rainfall erosivity estimation for southern Italy and southeastern Australia.' Hydr. Sc. J. Vol. 44., N° 1, pp. 3-24.

HERWEG, H. et M.W. OSTROWSKI (1997) *The influence of errors on erosion process analysis*. Uni. Berne, 24 p.

MAIGNIEN, R. (1959) *Les sols de la Presqu' île du Cap-Vert*. ORSTOM, 163p.

MAIGNIEN, R. (1959) *Presqu'île du Cap-Vert" Carte pédologique 1/50.000e, feuille Sud-Est*.

MARTIN, A. (1970) *Les nappes de la Presqu'île du Cap-Vert.' Leur utilisation pour l'alimentation en eau de DakarBRGM*, 55 p.

NAHON, D. et D. DEMOULIN (1971) *Contribution à l'étude des formations cuirassées du Sénégal Occidental (pétrographie, morphologie, et stratigraphie relative)* BRGM, 1971.

NILLS, D.; U. SCHWERTMANN; U. SABEL-KOSCHELLA; M. BERNHARD et J. BREUER (1996) *Soil erosion by water in Africa. principles, prediction and protection*. Schriftenreihe der GTZ, No 257. GTZ TZ-Verlag, 292 S.

RIOU, G. (1990) 'L'eau et les sols dans les geosystèmes tropicaux.' Paris, ed. Masson, collection Géographie, 221 p.

RODIER, J., et C. AUVRAY (1965) *Estimation des débits de crues décennales pour des bassins de superficie inférieure à 200 km_ en Afrique Occidentale* ORSTOM, Juillet 1965, 46 p.

RODIER, J. et P. RIBSTEIN (1988) *Estimation des débits de crues décennales pour les petits bassins versants du Sahel couvrant de 1 à 10km_*, ORSTOM, 133p.

ROOSE, E. (1977) *Erosion et ruissellement en Afrique de l´Ouest. Vingt années de mesure en petites parcelles experimentales*. Paris, Travaux et documents de l´ORSTOM, 108 S.

SCHRAMM, M. (1994) *Ein Erosionsmodell mit räulich und zeitlich veränderlicher Rillenmorphologie*. Dissert. Inst. für Wasserbau und Kulturtechnik, Uni. Karlsruhe, 196 S.

STEINER, K.J. (1996) ‘Causes de la dégradation des sols et approches pour la promotion d´une utilisation durable des sols dans le cadre de la coopération au développement.’ projet pilote ‘gestion durable des sols.’ Margraf Verlag, 97 S. + Ann.

TAUER, W. et G. HUMBORG (1993) *Irrigation par ruissellement au Sahel. Télédétection et systèmes d´informations géographiques pour déterminer des sites potentiels*. CTA, verlag josef margraf 199 p.

THIOUBOU, A. (1996) *Etude des conditions environnementales de production et de transfert des écoulements de surface dans la Communauté Rurale de Diass*. Mém. DEA Uni. Dakar, 56S.

USAID / DAT / RSI (1986) *Cartographie et télédétection des ressources de la république du Sénégal.’ Étude de la géologie, de l’ hydrologie, des sols, de la végétation et des potentiels d’utilisation des sols*, 653 p.

USDA (1997) *Water Erosion Prediction Project Model Version 98.4*. NSERL, USDA-ARS, West Lafayette, Indiana.

WERNER, M.V. (1995) *GIS-orientierte Methoden der digitalen Reliefanalyse zur Modellierung von Bodenerosion in kleinen Einzugsgebieten*. Dissertation an der Freien Universität Berlin, 107 S. + anh.

Trends in soil erosion and sediment yield in the alpine basin of the Austrian Danube

E. Klaghofer[1], K. Hintersteiner[1], and W. Summer[2]
[1]Federal Institute for Land and Water Management Research, A-3252 Petzenkirchen, Austria
[2]Chartered Engineering Consultant for Hydraulic Engineering and Water Management, Brennleitenstrasse 59-61/3, A-2202 Hagenbrunn, Austria

Introduction

The Austrian part of the drainage basin of the Danube with its strong alpine characteristics has a size of approx. 75000 km^2. As a geological young mountain system the Alps still represent an active source of various types of natural sediments, e.g. landslides of all different sizes during storm events. However, intensifying human activities (the development of alpine tourism and new settlements requiring flood protection schemes and often causing deforestation, agriculture in (sub) alpine regions etc.) are disturbing the fragile status of the natural sedimentological balance of the Alps.

Trend analyses show that agriculture represents the cause for the major negative impact of soil erosion in the (sub) alpine region (Summer and Klaghofer, 1989; Klaghofer and Summer, 1990; Klaghofer and Hintersteiner, 1993; Klaghofer et al., 1994). The expansion of farm land into hilly/mountainous areas with steep slopes and changes in land use as well as in land management techniques, often enforced on the farmers by economic pressure, significantly increased the soil erosion rates as well as the sediment yields from the different subcatchment within the Danube's drainage basin within the last 40 years. These impacts on the sedimentological behaviour of the Austrian Danube have been recently observed and reported (Radler et al., 1993; Summer et al., 1994a, b; Summer and Zhang, 1994).

This is the first study that quantitatively estimates the changes of agricultural rates of soil erosion as well as sediment yields within the overall Austrian drainage basin of the Danube and three relevant tributaries (Figure 1). Based on the Universal Soil Erosion Equation (USLE) average soil erosion rates have been estimated (Wischmeier and Smith, 1962). By the application of specifically adapted Sediment Delivery Ratios (SDR) for alpine areas (Vanoni, 1975; Klaghofer et al., 1992) the sediment yields for the major subcatchments of the Inn-, Enns- and Traun-river watershed have then been calculated. To carry out this study, land use information for the years 1950 to 1990 (Austrian Statistical Central Office, 1950; 1960; 1970;

1979; 1990) presented an important source of data, besides topographic information on slope characteristics, which could be gained from the digital elevation model (DEM) of Austria. Its grid size ranges between 30x30 m and 50x50 m.

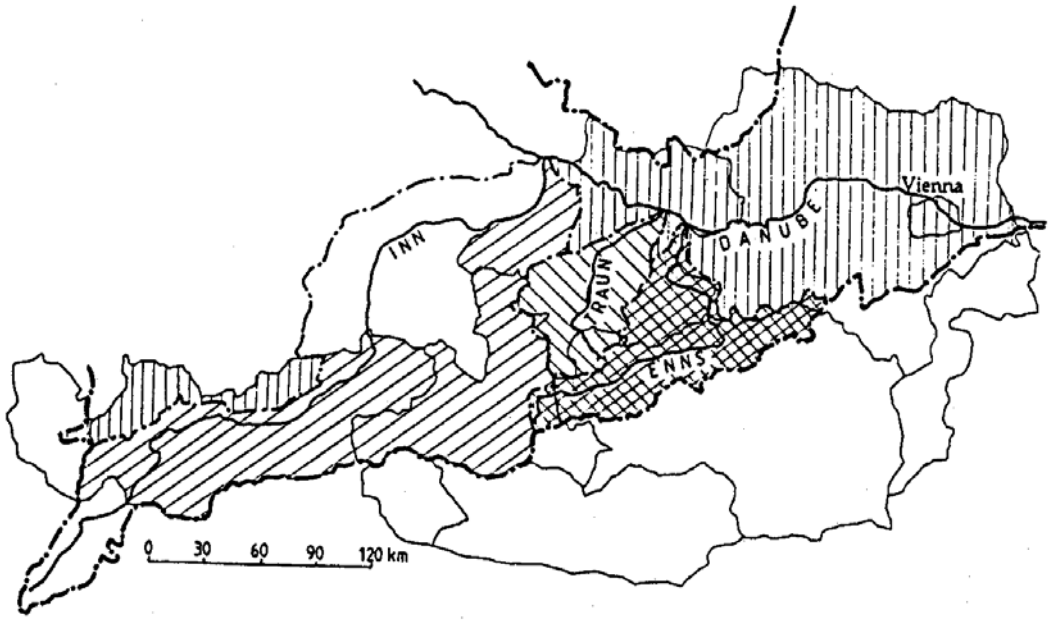

Fig. 1 Map of the overall Austrian Danube basin showing the three chosen watersheds of the Inn-, Enns- and Traun-river

The Inn-river watershed

The total watershed area of the Inn-river in Austria is around 1,7mil ha. 43% of this is used in agriculture, 35% in forestry and 22% is unproductive area. The size of the overall agricultural area hardly changed from the year 1950 to 1990, whereas its portion of farm land was reduced while grass land increased. A crop analysis shows that the part of the maize planted area was 2% in 1950 and 25% in 1990. The quantitative changes of the other erosion relevant crops such as beet, potatoes and spring corn have hardly any impact on the sediment loads. Assuming a rainfall erosion index R of 100 kJ.mm/m^2/h and a soil erodibility index K of 0,5 the estimates of the erosion rates were carried out by the USLE. Under the common Austrian land management practice it can be further assumed that 75% of the corn and maize as well as 25% of the potatoes and beet are planted in the sloped area. The average slope gradient S is estimated at 10%, the typical slope length L is of 50 m. Therefore a slope factor LS of 1,76 is gained from this. The crop practice factor C for maize is 0,33, for potatoes 0,24, for beet 0,21 and for spring corn 0,06.

In the year 1950 around 460000 t of soil was eroded. The average subcatchment size for each relevant tributary to the Inn-river is ca. 13 km^2. This gives a sediment delivery coefficient (SDR) of 0,2. Hence, a sediment yield of 92000 t/year can be calculated. Under the

same previous conditions in 1990 a sediment yield of 128000 t is reached in changed crop proportions of the Inn-river watershed.

The Enns-river watershed

The Enns-river watershed covers approx. 0,90mil ha. In the year 1950 37% was used in agriculture, 46% in forestry and 17% consisted of unproductive area. The agricultural land decreased up to the year 1990 by ca. 5% while the used forestry increased by the same amount. In the year 1950 there was no maize planted. Until 1990 the amount of planted maize areas increased up to 23% of the agricultural area. The amount of potatoes, beet and spring corn lowered itself slightly up to 1990. The calculation of the soil erosion was carried out under very similar climatic, topographic and morphologic assumptions as in the watershed of the Inn-river. The erosion yield estimated by the USLE totalled at 227000 t for 1950. With a SDR coefficient of 0,2 for appropriate subcatchments of a size of ca. 15km^2 a sediment inflow into the Enns-river of 45400 t/year has been calculated. In 1990, under a changed land use management, 407000 t of soil eroded, giving a sediment yield of 81400 t.

The Traun-river watershed

The complete watershed of the Traun-river has a size of ca. 0,5mil ha. In 1950 43% of this area was used by agriculture, 40% consisted of forests and the unproductive area had a proportion of 17%. While the size of the agro-land did not change significantly until 1990, the intensive farming increased dramatically in the same way as the grassland was reduced. The quantitative crop analysis shows clearly within this forty year period the expansion of maize areas from non-existence in 1950 to 25% in 1990. Therefore the areas of potatoes, beet and spring corn had to decrease. Under comparative catchment conditions of the Traun-river to the other watersheds, the soil loss computation resulted in an amount of approx. 326000 t for the year 1950. This gives under an assumption of an SDR coefficient of 0,2 (the sizes of the relevant subcatchments range between 10 to 15 km^2) an input into the river of ca. 65000 t/year. Under the different land use and/or crop situation in 1990 the similar calculation for this year gives a soil loss rate of 642000 t and ca. 128000 t of sediment was delivered into the river.

The remaining basin of the Austrian Danube

The remaining size of the overall Austrian basin of the Danube (excluding the Enns-, Traun- and Inn-river watershed) is about 4,4mil ha. In 1950 the agricultural use of this area was 52% and 34% was forestry. The unproductive area had a size of 14%. Up to 1990 the agricultural area lowered to 49% whereas the forest areas rose to 39%. The portion with maize production increased in the Danube basin between 1950 and 1990 by 12% from 4% to 16%. An increase of wintercorn was observed while potatoes and beet areas had decreased.

In the remaining Danube regions an average R index of 70 was assumed. These locations basically refer to several catchments characterised by flat areas, basins and plateaux with levelled topography of none or only a slight gradient. Overlaying a crop map onto a topographic map showed that for these regions only 50% of corn and maize production and only 25% of potato and beet farming was situated on hillslopes. A reasonable assumption for an average slope length L of 75 m could be found and a mean slope gradient S of 10% for the hilly sections of the area was evaluated. Hence a LS factor of 2,15 was found and the value of 0,5 was assumed for the K factor. Under the assumption of the just mentioned crop portion and the areal expansion as well as the average climatic and geomorphologic conditions an annual rate of soil loss of 1969000 t was estimated. Applying again a reasonable SDR coefficient of 0,2 gives a sediment yield of ca. 394000 t for the year 1950. Having considered the land use changes up to 1990, the soil erosion rate is estimated at 2209000 t/year and the sediment yield at ca. 442000 t/year.

Sediment impact of the German basin on the Austrian Danube

The sediment dynamics of the Austrian Danube is not only influenced by the northern alpine regions of the Austrian Danube basin, but also by the intensively used agricultural areas of the catchments in southern Germany with partly subalpine characteristics. The area of potential soil erosion has a size of about 2,1mil ha. With reference to the annual soil erosion rate of 17,1mil t/year (Auerswald and Schmidt, 1986) a sediment input into the German Danube of around 3,4mil t/year can be estimated, again under the assumption of a plausible SDR coefficient of 0,2. It is thus evident that the German sediment yield is much higher in comparison to the input from the Austrian basin. This can be explained by the following two factors:

1. Larger portions of intensively used agriculture areas exist in the German catchments in comparison to that in the Austrian ones;
2. Soil erosion rates are higher in Germany (8,1 t/ha/year) than in Austria (3,0 t/ha/year) due to the intensity of different land use practices in farming between these two countries.

However, this only available German data set represents a status-quo situation from the eighties and is not eligible to show a trend over a certain period of time.

Discussion

From 1950 to 1990 the changes within each of the major subcatchments of the Austrian Danube basin showed regionally a highly variable increase of the sediment dynamics (erosion rate as well as sediment yield). In the Inn-river watershed an increase from 100% to ca. 140% was estimated, 100% to ca. 180% in the Enns-river watershed and an almost doubling of the sediment dynamics in the Traun-river watershed. The remaining part of the Austrian basin showed an increase of ca. 12%. Hence, for the entire Austrian basin (including the three listed watersheds plus the remaining part of the total basin) an average increase of 32% could be derived for the forty-year period.

The impacts in the eastern parts of the Danube basin were more dramatic than in the alpine locations of western Austria. Three plausible reasons can be given as an explanation for this negative development in the sediment dynamics:

1. Intensified agricultural activities in the lower alpine areas of eastern Austria in comparison to western Austria with its alpine characteristics. Intensive agriculture is practised and extended in the subalpine areas of eastern Austria. Forestry and grassland with stock-farming is the tradition, hence, the dominating form of land use in western Austria. Spatial restriction of the availability of suitable farm land for intensive agriculture due to extreme topographic, climatic, etc. conditions is limits the increase in soil erosion and sediment yield in this region.
2. The increase of the economically beneficial maize production areas in the Danube basin from 4% in 1950 to 16% in 1990 (Figures 2 and 3)
3. The new maize production areas in the subalpine regions were often set up on high slope gradients without considering contour farming or other appropriate soil erosion strategies. The young maize plants in particular do not cover the soil properly during the spring rainfall season in the Alps, which is characterised by high precipitation intensities caused by severe storm systems of small areal extension.

Although the changes in land use, management practices and areal expansion alone can't explain all of the recent developments in the sediment dynamics of the Danube, they represent a strong indication.

It also should be mentioned that the applied calculation procedures for soil loss rates and the sediment yield only provide a very rough technique. But the gained estimates coincide with the monitored long-term sediment dynamics in the listed rivers. Nevertheless, the results of this study can't explain the sediment dynamics of single storm events with relevant floods.

However, for the first time the outlined results not only focus on the dramatic development in parts of the Alps on a large-scale as well as from an on-site point of view, they also indicate the location and the source of the problem. In addition, Klaghofer and Hintersteiner (1993) represented the first available data analysis indicating the goal for future research activities in soil erosion control in the Alps. For these purposes only physically-based approaches that have the capability to consider the surface transport in combination with the geomorphologic complexity of the alpine landscapes can give a proper picture of the non-point source erosion dynamics (Tayfur and Kavvas, 1994). Only such a tool will then allow the predictive development of efficient soil conservation strategies, considering urgently needed integrated watershed management for this region.

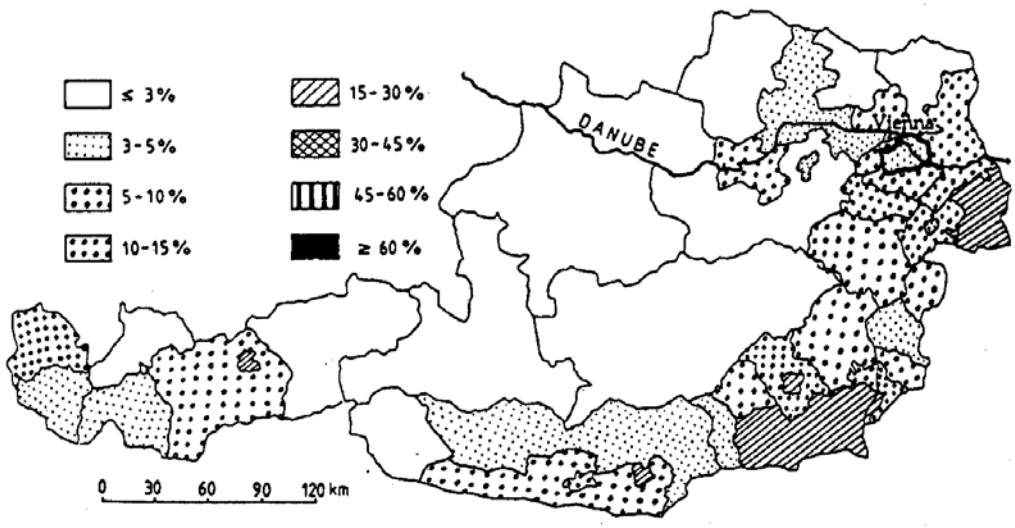

Fig 2 Soil loss rates from the Bavarian region of the Danube basin (Auerswald and Schmidt, 1986)

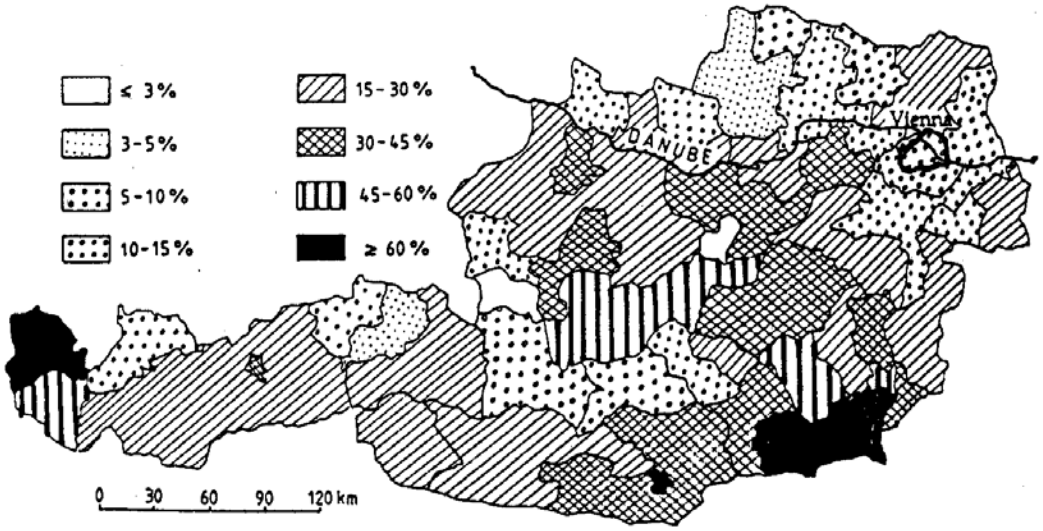

Fig. 3 The spatial expansion of maize farming in Austria between 1960 and 1986 (Klaghofer and Hintersteiner, 1993)

Concluding summary

For the first time this study quantifies the increase of the soil erosion and sediment yield within the overall alpine basin of the Austrian Danube as well as the catchments of three typical major tributary rivers. The research is based on topographic data as well as land use information for the period from 1950 to 1990, which was published by the Austrian Statistical Central Office. Due to the large-scale approach, the simplicity of the Universal Soil Loss Equation was used to calculate average soil erosion rates for typical erosion controlling parameter combinations found in the basin. By the application of an adapted sediment delivery ratio the sediment yields for the sub-catchments of the major watersheds have then been estimated. Recently monitored suspended sediment concentration in the draining rivers indicated an increasing trend of the sediment yield. The results not only confirmed this development, but can also partly be explained by the changes in land use as well as agricultural management practices, especially the spatial expansion of maize areas often onto the steep hillslopes of the subalpine regions.

Bibliography

AUERSWALD, K. and F. SCHMIDT (1986) *Atlas der Erosionsgefährdung in Bayern* (in German).' GLA-Fachberichte, Bayrisches Geologisches Landesamt, Munich.

AUSTRIAN STATISTICAL CENTRAL OFFICE (1950, 1960, 1970, 1979, 1990) *Ergebnisse der landwirtschaftlichen Statistik* (in German). Copy Rights: Rep. Austria, Vienna.

KLAGHOFER, E. and K. HINTERSTEINER (1993*) Abschätzung der Veränderung der potentiellen Erosion auf landwirtschftlich genutzten Flächen im Einzugsgebiet der Donau*. (in German) Österr. Donaukraftwerke AG, Vienna.

KLAGHOFER, E.; K. HINTERSTEINER and W. SUMMER (1994) 'Aspekte zum Sedimenteintrag in die österreichische Donau und ihrer Zubringer.' (in German with an English summary) In: *XVIIth conference of the Danube countries on hydrological forecasting and hydrological basis of water management*, 5-9 Sept., Budapest.

KLAGHOFER, E. and W. SUMMER (1990) 'Estimation of soil erosion from a lower Alpine catchment.' In: *Hydrology in mountainous regions II - artificial reservoirs - water and slopes*, (Proc. of 2 Lausanne Symp.), IAHS Publ. No. 194.

KLAGHOFER, E.; W. SUMMER and J.P. VILLENEUVE (1992) 'Some remarks on the determination of the Sediment Delivery Ratio.' In: *Erosion, debris flows and environment in mountain regions*, (Proc. of the Chengdu Symp.), IAHS Publ. No. 209.

RADLER, S.; W. SUMMER; T. STROBL and H. SCHEUERLEIN (1993) 'Der Sedimenthaushalt der österreichischen Donau.' (in German) Österr. Donaukraftwerke AG, Univ. Bodenkultur, Inst. Water Manag., Hydrol. and Hydraul., Vienna, and Techn. Univ. Munich, Inst. and Res. Lab. for Hydraul. Engr. and Water Manag., Obernach-Walchensee.

SUMMER, W. and E. KLAGHOFER (1989) 'Studie über das Erosions- und Schwebstoffgeschehen am Beispiel des Einzugsgebietes Ybbser Mühlbach.' (in German) Österr. Donaukraftwerke AG, Vienna.

SUMMER, W.; W. STRITZINGER and W. ZHANG (1994a) 'The impact of run-of-river hydropower plants on the temporal suspended sediment transport behaviour.' In: *Variability in stream erosion and sediment transport*, (Proc. of the Canberra Symp.), IAHS Publ. No. 224.

SUMMER, W. and W. ZHANG (1994) 'An impact analysis of hydraulical and hydrological changes on the suspended sediment trasport on the Austrian Danube.' In: *XVIIth conference of the Danube countries on hydrological forecasting and hydrological basis of water management*, 5-9 Sept., Budapest.

SUMMER, W.; W. ZHANG and W. STRITZINGER (1994b) 'Consequences of human impacts on the sediment transport process.' J. Rural Eng. and Development, vol. 35/6.

TAYFUR, G. and M.L. KAVVAS (1994) 'Spatially averaged conservation equations for interacting rill-interrill area overland flows.' J. Hydraul. Engr., ASCE, 120 (12).

VANONI, V.A. (1975) *Sedimentation engineering*. American Society of Civil Engineering, New York.

WISCHMEIER, W.H. and D.D. SMITH (1962) 'Soil loss estimation as a tool in soil and water management planning.' Int. Assoc. Scient. Hydrol. Pub. 59.

Suspended sediment structure: implications for sediment transport/yield modelling

I.G. Droppo[1,2], D.E. Walling[2] and E.D. Ongley[1]
[1]National Water Research Institute, Environment Canada, PO Box 5050, Burlington, Ontario, Canada, L7R 4A6 and [2]Department of Geography, University of Exeter, Exeter EX4 4RJ, UK

Introduction

The settling velocity of a particle is the primary mechanism (behaviour) that dictates the fate (i.e. transport) of sediment and associated contaminants. Settling velocity (measured, derived or assumed) is a key predictor within all sediment transport models. The knowledge that cohesive particles exist primarily as flocculated particles, and not as the traditionally viewed primary particle, complicates the quantification of particle (floc) settling velocity. As flocculated particles have significantly different hydrodynamic characteristics compared to absolute primary particles due to effectively different particle size, density, porosity and shape (Li and Ganczarczyk, 1987; Krishnappan, 1990; Ongley et al., 1992; Phillips and Walling, 1995; Nicholas and Walling, 1996; Droppo et al., 1997, 1998), the use of traditionally obtained absolute particle size distributions and Stokes' Law derived settling velocities to characterize sediment in sediment transport/yield models would result in erroneous results. It is likely that models based on these traditional derived settling velocities and absolute grain sizes would overestimate storm event sediment loadings to receiving water bodies, since finer particles will be transported further in a turbulent flow than larger flocculated particles (assuming no floc breakage).

The settling velocity/transport of sediment in aquatic systems is controlled to a degree by the structure of the sediment, which in turn is influenced by the conditions prevailing in the fluid medium (e.g. shear, organic content, mineralogy of the sediment). This paper evaluates, experimentally, the structural components of flocs (floc size, shape, density and porosity) and how these influence the settling velocity and transport of flocculated particles. By obtaining a better understanding of the settling/transport characteristics of flocs and how structure can influence this function, more accurate models of sediment transport/yield can be developed.

Sample sites

Samples collected from the fluvial environment were from two river systems; Sixteen-Mile Creek (sampled from February 1997 to May 1998) and Fourteen-Mile Creek (sampled on November 3, 1997). These sites are located in southern Ontario, Canada and have been studied previously. As this paper is concerned more specifically with the form and function of flocculated material and how this may influence transport, rather than the characterization of a particular site, detailed descriptions of the sites are not provided. The reader is referred to the following publications for their hydrological and geomorphological characteristics (16-Mile Creek - Droppo and Ongley, 1992; Droppo and Ongley, 1994; 14-Mile Creek - Ongley, 1974).

Lacustrine floc samples were collected from two locations; Hamilton Harbour, Lake Ontario, Canada (sampled from August 17 to August 24, 1995) and Lake Biwa, Japan (sampled on June 12, 1995). Suspended sediment floc samples were also collected in Hamilton Harbour. Full descriptions of these systems are given in the following publications (Hamilton Harbour - Amos and Droppo, 1996; Lake Biwa - Murphy et al., 1995; Okuda et al., 1995).

Methodology

Samples for floc size and morphological characterization were collected following the method of Droppo et al. (1997). This method allows for the non-destructive direct sampling and observation/measurement of flocculated material within a settling column (plankton chamber). The flocs are imaged (sized) down to a lower resolution of approximately 2 μm (10x objective) using a Zeiss Axiovert 100 microscope interfaced with an image analysis system (Northern Exposure™ - Empix Imaging, Inc.). Distributions of particle size (percent by number and volume) and two shape parameters are derived from the digitized data. The shape parameters used were to describe the shape of a floc and to assess the impact of floc shape on floc settling. These were; 1) Aspect ratio; which is simply the ratio of floc length to floc width. This ratio provides a good indication of floc elongation (i.e. the larger the ratio above one, the more elongated it is) and 2) Shape Factor (S_f) (Equation 1); which provides a measurement of the irregularity of the shape. It is defined in the equation below. (S_f = 1 for a perfect circle, successively lower factors represent a more convoluted floc, and close to 0 = approaching a line).

$$S_f = \frac{4\pi.Area}{Perimeter^2} \tag{1}$$

Settling experiments were performed following the methods of Droppo et al. (1997). A drop of sediment collected with a wide mouth pipette (3.74 mm) from a gently homogenized sample bottle was introduced into an insulated 2.5 L capacity settling column. As the flocs pass through the field of view of the microscope they are video taped on a SVHS VCR through a CCD camera interface. Using Northern Exposure™, the settling velocity was derived by digitally overlaying two video frames separated by a known time interval. In this way the same particle appears on the newly combined image twice and the distance of settling (over a known time),

particle size, and settling orientation can be digitized.

The density of a floc [expressed as excess density (1 - wet floc density)] was estimated using Stokes' Law (Equation 2). As Stokes' Law is based on the settling of single impermeable spherical particles in a laminar region (Reynolds Number < 0.5), it is not ideal for the determination of floc density due to the heterogeneous structure and irregular shape of flocs (Hawley, 1982). Nevertheless Stokes' Law or a modification thereof has often been used to determine the wet density of singular flocs (Li and Ganczarczyk, 1987; Droppo et al., 1997), and does provide an indication of how aggregate settling velocity, density, and porosity are related to aggregate size. The floc porosity can be expressed by a mass balance equation (Equation 3) assuming a typical density of dried silt and clay of 1.65 g/cm^3.

$$\varpi = \frac{1}{18} D^2 (\rho_f - \rho_w) \frac{g}{\mu} \quad (2)$$

where: ϖ = settling velocity,
D = diameter,
ρ_f = wet density of the floc,
ρ_w = density of the water,
μ = dynamic viscosity (kinemetic viscosity x ρ_w)
g = acceleration due to gravity

$$\varepsilon = (\rho_s - \rho_f)/(\rho_s - \rho_w) \quad (3)$$

where: ε = floc porosity,
ρ_s = density of the dried solid material

Results and discussion

The relationship of floc settling velocity to floc size

It is well documented that flocs do not conform to the assumption of solid spherical particles as required by Stokes' Law and have densities well below that of quartz particles (e.g. Li and Ganczarczyk, 1989, 1990; Droppo et al., 1997, 1998). In addition many of the larger floc sizes are found to not settle within the Stokes' region of Reynolds Numbers. Figure 1 illustrates a plot of Reynolds Numbers (R_e) calculated for a range of floc sizes (ϖ derived from linear regression of size to measured settling velocity) and demonstrates that for fluvial and lacustrine sediments only those flocs below 100 - 150 μm will generally settle within the Stokes' region (Re <0.2). These results pose a problem for modelling of sediment transport where the volume or mass of the sediment transported is of importance (for example reservoir in-filling modelling). This is because often the majority of the sediment volume is represented by the larger particles which settle outside of the Stokes' region, although they may only represent a relatively small proportion of the total number of particles (Droppo and Ongley, 1994). For most of the rivers in Southern Ontario, however, the flocs are generally small (<100 μm) and as such will settle within the Stokes' region. Such a finding does not however imply that the Stokes' Equation is still appropriate for sediment transport models (calculating settling velocities and deriving floc

density and porosity), as the assumption of solid, spherical, smooth rigid particles is still not met.

In studying numerous samples from both the fluvial and lacustrine environment, some consistent trends were observed. It was consistently found that the traditionally used Stokes' Equation for the prediction of settling velocity overestimated the settling velocity of flocculated particles. Table 1 provides examples of both the lacustrine and riverine settling velocity (as based on the linear regression of floc size to measured settling velocity) as compared to calculated Stokes' values for set floc sizes. For these examples, Stokes' Law over-predicts settling velocities

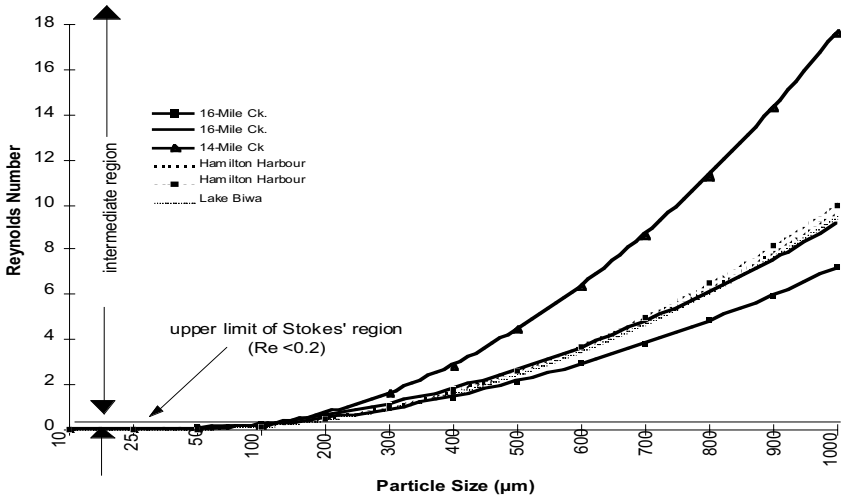

Fig. 1 The relationship of Reynolds Number to particle size for different environments

by orders of magnitude for larger flocs. The agreement converges only for very small flocs. The poor performance of Stokes' Equation to predict the settling velocities of flocculated particles is related to the varying morphology (shape, porosity) and composition (organic/inorganic composition and water content) of flocs from that of the assumed solid spherical particle (Nicholas and Walling, 1996). Very small flocs approximate a solid particle and therefore have settling velocities closely predicted by Stokes'. While it is evident that floc size is a dominant factor which will influence settling velocity, the other characteristics of density, porosity and shape (discussed below) all combine to provide a particle settling velocity which is well below that predicted by Stokes'. Any sediment transport/yield modelling will need to take these factors into account.

Given the inappropriateness of the Stokes' Equation for the calculation of floc settling velocity and the difficulties in estimating floc density (described below), it is important to measure the fall velocity of flocculated particles directly. In the many settling experiments performed in this work from different environments (> 100 experiments), a positive relationship of floc size to settling velocity was consistently found, where settling velocity is proportional to the diameter of the particle (Figure 2). This is different from the Stokes' Equation, which states that settling velocity is proportional to the diameter of the particle squared.

Table 1 Calculated (Stokes' Law) versus measured settling velocities for three different environment examples (2.65 g/cm^3 assumed in Stokes' Equation calculations)

Particle size (μm)	Calculated Stokes' settling velocity (mm/s)	16-Mile Ck. measured settling velocity (mm/s)	Hamilton Harbour measured settling velocity (mm/s)	Lake Biwa, Japan measured settling velocity (mm/s)
500	225.00	4.30	5.09	4.88
300	81.00	3.10	3.27	3.06
100	9.00	1.91	1.45	1.24
50	2.25	1.61	1.00	0.79
20	0.36	1.43	0.73	0.51

While the regression lines fitted to the relationship between settling velocity and floc size are generally significant (α =0.05) (Figure 2), the r^2 values are often low. This low r^2 reflects the wide range of morphologies (shape, porosity) and composition (organic/inorganic composition and water content) of individual flocs which result in a high variation in floc settling velocity for a given floc size.

The relationship of floc settling velocity to floc shape

The shape of a floc is generally influenced by its origin/source and composition and by the flow field in which it is transported/eroded. Floc shape is known to affect settling/transport due to resistance effects against flow (fluid drag forces) (Richards, 1982; Li and Ganczarczyk, 1987). Flocs which possess the same density and radius as an equivalent sphere but have a different shape will generally settle at different rates (Krumbein, 1942; Lerman, 1979; Richards, 1982; Ozturgut and Lavelle, 1984). Cylinders and disk- and cap-shaped particles settle more slowly than ellipsoids and needle-like shapes (depending on their orientation). Droppo et al. (1998) found that during a spring melt period on the Sixteen-Mile Creek, elongated flocs (aspect ratio > 2) settled slower in a quiescent settling tube than did more spherical flocs (aspect ratio < 2). Theoretical computations by Lerman (1979) of the influence of shape factor on settling velocity have shown that the settling velocities of non-spheres of equivalent spherical volume vary within a factor of two of the settling velocity of the sphere. It is difficult to determine experimentally the individual effect of floc shape on settling velocity, as it is not possible to control floc mass and density within the laboratory.

Figure 3 illustrates that for a given size floc in a fluvial or lacustrine environment there can be a wide range of shapes. While the relationship is generally poorly defined, a power function of the form $S_f = ad^m$ can be fitted to most of the data sets, where: S_f is the shape factor, d is diameter and *a* and *m* are parameters which are likely to depend on the type of particle being investigated and the conditions under which the flocs were produced (*a* and *m* are derived empirically). Generally as floc size increases the shape factor decreases, suggesting that larger flocs are generally more irregular in shape and more elongated. COM observations generally support this finding (Figure 4).

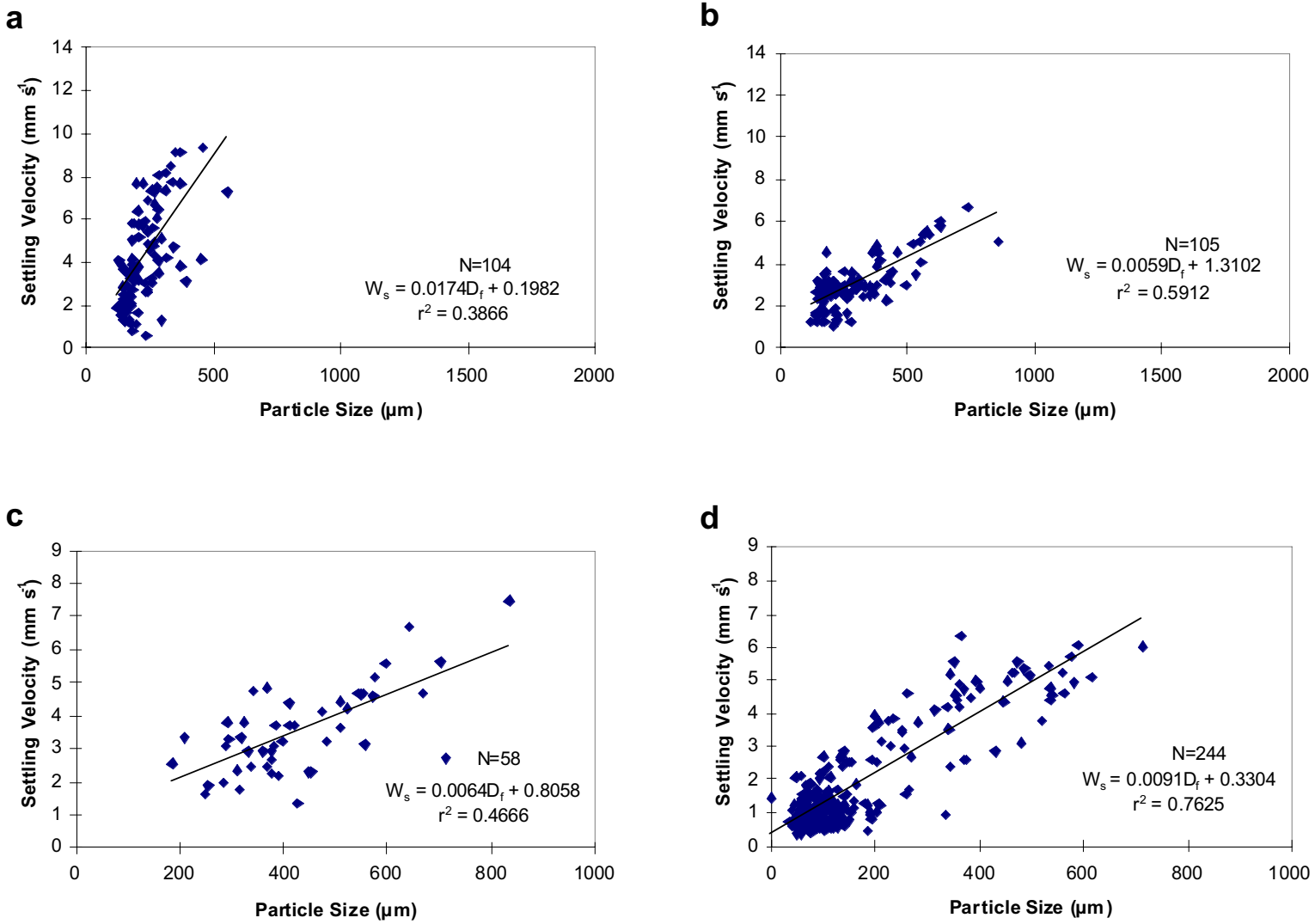

Fig. 2 Example plots of settling velocity versus floc particle size for fluvial and lacustrine sediments [a) 14-Mile Creek, November 3, 1997; b) 16-Mile Creek, January 10, 1998; c) Hamilton Harbour, August 18, 1995; d) Lake Biwa, June 12, 1995]

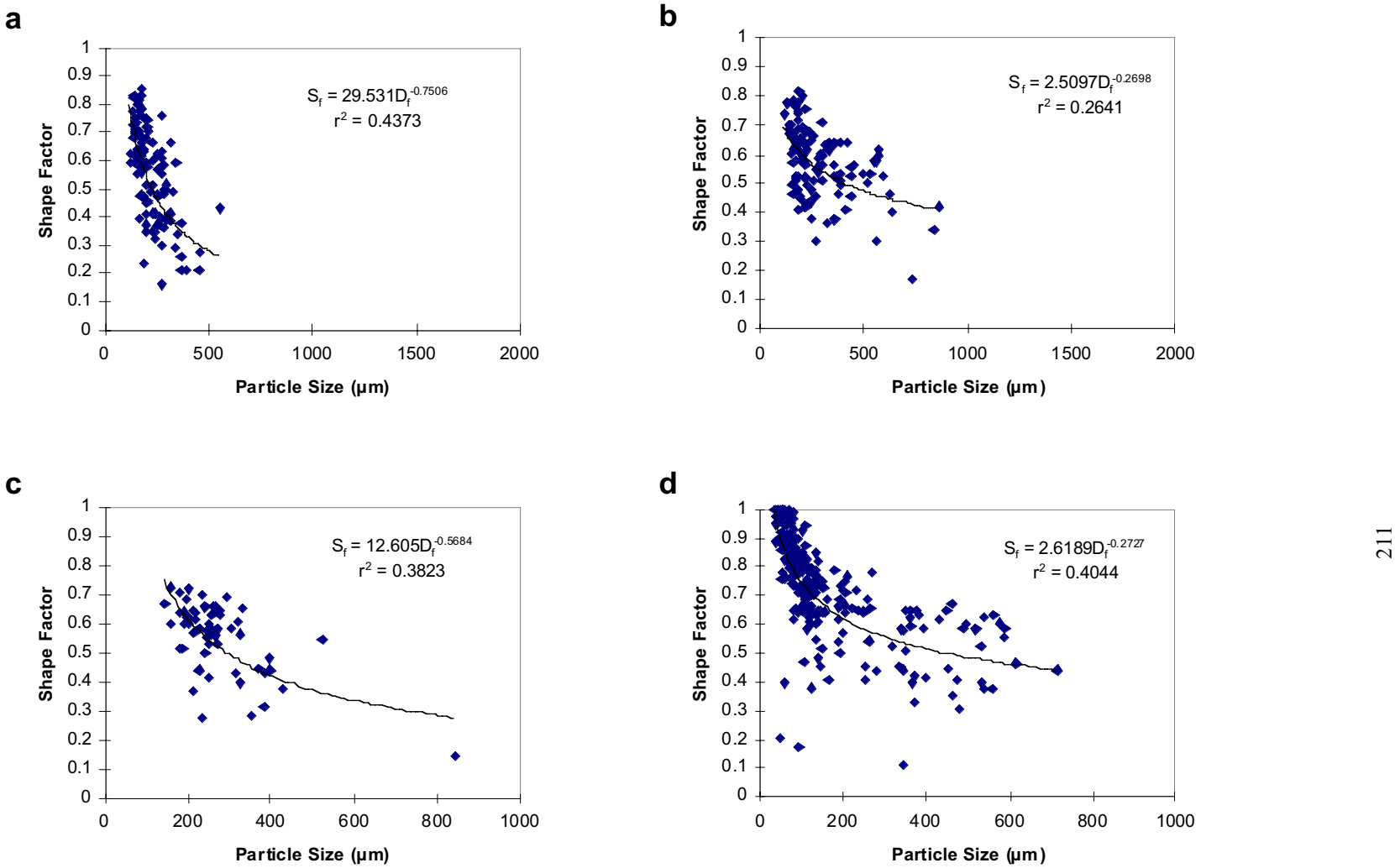

Fig. 3 Example plots of shape factor versus particle size for selected fluvial and lacustrine sediments [a) 14-Mile Creek, November 3, 1997; b) 16-Mile Creek, January 10, 1998; c) Hamilton Harbour, August 18, 1995; d) Lake Biwa, June 12, 1995]

Contrary to the above information, the flocs in this study generally revealed a decrease in floc settling velocity as the particles approached a spherical shape. Evaluating the same data in a similar manner to that proposed by Droppo et al. (1998) (i.e. settling velocity versus aspect ratio rather than shape factor) failed to confirm the relationship that they found for the Sixteen-Mile Creek spring melt periods (i.e. higher settling rate for spherical particles) for other times of the year or other sample sites. Given that the findings of this work go against traditional theory, this would suggest that shape appears to have a minimal impact on settling velocities (at least for the natural flocs observed). Furthermore, this may suggest that size and density are far more important in influencing the settling of a floc and for consideration in sediment transport/yield models. The observation of more irregular flocs settling faster is therefore more likely to be related to the observation that larger flocs, which settle faster due to their size, tend to represent the greatest population of irregular flocs.

While shape did not appear to have an influence on settling velocity, a preference of settling orientation was observed. Settling orientation is simply the angle at which a floc settles relative to its long axis. As with Droppo et al. (1998), many of the flocs encountered revealed a preference to settle with their long axis parallel to the direction of settling. This is seen in Figure 5 which shows bell shape distributions [note that at the bottom of the bell the flocs are approaching a circular shape (i.e. close to 1) and exhibit no preference of orientation]. While difficult to see in the plots, 15 to 30% of the flocs measured settle with their long axis exactly parallel to the direction of settling (i.e. 90°). In reality, flocs generally settle in a turbulent flow (particularly in a fluvial environment) which will result in the "tumbling" of the floc and as such would further suggest that the influence of shape and orientation on settling velocity is not an important factor to be considered when modelling the transport of sediment in natural or engineered environments.

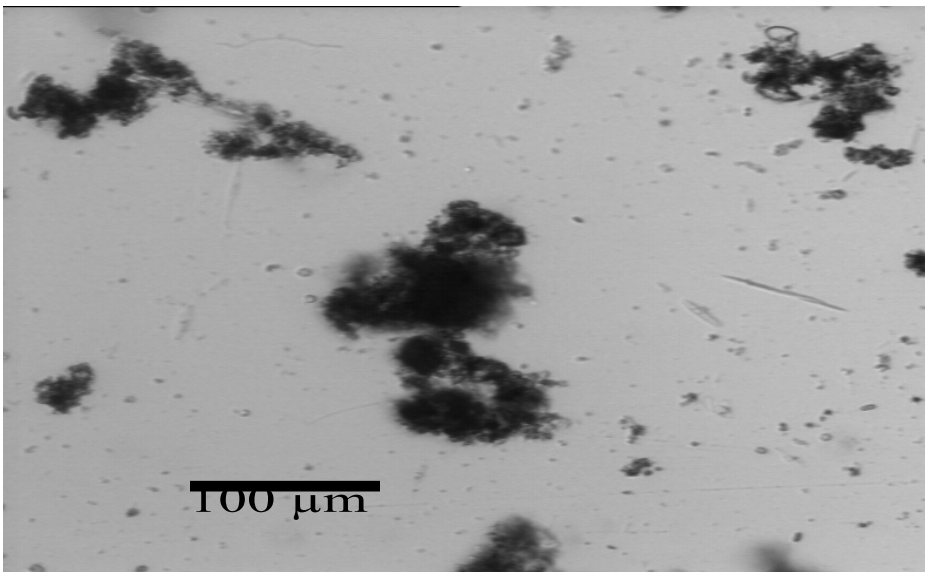

Fig. 4 Large irregular shaped flocs from a 16-Mile Creek Sample

The relationship of floc settling velocity to floc density

The density of a floc is influenced by, firstly, its composition (inorganic and organic particles, EPS, water content, etc.) and, secondly, its porosity (pore size and structure). The potential influence of particle density on settling velocity is illustrated below using data from the rising and falling limbs of the 1997 spring melt for the Sixteen-Mile Creek. Other samples are also used to demonstrate trends in the data and to demonstrate the application of an equation for describing the relationship between floc size and density. Regression equations are used to illustrate differences between sample settling velocities and densities. Variations in the slope and y-intercept of the regression lines were statistically analyzed for significant differences based on the t-statistic according to Equation 4.

$$-1.96 \leq \frac{(b_1 - b_2)}{\sqrt{\left[Var(b_1) + Var(b_2)\right]}} \leq 1.96 \qquad (4)$$

where: b_1 = first data point (slope or y-intercept)
b_2 = second data point (slope or y-intercept)
Var = variance of $b_{1 \text{ or } 2}$ = (standard error of $b_{1 \text{ or } 2}$)^2

If the test statistic is within the range specified in Equation 4 then there is considered to be no significant difference at the 95% confidence limit ($\alpha = 0.05$). Again, it is difficult to determine experimentally the effects of natural floc density on settling as it is not possible to control floc density.

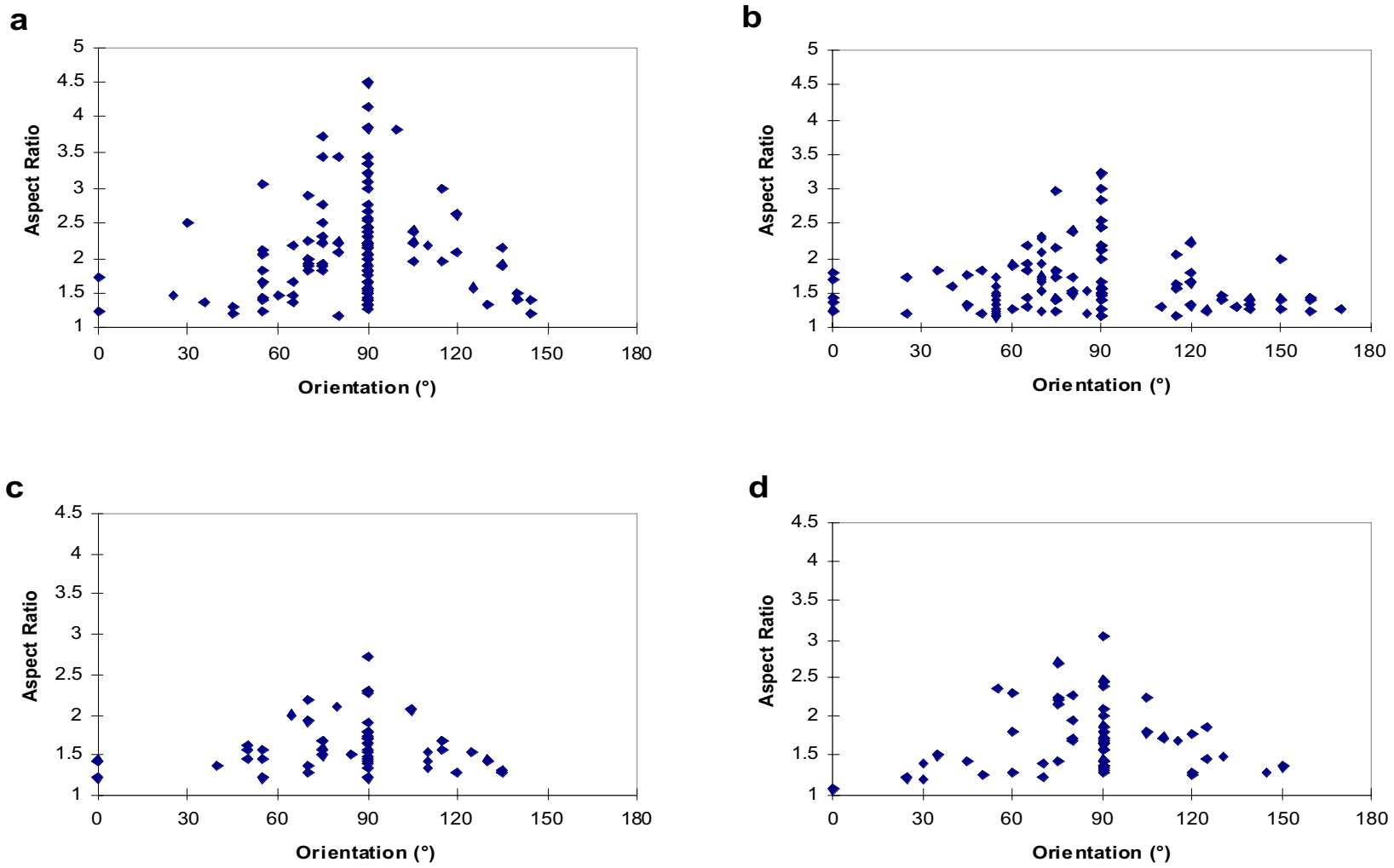

Fig. 5 Example plots of floc settling orientation versus aspect ratio (floc length / floc width) for fluvial and lacustrine sediment samples (no data for Lake Biwa available) [a) 14-Mile Creek, November 3, 1997; b) 16-Mile Creek, January 10, 1998; c) and d) Hamilton Harbour, August 18, 1995]

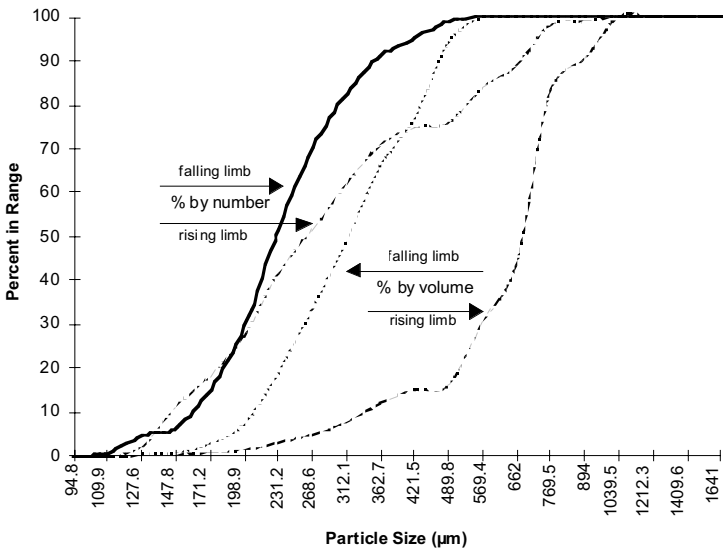

Fig. 6 A comparison of the floc size distributions (by number and volume) for both the falling and rising limbs of the Sixteen-Mile Creek

Extreme variations in flow occurred during the 1997 spring melt for Sixteen-Mile Creek and samples were collected on both the rising limb and falling limb of the hydrograph. A significant difference was found between the two distributions representative of the hydrograph limbs for both the percent by volume and number distributions (Figure 6) as measured using the settling chamber (modified Kolmogorov-Smirnov test, $\alpha = 0.05$). The significant difference between the volume distributions is related to their sensitivity to the presence of only a few large volume particles. Of the two samples settled, the rising limb possessed much larger particles as seen in Figures 6 and 7. These larger particles are likely to represent rip-up flocs originating as biofilm-type material eroded from the bed of the creek as bed shear stress increases with stage. A distinct difference was found between the statistically significant regression lines ($\alpha = 0.05$) fitted to the relationship between settling velocity and floc size for the two hydrograph limbs (Figure 7).

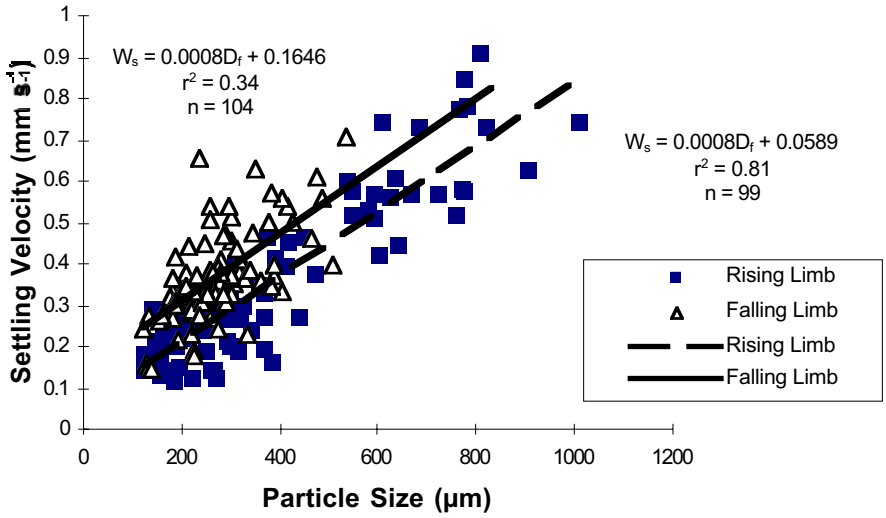

Fig. 7 Plots of settling velocity versus floc size for the 1997 spring melt on 16-Mile Creek

While the rate of change is constant (Figure 7) (i.e. same slopes, no significant difference at $\alpha = 0.05$, t-test as per Equation 4), particles on the rising limb have lower settling rates as indicated by a significantly different y-intercept of the regression lines ($\alpha = 0.05$, t-test as per Equation 4). This may indicate that the flocs associated with the rising limb are characterized by lower densities, more irregular shapes and higher porosities. The differences in settling velocities are likely to reflect the changing source material over the spring melt hydrograph. For example, as suggested above, the rising limb may contain more low density biofilm flocs (high porosity, high bio-content) ripped up from the bed while the falling limb sample may contain more high density (low porosity, high inorganic) eroded water stable soil aggregates (the source of biofilm would be depleted by this time). Density estimates from statistically significant power function regression lines ($\alpha = 0.05$) confirm an increase in floc density for the falling limb for the range of floc sizes measured (See Figure 6 and Equations 5 and 6 below), as there was a significant difference between the slopes and the y-intercepts of the two lines (Equation 4, $\alpha = 0.05$).

$$\text{rising limb} \quad \rho_f = 1 + 6.021 D_f^{-1.212} \quad (r^2 = 0.85); \tag{5}$$

$$\text{falling limb} \quad \rho_f = 1 + 23.971 D_f^{-1.402} \quad (r^2 = 0.78) \tag{6}$$

where: ρ_f = floc density (note that $\rho_f - 1$ = excess density)

D_f = floc diameter

The greater slope (i.e. greater rate of change in density with floc size) associated with the falling limb is likely to reflect an accompanying greater decrease in porosity with size than for the rising limb (this is tested below). Petticrew and Droppo (1998) found two distinct populations of particle densities within western Canadian streams, which exhibited different settling velocities. It was hypothesized that the denser flocs/aggregates characterised by faster settling were derived from the cobble bed while the less dense flocs characterised by slower settling were derived from flocculation within the water column.

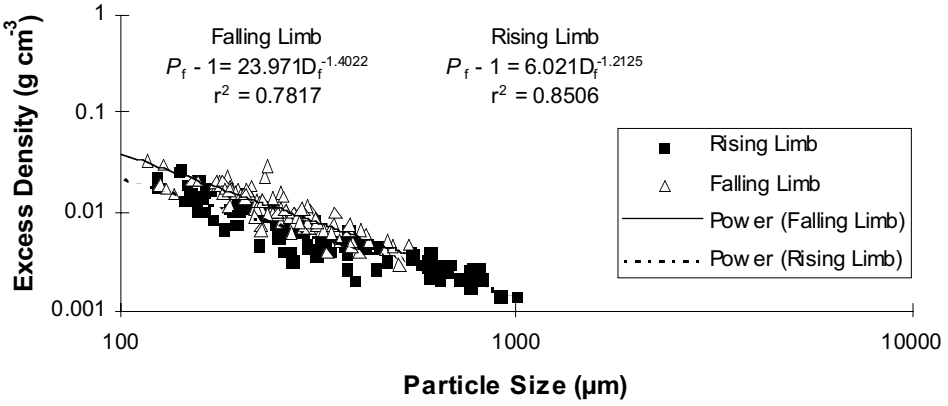

Fig. 8 Plots of excess density versus floc size for the 1997 spring melt on 16-Mile Creek

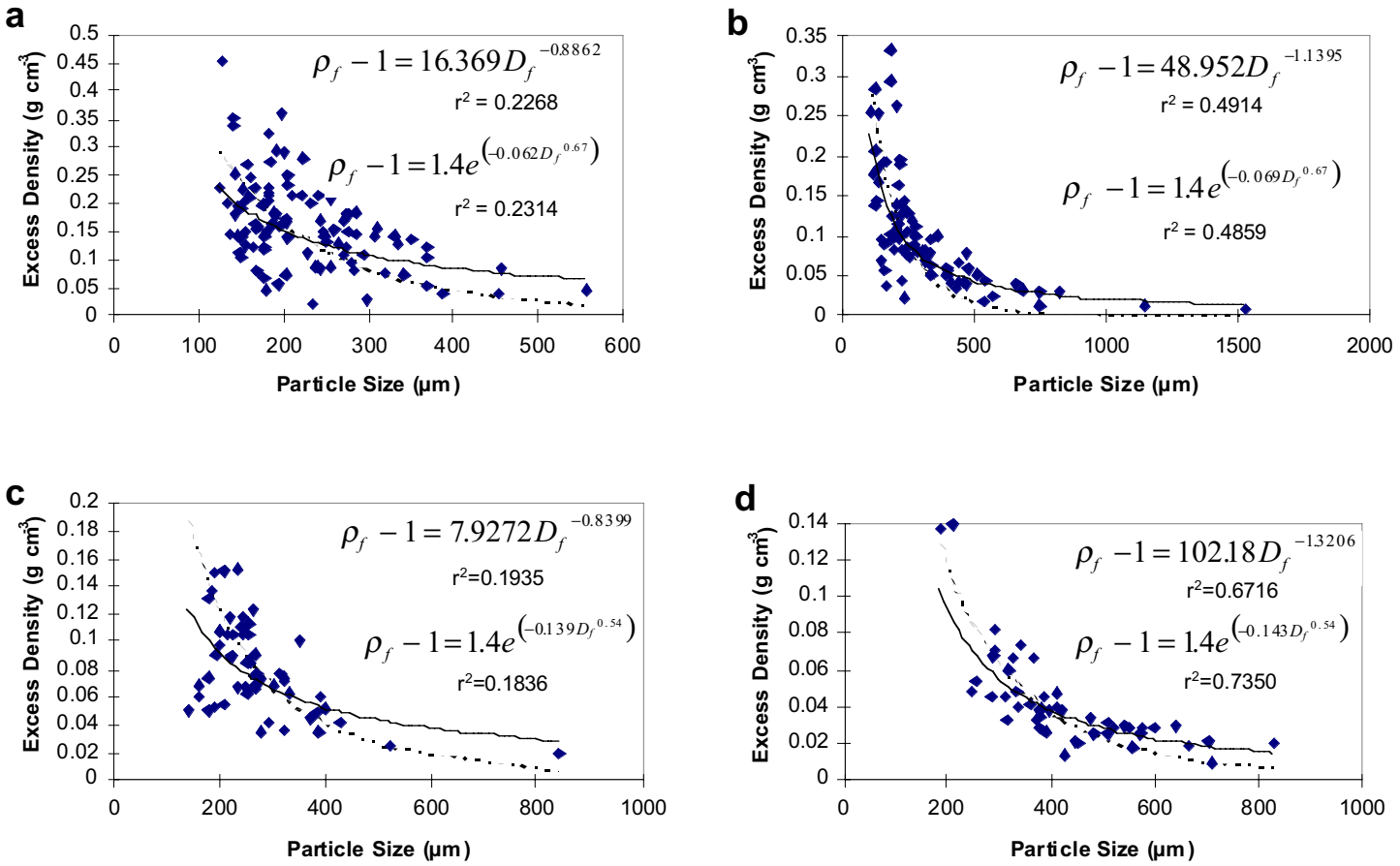

Fig. 9 Examples of the negative relationship which exists between excess density and particle size for fluvial and lacustrine sediment samples The data has been fitted with both a power (solid line) and exponential (dashed line) function (see Equation 7). [a) 14 Mile Creek, November 3/97; b) 16 Mile Creek, February 18/97; c) and d) Hamilton Harbour, August 18th]

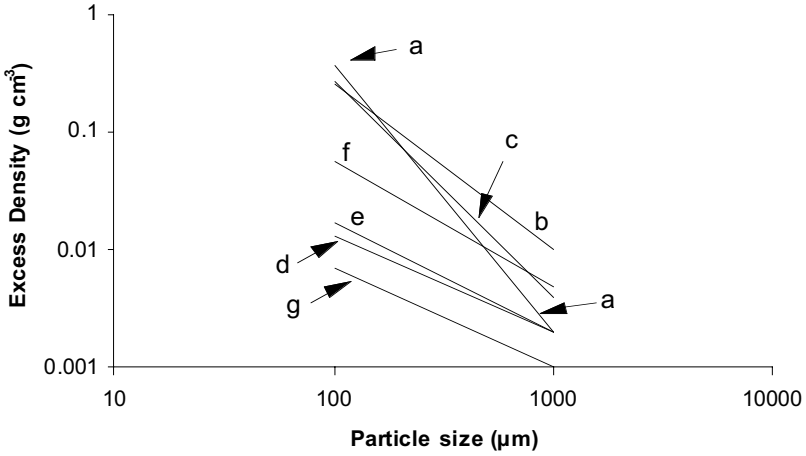

Fig. 10 Comparative results of excess density with floc size for different environments. a = Fourteen-Mile Creek (this study), b = Sixteen-Mile Creek (this study), c = Hamilton Harbour (this study), d = Fennessy et al. (1994) (marine flocs), e = Gibbs (1985) (estuarine flocs), f = Hawley (1982) (lacustrine flocs), g = Andreadakis (1993) (activated sludge - waste water)

The decrease in density with increasing particle size observed in Figure 8 is evident for all floc samples analyzed within this work (examples given in Figure 9). Figure 10 also demonstrates that numerous other researchers have found similar trends for different environments. The substantial variation between the lines is reflective of the different factors and relative importance of each, in influencing floc growth between environments. It has been suggested that the slope of these lines (log excess density vs. log particle size) has a close relation to floc structure (Li and Ganczarczyk, 1989, 1990). The decrease in density with increasing size, irrespective of environment, reflects an increase in porosity with increasing size (see below). As a floc grows and encompasses more and more particles, it also creates more void space for the entrapment of water. It is the high water content which results in the density of larger flocs approaching that of water (Droppo et al., 1998). Given that the density of the very large flocs approaches that of water, it is puzzling as to why such flocs still settle with such a fast rate relative to the smaller more dense flocs. A possible explanation may be that flow through the floc (via large pores) during settling helps to increase the settling velocity of such low density flocs. This is discussed further below.

In assessing the relationship of floc size to density, often the power function is used to provide a "good fit" (Figure 9) (Zahid and Ganczarczyk, 1990; Andreadakis, 1993; Li and Ganczarczyk, 1993). The power function, however, does not have any physical meaning with regards to this relationship. The exponential function on the other hand is more physically based in relation to how floc size and density vary and as such can be used to explain the relationship of floc size and density (based on sound physical principles observed in this work). As such, while the power function used within this work and highly cited within the literature provides a good fit for the data, the exponential function described below makes more physical sense.

As described above, as a floc increases in size its density approaches that of water.

Conversely, as a floc approaches the size of a constituent (absolute) single particle its density approaches that of the density of the sediment. This relationship can be described mathematically below (Lau and Krishnappan, 1997);

$$\rho_f - \rho_w = (\rho_s - \rho_w) e^{-(C_1 D_f^{C_2})} \quad (7)$$

where: C_1 = empirical constant 1
C_2 = empirical constant 2
D_f = floc diameter
ρ_f = floc density
ρ_s = solid particle density
ρ_w = water density
$(\rho_f-\rho_w)$ = excess density

As $D_f \longrightarrow \infty$ $(e^{-\infty} = 0)$ then $\rho_f-\rho_w = 0$ and therefore $\rho_f = \rho_w$
As $D_f \longrightarrow 0$ $(e^{0} = 1)$ then $\rho_f-\rho_w = \rho_s-\rho_w$ and therefore $\rho_f = \rho_s$

A simple curve fitting exercise was used to fit an exponential curve (based on Equation 7) to the data provided in Figure 9 by varying C_1 and C_2 until the lowest sums of squares errors (SSE) was derived. The r^2 value for each curve was calculated and compared to the power function curve and r^2 provided on the plots in Figure 9. A value of 2.4 was assumed for ρ_s given that the natural environment flocs will be made up of both mineral particles and organic material. The parameter ρ_w was assumed to be 1.0 and as such $\rho_s-\rho_w = 1.4$. Clearly the exponential model provides a reasonable fit relative to the more widely used power function in describing the relationship of floc size to floc density. This is demonstrated by both fitted lines explaining essentially the similar amounts of variance within the data (i.e. similar r^2 values - see Figure 9). Interestingly, for both the fluvial and lacustrine examples (Figure 9), the exponential function under-predicts the density for larger size particles and, to a lesser degree, over-predicts the density of the smaller particles. The under-prediction of floc density for large flocs is of less concern as generally these particles only make up a small population of the over all sediment in transport. The constants of the equations were found to be relatively similar within environments, but quite different between the environments. This suggests that factors influencing floc density and size are consistent within an environment but are different between the fluvial and lacustrine environments studied. Given the physically based nature of Equation 7, numerical descriptions of floc size to density for modelling efforts would be better suited to use such a relationship rather than the more commonly used power function.

Given the observation that as floc size increases, settling velocity increases but floc density decreases, it would appear that, although differences in density are found between flocs, density's relative importance may be minimal in relation to a change in floc diameter as related to floc settling. Floc densities (Figure 9) are typically low ranging between the density of water and 1.4 g cm^{-3} (the majority of flocs observed were below 1.1 g cm^{-3}). Other researchers have found similar densities [Riley (1970) - 1.152 g cm^{-3} for 2-6 μm particles, 1.033 g cm^{-3} for higher organic content flocs with sizes >60 μm; Krone (1972) - 1.164-1.056 g cm^{-3} for <1 mm diameter flocs; Shiozawa et al., (1985) - 1.38-1.03 g cm^{-3} for flocs ranging from 1.0-0.01 mm respectively].

Given 1) that larger flocs generally have the lowest density, and yet, exhibit the greatest settling velocity, 2) the minimal changes in density over the range of floc sizes examined and 3) the relative small difference between floc density and water density, it is likely that the size of the floc will have a greater influence over settling than the density of the floc. In general, it can be concluded that changes in floc density in time or space, or with floc size appears to have a minimal impact on floc settling. For large flocs where densities are very low (approaching that of water) it is possible that an open floc matrix with large pores will have a strong influence on floc settling (discussed further below). Because estimates of floc density are derived from the settling velocity, a statistical comparison of these two variables is not possible.

The relationship of floc settling velocity to floc porosity

Pores probably represent the most important structural entity of a floc. Floc pores are responsible for much of the physical, chemical and biological behaviour exhibited by flocs, as they are the primary physical factor, which controls water content and movement within a floc. As such, floc pores influence floc density and transport as well as potential advective, diffusional and electrochemical gradients within the floc (Sherman, 1953; Li and Ganczarczyk, 1988; Logan and Hunt, 1987, 1988). Porosity cannot be measured directly, due to the three dimensional and tortuous nature of flocculated sediment. It is generally derived from the mass balance between the density estimates for the wet floc (measured or derived through settling experiments), dry material density and water (Equation 3) (Li and Ganczarczyk, 1987; Andreadakis, 1993; Droppo et al., 1998).

Porosity influences settling velocity both directly and indirectly. As indicated above, porosity indirectly influences settling velocity by being one of the primary factors controlling density. As described above, this is primarily related to the water content of a floc, which is directly proportional to the porosity. The greater the porosity, the greater the water content, the lower the density, and, in theory, the slower its settling velocity (assuming constant floc size and no flow through the floc). More directly, however, porosity may influence settling velocity by the individual large pores potentially acting as passages for the flow-through of water during settling. Such movement of water through the floc will, in theory, increase the settling velocity of the floc due to a reduction in drag (Zahid and Ganczarczyk, 1990).

Figure 11 indicates that as fluvial and lacustrine floc size increases, the porosity of the floc also increases, approaching 100% (fitted lines are discussed by Equation 8 below). This finding is consistent with the findings of other researchers (Tambo and Watanabe, 1979; Logan and Hunt, 1987; Li and Ganczarczyk, 1987, 1988; Andreadakis, 1993). This relationship is reasonable, given that settling velocity of flocs is not, as suggested by Stokes' law, related to the square of the size. This would indicate that the floc density must decrease and floc porosity increases with increasing floc size (Logan and Hunt, 1987). As a floc grows, the amount of open void space increases simply due to the nature of the contact points between particles (organic and inorganic) forming the matrix. In the hundreds of high resolution TEM images observed, no floc was found to be completely devoid of pores such as might occur with face to face stacked clay platelets. In all cases the flocs were characterized by a highly open matrix such as that seen in Figure 12.

As with floc density, a power function (Figure 11) is often used to describe the relationship of floc size to porosity. Such a function did not provide an adequate fit and was very poor in both the larger and smaller floc sizes. As with the density, the power function fit has no physical basis associated with it. As such a new function for the description of the relationship between floc porosity and floc size was developed given the following observations. 1) As floc size increases porosity approaches 1 (or 100%) and 2) as the floc size approaches a single individual constituent particle the porosity approaches 0 (or 0%). Such physical constraints can be adequately explained in the following equation:

$$Por = \frac{D_f}{C_1 + C_2 D_f} \tag{8}$$

where Por = Porosity (as a decimal)
C_1= Empirical constant 1
C_2= Empirical constant 2

The empirical constants are derived through a spurious correlation of $\frac{D_f}{Por}$ to D_f , which from a truly statistical sense should be avoided. However, as this spurious relationship is only used for the derivation of constants for fitting of a line based on Equation 8 to the observed data, such a statistical rule can be relaxed. C_1 and C_2 are derived from the regression of the above relationship in the form;

$$\frac{D_f}{Por} = C_1 + C_2 D_f \tag{9}$$

The curve derived from Equation 9 are fitted to the data in Figure 11 for both the fluvial and lacustrine sample examples. It is evident that Equation 8 fits the data better than the power function, particularly in the larger size classes where the power function predicts values in excess of 100% much sooner than Equation 8. Equation 8 predicts porosity better than the power function for the smaller floc sizes although there is still room for improvement. In 85% of the samples analyzed, Equation 8 resulted in a slightly higher explanation of the variance. For both the fluvial and lacustrine examples, constant C_2 (the slope of Equation 9) is reasonably similar, however, C_1 is more variable within and between environments. As C_1 and C_2 are derived from a spurious correlation little inference can be made from these. However, Table 2 provides the fitted predictions for various floc sizes from Equation 8 and suggests that, like with the density, there may be some differences between environments. In the smaller floc sizes, the lacustrine samples exhibit a higher porosity. This may be attributed to flocs in a lacustrine environment generally being formed under lower shear conditions as compared to a fluvial environment resulting in a more open floc matrix. The flocs formed in a fluvial environment under higher shear are more likely to be less porous due to stronger impaction as a result of stronger collisions. The fact that the porosities predicted by Equation 8 for the larger floc sizes are similar between environments (Table 2), supports the concept that larger flocs approach 100% porosity (i.e. the density of water) regardless of the environment.

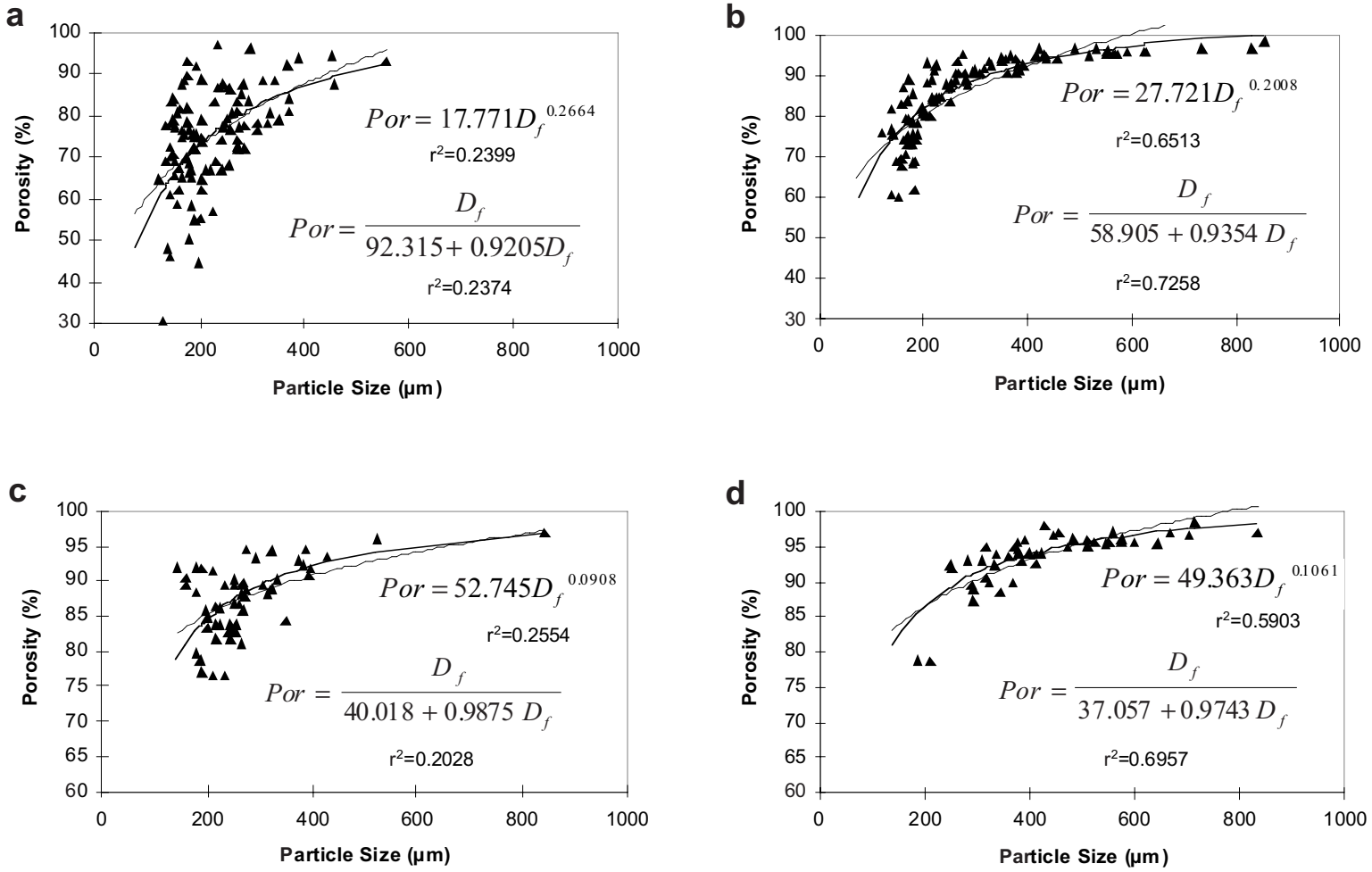

Fig. 11 Examples of the relationship between porosity and particle size for fluvial and lacustrine sediment samples. The data has been fitted with both a power function (thin line) and with Equation 8 described below (thick line). [a) 14 Mile Creek, November 3/97; b)16 Mile Creek, February 18/97; c) and d) Hamilton Harbour, August 18th]

Table 2 Estimations of fluvial and floc porosities using Equation 8 and the examples provided in Figure 11

Floc size	Fluvial mean floc porosity	Lacustrine mean floc porosity
50 µm	45.9%	60.6%
100 µm	63.8%	75.8%
200 µm	79.5%	86.6%
500 µm	93.5%	94.9%
1000 µm	99.2%	98.0%

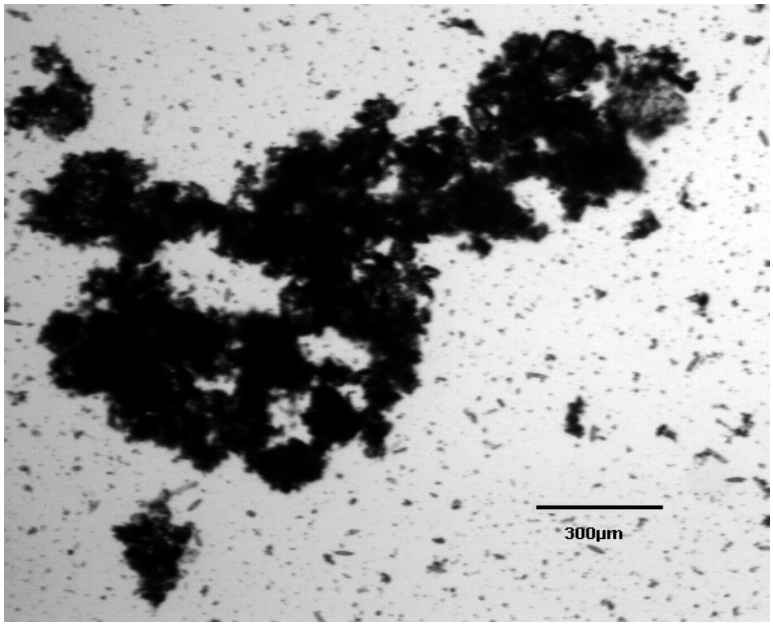

Fig. 12 A large open matrix floc from Sixteen-Mile Creek (February 18, 1997)

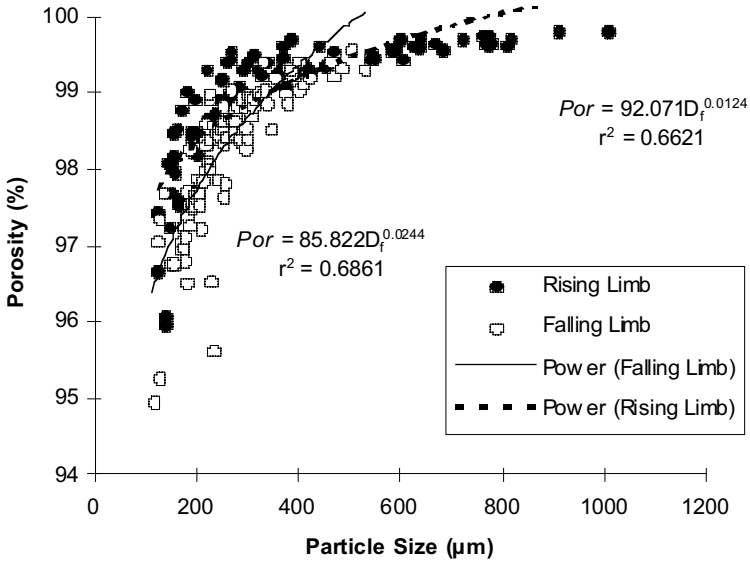

Fig. 13 Plot of porosity versus floc size for the 1997 spring melt on Sixteen-Mile Creek

Figure 13 plots the relationship of porosity to floc size for both the rising and falling limb of the Sixteen-Mile Creek spring melt samples previously described. An evaluation of the regression lines shows significant differences between the two limbs of the hydrograph for both the slope and y-intercept (based on Equation 4). This is suggestive of differences between the porosity of the rising and falling limb flocs, with the data plotted in Figure 13 showing that the rising limb generally has a higher porosity than the falling limb flocs. This is consistent with the significant differences in density seen for the same samples above. Such a link is expected because of the strong relationship between porosity, water content and density (i.e. the higher the porosity, the greater the water content and the lower the density).

As stated above, if water is able to flow through the floc via the pore structure during settling, this can have an influence on the settling velocity of the floc.

Theoretically, a solid sphere, having the same size and density as a highly porous sphere, will settle slower than the porous sphere, because the flow through the permeations of the porous sphere will reduce the hydrodynamic resistance that will be experienced by the solid sphere (Neale et al., 1973; Namer and Ganczarczyk, 1993). Zahid and Ganczarczyk (1990) concluded that the traditional computation of settling velocity by Stokes' Law from size and density measurements may lead to erroneous results if particle permeability is not considered. Given that, for the floc sizes studied, that there is a continuous increase in settling velocity with size (Figure 2), even though the density is approaching that of water (Figure 9), it is reasonable to expect that such a mechanism (flow through pores) is at work to allow large, low density flocs to settle. General observations show that only the large flocs possess pores which may be large enough for water flow (Figure 12).

There are opposing opinions within the literature as to the significance that flow through pores will have on floc settling velocity. In mathematical modelling, the behaviour of marine flocs, Logan and Hunt (1987) found that, even with a wide range in floc dry density (2.65 - 1.06 g cm^{-3}), intra-floc flow had a negligible effect on the settling velocity of flocs up to 1 mm in diameter. Li and Ganczarczyk (1988) demonstrated experimentally that the settling velocity of activated sludge flocs was reduced when the porosity of the flocs was reduced by the presence of impermeable blockers of activated carbon, coke and resin. This reduction in settling velocity occurred even though the blockers gave the floc a higher density. Adler (1981) found that flocs < 40 μm in diameter will have no intra-floc flow. It should be noted that existing models of flow through flocs are based on simplified floc structures which restrict the analysis to highly porous flocs typical of marine systems and to flocs in pure bacterial cultures (Logan and Hunt, 1987). Often porous plastic or steel-wool mesh balls are used in evaluating the influence of inter-flow on floc settling velocity (Masliyah and Polikar, 1980). Given the simplifying assumptions made about flocs in mathematical models and the fact that the physical structure of the flocs used in experiments does not approximate the true nature of a floc, it is likely that such modelling and experimental results do not represent reality for small freshwater flocs. In an analysis of Lake Mead flocs (0.5 to 1000 μm), Sherman (1953) found that because the floc pores were small and their permeability low, the water could be considered trapped and an integral part of the floc structure. As the majority of freshwater flocs observed in this study are relatively small (<100 μm), it is unlikely that there is any substantive flow of water through the floc during settling. Any flow gradients within the floc are likely to be diffusional. This is due to the complex matrix of the natural flocs observed which possesses thousands if not millions of micro pores (Liss et al., 1996). These pores, because of their very small nature (the fibrils making up the pore walls have diameters as small as 4 nm) will possess very strong hydrostatic forces, which will cause the retention of water. For the larger flocs, however, which can make up the majority of the volume of sediment in transport, flow through the pores of a floc is likely to contribute to the observed high settling velocity of low density flocs. As such, as stated above for density, it is likely that for the majority of flocs in the aquatic environment, floc size will influence settling velocity more than porosity. Direct statistical comparisons of porosity and settling velocity are not possible here as the porosity is derived from the settling velocity measurement.

Conclusion

The transport of sediment in aquatic systems is strongly influenced by the velocity and shear of the flow and by the structure of the sediment. Flocs were found to not conform to Stokes' Law, primarily due to the inappropriateness of the assumption of solid spherical particles for flocculated sediment. Floc settling velocity was found to generally be proportional to floc size and not to the square of the size as suggested by Stokes' Law. Although flocs can have densities as low as water, due to high porosity and organic content, they tend to settle faster than their constituent primary particles, due to their larger size and the potential impact of flow through the floc pores increasing their settling velocity. As such floc size, relative to density and porosity, is believed to be the dominant floc characteristic influencing settling. Floc shape was generally found to have a minimal influence on floc settling velocity/transport.

It should be realized that most of the discussion of floc settling velocity, porosity and density presented above is based on quiescent settling experiments. In reality, particles rarely settle within a quiescent zone of an aquatic environment. This is particularly true for the fluvial environment where backwater areas are of limited extent (with the exception of in-river lakes and reservoirs), relative to the total area of the river channel. While it is reasonable to assume that the strength of a floc will dictate its behaviour in a turbulent environment, individual floc strength is difficult to measure. The factors of size, shape, density and porosity discussed above will still exert a significant influence over the settling velocity and transport of flocs in a flowing turbulent environment, but their influence on the rate of settling will be distorted (relative to quiescent settling) due to the turbulent nature of flow. Nevertheless, because of the inherently different transport behaviour of flocs over their constituent particles, it is important that future models of sediment transport/yield take into account the structure of flocs and how this may influence their settling/transport behaviour. The development of such models will result in more accurate and meaningful estimates of sediment and contaminant source, fate and effect for the management of our aquatic ecosystems.

Acknowledgements The authors thank C. Jaskot for technical support with image analysis.

Bibliography

ADLER, P.M. (1981) 'Streamlines in and around porous particles'. J. Colloid Interface Sci., 81, p. 531-535.

AMOS, C.L. and I.G. DROPPO (1996) 'The stability of remediated lake bed sediment, Hamilton Harbour, Lake Ontario, Canada'. Geological Survey of Canada Open File Report # 2276.

ANDREADAKIS, A.D. (1993) 'Physical and chemical properties of activated sludge floc'. Wat. Res., 27, p. 1707-1714.

DROPPO, I.G. and E.D. ONGLEY (1992) 'The state of suspended sediment in the freshwater fluvial environment: a method of analysis'. Wat. Res., 26, p. 65-72.

DROPPO, I.G. and E.D. ONGLEY (1994) 'Flocculation of suspended sediment in rivers of southeastern Canada'. Wat. Res., 28, p. 1799-1809.

DROPPO, I.G.; G.G. LEPPARD; D.T. FLANNIGAN and S.N. LISS (1997) 'The freshwater floc: a functional relationship of water and organic and inorganic floc constituents affecting suspended sediment properties'. Wat. Air Soil Pollut., 99, p. 43-53.

DROPPO, I.G.; D.E. WALLING and E.D. ONGLEY (1998) 'Suspended sediment structure: implications for sediment and contaminant transport modelling'. In: W. Summer, E. Klaghofer and W. Zhang (eds.), *Modelling soil erosion, sediment transport and closely related hydrological processes*. (Proc. International Symposium, Vienna, Austria, July 1998). IAHS Publ. No. 249, p. 437-444.

FENNESSY, M.J.; K.R. DYER and D.A. HUNTLEY (1994) 'INSSEV: An instrument to measure the size and settling velocity of flocs in situ'. Mar. Geol., 117, p. 107-117.

GIBBS, R.J. (1985) 'Estuarine flocs: their size, settling velocity and density'. J. Geophys. Res., 90 (C2), p. 3249-3251.

HAWLEY, N. (1982) 'Settling velocity distribution of natural aggregates'. J. Geophys. Res., 87(C12), p. 9489-9498.

KRISHNAPPAN, B.G. (1990) 'Modelling of settling and flocculation of fine sediments in still water'. Can. J. Civil Eng., 17, p. 763-770.

KRONE, R.B. (1972) 'A field study of flocculation as a factor in estuarial shoaling processes'. U.S. Corps of Engineers, Committee on tidal hydraulics, Technical Bulletin, 19, 62 p.

KRUMBEIN, W.C. (1942) 'Settling-velocity and flume-behaviour of non-spherical particles'. Am. Geophys. Union Transact., 23, p. 621-632.

LAU, L.Y. and B.G. KRISHNAPPAN (1997) 'Measurements of size distributions of settling flocs'. NWRI Contribution # 97-223, CCIW, Burlington, Ontario, Canada.

LERMAN, A. (1979) *Geochemical processes: water and sediment environments*. John Wiley and Sons, New York, 481 p.

LI, D.H- and J. GANCZARCZYK (1987) 'Stroboscopic determination of settling velocity, size and porosity of activated sludge flocs'. Wat. Res., 21, p. 257-262.

LI, D.H- and J. GANCZARCZYK (1988) 'Flow through activated sludge flocs'. Wat. Res., 22, p. 789-792.

LI, D.H- and J. GANCZARCZYK (1989) 'Fractal geometry of particle aggregates generated in water and wastewater treatment processes'. Envir. Sci. Technol., 23, p. 1385-1389.

LI, D.H- and J. GANCZARCZYK (1990) 'Structure of activated sludge flocs'. Biotechnol. Bioengng., 35, p. 57-65.

LI, D.H- and J. GANCZARCZYK (1993) 'Factors affecting dispersion of activated sludge flocs'. Wat. Environ. Res., 65, p. 258-263.

LISS, S.N.; I.D. DROPPO; D.T. FLANNIGAN and G.G. LEPPARD (1996) 'Floc architecture in wastewater and natural riverine systems'. Environ. Sci. Technol., 30, p. 680-686.

LOGAN, B.E. and J.R. HUNT (1987) 'Advantages to microbes of growth in permeable aggregates in marine systems'. Limnol. Oceanogr., 32, p. 1034-1048.

LOGAN, B.E. and J.R. HUNT (1988) 'Bioflocculation as a microbial response to substrate limitations'. Biotechnol. Bioeng., 31, p. 91-101.

MASLIYAH, J.H. and M. POLIKAR (1980) 'Terminal velocity of porous spheres'. Can. J Chem. Eng., 58, p. 299-302.

MURPHY, T.P.; I.G. DROPPO; C. NALEWAJKO; D.G. RANCOURT and A. MOLLER (1995) 'Akanoi Bay, Lake Biwa bench-scale sediment treatment 1995'. Contributed as a Lake Biwa Research Institute Report, Japan.

NAMER, J. and J. GANCZARCZYK (1993) 'Settling properties of digested sludge particle aggregates'. Wat. Res., 8, p. 1285-1294.

NICHOLAS, A.P. and D.E. WALLING (1996) 'The significance of particle aggregation in the overbank deposition of suspended sediment on river floodplains'. J. Hydrol., 186, p. 275-293.

NEALE, G.; N. EPSTEIN and W. NADER (1973) 'Creeping flow relative to permeable spheres'. Chem. Eng. Sci., 28, p. 1865-1874.

OKUDA, S.; J. IMBERGER and M. KUMAGAI (1995) 'Physical processes in a large lake: Lake Biwa, Japan'. Coastal and Estuarine Studies 48, American Geophysical Union, Washington, DC.

ONGLEY, E.D. (1974) 'Hydrophysical characteristics of Great Lakes tributary drainage, Canada'. Pollution and Land Use Activities Reference Group (PLUARG), Task D, Activity 1, Sub-Activity 1, International Joint Commission, Windsor, Ontario, Canada.

ONGLEY, E.D.; B.G. KRISHNAPPAN; I.G. DROPPO; S.S. RAO and R.J. MAGUIRE (1992) 'Cohesive sediment transport: emerging issues for toxic chemical management'. Hydrobiologia, 235/236, p. 177-187.

OZTURGUT, E. and J.W. LAVALLE (1984) 'New method of wet density and settling velocity

determination for wastewater effluent'. Envir. Sci. Technol., 18, p. 947-952.

PETTICREW, E.L. and I.G. DROPPO (1998) 'Sediment flocculation: an important consideration for transport studies in fluvial geomorphology'. NWRI Contribution No. 98-07, Burlington, Ontario, Canada.

PHILLIPS, J.M. and D.E. WALLING (1995) 'Measurement in situ of the effective particle-size characteristics of fluvial suspended sediment by means of a field-portable laser backscatter probe: some preliminary results'. Mar. Freshwater Res., 46, p. 349-357.

RICHARDS, K. (1982) *Rivers: form and process in alluvial channels*. Methuen and Co., New York, 358 p.

RILEY, G.A. (1970) 'Particulate matter in sea water'. Adv. Mar. Bio., 8, p. 1-118.

SHERMAN, I. (1953) 'Flocculent structure of sediment suspended in Lake Mead'. Trans. AGU., 34, p. 394-406.

SHIOZAWA, T.; K. KAWANA; A. HOSHIKA and T. TANIMOTO (1985) 'Suspended matter and bottom sediment in the Seto Island Sea'. Bull. Coastal Oceanog., 22, p. 149-156.

TAMBO, N. and Y. WATANABE (1979) 'Physical characteristics of flocs 1: the floc density function and aluminum floc'. Wat. Res., 13, p. 409-419.

ZAHID, W.M. and J. GANCZARCZYK (1990) 'Suspended solids in biological filter effluents'. Wat. Res., 24, p. 215-220.

On assessment of erosion and model validation

B. Hasholt
Institute of Geography, University of Copenhagen,
Øster Voldgade 10, Denmark 1350 K

Introduction

Since the early attempts to model soil erosion (e.g. Wischmeier and Smith, 1978), many new and more sophisticated models have been developed, (e.g. Nielsen and Styczen, 1986; Morgan, 1995; Boardman and Favis Mortlock, 1998). Much of this progress is due to the rapid development in EDP and the development of GIS which makes it possible to incorporate spatial distributions of important parameters and land use classes.

A similar rate of development has not taken place with respect to techniques for erosion monitoring. In many cases, it remains necessary to undertake field observations on a manual basis. In particular, dynamic observations of mass transport caused by erosion have to be based to a large extent on manual sampling strategies. Nevertheless, a number of significant advances have occurred. These include the development of data loggers capable of providing quasi-continuous data records with minimum power consumption and the development of space borne platforms which have made it possible to monitor large-scale features of erosion. Satellite images can be used as input for the computation of spatial distributions of erosion features and for creating DTMs. GIS systems, e.g. ARCINFO facilitate automatic computation of streamlines, drainage areas and contour intervals, features that make it much easier to pin point areas at risk to erosion.

The aim of this chapter is to provide a brief review of some recent methods used for monitoring erosion at different scales in Denmark. The shortcomings of the methods are described and their potential for validating the output from available erosion models is evaluated. The discussion relies mainly on the personal experiences of the author while carrying out fieldwork for individual projects or participating in joint programmes such as the NPo-programme (Nitrogen, Phosphorus and organic matter), the Danish Strategic Environmental Monitoring programme (STM) or the development of the EUROSEM model. Although Denmark is known to have only moderate erosion, it is believed that the methods, ideas and recommendations discussed are more generally applicable.

Experiences with erosion monitoring

In the following discussion, erosion monitoring at different scales is described with reference to technical problems, accuracy and its potential for helping to validate erosion models.

Splash erosion is responsible for the detachment of particles and breakdown of soil aggregates. The influence of wind speed on splash erosion has been studied using splash cups and some results are found in Pedersen and Hasholt (1995). Such studies revealed that the aspect of splash cups and slope in relation to wind direction during effective rainfall are important factors influencing the volumes of sediment collected. When such factors are taken into account it was shown that high wind speeds during rainfall, and thereby increased energy inputs, could explain outliers in the relationship between rainfall energy and the amounts of sediment detached by splash erosion. It was also demonstrated that short duration high intensity rainfall was responsible for the most significant levels of erosion. This reflects the fact that short bursts of intense rainfall produce more energy and may exceed the local infiltration capacity and thereby create Hortonian overland flow. Many rainfall intensity records comprise 5 to 10 minute intervals and thereby frequently fail to record short duration extreme storms and associated overland flow. In order to include such factors in an erosion model, rainfall data with a time resolution of 1 minute are needed together with wind speed and direction.

Recognition of the importance of overland flow led to the question of how to monitor it. In response to this problem, the author constructed a small sampler for the collection of water and sediment (see Figures 1 and 2).

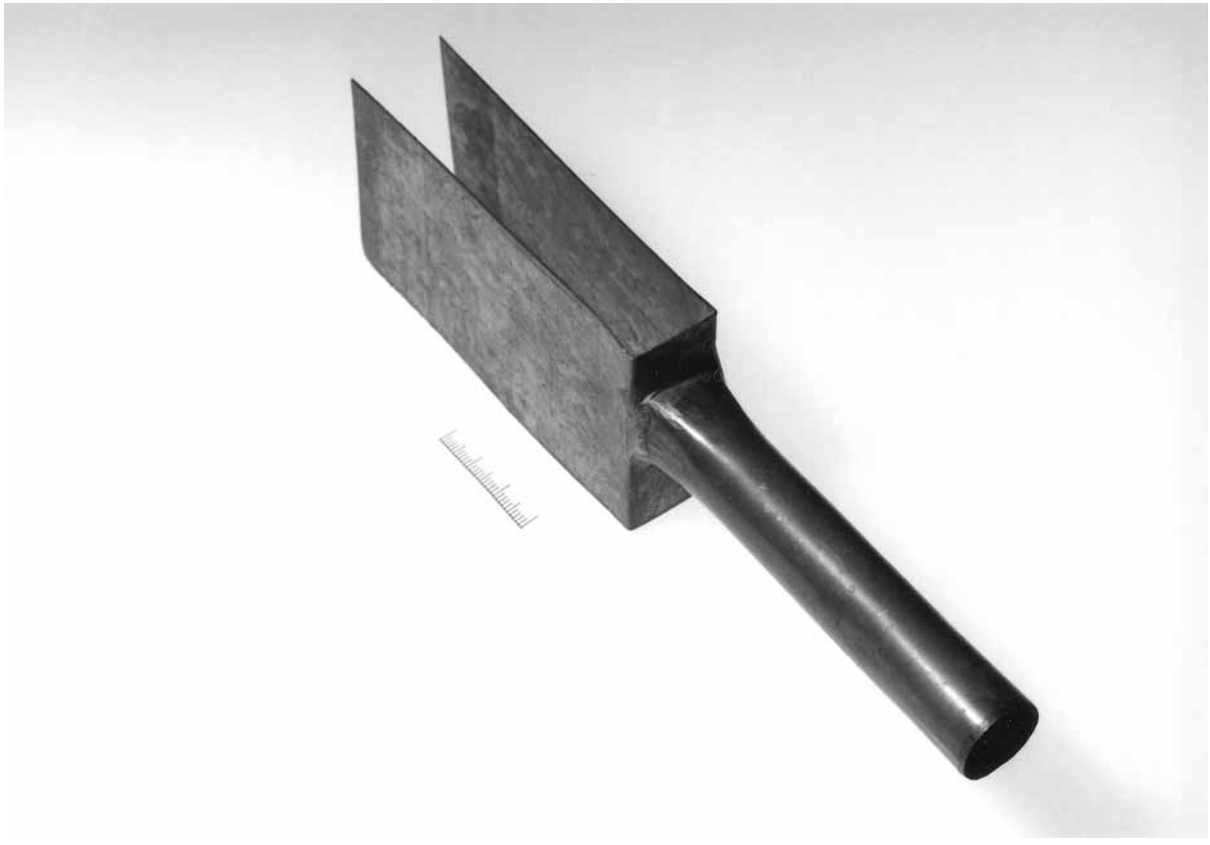

Fig.1 Mouthpiece of overland flow sampler. Water and sediment enter top left and are directed to a collecting bottle via a tube connected to the tube section of the mouthpiece. The length of the scale bar below is 3 cm

Fig.2 Overland flow sampler in measuring position, seen from above. The tube leading to the collecting bottle is seen

The small size of the sampling device is predetermined by the potential need to place the sampler in small depressions in the terrain and by the fact that it should be easy to install and should not interfere with the management of agricultural fields. The flanges in the intake section assist water intake, prevent undercutting by running water and define the width of the intake area. Knowledge of intake area is essential for making quantitative measurements of erosion, however, it is nevertheless very difficult to determine this area precisely. The time sequence of overland flow could be recorded by installing a pressure transducer in the collecting bottle. However, until now the sampler has mainly been used to prove if overland flow has taken place within a predefined area over a certain time. It is not possible with a few samplers to cover a whole slope, however, by choosing representative 'worst case' spots as locations for the samplers it is believed that it is possible to determine whether or not overland flow has occurred. 'Worst case' spots commonly coincide with the concave parts of slopes with small depressions, proto-rills or the previous pathways of running water.

Overland flow and erosion on slopes have also been monitored using Gerlach troughs. However, although some useful information has been obtained by using these sampling devices in Denmark, many problems have been experienced. Due to the size of these troughs the collection bottle must necessarily be larger and it is therefore more difficult to install. The lip of the sampler has proved difficult to insert without disturbing the soil and several cases of undercutting have been observed. In areas of frost, the lip and the whole trough can be displaced. Also the cavity for the collecting bottle is frequently disturbed by frost action and the bottle drowned because meltwater is not able to drain away. Due to its relatively small size and the difficulty of defining the contributing area, this sampler has been used mainly as an indicator of erosion and for helping to determine sediment concentration levels, which can be used for comparisons with the concentrations computed by existing models of sediment delivery.

Plot studies of erosion on slopes were initiated during a project within the NPo-programme (Hasholt et al., 1990). In each of two research catchments, two erosion plots were

installed at representative 'worst case' locations, on steep slopes close to watercourses. These plot installations consisted of a large collecting gutter at the foot of the slope. Water and sediment from the upslope watershed were collected from a slope width corresponding to the length of the gutter. Slope lengths of approx. 100 m and widths of 30-50 m were commonly used. From the centre of the gently sloping gutter, water and sediment were directed into a tank in a cellar and overflow from the tank passed through a Thomson weir. Discharge was recorded by measuring the stage in the tank. Water from the weir passed into a tipping bucket sampler from where subsamples were collected each time the bucket tipped. The whole installation had to be installed in a rather deep (2-3 m) cellar which was drained and above the groundwater surface. However, several important reservations were identified with respect to the feasibility of this preliminary plot installation. Firstly, preferential sediment transport is observed, with the result that sand, gravel and larger aggregates become trapped in the gutter whilst only silt and clay pass through to the tank, where sedimentation takes place before the tipping bucket sampler. This means that the simultaneous transport of sediment cannot be recorded adequately. After a major erosion event, the gutter has to be cleaned and the sediment collected should be weighed in order to compute the amount of sediment eroded from the slope. Therefore in spite of the high resolution of the runoff record, this installation can only record the sum erosion caused by an effective rainfall event. Consequently, this type of plot is not suited to detailed studies of erosion, which are necessary for assisting the development of time distributed erosion models. Furthermore, the results from such plot studies showed very low levels of surface runoff (only 0.1 - 1.5 % of the precipitation), whilst the erosion from these slopes was very low (less than 2 t/km^2/year), which is well below the annual load in nearby watercourses. A possible explanation for these low values could be, that despite slope steepness ranging from 4 - 12%, the use of a deep cellar at the end of the slope hinders the natural development of saturated overland flow, which is often believed to be an important mechanism for causing surface runoff.

In 1989, additional plot studies were initiated for two soil types, a Typic Hapludult and a Typic Agrudalf, at the Foulum and Ødum research stations, respectively (Schjønning et al., 1995). These plots were similar to standard Wishmeier plots and were tilled and sown with typical crops in order to test the effect of land use on the amount of erosion. The author participated with a special investigation of rill formation. In these plots a gutter was placed at the end of the slope, at a right angle to the flow and both water and sediment were collected in a plastic tank situated further down the slope and connected to the gutter by a tube. The tank and the gutter had to be emptied after a major event, or sometimes even during an event, to prevent overflow. The system proved successful, but experienced the same problems as above with respect to particle separation and sediment trapping. In order to improve time resolution, water samples were collected during events, and transmissometers were placed in the flow. The triggering of the sampling relied upon either the rise of stage in the tank, or a critical flow rate. These experiments showed that any obstruction of the water and sediment flow causes sedimentation. It was also shown that high sediment concentrations cause clogging of the sampling tubes. Therefore, because of the particle separation and the poor time resolution, these plots should only be used for validating the summed output of an erosion model and not for validating fluctuating sediment concentrations during individual runoff events.

These findings were taken into account when new investigations were initiated in 1993. One aim of the new investigations was to improve understanding of the initiation of rills under Danish conditions, whilst another aim was to design a system for the automatic recording of soil erosion. The most accurate methods for investigating erosion processes rely

upon the use of manned research plots or laboratory installations. When the installations are manned it is quite easy to collect in stream manual samples without causing the separation of particle sizes experienced with the use of some automated samplers. However, when sampling is necessary at a remote location and when the occurrence of erosion is determined by natural weather conditions instead of simulated rainfall, it is not practical to sustain manual sampling over long time periods. Therefore automation is necessary.

The following improvements were identified for the revised soil erosion plots:

(a) The system (automated plot) should be compatible with the other plots so that manual sampling of accumulated sediment could be carried out after an erosion event. A collecting tank is therefore placed in the measuring cellar.

(b) The inlet from the plot to the cellar should be sedimentation free. This means that all particle sizes and aggregates should pass through to the collecting tank, without any losses caused by sedimentation.

(c) In order to encourage natural runoff, the groundwater level around the measuring cellar should be allowed to fluctuate naturally, without any artificial drainage.

(d) The volume of water and sediment in the collecting tank should be recorded continuously.

(e) The weight of water and sediment in the collecting tank should be recorded continuously.

(f) Flow-proportional samples of water and sediment should be collected.

(g) During an erosion event, different types of erosion should be registered by use of a video-recorder.

The first version of the revised plot system and some preliminary results are described in Hasholt and Hansen (1995). Many problems were encountered and resolved. The cellar was made with corrugated steel and kept in place using the weight of the overlying soil on flanges at the bottom in order to counteract buoyancy due to groundwater fluctuations. This component of the plots has now stayed in place for 5 years without leaking, in spite of buoyancies of ca. 9 tons caused by fluctuating ground water levels. The sampler intake, built of smooth stainless steel and sloping more steeply than the surrounding plot, did not trap much sediment. An exception was seen when falling leaves were blown into it and blocked the inlet to the tube to the cellar. The weighing of the collecting tank proved reliable and accurate to ± 0.2 kg, which is acceptable for validating sediment transport during an erosion event. The recording of volume was based on the very stable construction of the collecting tank, which maintained an area of one square meter without bulging during fill-up. It was, however, not possible to monitor the stage with an accuracy better than ± 1.5 mm, equivalent to ± 1.5 kg. This is not satisfactory for detailed validation of modelled sediment delivery during a single erosion event.

Hasholt and Hansen (1995) also indicate that samples were collected by tipping part of the flume leading to the collecting tank backwards, so that the water in the flume was passed into a funnel, leading to 250 ml collection bottles placed on a conveyor belt. Flow proportional sampling was achieved by triggering the sampler on the basis of weight (e.g. every 1 kg) or stage (e.g. every 1 cm) increments. The rate of flow was computed by the datalogger using the time interval between each discrete sample. Based on this flow rate, the time for filling the sampling bottle was computed. The funnel was kept open so that the sampling bottle was 3/4 full. From recorded time and volume in the bottle a flow rate could be computed. Comparing results of sediment transport, computed by use of the discrete water samples and transport found by drying and weighing the sediment in the collecting tank, it was found that the load based on the sediment samples was up to 10 times lower than the true load. This was quite puzzling until the sampling was observed during a storm. It was observed that when the funnel tipped backwards to allow sampling, the flow was reversed

and the coarser grains were difficult to accelerate in the opposite direction. Therefore a serious particle separation took place. This demonstrated that an apparently right solution might prove wrong because an important process is overlooked.

Due to this problem, the sampler had to be modified because it is essential that the samples should be collected without problems associated with sedimentation or particle separation. Several alterations were tested, but the one that needed the least modification of the sampler was the incorporation of a 'tipping funnel'. In the no sampling position, water and sediment pass from the plot to a moveable funnel, kept over a flume leading to the collecting tank by a spring. When sampling is triggered, a solenoide causes the moving funnel to swing into position above a fixed funnel leading to the sample bottle on the conveyor belt (Hasholt et al., 1996). The installation is shown on Figures 3 and 4. This modification represented the final alteration to the automatic sampler and as a result of these changes the sediment concentrations in the samples were found to be more representative.

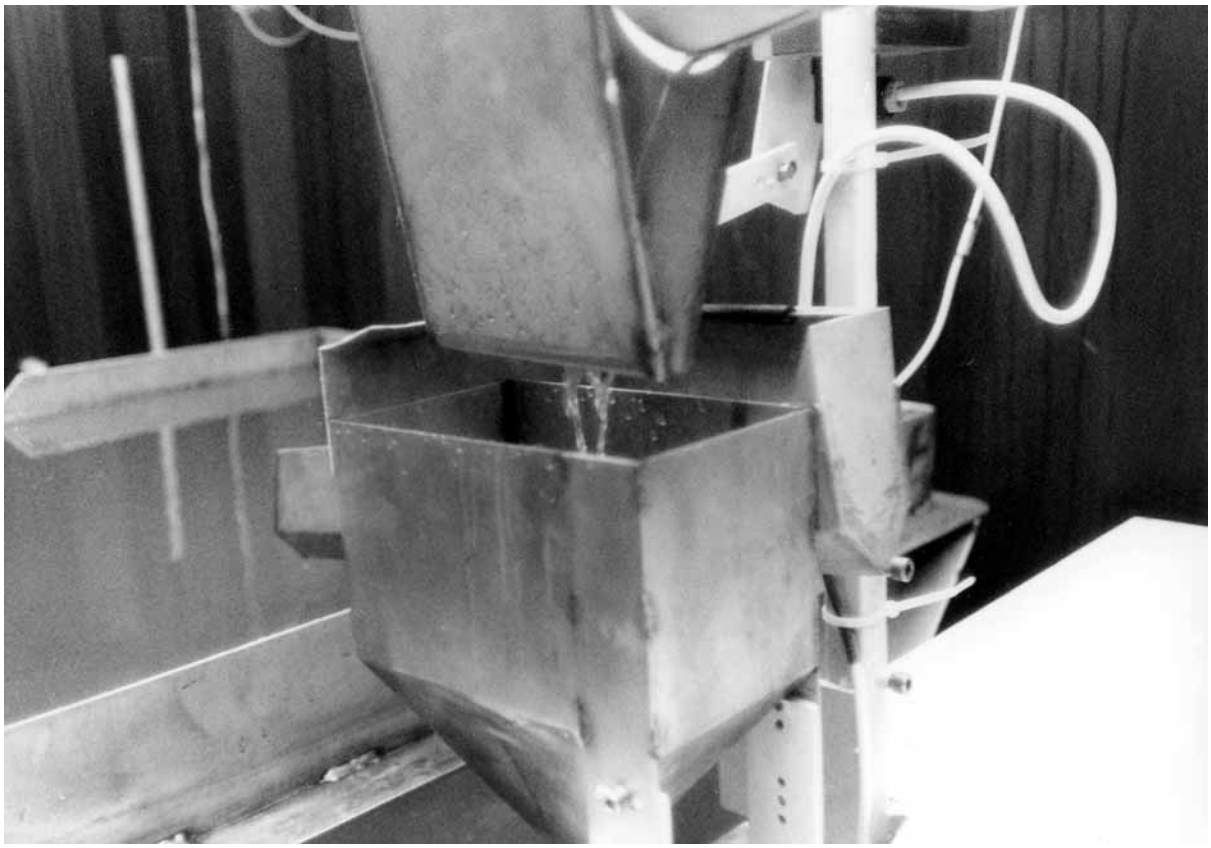

Fig.3 Sediment sampler. Inlet tube from plot enters moving funnel from top of picture. Below left is seen the flume leading to the collecting tank and the upper corner of the tank. In the centre of the picture is seen the fixed funnel leading to the sampling bottles placed on the conveyor belt

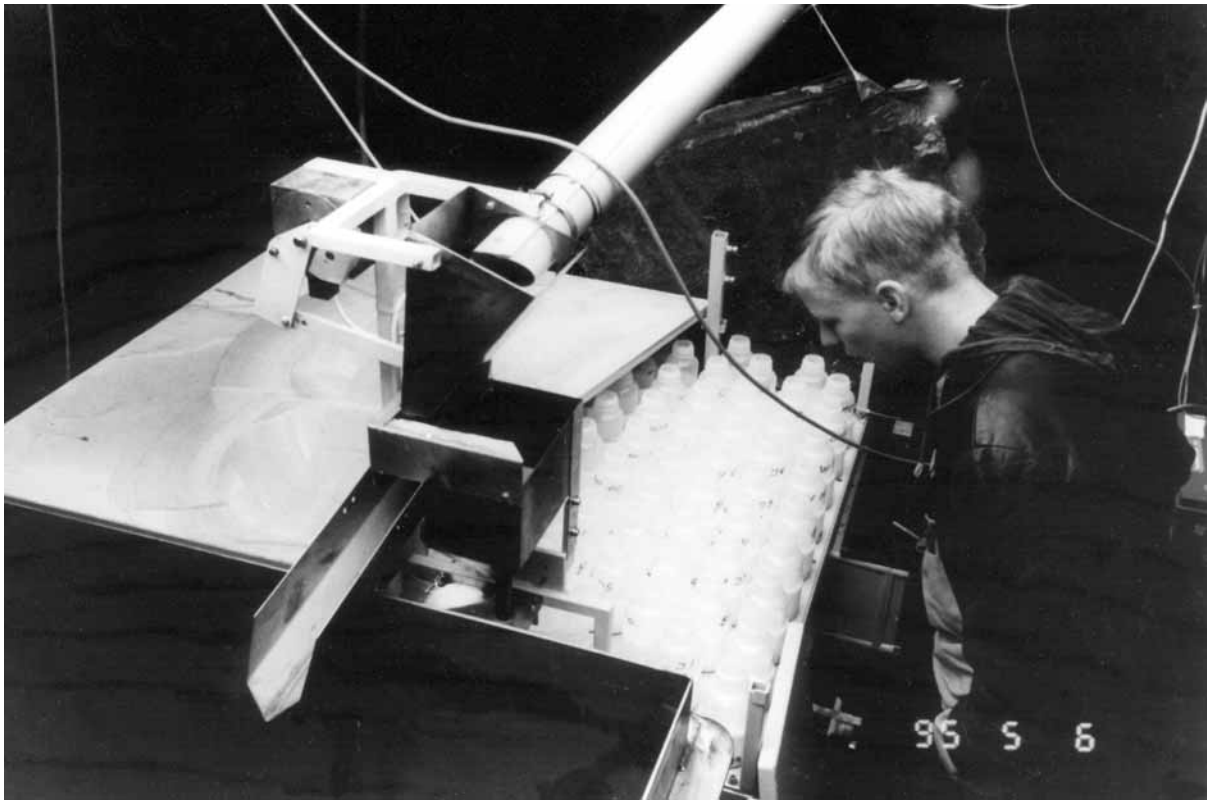

Fig.4 The moving funnel and the fixed funnel seen during sampling. Behind is seen the flume leading to the collecting tank, which is now full

This sampling equipment is useful for helping to validate sediment concentration levels predicted by the use of a model and to obtain in situ samples for the determination of aggregate grain sizes. However, it was found that the results from replicate plots situated only 10 m apart could differ by as much as 50%. Video-recording has proved useful for explaining such differences. For example, during one winter the videotapes showed that a large snowdrift formed at the intake of the instrumented plot. During snowmelt, when high concentrations and high transport rates usually occur, only low concentrations were recorded. This was because much of the water that should have run down the slope, now melted close to the intake, without being able to detach and mobilise sediment. Besides, water from the upper end of the slope was trapped in the snowdrift and depleted of its sediment. Such conditions are quite unusual, and if it had not been for the video-recording the low erosion during this snowmelt period would have been very difficult to explain.

When rills are formed, the sediment yield from a field increases significantly (e.g. Bryan, 1987; Hasholt, 1995). This knowledge is based on in situ measurements of rill volume and frequency for a defined area. The monitoring of rill erosion is very time-consuming, especially when this type of erosion is well developed on a slope. Therefore, a way to reduce the amount of surveying has to be found. The computation of the volume of soil eroded from a rill is commonly based on cross-sections measured at regular intervals along the rill and by measuring the rill length. The effect of different spacing on the estimate was tested against the 'correct' volume, based on a regular spacing of 0.5 m. It was shown, (Madsen, 1992), that a spacing of 5 m between the cross sections gave results that deviated less than 20% from the 'correct' value. The total amount of sediment eroded by rill erosion on a slope is found by multiplying the estimated volume of removed soil by the number of rills. Estimates of rill

erosion determined in this way on fields in Denmark could be as high as 2000 t/km^2 for field sizes up to 0.03 km^2 (Hasholt, 1995). This figure is probably correct to within ± 50%. It is therefore, not possible to validate the results of modelling rill erosion on a whole hillslope more rigorously, without considerable effort and time consumption. The net contribution of eroded sediment, to a watercourse situated at the foot of the slope, is found by measuring the amount of sediment accumulated in an alluvial cone at the lower end of the rill, and subtracting this volume from the volume of the rill. Determining the volume of deposited sediment is more difficult than determining the total volume removed from the rill, because the margins are often more diffuse. The resulting estimates of net transport are therefore less accurate. Results from Denmark indicate that although sedimentation is often found at the foot of a slope, sediment released by rill erosion is frequently routed directly to watercourses. However, due to the limited accuracy of field measurements of sediment delivery, it is difficult to test the ability of a model to route the sediment correctly.

The inclusion of rill erosion is different from one model to another, e.g. in EUROSEM the occurrence of rills has to be specified in advance, whilst in the model by Nielsen and Styczen (1986) a measure of rill formation is built in. Concerning the importance of rill erosion, it is essential for model validation to check if rills are actually present if predicted by the model. Data from the NPo-project has been used to verify predictions of rill occurrence using soil erosion models (Hasholt and Styczen, 1993). Although there is a reasonable agreement between the predicted and recorded occurrence of rills, it is meaningful firstly, to run a model and, secondly, to carry out field checks at the precise spots where the model predicts rill erosion.

Erosion monitoring at the catchment scale is described in Hasholt (1987, 1992) and Sibbesen et al. (1996). Such investigations have demonstrated that the sampling or monitoring frequency at the basin outlet should be high enough to ensure that no peak events are left unrecorded. In Denmark, investigations have indicated that one to two daily samples collected using an automatic sampler are sufficient to give annual sediment load estimates correct to within ± 5%. This was tested by use of transmissometers that measured every 2 minutes. However, daily samples are not satisfactory for describing sediment transport during single events and interpolation of the sediment concentration record is therefore necessary. Alternatively, automatic samplers can be programmed to pool more frequent samples into a single bottle, to exploit the small number of sample bottles comprising most samplers. Another possibility is to collect flow- or load-proportional samples. The amount of sheet erosion in a catchment can be determined by measuring erosion contributions e.g. bed- and bank erosion and rill erosion and by subtracting these from the total flux estimated for the basin (Hasholt, 1991). This approach is very labour intensive and relies upon the precondition that material released in the catchment will pass the monitoring station at the outlet within the recording period. The construction of sediment budgets is therefore easier in smaller catchments, e.g. with areas up to ca. 10 km^2. Validating sediment routing by measuring the individual components of sediment delivery is therefore a difficult task. Use of tracers offers considerable potential in this respect, but because of rigorous restrictions on the use of tracers this approach has not been tested in Denmark.

Discussion

The above discussion has briefly described a spectrum of available methods for monitoring soil erosion and sediment delivery. Despite a range of shortcomings, the methods described provide satisfactory qualitative and quantitative information. However, a major constraint on their widespread use is that the methods are often tedious, and consume large amounts of manpower and time. Nevertheless, more sophisticated methods are rather expensive because of high instrumentation costs. In combination, such constraints commonly prevent coverage of larger catchments. The time resolution of sampling procedures is critical with respect to the timescale of the processes under scrutiny e.g. sediment delivery during discrete storms. Another critical temporal consideration is that the time of storm arrival at a certain spot is difficult to predict with the result that considerable resources must be spent on automatic monitoring equipment. Another critical factor is the timing of tillage operations by farmers. Even within a rather small area in Denmark, there can be large individual differences in the timing of ploughing. As a result of this 'time window', longer-term monitoring programmes are more useful for helping to ensure that such activities are not missed. This again stresses the importance of costly readiness and the advantages of automatic monitoring equipment. Above all, it is important to realise that it is not possible to fulfil the ideal demands of a complete monitoring programme for erosion over larger areas e.g. catchments. Therefore there is a need for guidelines to assist the determination of 'optimal' monitoring strategies. Some thoughts on this problem are dealt with above. The following discussion attempts to demonstrate how the collection of representative point data by erosion monitoring programmes could be combined with the spatial extrapolation capabilities of modelling in a fruitful manner.

The performance of a model is measured by its ability to reproduce, within certain limitations, the modelled part of the physical environment and the processes taking place. It is essential that the reproduction is in accordance with physical laws and able to produce results that are quantitatively correct. The closest approximation to these ideal requirements is found in physically based fully distributed models ('white box models'). At the end of the day there must be a compromise between required data and the available funding. Therefore simple models, e.g. regression based ('black box') models are found to be satisfactory in many cases, especially for technical purposes. The present discussion focuses mainly upon more sophisticated modelling, partly because, from a scientific point of view, this is the most interesting, and partly because it is believed that the need for a more complete understanding of our physical environment will continue to grow in the future.

The process of evaluating a model in relation to the demands or requirements is often termed model validation. There is no acknowledged standard validation procedure. Examples of validation procedures can be found in Refsgaard and Knudsen (1996) and Quinton (1994), referring mainly to the EUROSEM model, but also with some general comments. According to Quinton (1994) it is very important to relate the validation to the actual purpose for which the model is designed. This is both true and fair, but in this contribution a more " idealistic" approach is presented.

There are a number of essential components in the 'ideal' physically distributed model. The more rigorous tests the model is able to pass, the better the model. These essential considerations include:

1. Incorporation of relevant physical processes.
2. Correct proportioning of relevant physical processes.
3. Correct representation of the interaction between processes, including feed back loops.

4. Accurate quantification of the relevant physical processes.
5. Quantitative results referring to 3. above.

What are the main criteria for fulfilling the above demands? Generally, the fulfilment of 1-3 can be judged by experts trained within the field of global geomorphology. It is obvious that models operating at higher latitudes and in high mountains should incorporate the effects of snow and processes in frozen soils in order to be representative. In unknown areas a certain time must be spent on skilled observation, before it can be confirmed that criteria 1-3 are satisfied. This process could be termed 'visual validation'. The authors personal experiences show that this can partly be obtained by the use of automated digital cameras or video recorders or on a larger scale by the use of remote sensing, especially as it is rarely possible to be 'on the right spot at the right time'. A way of optimizing the use of 'visual validation' procedures and of monitoring equipment, is to identify critical thresholds and key areas, for instance 'worst case' areas, or indicator areas. An example of this could be to check the occurrence of surface runoff at a given spot at a given time. As surface runoff is a prerequisite for major erosion, this could be considered a critical test. Another example is the formation of rills. It is now well established that erosion rates increase by several orders of magnitude when rills replace sheet erosion. Therefore the inclusion of rill erosion in a model is important, but the ability of the model to predict accurately where and when rills will develop is even more important. This is again a crucial test of model performance. Equipment should in the first phase be located at such key locations where it can be used to test the critical behaviour of a catchment system and to quantify the maximum values of erosion. In some cases this information is enough, especially when the maximum values are below sustainable limits for soil loss. However, a further consideration is the collection of representative data for validating modelled erosion estimates for larger areas or whole catchments. If a model passes these first tests satisfactorily, it could be assumed with some confidence that it works in other areas too.

The model could then be used to point at locations for further testing, and an interactive process between model creation, testing and direct monitoring should take place. This relies upon co-operation between the modeller and the monitoring fieldworker. In order to limit the amount of work and data requirements, a number of available models are event-based. Many of these models are very sensitive to the starting conditions or the initialization of the model e.g. EUROSEM (van der Keur and Hasholt, 1996). A way to overcome this is to run erosion models 'on top' of hydrological models, e.g. the SHE model, so that erosion might be computed 'on line'. A validation of the model could then be carried out by field checks of measured versus predicted erosion after an erosion event. This will cost more computer time, but the costly need for readiness can be avoided.

A topic requiring further research is the routing of sediment through entire catchments. Although useful in this respect, grid-based models are sensitive to grid size and have some shortcomings in producing correct slope angles and also in routing across grid borders and in watercourses. On the monitoring side it has been shown that very frequent sampling is needed to give a satisfactory description of the sedigraph through time. Although transmissometers might overcome some of the problems, they are very sensitive to changes in grain size, and frequent calibration is necessary. Consequently, there is certainly a need for new instrumentation and models for measuring or predicting sediment load. Co-operation between modeller and field worker should prove useful in this respect.

Acknowledgements The research described in this chapter is sponsored by the NPo-Project, by EC within the STEP programme, the NORPHOS programme and the Danish strategic environmental programme, STM.

Bibliography

BOARDMAN, J. and FAVIS-MORTLOCK, D.T. (eds.) (1998) *Modelling soil erosion by water*. Springer-Verlag NATO-ASI Series I-55, Berlin.

BRYAN, R.B. (1987) 'Processes and significance of rill development'. Rill Erosion. Catena Supplement, 8. p. 1-15.

HASHOLT, B. (1988) 'On identification of sources of sediment transport in small basins with special reference to particulate phosphorus'. In: M.P. Bordas and D.E. Walling (eds.), *Sediment budgets* (Proc. International Symposium, Porto Alegre, December 1998). IAHS Publ. No. 174, p. 241-250.

HASHOLT, B.; H.B. MADSEN; H. KUHLMAN; A.C. HANSEN and S.W. PLATOU (1990) 'Erosion og transport af fosfor til vandløb og søer.' *Npo-forskning fra Miljøstyrelsen C12*.

HASHOLT, B. (1991) 'Influence of erosion on the transport of suspended sediment and phosphorus'. In: N.E. Peters and D.E. Walling (eds.), *Sediment and stream water quality in a changing environment: trends and explanation* (Proc. International Symposium, Vienna, August 1991). IAHS Publ. No.203, p. 329-338.

HASHOLT, B. (1992) 'Monitoring sediment load from erosion events'. In: J. Bogen, D.E. Walling and T.J. Day (eds.), *Erosion and sediment transport monitoring programmes in river basins* (Proc. International Symposium, Oslo, August 1992). IAHS Publ. No. 210, p. 201-208.

HASHOLT, B. and M. STYCZEN (1993) 'Measurement of sediment transport components in a drainage basin and comparison with sediment delivery computed by a soil erosion model'. In: R.F. Hadley and T. Mizuyama (eds.), *Sediment problems: strategies for monitoring, prediction and control* (Proc. International Symposium, Yokohama, July 1993). IAHS Publ. No.217, p. 147-159.

HASHOLT, B. (1995) 'Formation of rills and their contribution to sediment yield'. Chapter 7 In: *Surface runoff, erosion and loss of phosphorus on two agricultural soils in Denmark-plot studies 1989-92*. SP-report No. 14, 1995, Danish Institute of Plant and Soil Science, Foulum.

HASHOLT, B.and B.S. HANSEN (1995) 'Monitoring of rill formation'. In: W. Osterkamp (ed.), *Effects of scale on interpretation and management of sediment and water quality* (Proc. International Symposium, Boulder, July 1995). IAHS Publ. No. 226, p. 285-291.

HASHOLT, B.; B.S. HANSEN and E. SIBBESEN (1996) 'An automatic system for continuous monitoring of rill development, surface runoff and delivered sediments'. In: *Proc. sediment and phosphorus*. NERI Tech. Report No.178, p. 33-36.

KEUR, P.V.D. and B. HASHOLT (1996) 'Validation of EUROSEM in a Danish Catchment'. Poster, STEP meeting in Bari, Italy.

MADSEN, S. (1992) Unpubl. rill erosion data.

MORGAN, R.P.C. (1995) *Soil erosion and conservation* . Longman Group, UK.

NIELSEN, S.A. and M. STYCZEN (1986) 'Development of an areally distributed soil erosion model.' In: *Proc. Nordic hydrological conference* (Reykjavik, August) p. 797-808.

PEDERSEN, H.S. and HASHOLT, B.(1995) 'Influence of wind speed on rainsplash erosion'. Catena, 24, p. 39-54.

QUINTON, J.N. (1994) 'The validation of physically-based erosion models, with particular reference to EUROSEM'. In: R. Rickson (ed.), *Conserving soil resources: European perspectives*. CAB International, Wallingford, p. 300-313.

REFSGAARD, J.C. and J. KNUDSEN (1996) 'Operational validation and intercomparison of different types of hydrological models'. Wat. Resour. Res., 32, p. 2189-2202.

SCHJØNNING, P.; E. SIBBESEN; A.C. HANSEN; B. HASHOLT; T. HEIDMANN; M.B. MADSEN and J.D. NIELSEN (1995) *Surface runoff, erosion and loss of phosphorus at two agricultural soils in Denmark.* SP Report No. 14, DIPSS.

SIBBESEN, E.; B.S. HANSEN; B. HASHOLT; C. OLSEN; P. OLSEN; P. SCHJØNNING and N. JENSEN (1996) 'Water erosion on cultivated areas - field monitoring of rill erosion, sedimentation and sediment transport to surface waters'. In: *Proc. sediment and phosphorus*. NERI Technical Report No. 178, p. 37-40.

WISCHMEIER, W.H. and D.D. SMITH (1978) *Predicting rainfall erosion losses*. USDA Agricultural Research Service Handbook 537.

Using ^{137}Cs measurements to test distributed soil erosion and sediment delivery models

D. E. Walling, Q. He
Department of Geography, University of Exeter,
Exeter, EX4 4RJ, UK

Introduction

Recent advances in the use of Geographical Information Systems (GIS) and Digital Elevation Models (DEMs) have promoted the development and application of spatially distributed models of soil erosion and sediment delivery at the catchment scale. (e.g. Lane and Nearing, 1989; Morgan et al., 1992; Moore et al., 1993; Ferro and Minacapilli, 1995; De Roo et al., 1996; Ferro, 1997; De Roo, 1998; Young et al., 1987, 1989; Wicks and Bathurst, 1996; Zhang et al., 1996; Bouraoui et al., 1997; Kothyari and Jain, 1997; Watson et al., 1998; Parson et al., 1998; Pitts et al., 1999; Choi and Blood, 1999; Perrone and Madramootoo, 1999). Use of a distributed approach permits both the spatial heterogeneity of catchment land use, soil properties and topography and the spatial variability and interaction of erosion and sediment delivery processes to be represented, and can therefore provide spatially distributed predictions of soil erosion and sediment redistribution for complex three-dimensional terrain (e.g. Moore et al., 1993; Kothyari and Jain, 1997; De Roo, 1998; Parson et al., 1998).

An important limitation of these developments has, however, been the lack of data for model validation and, more particularly, for validating the spatial pattern of sediment redistribution *within* a catchment predicted by the model. Validation of such distributed models has commonly been restricted to comparison of measured and predicted catchment outputs, as represented by storm hydrographs and associated sedigraphs and both event and longer-term sediment yields. Close agreement of modelled and measured outputs will afford some degree of validation, but it cannot provide conclusive validation of the internal functioning of the models and thus of the predicted erosion and deposition rates. Close correspondence between observed and predicted outputs could still be obtained in situations where both the magnitude and the pattern of erosion and deposition rates within the catchment predicted by the models differed substantially from the actual values. For example, over-estimated erosion rates or the occurrence of erosion over a larger area than existing in reality could be balanced by over-estimation of the deposition rates or the area experiencing deposition. Equally, under-estimated erosion rates or under-prediction of the area experiencing erosion could be balanced by under-estimation of the deposition rates or the area

experiencing deposition. Spatially distributed information on erosion soil redistribution rates is an essential requirement for rigorous testing of existing distributed erosion and sediment yield models. Furthermore, future refinement and development of distributed erosion and sediment delivery models will depend heavily on the availability of a means of validating both the magnitude and the spatial patterns of erosion and sediment deposition rates predicted by the models. The use of fallout ^{137}Cs measurements to quantify soil redistribution at the catchment scale affords one means of assembling spatially distributed information on longer-term rates of soil redistribution within a catchment that could be used to meet this need.

Caesium-137 (Cs-137 or ^{137}Cs) is a man-made radionuclide (half-life 30.2 years) that was introduced into the environment primarily by the atmospheric testing of thermonuclear weapons during the period between the mid 1950s and the early 1970s. On reaching the ground surface, the resulting ^{137}Cs fallout was strongly adsorbed by soils and sediments and its subsequent redistribution within the landscape was primarily associated with the redistribution of soil and sediment particles through physical processes, such as water-induced soil erosion. Deviation of the current spatial pattern of ^{137}Cs inventories within a catchment from that associated with the original fallout input will therefore directly reflect the redistribution of soil and sediment particles within the catchment during the period between the fallout input and the time of collection of soil cores for ^{137}Cs analysis. The potential for using ^{137}Cs measurements in soil erosion and sediment budget investigations has attracted increasing attention in recent years (cf. Ritchie and McHenry, 1990; IAEA, 1998; Walling and Quine, 1990, 1992, 1995; Walling, 1998; Walling and He, 1999). Studies undertaken in a wide range of environments in many different areas of the world have demonstrated that ^{137}Cs measurements afford a valuable means of estimating medium-term rates of soil loss and sediment deposition, that has many advantages over conventional monitoring techniques. These advantages include the potential for deriving retrospective estimates of erosion and deposition rates based on a single site visit and for assembling distributed information for individual points in the landscape that can be used to study spatial patterns of soil redistribution (cf. Walling, 1998; Walling and He, 1999)

The potential for using soil ^{137}Cs data to calibrate and validate distributed soil erosion and sediment delivery models has been recognised by several workers in recent years (e.g. De Roo and Walling, 1994; Chappell, 1996; Govers et al., 1996; Ferro, 1997; He and Walling, 1998; Walling and He, 1998), but exploitation of this potential has to date been limited. This contribution presents some preliminary results from a study undertaken in a small agricultural catchment near Crediton, Devon, UK, aimed at using ^{137}Cs measurements to test and validate four distributed models, including, a topography-based sediment delivery model, a topography-driven soil erosion model, and the AGNPS and ANSWERS models. Two approaches have been employed. The first involves using the ^{137}Cs measurements to obtain spatially distributed estimates of soil redistribution rates within the catchment that can be used alongside measurements of catchment output for model validation, whilst the second involves coupling an erosion and sediment redistribution model with a model of ^{137}Cs redistribution and testing the ability of that model to reproduce the measured pattern of ^{137}Cs inventories.

Study site and data acquisition

Site description

The study focused on the small (0.52 km^2) Keymelford catchment located near Crediton in Devon, UK. The topography of the catchment is depicted in Figure 1. The catchment soils are typical loamy and gravelly brown earths developed on Permian breccias and conglomerates (Crediton series). Cultivated land accounts for ca. 64% of the catchment, and the remaining area is under permanent pasture. The main crops are maize and winter barley. The catchment comprises a single valley, drained by a small first order tributary, and has a mean slope of ca. 14%. The mean annual precipitation over the catchment is ca. 800 mm, and most storm runoff events occur during the winter season, which extends from November to February. Fields used for growing maize are commonly left bare during the winter and these frequently experience significant soil loss.

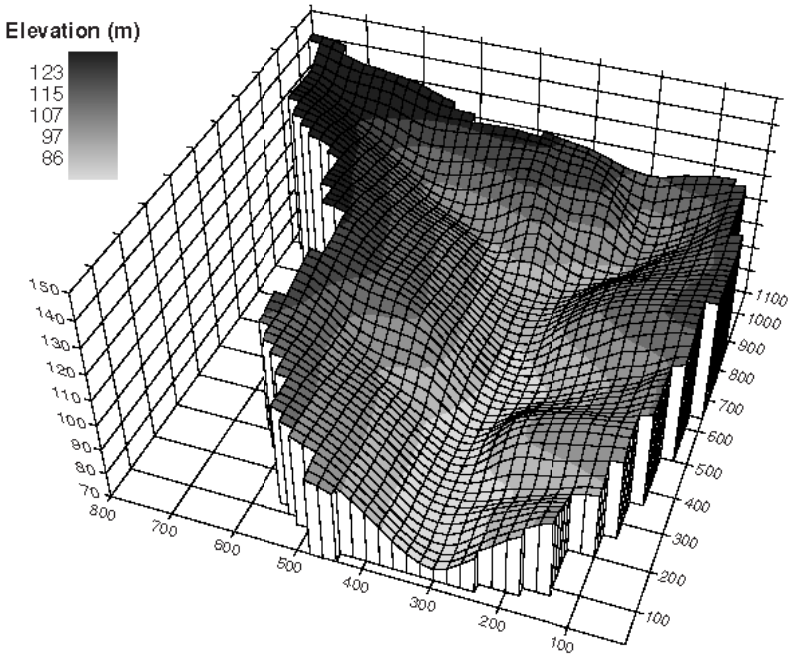

Fig. 1 A DEM of the Keymelford catchment

Instrumentation

From late 1996, a rain gauge was installed within the catchment to collect the precipitation data which are required as input to the AGNPS and ANSWERS models. To measure the runoff and sediment output associated with individual storm events, water level and turbidity sensors coupled to a data logger and two EPIC automatic samplers were installed at the catchment outlet. The automatic samplers were programmed to collect individual water samples at regular 8 hourly intervals and at 15 minute intervals during storm events. Measurements of suspended sediment concentration undertaken on these samples were used to calibrate the turbidity sensor and the resulting continuous record of suspended sediment

concentration was used in conjunction with the record of water discharge to calculate the suspended sediment output from the catchment associated with individual storm events and the overall study period.

Collection of sediment and soil samples

Suspended sediment samples were collected from the main stream during storm events. Analysis of these samples provided information on the ^{137}Cs content and grain size composition of mobilised sediment, which is needed when converting the values of ^{137}Cs inventory obtained for soil cores collected from the catchments to estimates of soil redistribution rates.

To document the spatial pattern of soil redistribution within the study catchment and the longer-term soil loss from the catchment and the associated sediment delivery ratio, soil samples were collected from both cultivated and pasture fields within the catchment for ^{137}Cs analysis. The soil sampling programme involved both slope transects and detailed grid-based coring in selected fields. Soil cores were collected using a motorised percussion corer equipped with a 6.9 cm diameter core tube. The corer penetrated to a depth of ca. 60 cm and a small sample was collected from the base of each core for subsequent radionuclide assay, in order to ensure that the core had penetrated to the full depth of the ^{137}Cs profile. Samples of surface soil were also collected immediately adjacent to the coring points for analysis of grain size composition. The local ^{137}Cs reference inventory was established by collecting a series of bulk cores from stable non-eroding areas in the pasture fields. For the slope transects, soil cores were collected from representative slope profiles in the fields at a spacing of 12 m. Only transects were used for sampling pasture fields. In the case of a ploughed field at Higher Walton Farm, more detailed sampling was undertaken. Bulk soil cores were collected at the intersections of a 20 m grid, and additional cores were collected from areas characterised by marked topographic change, in order to increase the representativeness of the sampling. A detailed topographic survey of both coring locations and the entire field was undertaken in parallel with the coring programme, using an electronic theodolite. These survey data were used to create a DEM of the field for use in subsequent data analysis and modelling.

Sample analysis

All soil cores and the samples of suspended sediment recovered from water samples collected during storm events were air-dried, ground and homogenised prior to measurement of their ^{137}Cs content by gamma-spectrometry. The measurements were undertaken using high resolution coaxial HPGe detectors. Cs-137 concentrations were obtained by measuring the activity at 662 keV. Count times were typically ca.10 hours and produced values of ^{137}Cs activity with a precision of ca. ±10% at the 95% level of confidence. Measurements of the absolute grain size composition of samples of surface soil and suspended sediment were undertaken using sieves and laser diffraction equipment, after appropriate chemical pre-treatment, including removal of the organic fraction and chemical dispersion.

Collection of other data required by the AGNPS and ANSWERS models

For both the AGNPS and the ANSWERS models the catchment to which the model is applied is subdivided into square cells and values for various parameters are assigned to each individual cell. Surface runoff and sediment mobilisation for individual storm events are simulated for each cell and routed to the basin outlet. A spatially distributed pattern of runoff and sediment generation and transfer is therefore obtained. The present study focused on testing and validating the sediment generation and routing components of the two models. Since detailed calibration of the two models for the study area was beyond the scope of the study and emphasis was placed on testing the consistency between the model-simulated and the observed data, values for some of the model parameters, such as the SCS Curve Number, the Manning coefficient, the K, C, and P factors from the USLE, the surface condition constant, total porosity, field capacity, antecedent soil moisture, were estimated using the guidelines suggested in the manuals for the models and the methods recommended by Wischmeier and Smith (1978).

The topographic data required for the study catchment by the AGNPS and ANSWERS models were obtained from the Ordnance Survey, in DTM format at a resolution of 10 m, both latitudinally and longitudinally. These data were used to generate topographic attributes including slope, slope curvature, flow direction and length, for each individual cell using the cell-based modelling tool provided by ARC/INFO GIS.

Documenting the spatial pattern of soil redistribution rates using ^{137}Cs measurements

For the field at Higher Walton Farm, where detailed ^{137}Cs sampling was undertaken, a DEM of the field was created from the surveyed elevation data using the cell-based modelling tool of the ARC/INFO GIS. This involved discretization of the study area into 8m×8m grid cells and application of the SPLINE surface interpolation method to the elevation data. The height data were expressed relative to an arbitrary datum. Figure 2 presents the DEM for the part of the field that represents a small single-outlet mico-catchment. A catchment unit is required by the

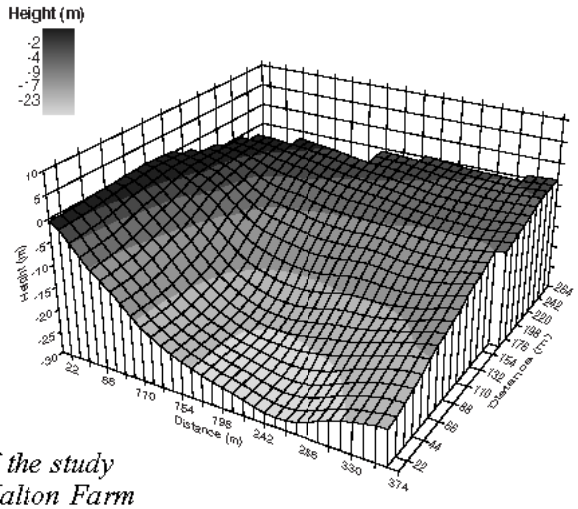

Fig. 2 A DEM of the study area at Higher Walton Farm

AGNPS and ANSWERS models and this area was used for testing all four distributed models. Figure 3A depicts the interpolated distribution of ^{137}Cs inventories within the field based on the measurements undertaken on the bulk soil cores. Significant spatial variability exists in these inventory values. Areas with reduced ^{137}Cs inventories are found along the ridge top and valley side, whilst areas located in depressions along the valley bottom are characterised by higher ^{137}Cs inventories. The average ^{137}Cs inventory for the field is ca. 2257 Bq m^{-2}.

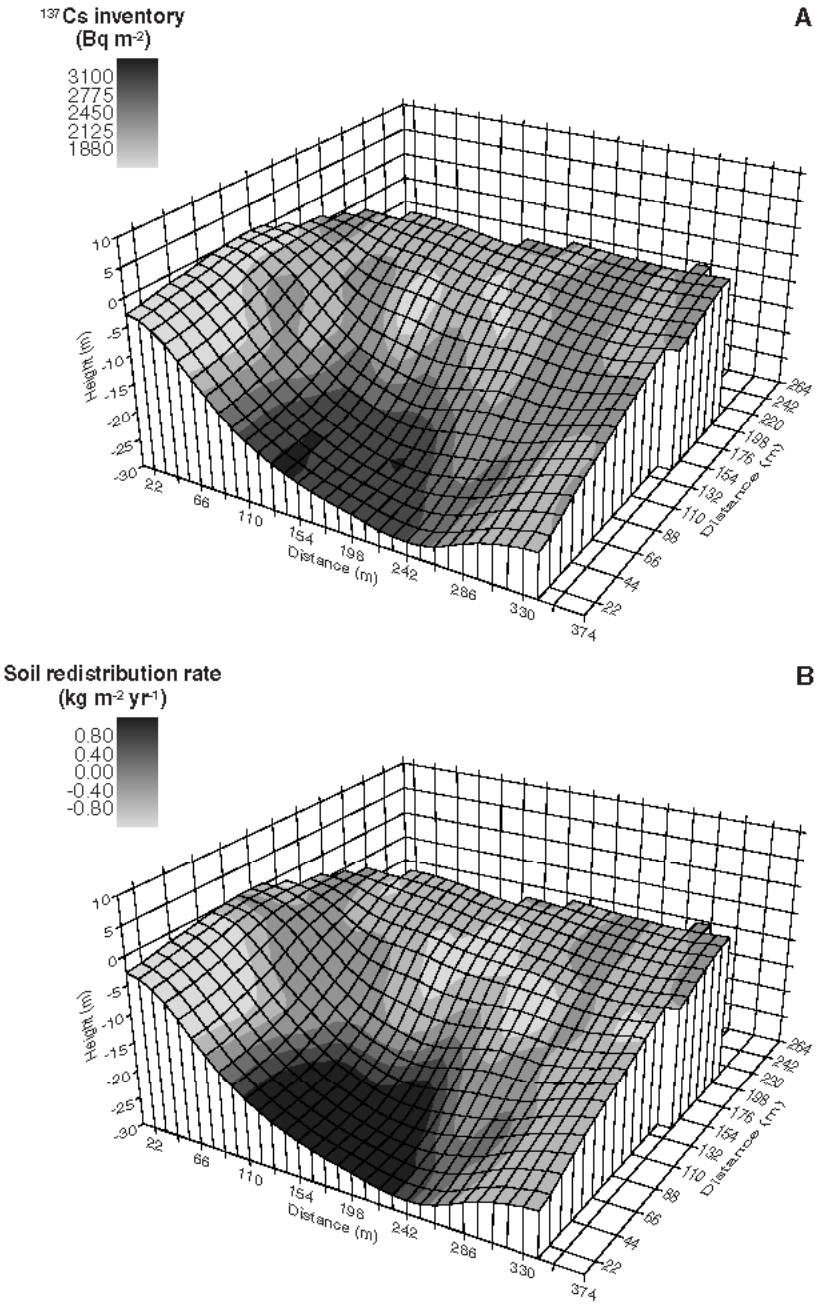

Fig. 3 The spatial distribution of ^{137}Cs inventories (A) within the study area at Higher Walton Farm and the soil redistribution rates (B) derived from the ^{137}Cs data using a mass balance approach

The estimated local ^{137}Cs inventory was estimated to be ca. 2500 Bq m^{-2} at the time of sampling, indicating that ca. 10% of the direct atmospheric ^{137}Cs input had been lost from the field as a result of soil loss associated with erosion.

A number of approaches have been employed to convert ^{137}Cs measurements into quantitative estimates of erosion and deposition rates for cultivated soils (cf. Walling and Quine, 1990; Walling and He, 1997, 1999). These existing methods include both empirical relationships and theoretical models and accounting procedures. Of these approaches, use of a mass balance model is arguably the most reliable, and in this study the mass balance model described by Walling and He (1997, 1999) has been employed to estimate the soil redistribution rates from the ^{137}Cs inventories obtained for the sampling points in the study field. This model provides a more realistic representation of the fate of ^{137}Cs in cultivated soil than many other mass balance algorithms, since it takes account of the fate of freshly deposited fallout, before its incorporation into the plough layer by cultivation. The resulting spatial distribution of soil redistribution rates within the study field is illustrated in Figure 3B. The mean erosion rate for the eroding areas was estimated to be 0.62 kg m^{-2} $year^{-1}$ (or 6.2 t ha^{-1} $year^{-1}$), and the mean deposition rate for depositional areas was 0.74 kg m^{-2} $year^{-1}$ (or 7.4 t ha^{-1} $year^{-1}$). A sediment delivery ratio of 0.66 was estimated for the micro-catchment.

The same approach was applied for the fields where cores had been collected from representative transects. The soil redistributon rates estimated for the transects were assumed to reflect those of the individual fields. Based on the soil redistribution rates estimated from both the transects and the detailed grid-based coring, the overall sediment delivery ratio for the Keymelford catchment (Figure 1) was estimated to be 0.54.

The data presented in Figure 3B afford one basis for validating existing soil erosion and sediment delivery models, by assessing their ability to replicate both the magnitude and the pattern of the erosion and deposition rates. It is, however, important to recognise that the estimates of erosion and deposition rates derived for the mico-catchment from the ^{137}Cs inventories represent longer-term averages (i.e. ca. 40 years) and that any model being tested would need to be run for a long period or with synthetic input data that were representative of the longer-term. Furthermore, the estimates of soil redistribution rates derived from ^{137}Cs measurements are themselves dependent on the conversion model used. Use of the spatial pattern of ^{137}Cs inventories shown in Figure 3A therefore arguably offers a better basis for model validation, if the erosion and soil redistribution model can be coupled with a model of ^{137}Cs redistribution.

The distributed soil erosion and sediment delivery models

The four distributed erosion and sediment delivery models tested using the ^{137}Cs measurements undertaken within the study catchment are outlined below.

A topography-based sediment delivery model

Spatial variability of both soil erosion and sediment transfer will occur at the catchment scale, due to interaction between soil erosion and sediment transport processes and the catchment topography and the spatial variability of soil properties and other catchment characteristics. A proportion of the eroded sediment will be transported to the catchment outlet, while a proportion may be deposited within the catchment. Recently, Ferro and Minacapilli (1995)

have developed a spatially distributed sediment delivery model for small catchments. In this model, a basin is divided into morphological units and the mean annual sediment delivery ratio D_i for the ith unit is related to its hydraulic path to the catchment outlet:

$$D_i = e^{-\beta t_{p,i}} = e^{-\beta \sum_{j=1}^{N_i} \left(\lambda_{i,j} / \sqrt{S_{i,j}} \right)} \quad (1)$$

where β is a constant, $t_{p,i}$ is the travel time of sediment to the basin outlet from the unit and $\lambda_{i,j}$ and $s_{i,j}$ are the length and slope of the jth morphological unit (with total number N_i) located along the hydraulic path. Ferro and Minacapilli (1995) tested several soil loss models in a number of basins in Italy, and found that the basin sediment delivery ratio D_b can be expressed as:

$$D_b = \sum_{i=1}^{N_p} e^{-\beta t_{p,i}} A_i / \sum_{i=1}^{N_p} A_i = e^{-1000 \beta \alpha_b} \quad (2)$$

where A_i is the soil loss from the ith unit, and N_p is the total number of morphological units. In Equation (2), α_b is a constant reflecting the topography of the catchment and is independent of the soil loss model selected. α_b is a measure of the efficiency of the basin in transporting sediment to its outlet. Once the basin sediment delivery D_b is known, the parameter β can be determined from Equation (2). Ferro (1997) has validated this model by comparing the model-predicted sediment yield from each morphological unit within a small Australian catchment with the ^{137}Cs loss relative to the local reference inventory. Further work is, however, required to test the validity of the model for other small catchments. Furthermore, since sediment yield is not necessarily a linear function of the ^{137}Cs loss relative to the reference inventory, a more rigorous approach to using ^{137}Cs measurements to validate the model would involve use of the rates and pattern of soil redistribution derived from the ^{137}Cs measurements. This approach is adopted here.

A topography-driven soil erosion model incorporating water erosion and tillage

In addition to rainfall erosivity and soil physical and chemical properties, topography can be expected to exert a primary control on soil erosion and sediment delivery (cf. Moore and Burch, 1986). Based on work reported by Kirkby et al. (1987), Govers et al. (1996) have proposed the following topography-driven transport-limited sediment transport function representing soil redistribution by both water erosion and tillage:

$$F_Q = \phi_1 (\sin \beta)^m S^n + \phi_2 \sin \beta \quad (3)$$

where F_Q (kg m^{-1} year^{-1}) is the sediment flux exported from a unit contour length downslope, β (°) is the angle of steepest slope, S (m^2) is the upslope contributing area, and m and n are constants. The first term on the right hand side of Equation (3) represents sediment transported by overland flow and the second term sediment transported by tillage movement.

Values for the constants ϕ_1 and ϕ_2 will be dependent on the cultivation methods, the rainfall regime, soil properties and the unit system adopted.

The AGNPS and ANSWERS models

The AGNPS and ANSWERS distributed soil erosion and sediment delivery models have been widely used in many areas of the world for studying erosion and sediment yield from agricultural catchments for individual storm events (cf. Beasley et al., 1982; Bouraoui et al., 1997; Young et al., 1987, 1989; Lenzi and Di Luzio, 1997; Rode and Frede, 1997; Perrone and Madramootoo, 1999). These models adopt a distributed representation of sediment mobilisation and transport within a catchment and therefore generate the spatial pattern of sediment redistribution within the catchment.

Testing the models using ^{137}Cs measurements at the micro-catchment scale

Although the estimates of soil redistribution derived from ^{137}Cs measurements are estimates of medium-term (i.e. ca. 45 years) rates, the first two models outlined above are commonly used for modelling erosion and soil redistribution over shorter timescales and the AGNPS and ANSWERS models are event-based models. It is, however, reasonable to assume that the basic spatial pattern of soil redistribution rates derived from the ^{137}Cs measurements should be similar to that for a single storm event or series of events, even though the absolute magnitude of the values will be different. All four models have therefore been tested in terms of their ability to reproduce the spatial distribution of either the ^{137}Cs inventories or the estimates of soil redistribution rates derived from the ^{137}Cs measurements for the micro-catchment at Higher Walton Farm. Since the modelling routines necessitates complex calculations involving three-dimensional natural terrain, the powerful GRID modelling tools provided by ARC/INFO GIS have been used to support the models.

Calibrating and validating the topography-based sediment delivery model

The spatial distribution of sediment delivery ratios within the micro-catchment can be derived from the data presented in Figure 3, and this can be used to calibrate and test the distributed sediment delivery model outlined above. Using the approach described by Ferro and Minacapilli (1995), the sediment transport efficiency α_b for the study area was estimated to be ca. 0.092 and using the sediment delivery ratio D_b estimated from the information presented in Figure 3B and Equation (2), β was estimated to be 0.002. The spatial pattern of sediment delivery ratios within the study field was derived from the information presented in Figure 3B. For each grid cell, the sediment delivery ratio D_{sbcs} for the sub-basin draining into the cell was calculated as:

$$D_{sbcs} = \frac{\sum_{e} R_e a - \sum_{d} R_d a}{\sum_{e} R_e a} \tag{4}$$

where a is the cell size, e represents cells in eroding zones and d the cells in depositing zones, and R_e and R_d are the interpolated ^{137}Cs-based estimates of the erosion and deposition rates for eroding and depositing cells respectively. The resulting spatial distribution of D_{sbcs} within the study area is presented in Figure 4. The sediment delivery ratios are highest on the side

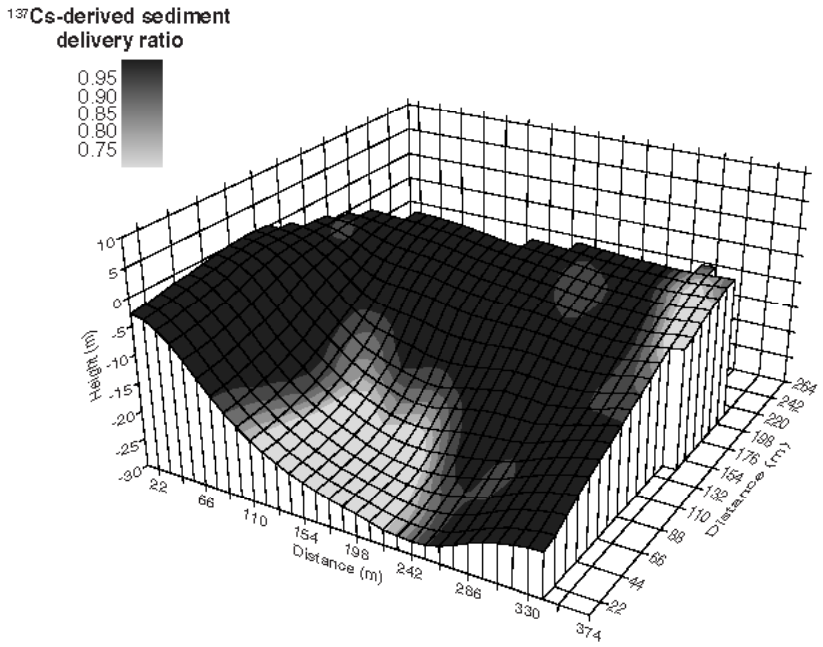

Fig. 4 The spatial distribution of the ^{137}Cs-derived sediment delivery ratios within the study area at Higher Walton Farm

slopes and decrease towards the central depression near the slope bottom, reflecting the sediment transport processes operating within the study area. Areas with low sediment delivery ratios are also found on the interfluves. To test the distributed sediment delivery model, the spatial distribution of the model-predicted sediment delivery ratio D_{sb} is required for comparison with that derived from the ^{137}Cs data. From equation (2) the sediment delivery ratio D_{sb} and the sediment transport efficiency α_{sb} for a sub-basin within a catchment can be calculated as:

$$D_{sb} = \sum_{i=1}^{N_{sb}} e^{-\beta t_{p,i}} A_i \Big/ \sum_{i=1}^{N_{sb}} A_i = e^{(\ln D_b / \alpha_b)\alpha_{sb}} \tag{5}$$

where N_{sb} is the number of morphological units within the sub-basin and α_{sb} is the sub-basin sediment transport efficiency related to its topography. For each sub-basin, the model-

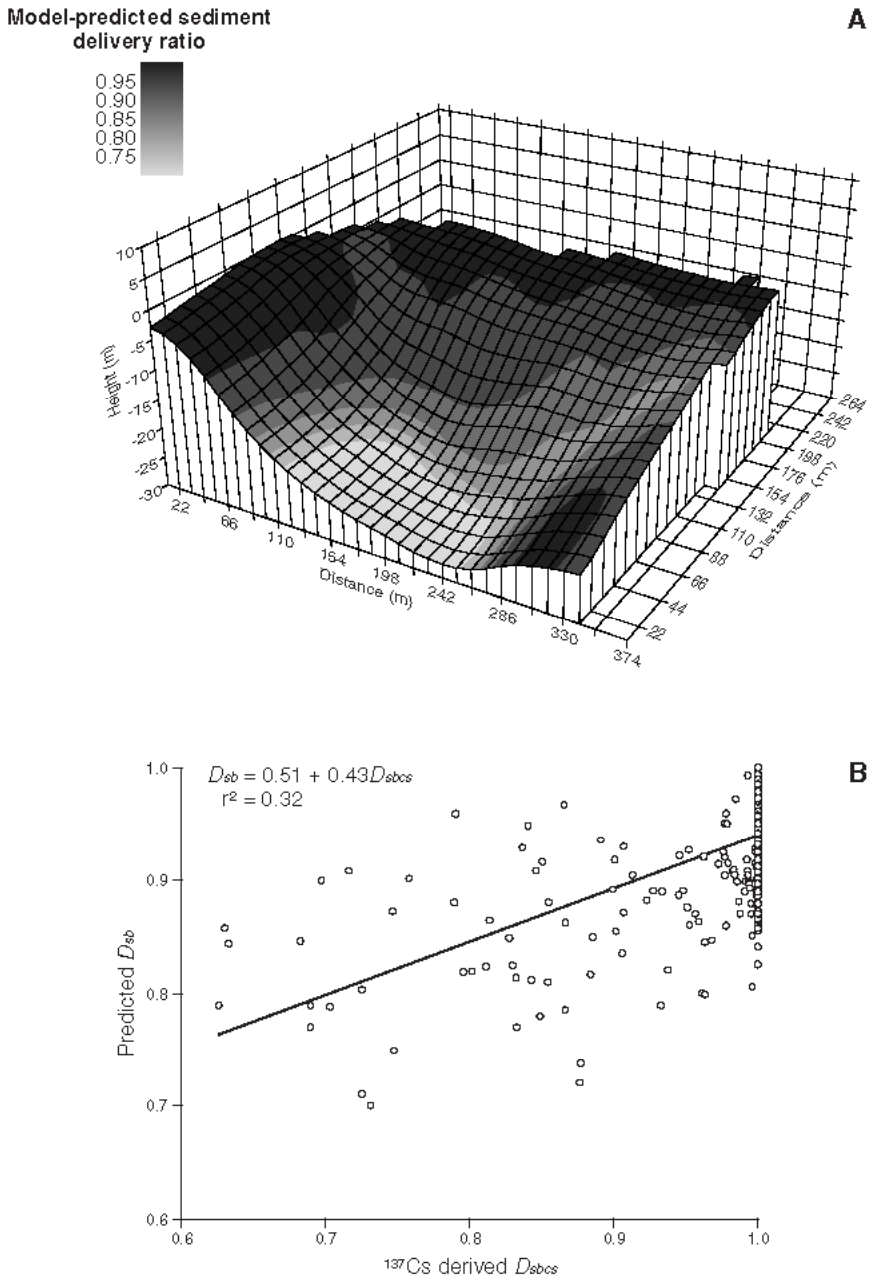

Fig. 5 The spatial distribution of the distributed sediment delivery model-predicted sediment delivery ratios within the study area (A) at Higher Walton Farm and the relationship between model-predicted and ^{137}Cs derived sediment delivery ratios (B)

predicted D_{sb} can be calculated using the same approach as used for calculating D_b. The spatial distribution of the model-predicted D_{sb} values is shown in Figure 5A. Figure 5B plots the relationship between the model-predicted and ^{137}Cs-derived sediment delivery ratios for the individual cells within study area. The general linear relationship between D_{sb} and D_{sbcs} indicates that the distributed sediment delivery model is able to represent the sediment delivery processes operating within the study area to some degree, and confirms that topography is one of the key factors influencing sediment mobilisation. However, the poor

correlation between the actual values of the model-predicted and ^{137}Cs-derived sediment delivery ratios also points to the need for an improved relationship between the sediment travel time $t_{p,i}$ and the morphological parameters $\lambda_{i,j}$ and $s_{i,j}$ for each morphological unit. An improved relationship between model-predicted and ^{137}Cs-derived sediment delivery ratios could also be obtained by calibrating the parameter β and the basin sediment transport efficiency α_b, using the spatial distribution of sediment delivery ratios derived from the ^{137}Cs data.

Calibrating and validating the topography-driven soil erosion model

The magnitude and spatial distribution of contemporary ^{137}Cs inventories within an area will reflect the cumulative effect of ^{137}Cs redistribution in association with soil and sediment redistribution, over the period since this radionuclide was introduced into the environment. It is therefore possible to use information on ^{137}Cs inventories to calibrate and validate soil erosion and sediment delivery models directly, if such models can be extended to simulate ^{137}Cs redistribution as well as soil redistribution. To test the topography-driven soil erosion model, water erosion and tillage redistribution have been assumed to be the primary processes controlling the movement of soil particles and ^{137}Cs within the study field and these processes have been incorporated into a topography-driven soil erosion and sediment delivery model, which is capable of simulating the magnitude and spatial pattern of contemporary ^{137}Cs inventories within the field. By comparing the measured and simulated ^{137}Cs inventories, it is possible to calibrate this model and to assess its ability to replicate the measured values and therefore to provide meaningful estimates of soil redistribution rates.

When the values for m, n, ϕ_1 and ϕ_2 are known, the net soil redistribution rate R_{Net} (kg m^{-2} year^{-1}) can be calculated as the gradient of the sediment transport flux. For a point within a study area, R_{Net} incorporates both tillage and water erosion contributions and can be expressed as:

$$\begin{aligned} R_{Net} &= R_T - R'_T + R_W \quad \text{for a point experiencing water erosion} \\ R_{Net} &= R_T - R'_T - R'_W \quad \text{for a point experiencing deposition by water} \end{aligned} \tag{6}$$

where R_T (kg m^{-2} year^{-1}) is the rate of tillage-induced downslope soil removal from the point and R'_T (kg m^{-2} year^{-1}) is the rate of tillage-induced deposition of soil from upslope areas. In equation (6), R_W (kg m^{-2} year^{-1}) is the water-induced erosion rate for a point experiencing erosion by water and R'_W (kg m^{-2} year^{-1}) is the water-induced deposition rate for a point experiencing deposition, respectively.

When the basic soil erosion model has been formulated, the spatial distribution of ^{137}Cs within the study area can be modelled. The process of soil redistribution by tillage differs from that by water, in that the former only produces movement of soil particles over a short distance, while the latter can transport the mobilised sediment over much greater distances. Sediment export from a field will only be associated with surface runoff. Following Walling and He (1997, 1999), variation of the ^{137}Cs inventory $A(t)$ (Bq m^{-2}) for a point experiencing water erosion can be expressed as:

$$\frac{\mathrm{d}A(t)}{\mathrm{d}t} = (1-\Gamma)I(t) + R'_T C'_T(t) - R_T C_T(t) - R_W C_W(t) - \lambda A(t) \tag{7}$$

where $I(t)$ (Bq m^{-2} year^{-1}) is the annual atmospheric ^{137}Cs deposition flux, λ (year^{-1}) is the decay constant of ^{137}Cs, $C_W(t)$ (Bq kg^{-1}) is the ^{137}Cs concentration in exported sediment by water, and $C'_T(t)$ (Bq kg^{-1}) and $C_T(t)$ (Bq kg^{-1}) are the concentrations of ^{137}Cs in deposited and exported sediment respectively. The second and third terms on the right side of Equation (7) represent the tillage-induced ^{137}Cs input flux from upslope and the output flux to downslope respectively, and the fourth term represents the water-induced ^{137}Cs output flux. Γ represents the percentage of the freshly deposited ^{137}Cs fallout removed by water-induced erosion before being mixed into the plough layer. Because the deposition of ^{137}Cs from the atmosphere is primarily associated with wet precipitation, a fraction of the annual ^{137}Cs input may be removed from the soil surface by water erosion associated with surface runoff before being incorporated into the plough layer by cultivation (cf. Walling and He, 1997, 1999).

For a point experiencing water-induced deposition, variation of the ^{137}Cs inventory $A(t)$ at a point experiencing deposition by water can be expressed as:

$$\frac{\mathrm{d}A(t)}{\mathrm{d}t} = I(t) + R'_T C'_T(t) - R_T C_T(t) + R'_W C'_W(t) - \lambda A(t) \tag{8}$$

where $C'_W(t)$ (Bq kg^{-1}) is the ^{137}Cs concentration in sediment deposited by water. The fourth term on the right side of equation (9) represents the water-induced ^{137}Cs input flux.

If it is assumed that the ^{137}Cs contained within the plough layer is uniformly distributed within the plough depth D (kg m^{-2}), the ^{137}Cs concentration $C_s(t)$ (Bq kg^{-1}) of soil within the plough layer can be expressed as:

$$C_s(t) = \begin{cases} \dfrac{A(t)}{D} & \text{for a net erosion point} \\ \dfrac{1}{D}\left[A(t) - \dfrac{|R_{Net}|}{D}\displaystyle\int_0^{t-1} A(t')\mathrm{e}^{-\lambda t'}\mathrm{d}t'\right] & \text{for a net deposition point} \end{cases} \tag{9}$$

For tillage erosion, the ^{137}Cs concentration in the deposited or exported sediment at a specific point may be assumed to be the same as that for the soil within the plough layer. However, for a point experiencing water erosion, the removal of the ^{137}Cs essentially comprises two components, the first of which is associated with the removal of the freshly deposited ^{137}Cs, and the second is associated with erosion of the accumulated ^{137}Cs stored in the soil. For a point experiencing water-induced deposition, the ^{137}Cs content of the deposited sediment will reflect the combination of sediment and its associated ^{137}Cs mobilised from all the eroding areas that contribute to the aggrading point, and can be estimated from the erosion rates and the ^{137}Cs concentrations of the sediment mobilised from the upslope eroding area S_e (m^2). The ^{137}Cs concentration of mobilised sediment can therefore be expressed as follows:

$$\begin{aligned} C_T(t) &= C'_T(t) = C_s(t) \\ C_W(t) &= P\left[C_s(t) + \frac{\Gamma I(t)}{R_W}\right] \\ C'_W(t) &= \frac{\displaystyle\int_{S_e} P' R_W C_W(t)\mathrm{d}S_e}{\displaystyle\int_{S_e} R_W \mathrm{d}S_e} \end{aligned} \tag{10}$$

where P is the particle size correction factor associated with mobilised sediment, and P' is the particle size correction factor associated with deposited sediment (cf. Walling and He, 1997, 1999). The introduction of P and P' takes into account of the effect on the ^{137}Cs content of sediment of the grain size selectivity in erosion and deposition processes.

The algorithms for modelling the spatial distribution of ^{137}Cs inventories described above and the ^{137}Cs inventory data collected from the cultivated field at Higher Walton Farm have been used to calibrate the sediment transport model outlined previously using a GIS cell-based modelling technique. When a study area is divided into cells and the mobilised sediment is assumed to move down the slope gradient (or flow direction, defined as the direction of steepest slope), the sediment transport equation presented as equation (1) can be used to establish a cell-based soil redistribution model: the difference between the amount of sediment exported from a cell Q_{Out} (kg year^{-1}) and the amount of sediment transported into the cell from the neighbouring cells Q_{In} (kg year^{-1}) will reflect the net soil loss or gain for the cell. The net soil redistribution rate R_{Net} can be calculated as:

$$R_{Net} = (Q_{Out} - Q_{In}) / a \tag{11}$$

where a (m^2) is the area of the cell. A positive value of R_{Net} implies net soil erosion and a negative value deposition. Values for the two exponents m and n can be derived experimentally (cf. Desmet & Govers, 1995). To evaluate the optimum values for the two constants ϕ_1 and ϕ_2 in equation (1), the predicted ^{137}Cs inventory A_P (Bq m^{-2}) for each cell can be linearly related to the measured ^{137}Cs inventory A_M (Bq m^{-2}) for the same cell, with the slope gradient ϕ_3 equal to 1.0:

$$A_P = \phi_3 A_M \tag{12}$$

The topographic attributes such as slope angle, flow direction and contributing area used to calculate soil redistribution rates were derived from the DEM of the study area using ARC/INFO GIS. Values for m and n were set at 1.2 and 1.4 respectively, based on values reported by other workers (cf. Moore et al., 1993; Desmet and Govers, 1995; Govers et al., 1994, 1996). It has been assumed that the topographic change at the study site over the past 40 years has been insignificant and that erosion and deposition rates have been essentially constant through time. Different values for ϕ_1 and ϕ_2 were input into the topography-driven erosion model and values for R_{Net}, R_T, R'_T, R_W and R'_W were then calculated. The calculated soil redistribution rates were then input into the model describing the redistribution of ^{137}Cs within the field, and the model was run to simulate the spatial distribution of ^{137}Cs inventories. Values of other parameters required by the model were estimated based on information on local soil and rainfall conditions, and the temporal variation of the atmospheric ^{137}Cs fallout flux was assumed to be the same as that for Milford Haven, UK (cf. Cambray et al., 1989), with the magnitude adjusted according to the estimated local reference inventory. Values of ^{137}Cs inventory were extracted from the simulated spatial distribution of ^{137}Cs inventories for those cells with the same co-ordinates as the sampled soil cores and compared with the measured ^{137}Cs inventories. The value of ϕ_3 was estimated according to Equation (12) and the values of ϕ_1 and ϕ_2 producing a value of ϕ_3 closest to 1.0 were taken to be the optimum values.

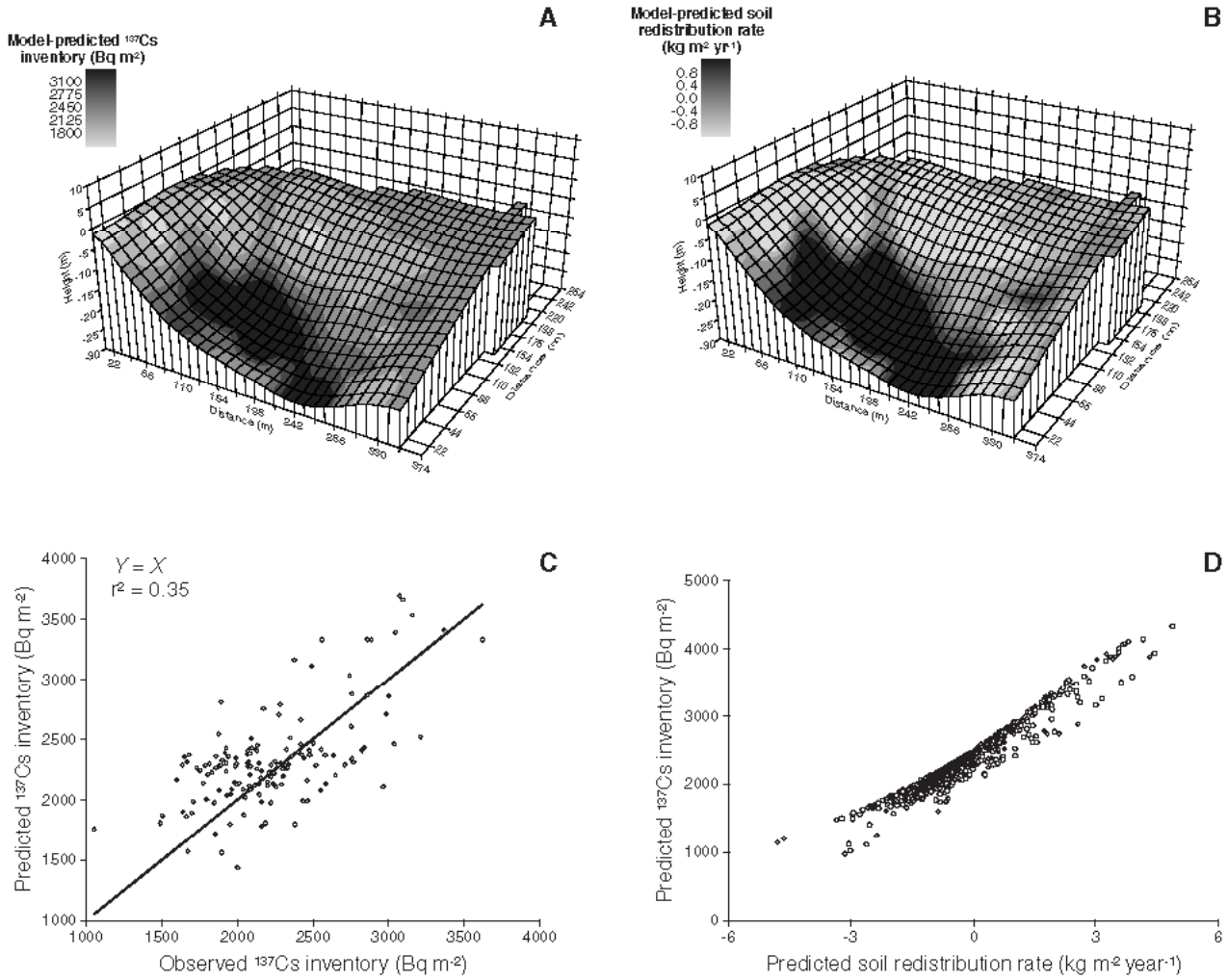

Fig. 6 The spatial distribution of ^{137}Cs inventories (A) and soil redistribution rates (B) predicted by the topography-driven erosion model at Higher Walton Farm and the relationships between model-predicted and measured ^{137}Cs inventories (C) for the sampling points in the study area (the smooth line is the theoretical line from equation (12)) and the model-predicted ^{137}Cs inventories and soil redistribution rates for the study area (D)

Figures 6A and 6B present the spatial patterns of ^{137}Cs inventories and soil redistribution rates within the study area predicted by the calibrated model and Figure 6C depicts the relationship between the measured and model-predicted ^{137}Cs inventories (with optimum values of 1.9 for ϕ_1 and 210 for ϕ_2, with r^2=0.35). In general, there is a linear relationship between the predicted and measured ^{137}Cs inventories, confirming the general validity of this distributed sediment transport model. Figure 6D shows the relationship between the predicted ^{137}Cs inventory and soil redistribution rate for the study area. This differs from that associated with the conventional conversion models used to estimate soil redistribution rates from ^{137}Cs measurements, in that the ^{137}Cs inventory is a multiple value function of the erosion rate for the model presented here, but a single value function for the conventional conversion models (cf. Walling and Quine, 1990). The relationship illustrated in Figure 6D reflects the influence of both water erosion and tillage in redistributing soil on arable land and their relative importance will vary between sampling points. The level of agreement between the model-predicted and measured ^{137}Cs inventories must be seen as

relatively low, and this may reflect the failure of the present model to represent fully the processes of soil and ^{137}Cs redistribution operating at the study site. Some inaccuracies may also be associated with the DEM of the study area derived from the surveyed elevation data using a GIS. Extension of this analysis to include use of data for two study areas characterised by similar soil and land use, with the ^{137}Cs inventory data from one area being used to calibrate the model and that from the other area being used to validate the predicted ^{137}Cs inventories, would increase its rigour.

Testing the AGNPS and ANSWERS models

To apply the AGNPS and ANSWERS models to the micro-catchment, values of the parameters needed for the grid cells were assigned, and the data were arranged in the format required by the models using a FORTRAN program written by the authors. The AGNPS (version 5.00) and ANSWERS (version 4.880215) models were run for an hypothetical rainfall event with a total precipitation of 18 mm fallen within 3.5 hours, which represents a large rainfall event for the study sites. Another FORTRAN programme was written to calculate cell erosion and sediment yield and the basin sediment delivery ratios from the model outputs and to produce the data in the format required by ARC/INFO for further data display and analysis. In view of the difficulty of directly comparing the soil redistribution rates for the single event predicted by the models with the estimates of longer-term mean annual rates derived from the ^{137}Cs measurements, emphasis has been placed on validating the spatial patterns of soil redistribution simulated by the models rather than the magnitude of the predicted erosion rates.

Figures 7A and 7B illustrate the spatial distribution of soil erosion rates simulated from the two models. Significant differences exist between the spatial patterns predicted by the models. The AGNPS model predicts higher soil erosion rates in the convex midslope areas, lower erosion rates in areas along the top of the slopes and soil deposition in concave areas at the foot of the slopes. There is a reasonable degree of similarity between the pattern of soil redistribution simulated by the AGNPS model and that provided by the ^{137}Cs measurements (Figure 3B). In contrast, the pattern of soil redistribution predicted by the ANSWERS model is characterised by lower erosion rates along the field boundaries and an increase in the erosion rates towards the field outlet. The ANSWERS model-simulated results show almost no sediment deposition within the field and the predicted sediment delivery ratio is nearly 1.0. This value is substantially higher than that of 0.59 predicted by the AGNPS model. The sediment delivery ratio predicted by the AGNPS model is much closer to the value of 0.66 estimated from the ^{137}Cs measurements than that predicted by the ANSWERS model. Figures 7C and 7D further compare the soil redistribution rates simulated by the two models with the soil redistribution rates estimated from the ^{137}Cs measurements. It is clear from Figure 7D, that there is essentially no agreement between the ANSWERS-simulated soil redistribution rates and the ^{137}Cs derived values. However, a clear linear correlation between the AGNPS-simulated soil redistribution rates and the ^{137}Cs-estimated soil redistribution rates exists. Figure 7 therefore indicates that, the AGNPS model provides a better representation of the soil erosion and sediment delivery processes operating within the micro-catchment than the ANSWERS models. For example, although both models predict some soil deposition along the bottom of the main valley, the pattern of soil redistribution on the slopes is very different. The AGNPS model predicts soil deposition in the concave areas on the valley sides, whereas the ANSWERS predicts increased erosion in those areas.

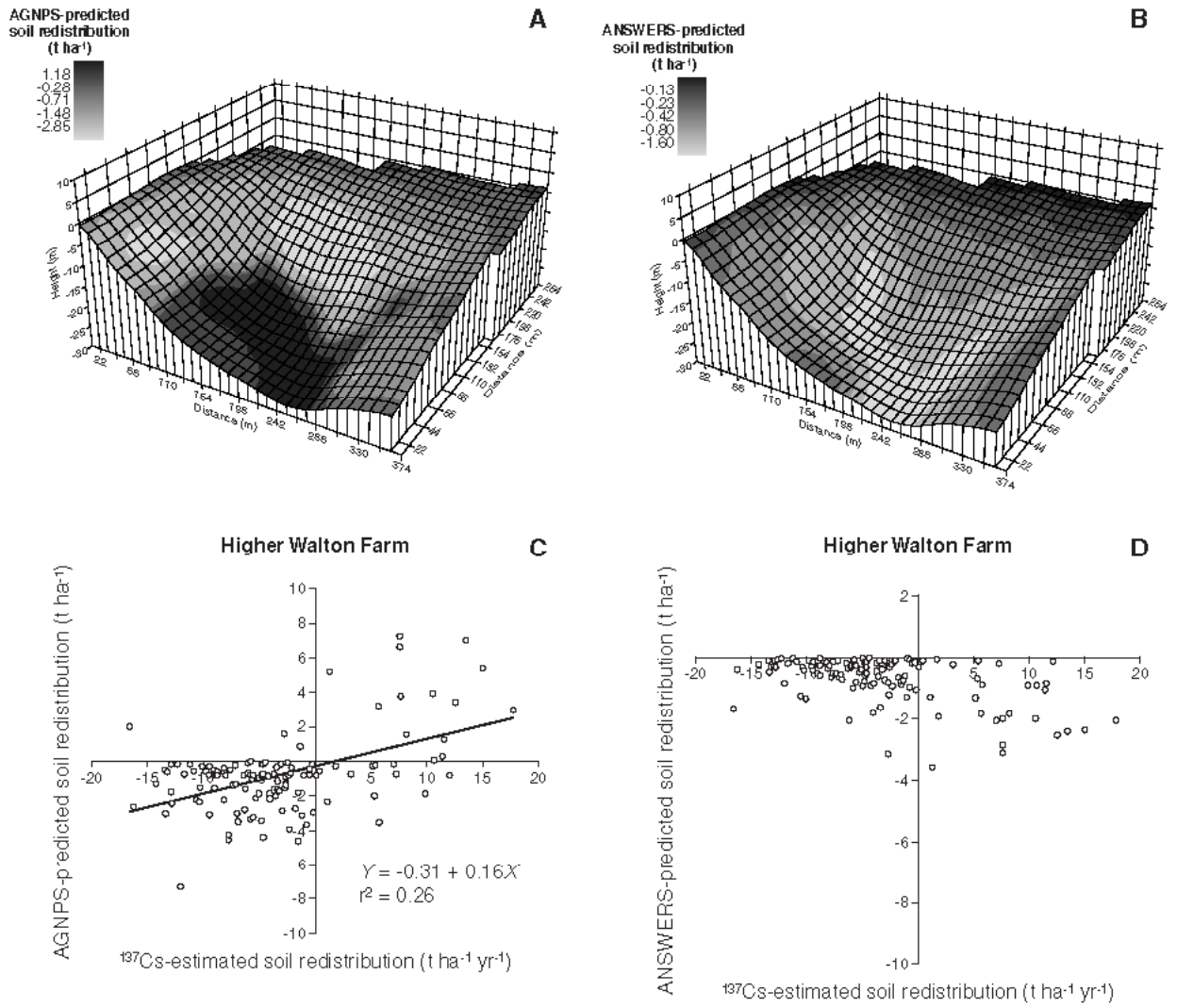

Fig. 7 The AGNPS and ANSWERS predicted soil redistribution rates (A and B) within the study area at Higher Walton Farm for the hypothetical rainfall events and the relationship between the model-predicted and ^{137}Cs-estimated soil redistribution rates (C and D)

Testing the AGNPS and ANSWERS models at the catchment scale

A further test of the AGNPS and ANSWERS models was undertaken at the catchment scale by comparing the basin sediment delivery ratio predicted for the entire Keymelford catchment by the models with those estimated from the ^{137}Cs measurements.

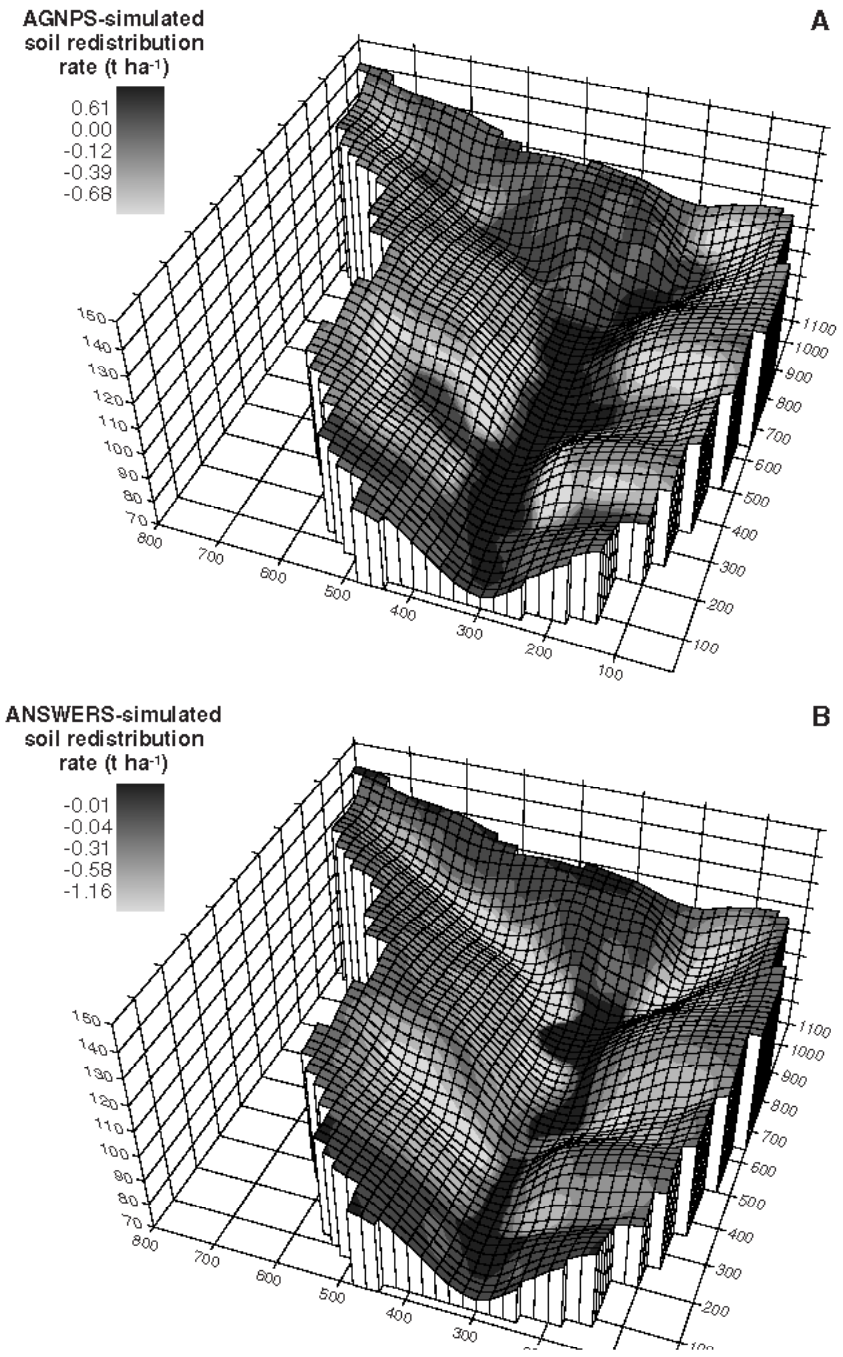

Fig. 8 Spatial pattern of cumulative soil redistribution within the Keymelford catchment simulated by the AGNPS (A) and ANSWERS (B) models for a series of storm events

Use of ^{137}Cs-derived basin sediment delivery ratios

To comply with the total number of cells that the models can process and to maintain the same cell size for both models, the 10 m grid DTM data obtained for the catchment from the Ordnance Survey were re-sampled to 20 m using the ARC/INFO RESAMPLE tool. This provided a total of 1291 cells for the catchment. The two models were run for a series of observed rainfall events to simulate the soil redistribution and the basin sediment delivery ratios were estimated for each storm. Figure 8 depicts the spatial pattern of cumulative

sediment redistribution associated with these events. Mean basin sediment delivery ratios for the storms predicted by the AGNPS and ANSWERS models were 0.37 and 0.91 respectively. The basin sediment delivery ratio predicted by the AGNPS model is considerably closer to the ^{137}Cs-estimated basin sediment delivery ratio of 0.54 than that predicted by the ANSWERS model. These results again suggest that the AGNPS model provides a better representation of erosion and sediment redistribution processes in the study area than the ANSWERS model.

Perspective

The spatial heterogeneity of soil properties and basin topography and their interaction with soil erosion and sediment transport processes necessitate the use of spatially distributed approaches to modelling erosion and sediment delivery processes at the catchment scale. Distributed soil erosion and sediment delivery models, such as AGNPS, ANSWERS and WEPP, are being widely used for predicting sediment mobilisation and delivery within agricultural catchments. Traditionally, calibration and validation of such models has been based on comparisons of model predicted and observed catchment outputs (e.g. runoff and sediment yields). Close agreement between model-predicted and measured outputs will afford some degree of validation, but it cannot provide conclusive validation of the magnitude and spatial distribution of soil redistribution rates within the catchment predicted by the model. Since the importance of spatially distributed modelling lies with its ability to provide spatially distributed information on soil loss and sediment transport which can be used for planning soil conservation and management strategies, validation of the spatial pattern of soil redistribution predicted by a model must be seen as an important requirement. There is, however, a general lack of distributed data on soil redistribution rates for use in such validation. The results presented in this contribution demonstrate that the information on soil redistribution rates provided by ^{137}Cs measurements can provide a basis for such model validation. The level of agreement between the ^{137}Cs-estimated and model-simulated results can be used to examine the performance of distributed models and therefore their representation of the soil redistribution processes. Although the results presented here are preliminary, the use of the information provided by ^{137}Cs measurements to validate spatially distributed models must be seen as representing an important advance in the testing and further development of such models.

Acknowledgement The work reported in this contribution was supported by a research grant from the UK Natural Environment Research Council (GR3/10293). The authors gratefully acknowledge this support, the generosity of local landowners in permitting access to the study area and the collection of soil samples for ^{137}Cs analysis, and the assistance of Mr Phil Whelan with hydrological monitoring in the study catchment. The study represents a contribution to the IAEA Coordinated Research Programme D1.50.5 through Technical Contract 9562/R2.

Bibliography

BEASLEY, D.B. (1982) 'Modelling sediment yield from agricultural watersheds'. J. Soil Water Conserv., 37, p.113-117.

BROURAOUI, F.; F. VACHAUD; G. HAVERKAMP and B. NORMAND (1997). 'A distributed physical approach for surface-subsurface water transport modelling in agricultural watersheds. J. Hydrol., 203, p.79-92.

CAMBRAY, R.S.; K. PLAYFORD and R.C. CARPENTER (1989) *Radioactive fallout in air and rain: results to the end of 1988*. UK Atomic Energy Authority Report AERE-R 10155, HMSO.

CHAPPELL, A. (1996) 'Modelling the spatial variation of processes in the redistribution of soil: digital terrain models and ^{137}Cs in southwest Niger'. Geomorphology, 17, p. 249-261.

CHOI, K.S. and E. BLOOD (1999) 'Modeling developed coastal watersheds with the agricultural non-point source model'. J. Am. Water Resources Association, 35, p.233-244.

DE ROO, A.P.J. (1998) 'Modelling runoff and sediment transport in catchments using GIS'. Hydrol. Process, 12, p.905-922.

DE ROO, A.P.J. and D.E. WALLING (1994) 'Validating the ANSWERS soil erosion model using ^{137}Cs'. In: R.J.Rickson (ed.), *Conserving soil resources: European perspective,* CAB, Wallingford, UK, p. 246-263.

DE ROO, A.P.J.; C.G. WESSELING and C.J. RITSEMS (1996) 'LISEM: a single event physcially-based hydrologic and soil erosion model for drainage basins. I: Theory, input and output'. Hydrol. Proc. 10, p. 1107-1117.

DESMET, P. J. J. and G. GOVERS (1995) 'GIS-based simulation of erosion and deposition patters in an agricultural landscape: a comparison of model results with soil map information'. Catena, 25, 389-401.

FERRO, V. (1997) 'Further remarks on a distributed approach to sediment delivery'. Hydrol. Sci. J., 42, p.633-647.

FERRO, V. and M. MINACAPILLI (1995) 'Sediment delivery processes at basin scale'. Hydrol. Sci. J. 40, 703-717.

GOVERS, G.; K. VANDAELE; P.J.J. DESMET; J. POESEN and K. BUNTE (1994) 'The role of tillage in soil redistribution on hill slopes'. European J. Soil Sci,. 45, p. 69-478.

GOVERS, G.; T.A. QUINE; P.J.J. DESMET and D.E. WALLING (1996) 'The relative contribution of soil tillage and overland flow erosion to soil redistribution on agricultural land'. Earth Surf. Proc. Landforms, 21, p. 929-946.

HE, Q. and D.E. WALLING (1998) 'Calibrating and validating a spatially distributed sediment delivery model using soil caesium-137 data'. In: *Proceedings of the Hong Kong international conference on modeling geographical and environmental systems with Geographical Information Systems*. Chinese University of Hong Kong Press, Hong Kong, p. 272-277.

IAEA (1998) *Use of ^{137}Cs in the study of soil erosion and sedimentation.* IAEA-TECDOC-1028, IAEA, Vienna, Austria.

KIRKBY, M.J.; P.S. NADEN; T.P. BURT and D.P. BUTCHER (1987) *Computer simulation in physical geography*. Wiley, Chichester.

KOTHYARI, U.C. and S.K. JAIN (1997) 'Sediment yield estimation using GIS'. *Hydrol. Sci. J*., 42, p. 833-843.

LANE, L. J. and M.A. NEARING (1989) *USDA-Water Erosion Prediction Project: hillslope profile model documentation*. NSERL Report No. 2, USDA-ARS, West Lafayette, Indiana.

LENZI, M. A. and M. DI LUZIO (1997) 'Surface runoff, soil erosion and water quality modelling in the Alpone watershed using AGNPS integrated with Geographic Information System'. European J. of Agron. 6, p.1-14.

MOORE, I. D. and G.J. BURCH (1986) 'Modeling erosion and deposition: topographic effects'. Trans. Am. Soc. Ag. Eng., 29, p.1624-1630.

MOORE, I.D.; P.E. GESSLER; G.A. NIELSEN and G.A. PETERSEN (1993) 'Soil attribute prediction using terrain analysis'. Soil Sci. Soc. Am. J., 57, p.443-452.

MORGAN, R.P.C.; J.N. QUINTON and R.J. RICKSON (1992) *EUROSEM documentation manual.* Silsoe College, Silsoe, Bedford, UK.

PARSON, S.C.; J.M. HAMLETT; P.D. ROBILLARD and M.A. FOSTER (1998) 'Determining the decision-making risk from AGNPS simulations'. Trans. ASAE, 41,.p.1679-1688.

PERRONE, J. and C.A. MADRAMOOTOO (1999) 'Sediment yield prediction using AGNPS'. J. Soil Water Conserv., 54, p.415-419.

PITTS, W.E.; K.H. YOO; M.S. MILLER-GOODMAN; W.L. DELOS SANTOS and K.S. YOON (1999) 'WEPP and GLEAMS simulations of runoff and soil loss from grazed pasture in the south-eastern United States'. J. Environ. Sci. Health Part A-Toxic/Hazardous Substances and Environ. Engineering, 34, p. 1397-1413.

RITCHIE, J.C. and J.R. MCHENRY (1990) 'Application of radioactive fallout cesium-137 for measuring soil erosion and sediment accumulation rates and patterns: a review'. J. Environ. Qual., 19, p.215-233.

RODE, M. and H.G. FREDE (1997) 'Modification of AGNPS for agricultural land and climate conditions in Central Germany'. J. Environ. Qual., 26, p.165-172.

WALLING, D.E. (1998) 'Use of ^{137}Cs and other fallout radionuclides in soil erosion investigations: Progress, problems and prospects'. In: *Use of ^{137}Cs in the Study of Soil Erosion and Sedimentation*, IAEA-TECDOC-1028, IAEA, Vienna, p.39-62.

WALLING, D.E. and Q. HE (1997) *Models for converting ^{137}Cs measurements to estimates of soil redistribution rates on cultivated and uncultivated soils (including software for model implementation).* Report to IAEA, University of Exeter, UK.

WALLING, D.E. and Q. HE (1998) 'Use of fallout ^{137}Cs measurements for validating and calibrating soil erosion and sediment delivery models'. IAHS Publ. 249, p. 267-278.

WALLING, D.E. and Q. HE (1999) 'Improved models for estimating soil erosion rates from ^{137}Cs measurements'. J. Environ. Qual., 28, p.611-622.

WALLING, D.E. and T.A. QUINE (1990) 'Calibration of caesium-137 measurements to provide quantitative erosion rate data'. Land Degrad. Rehabil., 2, p.161-175.

WALLING, D.E. and T.A. QUINE (1992) 'The use of caesium-137 measurements in soil erosion surveys'. In: *Erosion and sediment transport monitoring programmes in river basins*. IAHS Publ. no. 210, p.143-152.

WALLING, D.E. and T.A. QUINE (1995) 'The use of fallout radionuclides in soil erosion investigations'. In: *Nuclear techniques in soil-plant studies for sustainable agriculture and environmental preservation*. IAEA Publication ST1/PUB/947.

WATSON, F. G. R.; R.B. GRAYSON; R.A. VERTESSY and T.A. MCMAHON (1998). 'Large-scale distribution modelling and utility of detailed ground data'. Hydrol. Proc., 12, p. 873-888.

WISCHMEIER, W. H. and D.D. SMITH (1978) *Predicting rainfall erosion losses: a guide to conservation planning*. Agricultural Handbook 537. USDA, Washington, DC, USA.

WICKS, J.M. and J.C. BATHURST (1996) 'SHESED: a physically based, distributed erosion and sediment yield component for the SHE hydrological modelling system'. J. Hydrol. 175, p.213-238.

YOUNG, R.R.; C.A. ONSTAD; D.D BOSCH and W.W. ANDERSON (1987) AGNPS: *an agricultural nonpoint source pollution model.* Conservation Research Report 35, USDA-ARS, Washington, D. C.

YOUNG, R.R.; C.A. ONSTAD; D.D BOSCH and W.W. ANDERSON (1989) 'AGNPS, Agricultural Non-Point-Source Pollution Model for evaluating agricultural watersheds'. J. Soil Water Conserv., 44, p.168-173.

ZHANG, L.; A.L. O'NEILL and S. LACEY (1996) 'Modelling approaches to prediction of soil erosion in catchments'. Environ. Software, 11, p.123-133.